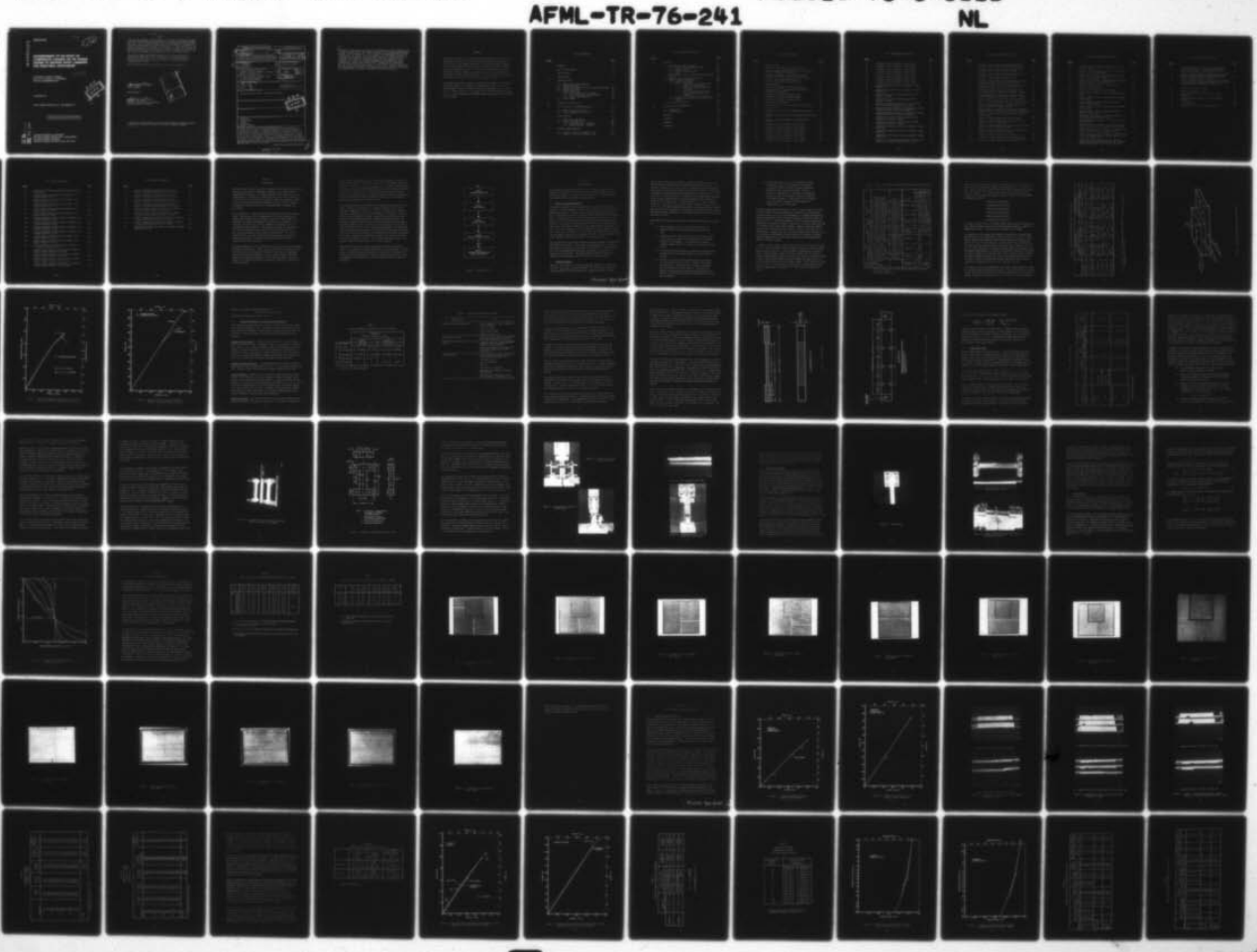
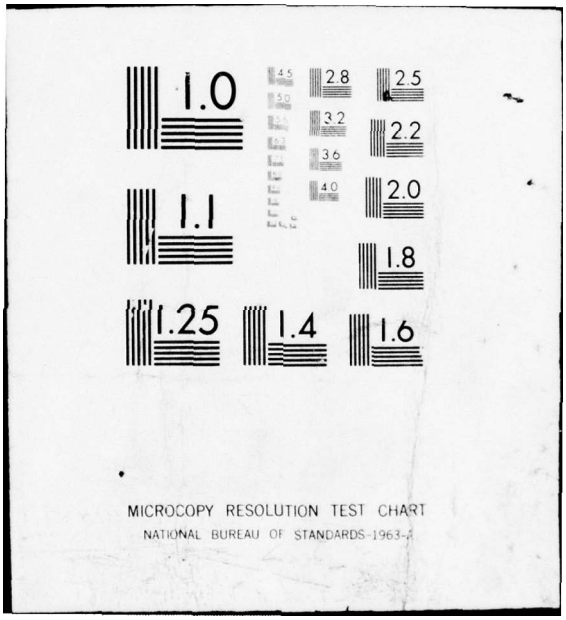
AD-A043 365 LOCKHEED-CALIFORNIA CO BURBANK RYE CANYON RESEARCH LAB F/G 11/4
ASCERTAINMENT OF THE EFFECT OF COMPRESSIVE LOADING ON THE FATIG--ETC(U)
DEC 76 J T RYDER, E K WALKER F33615-75-C-5118

UNCLASSIFIED AFML-TR-76-241 NL

1 OF 3

AD A043 365




1.0
1.1
1.25
1.4
1.6
1.8
2.0
2.2
2.5
2.8
3.2
3.6
4.0
4.5
5.0
MICROCOPY RESOLUTION TEST CHART
NATIONAL BUREAU OF STANDARDS-1963-A

AD A043365

AFML-TR-76-241

ASCERTAINMENT OF THE EFFECT OF COMPRESSIVE LOADING ON THE FATIGUE LIFETIME OF GRAPHITE EPOXY LAMINATES FOR STRUCTURAL APPLICATIONS

410347

LOCKHEED-CALIFORNIA COMPANY
RYE CANYON RESEARCH LABORATORY
BURBANK, CALIFORNIA 91520

DDC
AUG 22 1977
C

DECEMBER 1976

FINAL REPORT FEBRUARY 1975 - SEPTEMBER 1976

Approved for public release; distribution unlimited

AD No.
DDC FILE COPY

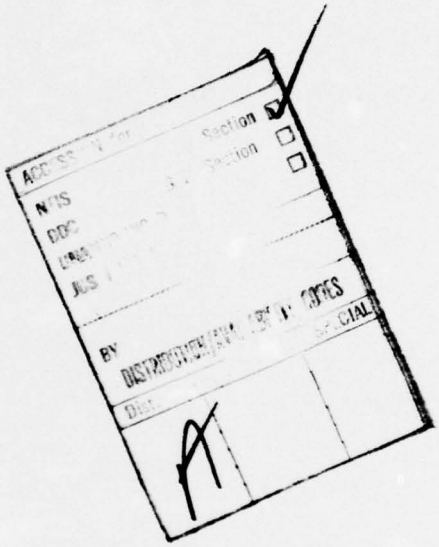
AIR FORCE MATERIALS LABORATORY
AIR FORCE WRIGHT AERONAUTICAL LABORATORIES
AIR FORCE SYSTEMS COMMAND
WRIGHT-PATTERSON AIR FORCE BASE, OHIO 45433

NOTICE

When Government drawings, specifications, or other data are used for any purpose other than in connection with a definitely related Government procurement operation, the United States Government thereby incurs no responsibility nor any obligation whatsoever; and the fact that the government may have formulated, furnished, or in any way supplied the said drawings, specifications, or other data, is not to be regarded by implication or otherwise as in any manner licensing the holder or any other person or corporation, or conveying any rights or permission to manufacture, use, or sell any patented invention that may in any way be related thereto.

This report has been reviewed and cleared for open publication and/or public release by the appropriate Office of Information (OI) in accordance with AFR 190-17 and DODD 5230.9. There is no objection to unlimited distribution of this report to the public at large, or by DDC to the National Technical Information Service (NTIS).

This technical report has been reviewed and is approved for publication.



James M. Whitney
JAMES M. WHITNEY
Project Engineer

FOR THE DIRECTOR

Stephen W. Tsai
STEPHEN W. TSAI, Chief
Mechanics & Surface Interactions Branch
Nonmetallic Materials Division

Copies of this report should not be returned unless return is required by security considerations, contractual obligations, or notice on a specific document.

AIR FORCE - 1 AUG 77 - 175

SECURITY CLASSIFICATION OF THIS PAGE (When Data Entered)

REPORT DOCUMENTATION PAGE

READ INSTRUCTIONS BEFORE COMPLETING FORM

1. REPORT NUMBER: AFML-TR-76-241	2. GOVT ACCESSION NO.
3. RECIPIENT'S CATALOG NUMBER	
4. TITLE (and Subtitle): ASCERTAINMENT OF THE EFFECT OF COMPRESSIVE LOADING ON THE FATIGUE LIFETIME OF GRAPHITE/EPOXY LAMINATES FOR STRUCTURAL APPLICATIONS	5. TYPE OF REPORT & PERIOD COVERED: Final Technical Report, 13 Feb 1975 — 22 Sept 1976
	6. PERFORMING ORG. REPORT NUMBER
7. AUTHOR(s): J. T. Ryder, E. K. Walker	8. CONTRACT OR GRANT NUMBER(s): F33615-75-C-5118
9. PERFORMING ORGANIZATION NAME AND ADDRESS: Lockheed-California Company, Division of Lockheed Aircraft Corporation, Burbank, California 91520	10. PROGRAM ELEMENT, PROJECT, TASK AREA & WORK UNIT NUMBERS: 73400399
11. CONTROLLING OFFICE NAME AND ADDRESS: Air Force Materials Laboratory (MBM), Air Force Systems Command, Wright-Patterson AFB, Ohio	12. REPORT DATE: December 1976
	13. NUMBER OF PAGES: 273
14. MONITORING AGENCY NAME & ADDRESS (if different from Controlling Office): 274 P.	15. SECURITY CLASS. (of this report): Unclassified
	15a. DECLASSIFICATION/DOWNGRADING SCHEDULE

16. DISTRIBUTION STATEMENT (of this Report)

Approved for public release: distribution unlimited

DDC PROCESSED AUG 22 1977 C

17. DISTRIBUTION STATEMENT (of the abstract entered in Block 20, if different from Report)

18. SUPPLEMENTARY NOTES

19. KEY WORDS (Continue on reverse side if necessary and identify by block number)

Composites
Graphite/Epoxy
Fatigue
Compression
Residual Strength

20. ABSTRACT (Continue on reverse side if necessary and identify by block number)

The main objective of this research investigation was the experimental determination of the effect of compressive loading on the fatigue response of graphite/epoxy laminates. The primary emphasis of the program was on the accumulation of a statistically significant data base. The data base was to be used for developing an analytical model with predictive capability to account for the effect of compressive loading. The test program included only unnotched coupons in a room temperature, laboratory air environment. The test program consisted of static tensile and compressive tests; tension-tension and tension-

DD FORM 1 JAN 73 1473 EDITION OF 1 NOV 65 IS OBSOLETE

SECURITY CLASSIFICATION OF THIS PAGE (When Data Entered)

410347

compression fatigue tests; and tensile and compressive residual strength tests of coupons tested either under tension-tension or tension-compression fatigue loading. The development of a large, statistically meaningful data base was accomplished. The general effect of compression on the fatigue response of a graphite/epoxy composite was determined. However, a general model with capability to account for compressive loading was not attempted. As an alternate, the concept of a fatigue threshold was postulated along with consideration of some substantiating data. Analysis of the data showed that due to the extent of data scatter, a model of the "wear-out" or similar type would predict the need for unacceptably low stress levels to achieve the high probabilities of survival required for aircraft structures.

FOREWORD

This report describes an investigation of ascertainment of the effect of compressive loading on the fatigue lifetime of graphite/epoxy laminates for structural applications performed by the Lockheed-California Company under Air Force Contract F33615-75-C-5118. The Air Force Project Engineer directing the program was Dr. J. M. Whitney of the Mechanics and Surface Interactions Branch, Nonmetallic Materials Division, Air Force Materials Laboratory at Wright-Patterson AFB, Ohio. Dr. J. T. Ryder was the Principal Investigator while Mr. E. K. Walker was the Program Manager.

The program was conducted through the Structures Department of the Lockheed-California Company. The support and contributions of Mr. W. E. Krupp, Group Engineer, Fatigue and Fracture Mechanics Laboratory; Mr. D. E. Pettit Dr. G. E. Bowie and Ms. K. N. Lauraitis, all of the same laboratory, and of Mr. L. D. Fogg of the Structural Methods Group, are gratefully acknowledged by the authors.

TABLE OF CONTENTS

Section		Page
	FOREWORD	iii
	LIST OF ILLUSTRATIONS	vi
	LIST OF TABLES	xi
I	INTRODUCTION	1
II	PROGRAM OVERVIEW	5
	2.1 Material Selection Background	5
	2.2 Laminate Selection	5
	2.3 Coupon Fabrication and Quality Assurance Procedures	16
	2.4 Program Test Matrix	23
	2.5 Testing Procedures	27
	2.5.1 Static Tension Test Procedures	27
	2.5.2 Static Compression Test Procedures	27
	2.5.3 Fatigue Test Procedures	35
	2.6 Data Analysis	38
III	MATERIAL CHARACTERIZATION	43
IV	STATIC TENSION AND COMPRESSION RESULTS	63
	4.1 Static Tension Test Results	63
	4.2 Static Compression Test Results	83
V	FATIGUE RESULTS	111
	5.1 Stress-Life Scan Results	113
	5.2 Extent of Fatigue Scatter	124
	5.2.1 Fatigue Behavior - Laminate 1	127
	5.2.2 Fatigue Behavior - Laminate 2	136
VI	RESIDUAL STRENGTH RESULTS	145
	6.1 Laminate 1 Residual Strength Results	145
	6.2 Laminate 2 Residual Strength Results	148

TABLE OF CONTENTS (Continued)

Section		Page
VII	DISCUSSION	157
	7.1 Comparison of Laminate Results	157
	7.1.1 Tension and Compression Results	157
	7.1.2 Fatigue Results	157
	7.1.3 Residual Strength Results	158
	7.1.4 Summary	161
	7.2 Comparison of 3- and 2- Parameter Weibull Analysis Results	162
	7.3 Extrapolation of Fatigue Life Results	167
	7.4 Residual Strength Degradation	170
	7.4.1 Physical Principles	172
	7.4.1.1 Damage Growth and Failure Modes Observed in this Program	173
	7.4.1.2 Comparisons Between Composites and Metals	177
	7.4.1.3 Nature of Required Failure and Damage Growth Expressions for Composites	183
	7.4.2 Evaluation of a Strength Degradation Model	185
	7.4.3 Summary; Direction of Future Research and Analysis	202
	7.5 Applications to Design	205
VIII	CONCLUSIONS AND RECOMMENDATIONS	207
	8.1 Conclusions	207
	8.2 Recommendations	209
	Appendix A	211
	Appendix B	221
	Appendix C	239
	REFERENCES	253

LIST OF ILLUSTRATIONS

Figure		Page
1	Program Outline	3
2	Diagram of Interlaminar and Normal Stresses	11
3	Predicted Tension Stress-Strain Curves for Laminate 1, T300/934 $(0/45/90/-45/-45/90/45/0)_s$	13
4	Predicted Compression Stress-Strain Curves for Laminate 1, T300/934, $(0/45/90/-45/-45/90/45/0)_s$	14
5	Predicted Axial Strength for Laminate 2, T300/934, $(0/45/0_2/-45/0_2/45/0_2/-45/0)_s$	15
6	Coupon Geometry	21
7	Location of Thickness and Width Measurements	22
8	Disassembled View of Compression Testing Fixture with Example Test Coupon	30
9	Geometry of Compression Testing Fixture	31
10	Extensometer Attached to Specimen Edges	33
11	Extensometer Attached to Specimen Sides	33
12	Test Coupon with Side Tabs	34
13	Compression Fixture and Test Coupon with Strain Gages	34
14	Fatigue Grip	36
15	Tension-Tension Fatigue Test Showing Failed Laminate 1 Coupon	37
16	Tension-Compression Fatigue Test Showing Single Buckling Guide	37
17	Influence of Shape Parameter k on Probability of Survival	42
18	Ultrasonic C-Scan of Laminate 1 Panel 1MJ578	46
19	Ultrasonic C-Scan of Laminate 1 Panel 1MJ580	47
20	Ultrasonic C-Scan of Laminate 1 Panel 1MJ582	48
21	Ultrasonic C-Scan of Laminate 1 Panel 1MJ583	49
22	Ultrasonic C-Scan of Laminate 1 Panel 1MJ594	50
23	Ultrasonic C-Scan of Laminate 1 Panel 1MJ596	51
24	Ultrasonic C-Scan of Laminate 1 Panel 1MJ601	52

LIST OF ILLUSTRATIONS (Continued)

Figure		Page
25	Ultrasonic C-Scan of Laminate 1 Panel 1MJ603	53
26	Ultrasonic C-Scan of Laminate 1 Panel 1MJ604	54
27	Ultrasonic C-Scan of Laminate 1 Panel 1MJ606	55
28	Ultrasonic C-Scan of Laminate 1 Panel 1MJ693	56
29	Ultrasonic C-Scan of Laminate 2 Panel 1NH696	57
30	Ultrasonic C-Scan of Laminate 2 Panel 1NH699	58
31	Ultrasonic C-Scan of Laminate 2 Panel 1NH727	59
32	Ultrasonic C-Scan of Laminate 2 Panel 1NH728	60
33	Tension Stress-Strain Curve for Laminate 1 Coupon 1MJ603-6A	64
34	Tension Stress-Strain Curve for Laminate 2 Coupon 1NH699-27B	65
35	Representative Static Tension Failure Modes of Laminate 1 Coupons	66
36	Representative Static Tension Failure Modes of Laminate 2 Coupons	67
37	Laminate 2 Coupons which Failed in Static Tension with Failure Modes Dominated by 45° Plies	68
38	Comparison Between Predicted and Experimental Average Tension Stress-Strain Curves for Laminate 1	75
39	Comparison Between Predicted and Experimental Average Tension Stress-Strain Curves for Laminate 2	76
40	Probability of Survival Versus Ultimate Tension Strength for Laminate 1 Coupons	79
41	Probability of Survival Versus Ultimate Tension Strength for Laminate 2 Coupons	80
42	Compression Stress-Strain Curve for Laminate 1 Coupon 1MJ601-23B	85
43	Compression Stress-Strain Curve for Laminate 1 Coupon 1MJ580-1A	86
44	Compression Stress-Strain Curve for Laminate 2 Coupon 1NH699-14C	87
45	Laminate 1 Failed Coupons; Specimens, Numbered Left to Right, are: 603-26A, 596-2B, 601-17B, 601-5A	89

LIST OF ILLUSTRATIONS (Continued)

Figure		Page
46	Laminate 1 Failed Coupons; Specimens Numbered Top to Bottom, are: 601-5A, 601-17B, 596-2B, 603-26A	89
47	Laminate 2 Failed Coupons; Specimens Numbered Top to Bottom, are: 727-34A, 699-29C, 728-12B	90
48	Laminate 2 Failed Coupons; Specimens, Numbered Top to Bottom, are: 728-12B, 699-29C, 727-34A	90
49	Laminate 2 Failed Coupon; Specimen 728-10B	91
50	Comparison Between Predicted and Experimental Average Compression Stress-Strain Curves for Laminate 1	98
51	Comparison Between Predicted and Experimental Average Compression Stress-Strain Curves for Laminate 2	90
52	Relationship Between Probability of Survival and Ultimate Compression Strength for Laminate 1 Coupons	103
53	Relationship Between Probability of Survival and Ultimate Compression Strength for Laminate 2 Coupons	104
54	Typical Tension-Tension Laminate 1 Fatigue Failures	114
55	Typical Tension-Compression Laminate 1 Fatigue Failures	115
56	Typical Delaminated Laminate 2 Coupons Which Failed Under Tension-Tension Fatigue Loading	116
57	Typical Laminate 2 Coupons Which Failed Under Tension-Tension Fatigue Loading Without Significant Delamination	117
58	Laminate 2 Tension-Tension Fatigue Failures Dominated by 45° Plies	118
59	Laminate 2 Tension-Compression Fatigue Failures	119
60	Laminate 1 Tension-Tension Fatigue Stress-Life Scan Results at σ_{min} = 0.0 MPa (ksi)	120
61	Laminate 1 Tension-Compression Fatigue Stress-Life Scan Results at σ_{min} = -69 MPa (10.0 ksi)	121
62	Laminate 1 Tension-Compression Fatigue Stress-Life Scan Results at σ_{min} = -110 MPa (16.0 ksi)	122
63	Laminate 2 Fatigue Stress-Life Scan Results	123
64	Laminate 1 Fatigue Stress-Life Scan Results for σ_{max}	125
65	Laminate 1 Fatigue Stress-Life Scan Results for $\Delta\sigma$	126

LIST OF ILLUSTRATIONS (Continued)

Figure		Page
66	Laminate 1 Tension-Tension Fatigue Results at σ_{min} = 0.0 MPa (ksi)	128
67	Laminate 1 Tension-Compression Fatigue Test Results at σ_{min} = -110 MPa (16.0 ksi)	129
68	Linear Plot of Laminate 1 Tension-Tension Fatigue Results at σ_{min} = 0.0 MPa (ksi)	130
69	Linear Plot of Laminate 1 Tension-Compression Fatigue Results at σ_{min} = -110 MPa (16.0 ksi)	131
70	Combined Plot of Laminate 1 Fatigue Results	137
71	Laminate 2 Fatigue Results	138
72	Linear Plot of Laminate 2 Fatigue Results	139
73	Distribution of Laminate 2 Static Tension Strength Data	143
74	Typical Laminate 1 Static Tension Residual Strength Failure Modes	150
75	Typical Laminate 1 Static Compression Residual Strength Failure Modes	151
76	Typical Laminate 2 Static Tension Residual Strength Failure Modes	152
77	Typical Laminate 2 Static Compression Residual Strength Failure Modes	153
78	Theoretical Prediction of the Effect of Moisture on the Compression Strength of Laminate 2	156
79	Comparison Between Laminate 1 and 2 Tension-Tension Fatigue Results	159
80	Comparison Between Laminate 1 and 2 Tension-Tension Fatigue Results on the Basis of Normalized Stress	160
81	Probability of Failure for Laminate 1 Tension-Tension Fatigue Results at σ_{max} = 290 MPa (42.0 ksi)	169
82	Effect of Sample Size on the Number of Fatigue Cycles at Specific Probability of Survivals (Laminate 1 Data at 0 to 290 MPa (42 ksi))	171
83	Comparison Between Analytical Fit and Laminate 1 Static Tension Residual Strength Data for Specimens Prior Fatigue Tested at 0 to 345 MPa (50.0 ksi)	196

LIST OF ILLUSTRATIONS (Continued)

Figure		Page
84	Comparison Between Analytical Fit and Laminate 1 Static Tension Residual Strength Data for Specimens Prior Fatigue Tested at 0 to 290 MPa (42.0 ksi)	197
85	Residual Strength Degradation with Time for a Composite Material; Comparison Between Theory and Experiment (Figure Duplicates Figure 9 of Reference 24)	200
86	Residual Strength Degradation and Truncation with Time for a Bonded Joint; Comparison of Theory and Experiment (Figure Duplicates Figure 10 of Reference 24)	201
1A	Template for Laminate 1 Panels	215
2A	Template for Laminate 2 Panels	216
3A	Identification of Laminate 1 Panels and Coupon Locations	217
4A	Identification of Laminate 2 Panels and Coupon Locations	218
5A	Coupon Geometry	219
6A	Location of Thickness and Width Measurements	220

LIST OF TABLES

TABLE		Page
1	Typical Input Material Properties for Hybrid Computer Program	8
2	Free-Edge Stresses in Quasi-Isotropic Test Coupons	10
3	Free-Edge Stresses in Selected 67% 0° Fiber Laminate	17
4	Quality Assurance Testing Outline	18
5	Program Test Matrix	24
6	Resin, Fiber, and Void Analysis Results of Laminate 1 Panels	44
7	Resin, Fiber, and Void Analysis Results of Laminate 2 Panels	45
8A	Tension Test Results of Laminate 1 Coupons	69
8B	Tension Test Results of Laminate 1 Coupons	70
9A	Tension Test Results of Laminate 2 Coupons	71
9B	Tension Test Results of Laminate 2 Coupons	72
10	Summary of Static Tension Test Results	74
11	Summary of Static Tension Test Parameters	77
12	Relationship Between Probability of Survival and Ultimate Tension Strength	78
13A	Tensile Test Results for Panel 1NH693, Laminate 1	81
13B	Tensile Test Results for Panel 1NH693, Laminate 1	82
14	Tension Test Results Using Strain Gages	84
15A	Static Compression Test Results of Laminate 1 Coupons	93
15B	Static Compression Test Results of Laminate 1 Coupons	94
16A	Static Compression Test Results of Laminate 2 Coupons	95
16B	Static Compression Test Results of Laminate 2 Coupons	96
17	Comparison of Static Compression Test Results	97
18	Summary of Static Compression Test Parameters	101
19	Relationship Between Probability of Survival and Ultimate Compression Strength	102
20A	Effect of Test Detail on Compression Results of Laminate 1 Coupons	105

LIST OF TABLES (Continued)

TABLE		Page
20B	Effect of Test Detail on Compression Results of Laminate 1 Coupons	106
21	Compression Test Results Using Strain Gages	108
22	Test Results for Determination of Poisson's Ratio	109
23	Weibull Parameters and Estimates for Laminate 1 Fatigue Data	133
24	Weibull Parameters for Two Parameter Fit to Fatigue Data of Laminate 1 Coupons	134
25	Fatigue Lives at Various Probabilities of Survival for Laminate 1	135
26	Summary of First Cycle Fatigue Failures of Laminate 2	141
27	Number of Fatigue Cycles to Which Laminate 1 Residual Strength Coupons were Subjected	146
28	Summary of Residual Strength Tests for Laminate 1	147
29	Residual Strength Study for Laminate 1	149
30	Summary of Residual Strength Tests for Laminate 2	154
31	Summary of Expected and Observed Failure Rates at $P_{.90}$ for Laminate 1	164
32	Summary of Expected and Observed Failure Rates at $P_{.95}$ for Laminate 1	165
33	Summary of Expected and Observed Failure Rates for Laminate 1	168
34	Summary of Observed Damage Growth and Failure Modes	176
35	Predicted and Actual Probability of Survival Values at F_{max} = 345 MPa (50 ksi)	194
36	Predicted and Actual Probability of Survival Values at F_{max} = 290 MPa (42 ksi)	195
1B	Stress Life Scan Tension-Tension Fatigue Test Results of Laminate 1	222
2B	Stress Life Scan Tension-Compression Fatigue Test Results of Laminate 1	223
3B	Stress Life Scan Tension-Tension Fatigue Test Results of Laminate 2	224

LIST OF TABLES (Continued)

TABLE		Page
4B	Stress Life Scan Tension-Compression Fatigue Results of Laminate 2	225
5B	Tension-Tension Fatigue Results of Laminate 1 at a Maximum Stress of 25 ksi	226
6B	Tension-Tension Fatigue Results of Laminate 1 at a Maximum Stress of 33.5 ksi	227
7B	Tension-Tension Fatigue Results of Laminate 1 at a Maximum Stress of 42 ksi	228
8B	Tension-Tension Fatigue Results of Laminate 1 at a Maximum Stress of 50 ksi	229
9B	Tension-Tension Fatigue Results of Laminate 1 at a Maximum Stress of 58 ksi	230
10B	Tension-Compression Fatigue Results of Laminate 1 at a Maximum Stress of 26 ksi	231
11B	Tension-Compression Fatigue Results of Laminate 1 at a Maximum Stress of 42 ksi	232
12B	Tension-Compression Fatigue Results of Laminate 1 at a Maximum Stress of 50 ksi	233
13B	Tension-Compression Fatigue Results of Laminate 1 at a Maximum Stress of 58 ksi	234
14B	Tension-Tension Fatigue Results of Laminate 2 at a Maximum Stress of 100 ksi	235
15B	Tension-Tension Fatigue Results of Laminate 2 at a Maximum Stress of 112 ksi	236
16B	Tension-Compression Fatigue Results of Laminate 2 at a Maximum Stress of 70 ksi	237
1C	Residual Tension Strength Test Results of Laminate 1 Coupons Fatigue Tested at 0 to 42 ksi	240
2C	Residual Tension Strength Test Results of Laminate 1 Coupons Fatigue Tested at 0 to 50 ksi	241
3C	Residual Tension Strensth Test Results of Laminate 1 Coupons Fatigue tested at -16 to 42 ksi	242
4C	Residual Tension Strength Test Results of Laminate 1 Coupons Fatigue Tested at -16 to 50 ksi	243

LIST OF TABLES (Continued)

TABLE		Page
5C	Residual Compression Strength Test Results of Laminate 1 Coupons Fatigue Tested at 0 to 42 ksi	244
6C	Residual Compression Strength Test Results of Laminate 1 Coupons Fatigue Tested at 0 to 50 ksi	245
7C	Residual Compression Strength Test Results of Laminate 1 Coupons Fatigue Tested at -16 to 42 ksi	246
8C	Residual Compression Strength Test Results of Laminate 1 Coupons Fatigue Tested at -16 to 50 ksi	247
9C	Residual Tension Strength Test Results of Laminate 2 Coupons Fatigue Tested at 0 to 100 ksi	248
10C	Residual Tension Strength Test Results of Laminate 2 Coupons Fatigue Tested at -30 to + 70 ksi	249
11C	Residual Compression Strength Test Results of Laminate 2 Coupons Fatigue Tested at 0 to 100 ksi	250
12C	Residual Compression Strength Test Results of Laminate 2 Coupons Fatigue Tested at -30 to +70 ksi	251
13C	Compression Strength Test Results of Laminate 2 Coupons Tested in Oct., 1976	252

SECTION I

INTRODUCTION

The main objective of this research investigation was the experimental determination of the effect of compressive loading on the fatigue response of graphite/epoxy laminates. The primary emphasis of the program was on the accumulation of a statistically significant data base. The intention was to use the data base to develop an analytical model with predictive capability to account for the effect of compressive loading. The test program included only unnotched coupons in a room temperature, laboratory air environment.

The development of a large, statistically meaningful data base was accomplished. The general effect of compression on the fatigue response of a graphite/epoxy composite was determined. However, a general model with capability to account for compressive loading was not attempted. As an alternate, the concept of a fatigue threshold was postulated and the substantiating data presented. The decision to explore the possibility of a fatigue threshold was made after an extensive analysis of the data and after appraisal of the associated implications. The analysis showed that the large data scatter implied the necessity of using low fatigue stress levels to achieve the high probabilities of survival required for aircraft structures.

The program emphasis on the accumulation of a large data base was considered necessary for two reasons. First, only a large set of data from more than one laminate would allow correct resolution of the effect of compressive loading on the fatigue properties. Second, numerous replications were needed to determine the reliability of any analytical model. The latter reason for an extensive data base was extremely important and needs to be further elucidated.

In many design applications, such as "safe life" components, the cost and safety implications of a failure are so high that an acceptable probability of survival must be $P_{.99}$, $P_{.999}$, $P_{.9999}$ or, as in helicopter applications, even higher. Analytical models for predicting residual strength degradation or fatigue failures should be reliable to these probability of survival levels. Thus, the usefulness for aerospace design of residual strength and fatigue models must be judged in regards to their ability to reasonably estimate high probability of survival values.

The principal features of the sequential investigation are shown in Fig. 1. Phase 1 consisted of fabrication of unnotched specimens with as nearly consistent properties as practical. In Phase 2, initial static strength (including stress-strain curves) distributions were determined. Following this, Phase 3 established the general stress-life (S-N) behavior of the material for both tension-tension and tension-compression fatigue. The preliminary screening tests at several load levels were used to determine the general shape of the S-N curves and aid in selection of load levels at which statistically based fatigue life distributions were to be determined. Using this information, the number of cycles for each load level which would give the most useful information on the distribution of tension and compression residual strengths was determined in Phase 4, and residual strength fatigue tests conducted. Phases 1 to 4 were conducted first using a quasi-isotropic laminate and then using a 67% 0° fiber laminate.

Experimental results were analyzed and analytical models considered in Phase 5. Data analysis included estimation of Weibull parameters. Investigation of analytical models was primarily concerned with evaluation of the "wear-out" type of model where the specific rate-decay equation and limits of integration are selected based on data trends and physical evidence of mechanisms.

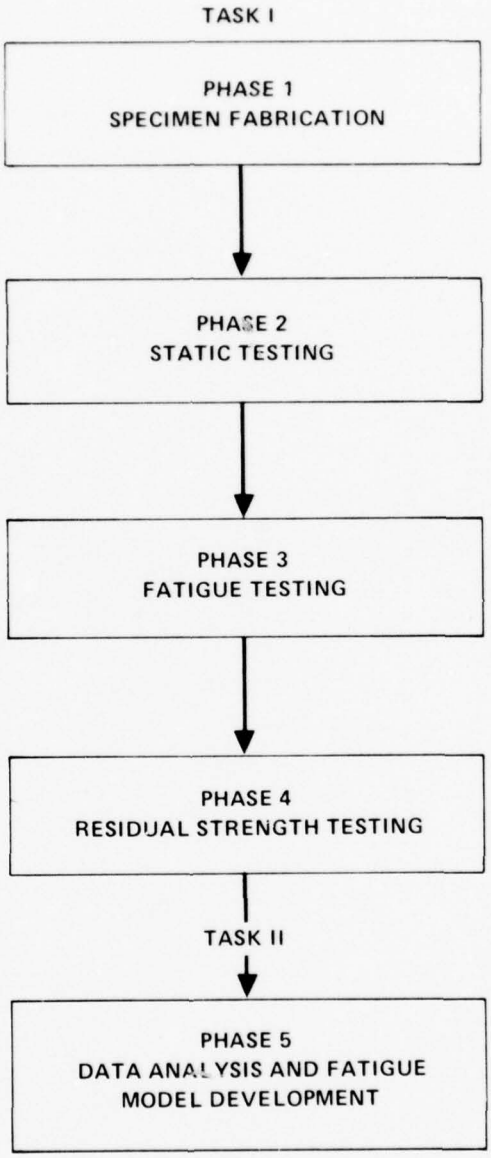


Figure 1. Program Outline

SECTION II

PROGRAM OVERVIEW

This research investigation emphasized the delineation of the effect of compressive loading on the fatigue behavior of graphite/epoxy laminates. This section presents a discussion of the rationale for material selection, program test matrix, and general test procedures.

2.1 Material Selection Background

The number of graphite material systems which have emerged in the recent history of advanced composites and which were viable for acceptance in this program were numerous. However, changes in system designation have been more a consequence of changes in the epoxy resin system than in the graphite fiber. An in-depth review of available graphite/epoxy systems led to the conclusion that the basic material selected for use on this program should consist of a low-cost, high strength graphite fiber such as the Hercules AS type or the Union Carbide Thornel 300. The matrix material was chosen as a 177°C (350°F) cure epoxy to be selected from one of the following: Hercules 3501, Narmco 5208, or Fiberite 934. The fiber/resin combinations considered for this program were Hercules' Magnamite (AS/3501), Narmco's Rigidite (T300/5208), Fiberite's HY-E-1034C (T300/934) and HY-E-1334C (AS/934).

The selected fiber/resin system was Fiberite system HY-E-1034C (Thornel T300 Fiber/Fiberite 934 Resin). Fiber/resin systems employing the AS fiber or 3501 resin were eliminated on the basis of limited data [1] which indicated that they had excessively wide property variations at the time of the inception of this program. The Narmco Rigidite (T300/5208) system was eliminated during discussions with the Air Force Program Manager.

2.2 Laminate Selection

Laminates for aircraft structures are typically selected for convenience from the $0_i/\pm45_j/90_k$ orientation family. The 0° direction is generally oriented parallel to the principal axial loading direction; $\pm45^\circ$ plies

Preceding Page BLANK

provide shear strength and stiffness or buckling resistance; and 90° plies provide additional strength in the transverse direction when required. The judicious addition of 90° plies to $(0_i/45_j)$ laminates reduces the Poisson's ratio, can be used to mitigate some of the free edge stresses, and can result in strength and stiffness benefits depending on the loading direction. However, the 90° plies may crack at a fraction of the ultimate tensile strength of the laminates complicating the fatigue phenomenon. Two laminates were chosen for the investigation: a quasi-isotropic, 25% 0° fiber laminate $(0/+45/90/-45_2/90/+45/0)_s$, and a 67% 0° fiber laminate $(0/+45/0_2/-45/0_2/+45/0_2/-45/0)_s$. The first laminate, designated 1, was chosen because of possible wide application and because the failure mode may be dominated by the matrix. The second laminate, designated 2, was chosen because the failure may be dominated by the fiber.

The selection of stacking sequences for the laminates considered the following:

(a) Mirror symmetry about the mid-plane was maintained to minimize warping or curling during manufacture or under load.

(b) Stacking order was considered because of the severe effects on the flexural stiffness and, consequently, the buckling behavior of the laminate. A wide column has a maximum buckling strength when the 0° plies are at or near the outer surface.

(c) For optimum load transfer the ply adjacent to a bonded joint was oriented with the fibers parallel to the direction of loading.

(d) Adjacent plies were oriented (when possible) to minimize the angle between adjacent plies. Studies [2] have shown microcracking can occur from curing stresses if adjacent plies are oriented at greater than 60°. The same rule applies to the transfer of interlaminar shear stresses [3]. While not normally affecting static strength, this can affect fatigue strength.

(e) The stacking sequence can cause interlaminar normal stresses to occur at the free edge of the laminate. Interlaminar tension stresses can cause delamination under both static and cyclic loading. The sign (tension or compression) of the normal stress depends both on the sign of the laminate in-plane loading and the stacking sequence. A given ply set can be stacked in such a way that maximum or minimum tension or compression, σ_z, can be obtained.

Obviously, simultaneous satisfaction of all the above criteria for a given structural element required compromises. Items (c) and (d) frequently conflicted with item (b), and the development of a stacking sequence that minimized interlaminar normal and shear stresses (item e) also conflicted with (b) and (c). Stacking the laminate so that the normal stresses are compressive is generally believed to increase the fatigue strength over that of a laminate with tensile normal stresses. However, cyclically applied loading with reversing direction results in reversal of the sign of the normal stress. Consequently, for the fatigue coupons of this program, which were subjected to compressive loading, laminae were stacked to minimize normal stresses over the entire range of loading and thus minimize their effects on fatigue strength.

A Lockheed computer program, SIGMZ, based on the method of Pagano and Pipes [4], was used to approximate the interlaminar stresses and aid in selecting optimum stacking sequences. Laminate ultimate strengths were calculated using a Lockheed program, HYBRID. Material property data for Fiberite's T300/934 graphite/epoxy unidirectional tape were taken from limited data made available from Lockheed Missiles and Space Company and adapted for use in Calac's "HYBRID" laminate characterization program. Where T300/934 test data were not available, the necessary information was estimated from data for AS/3002 graphite/epoxy in Reference [5]. These data are summarized in Table 1.

TABLE 1. TYPICAL INPUT MATERIAL PROPERTIES FOR HYBRID COMPUTER PROGRAM

		Direction, Type of Property	Symbol	Units	Material T300/934 GR/EP[a] Average Properties at RT, ΔT = 111°C (200°F)
Extensional Moduli		L, Initial Tensile	EA1(m,1,1)	GPa(psi x 10^6)	150.3 (21.8)
		L, Initial Compres.	EA1(m,1,2)		151.0 (21.9)
		L, Second Tensile	EA1(m,2,1)		150.3 (21.8)
		L, Second Compres.	EA1(m,2,2)		68.0 (9.87)
		T, Initial Tensile	EB1(m,1,1)	GPa(psi x 10^6)	9.65 (1.40)
		T, Initial Compres.	EB1(m,1,2)		10.96 (1.59)
		T, Second Tensile	EB1(m,2,1)		9.65 (1.40)
		T, Second Compres.	EB1(m,2,2)		8.67 (1.285)
Shear Mod.		LT, Initial Shear	G1(m,1)	GPa(psi x 10^6)	5.17 (0.750)[b]
		LT, Second Shear	G1(m,2)		2.21 (0.320)[b]
		LT, Major Poisson's	MUAB(m)		.21[b]
Therm Exp.		L, Coef. of Exp.	ALA(m,1)	mm/mm/°C (in./in./°F) x10^6	0.97 (0.54)
		T, Coef. of Exp.	ALA(m,2)		30.4 (16.9)
Strains	Tensile	L, Yield Tensile	EPT(m,1,1)	10^{-3}mm/mm	10.7
		T, Yield Tensile	EPT(m,1,2)		4.5
		L, Ultimate Tensile	EPT(m,2,1)		10.7
		T, Ultimate Tensile	EPT(m,2,2)		4.5
	Compr.	L, Yield Compr.	EPC(m,1,1)	10^{-3}mm/mm	7.0
		T, Yield Compr.	EPC(m,1,2)		11.0
		L, Ultimate Compr.	EPC(m,2,1)		9.3
		T, Ultimate Compr.	EPC(m,2,2)		17.0
	Shear	LT, Yield Shear	EPS(m,1)	10^{-3}mm/mm	10.0[b]
		LT, Ultimate Shear	EPS(m,2)		18.0[b]
Auxiliary Data		Fiber Volume			65%
		Density		kg/m^3(lbs/$in.^3$)	157.2 (0.057)
		Ply Thickness		mm(in.)	0.142(.0056)

a - Based on Average of Data from Lockheed Missiles & Space Co. Normalized at 65%

b - Est. from AS/3002 Data

From "HYBRID" the respective Y direction stresses for the 0°, ± 45°, and 90° plies of the quasi-isotropic laminate were determined at σ_x = 84.1 MPa (12.2 ksi). These stresses were used in the "SIGMZ" computer program to calculate free edge stresses. The "SIGMZ" program simply calculated the σ_z and τ_{zy} stresses by the approximation method of Pagano and Pipes [6]. The laminates investigated included:

$$(0/45/90/-45/-45/90/45/0)_s$$
$$(45/90/-45/90/-45/0/45/0)_s$$
$$(0/45/90/-45/90/-45/0/45)_s$$
$$(90/45/-45/0/-45/90/45/0)_s$$
$$(90/45/-45/90/-45/45/0/0)_s$$
$$(0/45/90/-45/90/-45/45/0)_s$$

Of these, the first two had the lowest normal tension and shear stresses and were chosen as primary and alternate quasi-isotropic laminates. Results are summarized in Table 2. Figure 2 shows a diagram of the stresses.

An examination of the maximum interlaminar and normal shear stresses demonstrated the fact that separating the +45° ply from the -45° ply by a 90° ply always reduced the interlaminar normal stresses compared to laminates that had the +45° and -45° plies adjacent. This was due to the fact that the σ_y in the 90° ply was almost balanced by the sum of the σ_y stresses in the +45° and -45° plies analogous to a beam with multiple supports and multiple loads. The minimum bending moment in the beam was obtained by locating the reactions as close as possible to the applied loads. The interlaminar shear strength was greater between plies that were 45° apart than between plies that were 90° apart. This fact together with reduced interlaminar normal stresses justified the separation of +45° and -45° plies by a 90° ply.

The laminates used in this program were, of course, stressed beyond the point of transverse cracking during cyclic loading. This altered the stress distribution, and another stacking sequence than that chosen may in fact be optimum. However, based on linear behavior to σ_x = 84.1 MPa (12.2 ksi), the laminate

TABLE 2. FREE-EDGE STRESSES IN QUASI-ISOTROPIC TEST COUPONS

	Primary Specimen $(0/45/90/-45/-45/90/45/0)_s$				Alternate Specimen $(45/90/-45/90/-45/0/45/0)_s$			
	Tension		Compression		Tension		Compression	
σ_x [a] MPa(ksi)	84.1(12.2)		-84.1(12.2)		-84.1(12.2)		-84.1(12.2)	
ΔT, °C (°F)	0 (0)	111 (200)	0 (0)	111 (200)	0 (0)	111 (200)	0 (0)	111 (200)
σ_y^0, MPa(psi)	1.43 (-208)	27.3 (3960)	1.33 (193)	9.94 (1442)	1.43 (-208)	27.3 (3960)	1.33 (193)	9.94 (1442)
σ_y^{45}, MPa(psi)	32.3 (4985)	34.4 (4985)	-32.2 (-4669)	-32.8 (-4754)	32.3 (4686)	34.4 (4985)	-32.2 (-4669)	-32.8 (-4754)
σ_y^{90}, MPa(psi)	-63.2 (-9174)	-94.4 (-13700)	63.1 (9150)	53.7 (7794)	-63.2 (-9174)	-94.4 (-13700)	63.1 (9150)	53.7 (7794)
σ_z^{max}, MPa(psi)	.32 (46)	1.70 (246)	.006 (9)	.38 (55)	.38 (55)	.39 (56)	2.67 (387)	.89 (129)
σ_z^{min}, MPa(psi)	-.069 (-10)	.28 (41)	-.32 (-46)	-.34 (-49)	-2.66 (-386)	-7.58 (-1100)	-.37 (-54)	-.50 (-73)

a - σ = 84.1 MPa(12.2 ksi) is the limiting stress for first ply failure, σ_{90}^{tu}, when ΔT is is assumed to be 111°C (200°F)

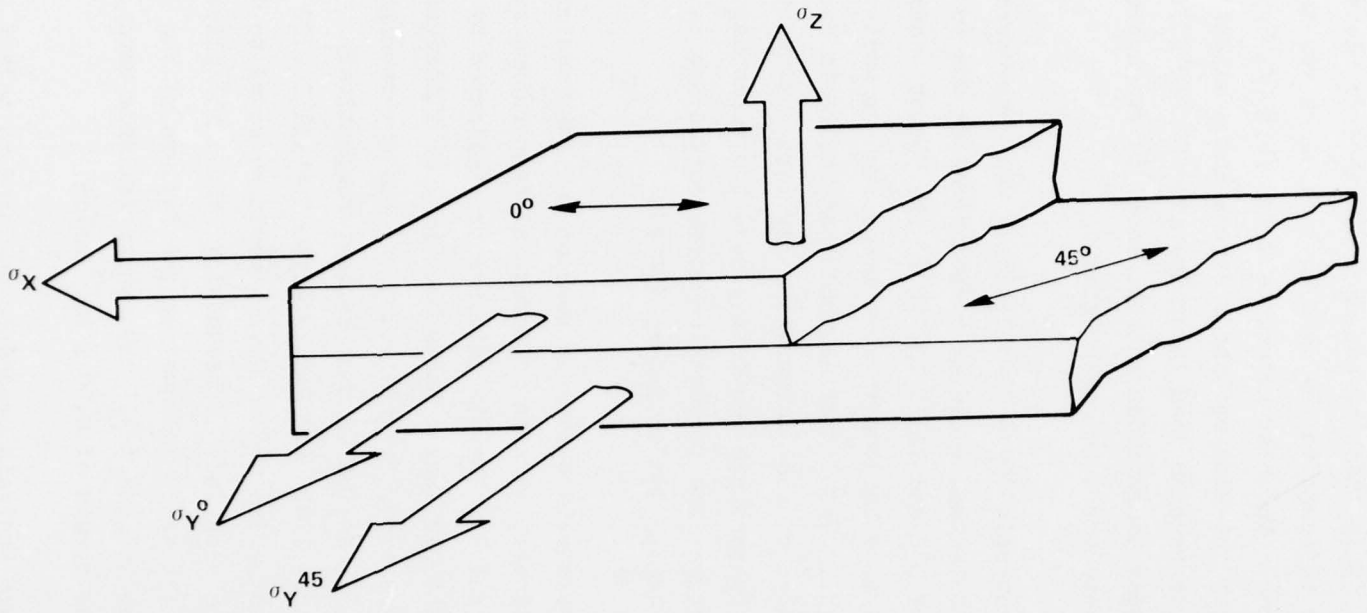


Figure 2. Diagram of Interlaminar and Normal Stresses

with the lowest σ_z, $(0/45/90/-45/-45/90/45/0)_s$, was selected as the quasi-isotropic laminate. This stacking sequence had the additional advantage of having the 0° plies adjacent to the loading tabs which was assumed to aid in reducing tab failures. The best alternate layup $(45/90/-45/90/-45/0/45/0)_s$ had a predicted lower interlaminar shear stress and a slightly higher normal stress during the compression load (assuming ΔT = 0°C (0°F)). Note that the interlaminar shear computation in Reference [6] was approximate and does not accurately reflect the true stress state.

The chosen quasi-isotropic $(0/\pm45/90)$ laminate was characterized in tension and compression with thermal residual curing stresses due to differential temperatures, ΔT, of 0°C and 111°C (200°F). The former assumed that the residual stress was ammeliorated by some means such as post-curing, and represented an upper bound. The latter assumed that the resin hardens near 149°C (300°F) and was cooled to room temperature for test. Since the computations were based on room temperature properties, and the resin has reduced properties at elevated temperature, the temperature differential was taken as 111°C (200°F) instead of 146 to 173°C (230 to 280°F).

The resultant stress-strain curves in tension and compression for the selected quasi-isotropic laminate, at both differential temperature extremes, are shown in Figures 3 and 4. The ply failures are indicated by symbols. The numeral indicates the ply angle; the subscript L or T indicates fiber direction, longitudinal or transverse, respectively; and the superscripts, tu or cu, indicate failure modes, tension or compression, respectively. The 90° ply was expected to fail at 84.1 MPa (12.2 ksi) with ΔT = 111°C (200°F). Note that if ΔT was assumed to be 156°C (280°F), σ_x would be equal to 14.1 MPa (2.04 ksi) when 90° ply failure occurred. Subsequently, the $\pm$ 45° plies were expected to fail at 221 MPa (32 ksi), followed by the failure of the laminate at 536 MPa (77.7 ksi). The 90° and $\pm$ 45° ply matrix failures were predicted on an allowable transverse strain of 4.50×10^{-6} mm/mm.

Essentially, the same analysis procedure was used to select the 67% 0° fiber laminate. Figure 5 shows the predicted axial strength of the 67% 0° fiber

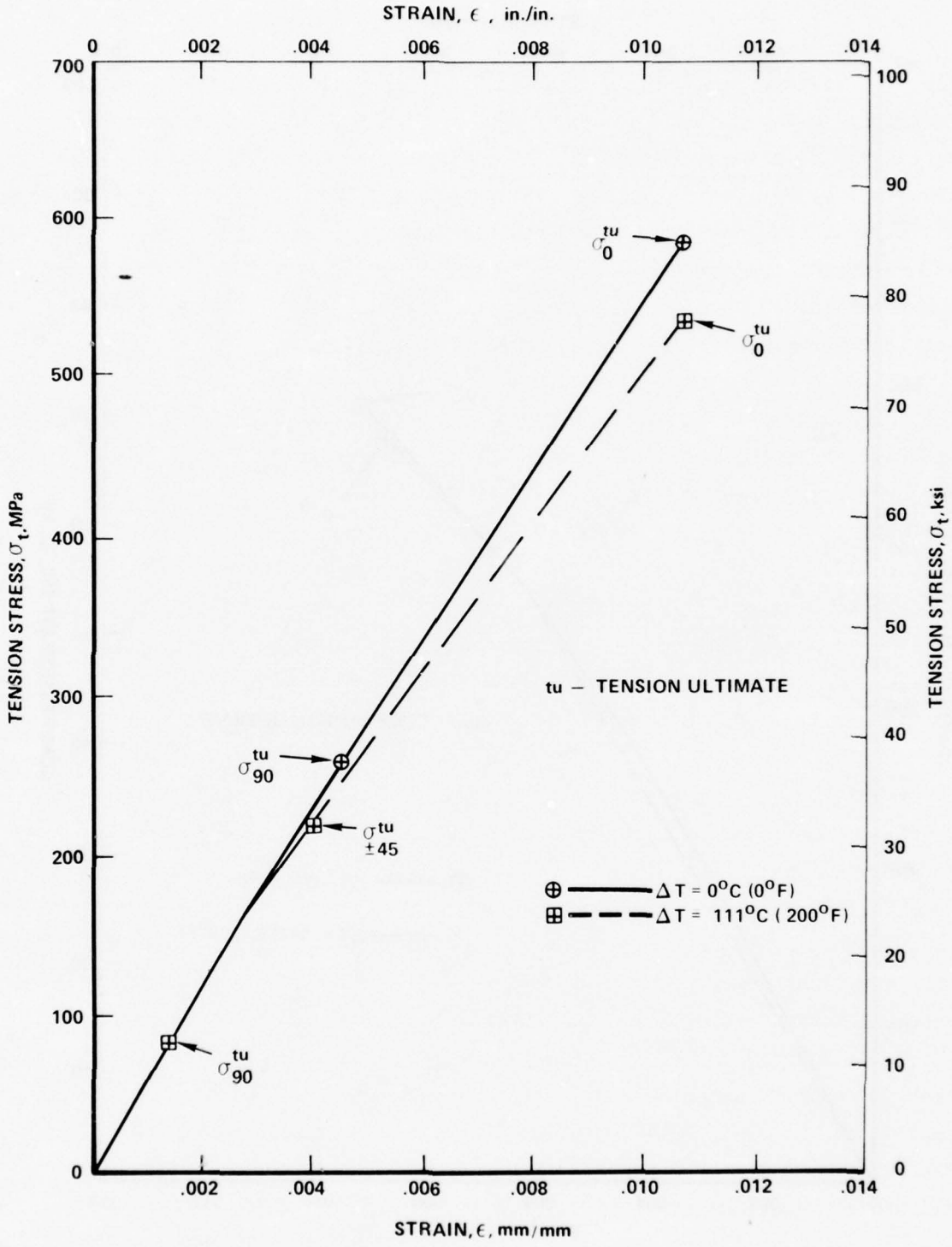


Figure 3. Predicted Tension Stress-Strain Curves for Laminate 1, T300/934, $(0/45/90/-45/-45/90/45/0)_s$

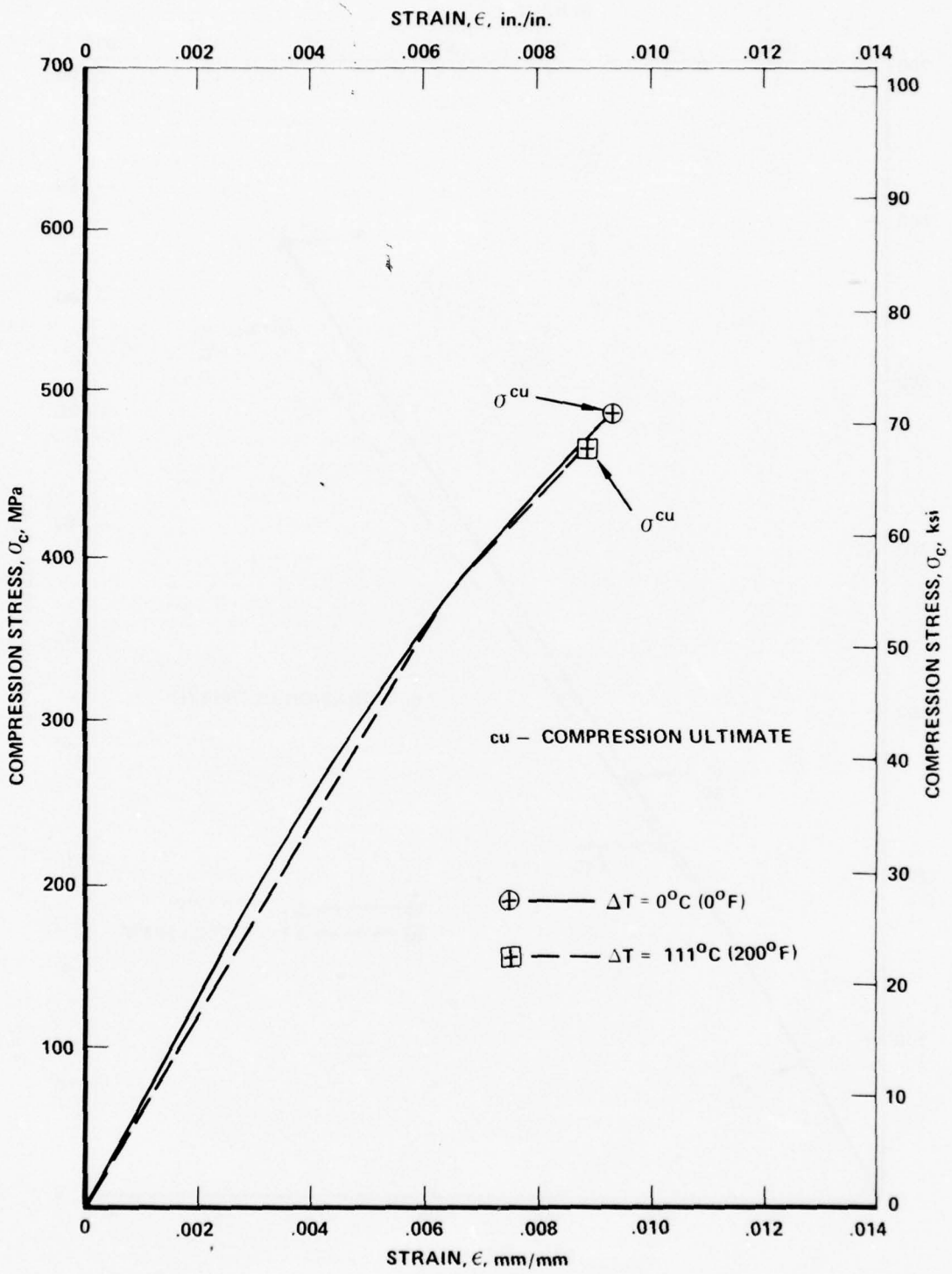


Figure 4. Predicted Compression Stress-Strain Curves for Laminate 1, T300/934, $(0/45/90/-45/-45/90/45/0)_s$

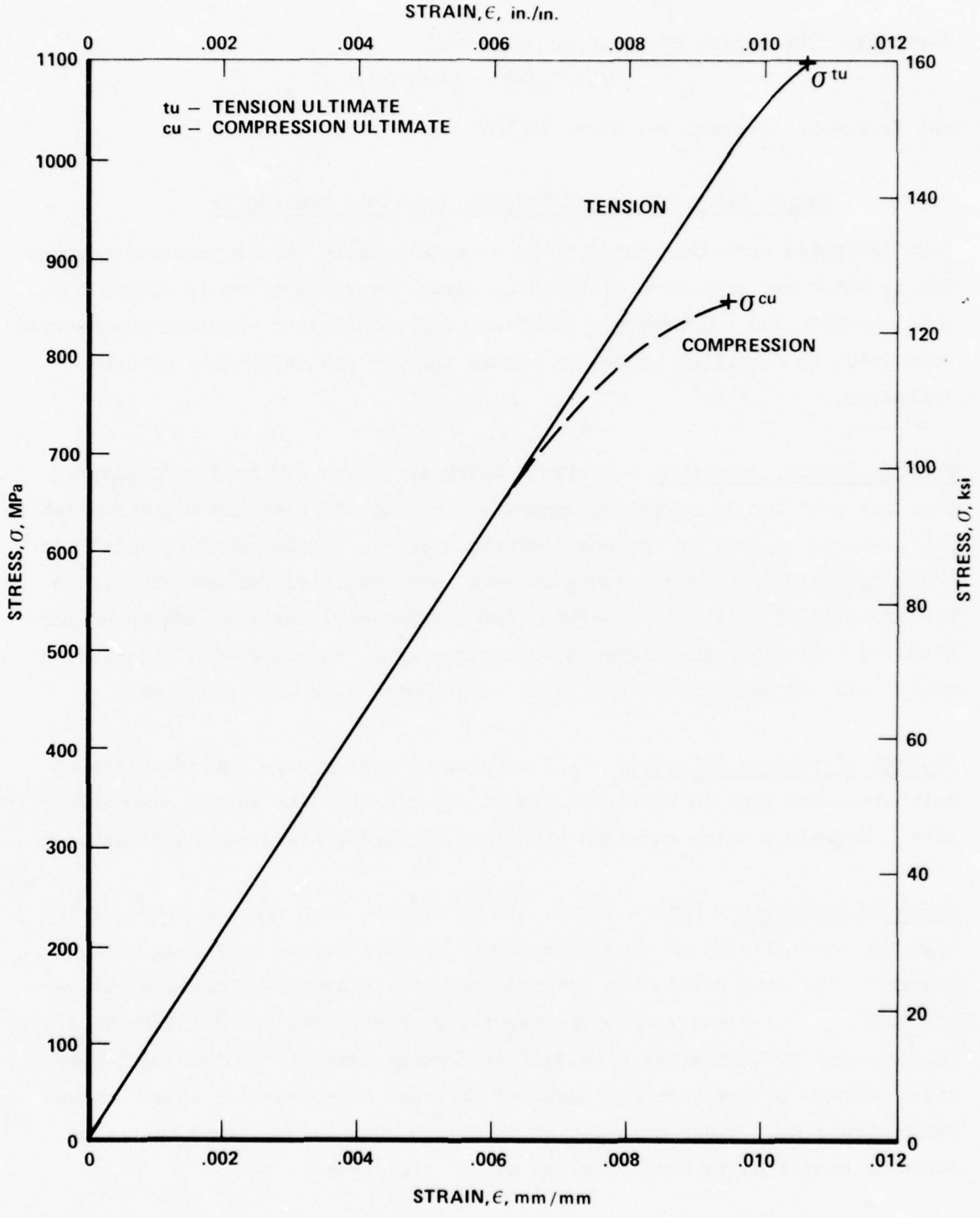


Figure 5. Predicted Axial Strength for Laminate 2, T300/934, $(0/45/0_2/-45/0_2/45/0_2/-45/0)_s$

laminate. The chosen stacking sequence was:

$$(0/45/0_2/-45/0_2/45/0_2/-45/0)_s$$

and free-edge stresses are given in Table 3.

2.3 Coupon Fabrication and Quality Assurance Procedures

Test laminates were fabricated in an autoclave using vacuum pressure augmented by autoclave pressure. Table 4 outlines the steps taken to assure test panel quality and uniformity. Manufacturing and quality assurance procedures were used, as described below, to ensure quality and uniformity of test laminates.

Prepreg Quality Assurance - A single batch of 305 mm (12 in.) wide prepreg tape was used for 10 of the 11 laminate 1 panels and a second batch for laminate 2 panels as well as for one laminate 1 panel. Resin content, volatiles content, and flow of the prepreg batches were inspected for conformance to specified tolerances upon receipt. Prepreg material was also inspected for flaws such as fiber misalignment, breakage, gaps, excess resin, and starved areas, and any portions of the batch with these flaws were rejected.

Storage of Prepreg Materials - All prepreg materials were stored in sealed moisture-proof bags in refrigerators at -17.8°C (0°F) to assure adequate shelf-life. Materials which exceeded specified storage periods were not used.

Layup of Laminates - Before layup, all materials, when removed from refrigerators, were allowed to come to room temperature before unsealing bags to prevent water condensation on prepreg surfaces. Layup of laminates was performed in a semi-clean room with temperature controlled to 21 ± 2°C (70 ± 5°F). This reduced contamination with dust or foreign matter. Controlled temperature assured proper tack and drape of prepregs and prevented water condensation problems. Fiber orientation in a layup was accomplished by use of suitable templates to meet required angle tolerances.

Curing of Laminates - The use of autoclave curing techniques permitted close control of pressure and temperature parameters. The autoclave incorporated

TABLE 3

FREE-EDGE STRESSES IN SELECTED 67% 0° FIBER LAMINATE

	Specimen B $(0/45/0_2/-45/0_2/45/0_2/-45/0)_s$			
	Tension		Compression	
[a] σ_x, MPa(ksi)	538 (78)		-538 (-78)	
ΔT, $^{\circ}C$ ($^{\circ}F$)	0 (0)	111 (200)	0 (0)	111 (200)
σ_y^{0}, MPa(psi)	-32.1 (-4660)	-6.55(-950)	22.2(3220)	33.0(4790)
σ_y^{45}, MPa(psi)	64.2 (9320)	13.2 (1910)	-44.4(-6440)	-66.0(-9580)
σ_z^{min}, MPa(psi)	-0.34(-50)	-0.07 (-10)	0	0
σ_x^{max}, MPa(psi)	0	0	.28(40)	.34(50)

a - σ_x is 2/3 of Ultimate Strength

TABLE 4. QUALITY ASSURANCE TESTING OUTLINE

Material Form	Test
Prepreg (receiving inspection)	- Visual examination (fiber uniformity, fiber alignment - Volatiles content - Uncured resin content - Control of shelf life
Layup (prior to cure)	- Visual examination of excess section for proper orientation of each ply
Curing	- Automated autoclave programming for control of cure parameters - Permanent records of cure temperature and pressure maintained for each autoclave run
Cured Laminates	- Visual examination (resin starvation, fiber wash-out, pinholes, etc.) - Thickness per ply - Cured resin content - Density - Void content (calculated) - Examination of cross-section under magnification - Nondestructive inspection of each test laminate by ultrasonic "C" scan

automatic programming instrumentation to control heating rates and dwell times. In the autoclave, pressure was not dependent upon tool or platen quality. These factors minimized the variations between separate cure operations. Test laminate fabrication required more than one autoclave cycle, but close controls reduced the possibility of significant test panel variations.

Bleeding was accomplished by use of a perforated releasable membrane placed in contact with the laminates and backed up with an absorbent material. This permitted escape of air and volatiles as well as bleeding of resin to reduce resin content of the laminates to specified levels. Pressure bags of suitable heat resistant plastic film were sealed in place over the layup.

An optimum cure cycle was developed prior to test laminate fabrication, see Appendix A. The proper combination of factors such as heat-up rate, dwell, venting, and time of pressure application were determined. This helped to ensure proper release of volatiles, resin flow, and wetting to minimize voids and porosity and provide maximum resin compaction and adhesion to fibers.

Prior to cure, an excess section of the layup was examined to ensure proper filament orientation in each ply. During the cure cycle, a complete permanent record was maintained of temperature, vacuum pressure, and autoclave pressure. This record included heat-up rates and times of pressure application and release.

Two throw-away panels of laminate 1 were fabricated and used to ensure the uniformity of the autoclave temperature cycle. Nine thermocouples were distributed at various places in the laminate, on the caul plates, and in the bleeder papers. Laminate temperatures varied ± 1.7°C (± 3°F) during heat-up and cool-down cycles and ± 1/2°C (± 1°F) during cure cycles.

Test laminates were visually examined for defects such as resin starvation, fiber wash-out, pinholes, voids, etc. Thickness per ply, cured resin content, and density were determined. These properties were used to estimate the void content from 25.4 mm (1.0 in.) wide strip in the middle of each panel,

perpendicular to the 0° fiber direction. Void content was determined according to ASTM D2734-70. This procedure requires accurate values for the density of fiber and neat resin. Unfortunately these values are not usually known accurately. An excess section of each laminate was sectioned and examined under magnification for voids and other defects on the surface and cut edges. All panels were fabricated such that a 25.4 mm (1.0 in.) wide edge could be trimmed off on all sides.

Each test laminate panel was nondestructively inspected by ultrasonic "C" scan procedure for voids, delaminations and other defects. One NDI standard reference panel for laminate 1 panels was fabricated identical to panels to be used in the test program except that 0.05 mm (0.002 in.) thick Teflon film pads of 3.2 to 12.7 mm (1/8 to 1/2 in.) diameter were placed at eight locations in the upper and lower halves of the standard panel. This panel was used as a standard for the NDI-C scan inspection of the laminate 1 test panels. For laminate 2 panels, three Teflon 0.05 mm (0.002 in.) thick film pads 3.2 to 12.7 mm (1/8 to 1/2 in.) diameter were placed in the corner of each fabricated test panel.

The panel and coupon fabrication procedure used in this program is attached to this report as Appendix A. For laminate 1, ten panels were fabricated of approximate dimensions, 610 x 660 mm (24 x 26 in.) and one panel of approximately 965 x 1372 mm (38 x 54 in.) dimensions. For laminate 2, four panels were fabricated of approximate dimensions, 965 x 1372 mm (38 x 54 in.). Coupon dimensions are shown in Figure 6 for laminate 1. Coupons for laminate 2 were identical except that the tabs were 40.8 mm (2 in.) long. For all tests, coupons were fabricated and machined identically so that any scatter in test results could not be attributed to variations in coupon fabrication procedures or geometry.

After fabrication and prior to testing, the thickness of all coupons was measured in eight places and the width in four places (see Figure 7 for these locations). The width of any one coupon varied at most ± 0.0127 mm (± 0.0005 in.) (± 0.06%) within the gage length. The width of all coupons varied by less than ± 0.10 mm (± 0.004 in.) within the gage lengths. The area of any one coupon was found to vary by less than ± 1.5% and that of all coupons by less than ± 4% within the gage length.

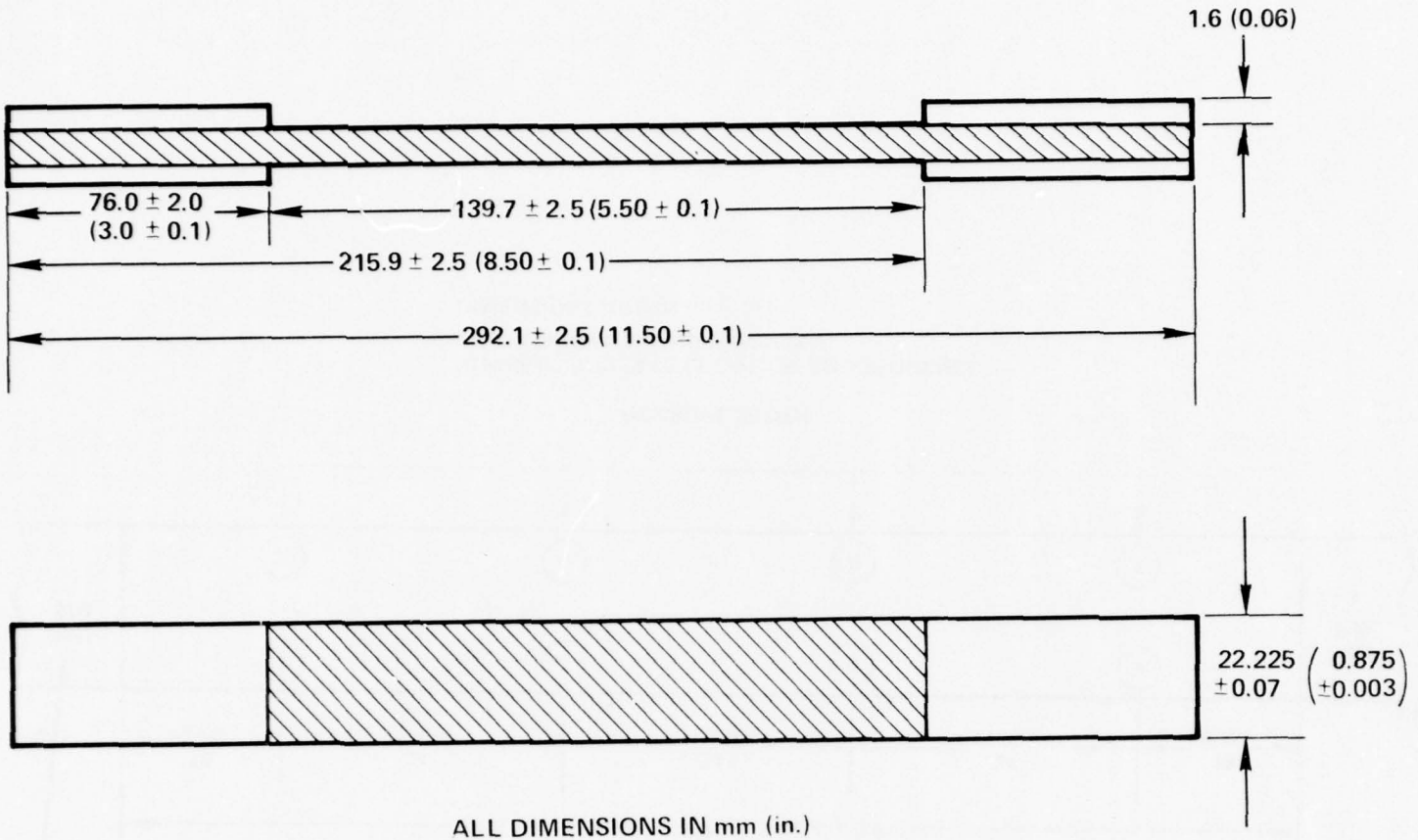


Figure 6. Coupon Geometry

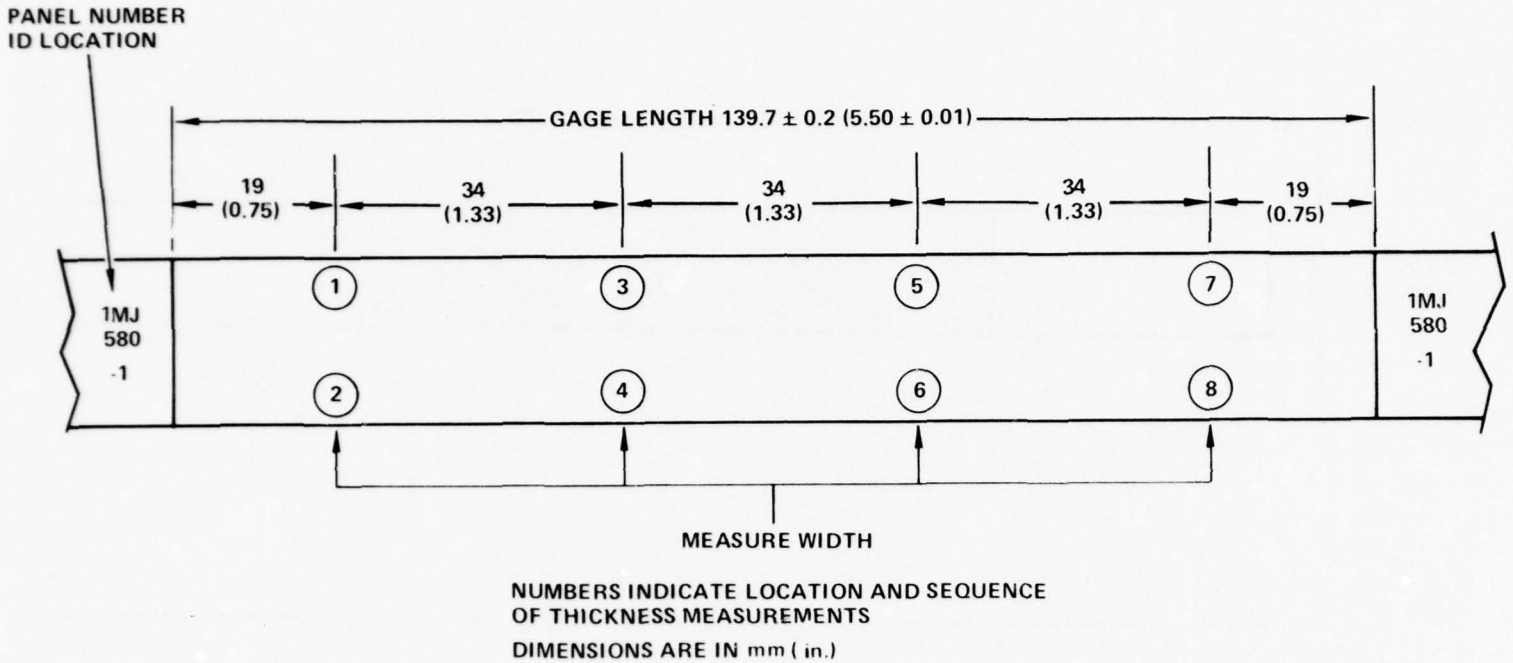
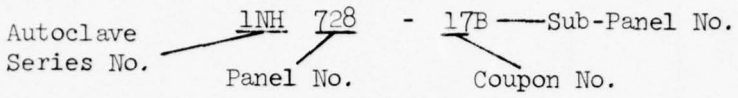


Figure 7. Location of Thickness and Width Measurements

All coupons were identified by the following system.



Autoclave and panel numbers are consecutive at Lockheed and are an internal reference number unique to each panel. The test panels were cut into 3 or 5 sub-panels, depending on whether the panel was laminate 1 or 2, and numbered from the top as A, B, C, D, or E. This system of coupon identification allowed for traceability of each coupon to previous panel location and of each panel to fabrication history.

2.4 Program Test Matrix

The test program matrix is given in Table 5. Tests were divided into three groups: static tension and compression tests, fatigue tests, and residual strength tests. For each testing condition (combination of load level or test type and laminate configuration), 25 specimens were originally intended to be tested. However, this was subsequently reduced to 20 coupons per test condition. All three types of testing included both laminate orientations.

All coupons were conditioned for at least 72 hours at 22 ± 1°C (72 ± 2°F) and 40 ± 10% RH in an environmental chamber prior to testing. All coupons were tested at 22 ± 1°C (72 ± 2°F) and 40 ± 10% RH and remained in the environmental chamber up until testing and returned to the chamber after testing.

Since a primary objective of this study was to establish a firm statistical basis for all test results, a random sampling procedure was written and encoded into computer software. Essentially, this program chose the order in which each sample was to be tested in a double-blind random manner.

The number of randomly selected coupons to be tested per condition was chosen to adequately insure a large enough data set for obtaining statistically meaningful and reliable distributions of fatigue life and static residual

TABLE 5. PROGRAM TEST MATRIX

Testing Category	Test Type	No. of Laminate Orientations	Minimum No. of Load Levels		Minimum No. of Coupons per Test Condition		Total No. of Data Points
			Lam 1	Lam 2	Lam 1	Lam 2	
Static	T	2	-	-	25	20	45
	C	2	-	-	25	40[a]	65
Fatigue							
T-T	S-N Curve	2	6	4	3	3	30
	Fatigue Scatter	2	5	2	20	20	107
C-T	S-N Curve	2	12	4	3	3	48
	Fatigue Scatter	2	4	1	20	20	125
Residual Strength							
T-T	T	2	4	1	20	20	60
	C	2	2	1	20	20	60
C-T	T	2	2	1	20	20	60
	C	2	2	1	20	20	60

a- laminate 2 tests repeated

strength. The number of test points at any particular condition needed to insure adequate statistical confidence (at least 90% and preferably 95% or better) depends upon the dispersion of the data. The particular distribution function, binomial, Poisson, multinomial, normal, Weibull or other chosen to represent data dispersion also affects the confidence that can be applied to the same data set. The two most common distributions in fatigue are normal [7] $Y = \frac{1}{\sigma\sqrt{2\pi}} e^{-\frac{1}{2}(x - \mu)^2/\sigma^2}$, where μ is the mean and σ the standard deviation, and Weibull [8] , $P(x) = \exp\left[-((x-e)/(v-e))^k\right]$, where e, v, and k are constants. With these thoughts in mind, the number of test specimens at each test condition required for acceptable confidence of the data dispersion and probability of survival of any one coupon was considered.

In essence, this problem of coupon sampling size is more a question of the probability of survival for each coupon under the test conditions specified than one of setting the confidence levels for the data dispersion. This conclusion results from the fact that one wants to be able to state the probability of survival of the test coupon or structural component before testing or vehicle use. Essentially, there are only few options [9] available for obtaining probability of survival and, hence, specimen sample size:

(1) Have available sufficient data for the particular material and test condition of concern.

(2) Adopt, in the case of a Weibull distribution assumption, the Weibull parameters obtained from a similar material where test results are available.

(3) Assume $e = 0$, or arbitrarily use the median S-N curve or median value of a strength distribution of a similar material as a characteristic value curve or value, assign a shape factor k and calculate:

$$x = v\left[- \log_e P(x) \right]^{1/k}$$

(4) Arbitrate a specific percent probability of survival curve or value by means of a factor such as $x_{.99}/x_{.50} \simeq 0.3$.

A combination of procedures 2 and 3, the most applicable in this case, led to the selection of a minimum sample size of 20.

The static tension and compression stress-strain curves, ultimate strength, and apparent modulus of elasticity were determined for each of the two laminate orientations. For constant amplitude fatigue (at 10 Hz), approximate tension-tension and tension-compression S-N curves were obtained for both laminates using three specimens at each of several load levels. Coupons were cycled to failure or to 10^6 cycles, defined as run-out, although many coupons were cycled longer. Based on the results of the approximate S-N curves, load levels were chosen from each S-N curve for study of data scatter under tension-tension and tension-compression fatigue testing. At each of the load levels, at least 20 specimens were cycled either to failure or to at least 10^6 cycles. This data supplied the necessary basis needed for a sound statistical analysis of the data.

The tension and compression residual strengths of specimens tested in tension-tension and tension-compression fatigue were determined. For each of the load levels selected, the number of cycles to be applied prior to residual strength testing was selected so that the chance of failing the specimens at the applied stress level was not large and yet the group of specimens was fatigue cycled long enough such that any significant change in strength and/or stiffness could be detected. For laminate 1, the number of cycles was selected equivalent to the life where 90% of the coupons could be expected to have survived as estimated from the prior data obtained to develop the fatigue life behavior. For laminate 2, the number of cycles was chosen as 10^6 cycles of fatigue loading. For each group of specimens, half were static tested in tension and the other half in compression. Stress-strain curves, ultimate strength, and apparent modulus of elasticity were recorded.

2.5 Testing Procedures

For both static tension and compression tests, load and deflection were continuously read out on an X-Y recorder so that stress-strain curves could be constructed. Ultimate strength, strain to failure, and the apparent modulus of elasticity were calculated. For laminate 1 coupons, stress was calculated using the minimum area because a previous Lockheed internally funded program indicated that the failure location might be the minimum area point. However, these coupons varied less than ± 1.5% in area within a coupon and no significant correlation of failure location to minimum area was observed. If the average area had been used for laminate 1 coupons, the calculated stress would have decreased by, at most, 1.5%. For laminate 2, the average area based on four locations equally spaced within the gage length was used to calculate stress.

2.5.1 Static Tension Test Procedures

Static tension tests were conducted in a 534 kN (120 kip) Baldwin static test machine. All testing was conducted similar to the procedures of ASTM D3039-74. Tests of laminate 1 coupons were conducted using modified fatigue grips while in tests of laminate 2 coupons, MTS hydraulic self-aligning grips were used. Alignment in the modified fatigue grips was ensured by a precise fixture, mounted within the grip, against which coupons were placed. For hydraulic grips, a special alignment fixture was constructed exterior to the grip assembly. Because coupon width varied only within ± 0.025 mm (± 0.001 in.), the alignment procedure assured end-to-end coupon alignment within ± 0.076 mm (± 0.003 in.). A 50.8 mm (2 in.) extensometer was used to record deflection. Testing was conducted at standard rates between 0.001 and 0.002 mm/mm/min.

2.5.2 Static Compression Test Procedures

Because, at present, there are no generally accepted testing standards for obtaining the ultimate compression strength of a composite laminate, the rationale and procedures used in this program will be discussed in detail. An advanced composite design guide document [10] prepared by Rockwell International Corporation discussed recommended test procedures for applications of the United States Air Force. Other test procedures have been proposed

and are presently used by various corporations and United States Government agencies [11-16]. Recently, a test method was issued by ASTM [17].

Essentially, there are two types of compression testing procedures that have been developed for composites, end loaded [11-13] and sandwich beams [14-16]. These two different types of procedures have been developed because of the numerous possible compression failure modes which exist for composites. Each mode may have a different ultimate strength. With any particular procedure, failure will occur at the lowest possible strength and in the corresponding failure mode. The range of possible failure strengths implies that the ultimate compressive strength of a composite laminate is not a precise term, but, is primarily one of definition.

For end loaded specimens, the two primary modes of failure are column buckling and shear crippling [10]. In filamentary composites, basic material failures are defined as filament fracture, failure of matrix stabilization, matrix failure, or dominant layer instability. Normally, failure loads corresponding to these failure modes are high and thus in practical design applications, column buckling may be the most important failure mode [10] .

Results of compression tests using end loaded coupons may be affected by end buckling, brooming, or splitting [10] . To obtain valid results, precise alignment was required. Since the test specimen beared on a plate, concern arose as to the extent of lateral restraining stresses acting on the coupon end due to Poisson's effect. This problem of end restraint due to Poisson's effect is, of course, not unique to composites, but is also a problem in compression testing of metallic specimens where, for example, the phenomenon of "barreling" occurs for cylindrical coupons.

In the region between the coupon end and the section where the unrestrained width is no longer affected, lateral compressive and shear loads are induced [10] . In this region, edge filaments can assume a curved shape causing a reduction in load carrying capacity. This region can be somewhat stabilized

by adding end guides or casting the ends in a suitable end block. Such procedures also help end brooming or splitting [10] . However, even if careful precautions against this problem are employed, the restraint problem and corresponding failure zone would most likely shift to a region further from the coupon end. Failure zones would then occur closer to the center of the gage section resulting in a supposedly more "valid" test, but, failure loads would not necessarily be higher and test validity would not necessarily be enhanced.

A final problem to consider in end loading of composites is termed progressive crushing failure [10] . This problem is due to the slight uneven length of the fiber ends caused by machining practice. These uneven lengths may cause only a few fibers to be loaded at first resulting in their local fracture succeeded by continuing local fracture of subsequently loaded fibers.

For this research study, an end loading test procedure for obtaining the ultimate compressive strength of large gage length graphite/epoxy composite coupons was used. The procedure employed a fully side supporting fixture, inspired by a fixture shown in Reference [18], and was designed to prevent coupon end brooming, splitting and column buckling. The large gage length was employed to ensure, as much as possible, a geometric similarity between fatigue, static tension and static compression test coupons.

Figure 8 shows both the compression testing fixture (exploded view) and a failed test specimen. Geometric details of the fixture are given in Figure 9. The testing apparatus was a fully side supporting fixture machined from medium strength steel. The fixture was designed such that the column length was slightly shorter ($\sim$ 3 mm or 1/8 in.) than the coupon gage length to allow for compression of the coupon. Width of the apparatus was the same as the coupon width although this was not a critical criterion. The testing fixture was designed to prevent buckling of the coupon and brooming of the ends. Teflon tape, 0.076mm (.003 in.) thick, was used on the inside surfaces of the

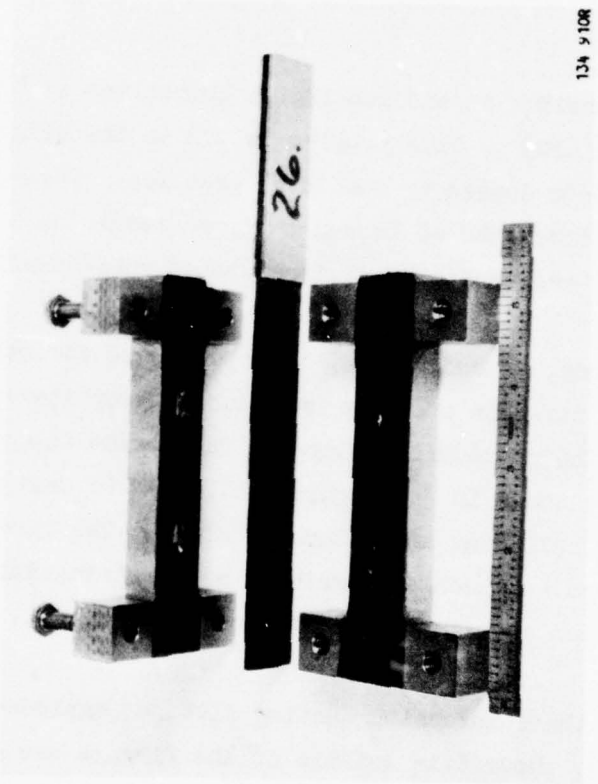
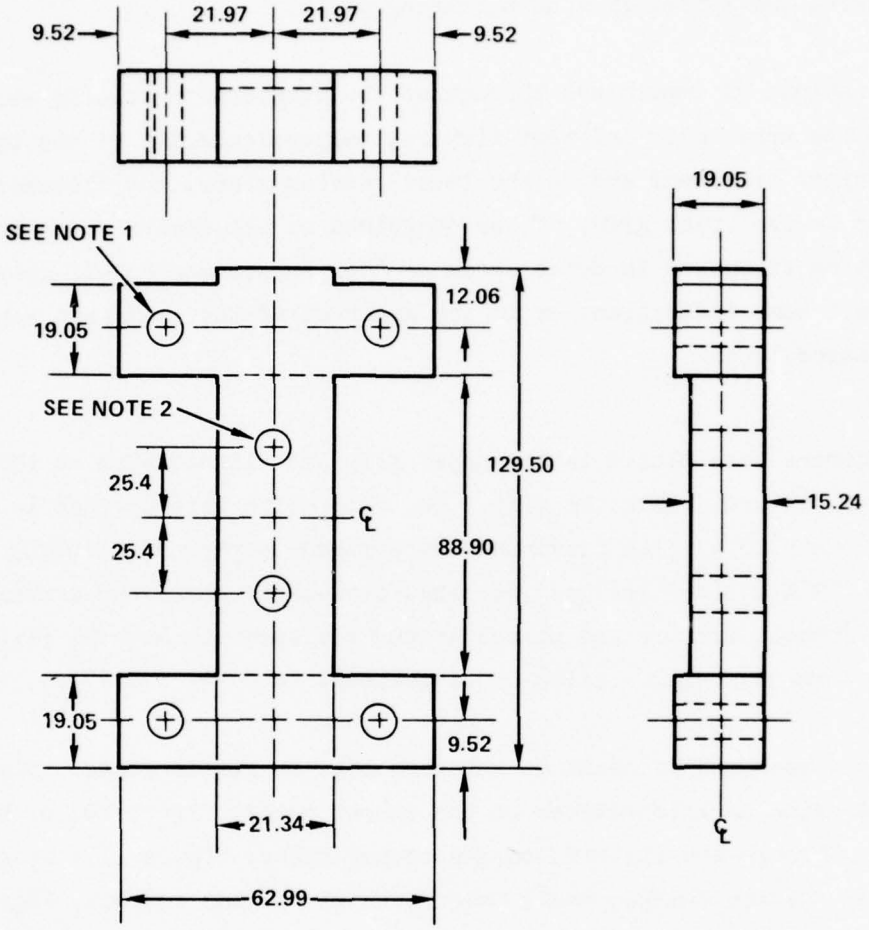


Figure 8. Disassembled View of Compression Testing Fixture with Example Test Coupon



NOTE:
1. Two Required: -1 Assembly Drilled and Tapped 1/4" -20 4 Places, -2 Assembly Drilled Only.
2. Hole Diameter as required for Extensometer and/or Strain Gages.
3. Material 1100-1240 MPa Steel.
4. All Dimensions in Millimeters.

Figure 9. Geometry of Compression Testing Fixture

fixture to reduce surface friction. In the testing procedure described below, specimens were end tabbed on one end. The other end was untabbed, cut square, and butted flat on a bearing plate.

Considerations of importance throughout the compression testing were: alignment of the upper grip and test fixture, perpendicularity of the upper grip to the upper crosshead and to the lower bearing plate, and alignment of the specimen in the upper grip. These questions of alignment, while important, will not be discussed in detail because they are common to all good testing practice. Some indications as to the accuracy of the alignment achieved will be discussed later.

The specimens were placed in the upper grip and aligned with an integral alignment fixture within the grip. The grip bolts were torqued in a criss-cross pattern to a value previously determined to prevent slipping of the coupon, 113 N·m (1000 in.·lbs), but insufficient to cause end crushing. The lateral support fixture was placed around the specimen and the fixture bolts lightly torqued, using a criss-cross pattern, to 0.339 N·m (3 in.·lbs).

Strain was measured by means of extensometers or strain gages. Strain was measured using an extensometer on the coupon edges, Figure 10, or by means of holes through the fixture, on the coupon sides, Figure 11. To study the effect of surface damage, small tabs were put on some coupons, Figure 12. The side tab material used in this study was of the same material as the coupons and attached with epoxy glue. Strain gages for specific coupons were placed on the coupon sides and centered beneath a fixture hole. Lead wires were brought through the side hole, Figure 13.

After extensometer attachment or strain gage lead wire hookup, the compression tests were run while recording both load and strain. Testing was conducted at constant crosshead speed although constant strain rate would, in general, be preferable. Standard testing strain rates between 0.001 and 0.002 mm/mm/min were used throughout the testing program.

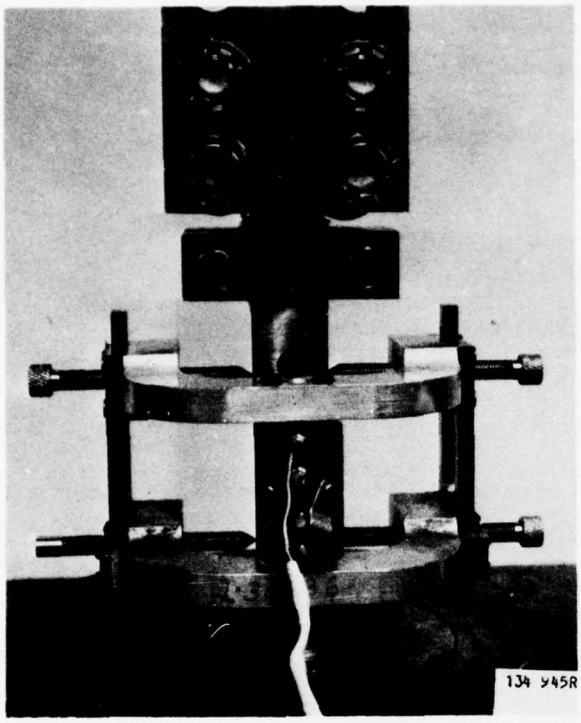


Figure 10. Extensometer Attached to Specimen Edges

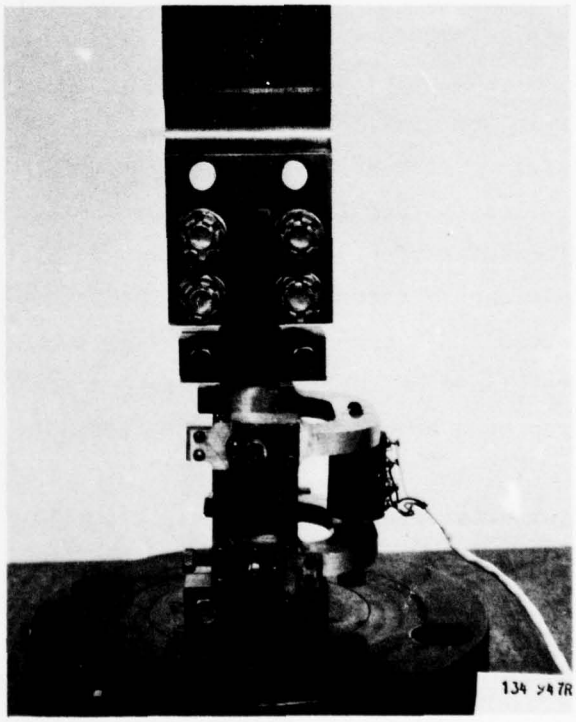


Figure 11. Extensometer Attached to Specimen Sides

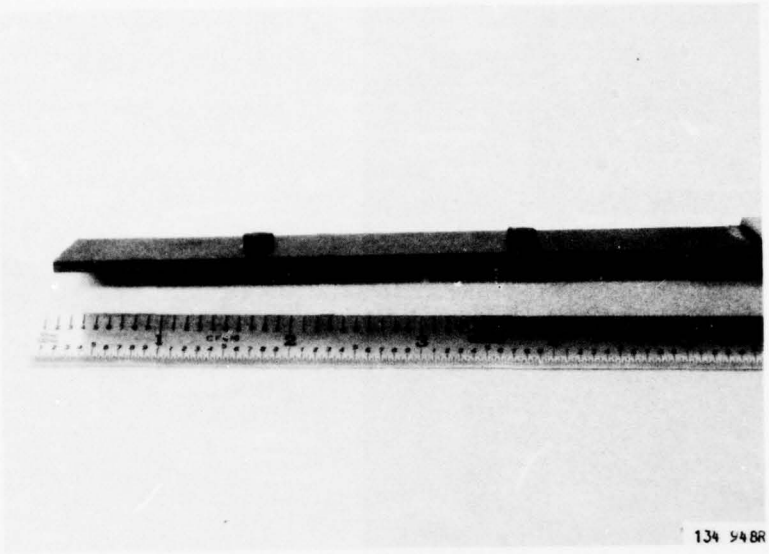


Figure 12. Test Coupon with Side Tabs

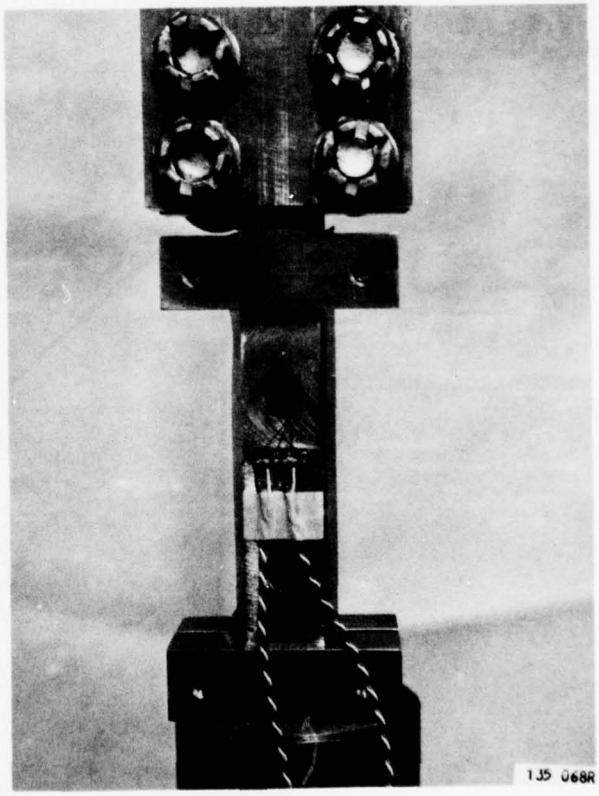


Figure 13. Compression Fixture and Test Coupon with Strain Gages

This compression testing procedure was by no means fully satisfactory. Signigicant improvements have been made at Lockheed expense and will be reported in the future. However, the procedure was internally valid for this program since the procedure was used to determine if any degradation in static compression properties had occurred due to fatigue.

2.5.3 Fatigue Test Procedures

Fatigue testing was accomplished using closed-loop electro-hydraulic servo controlled testing machines of various capacities from 89 to 220 kN (20 to 50 kips) maximum allowable load. Each machine was equipped with a peak and valley load monitoring system which allowed continuous monitoring of the load signal maximum peak, maximum valley, and minimum peak and minimum valley such that load accuracy was maintained within ± 1.0% of full-scale reading. Fatigue grips were of the friction bolt type with integral internal alignment fixtures, see Figure 14. Coupon alignment was maintained within ± 0.0762 mm (± 0.003 in.) in any direction. All tests were conducted at 10 Hz. Figure 15 shows a typical tension-tension fatigue test.

Tension-compression (T-C) fatigue tests were conducted using one or two buckling guide fixtures for stiffness, see Figure 16. The two guide fixtures used for most T-C tests were spaced 50.8 mm (2 in.) apart; had teflon tape on the faces towards the coupons; and had tie-down nuts which were torqued to approximately 0.224 N·m (2 in.·lbs). The maximum compression load for T-C tests was chosen as that compression stress at which the maximum coupon deflection within the gage length exceeded 0.0254 mm (0.001 in.) with stiffeners attached. Minimum load in tension-tension (T-T) fatigue tests was approximately 220 N (50 lbs).

A chosen minimum load was held constant during the tension-compression fatigue test program of each laminate while the effect on coupon life of different maximum stresses was evaluated. Other alternatives to holding the minimum load constant, such as constant mean stress or stress ratio, were discarded because the maximum load in tension would have been related to the maximum obtainable compression load. Thus, as the maximum load was reduced, the amount of compression would also be reduced. Holding the minimum load constant

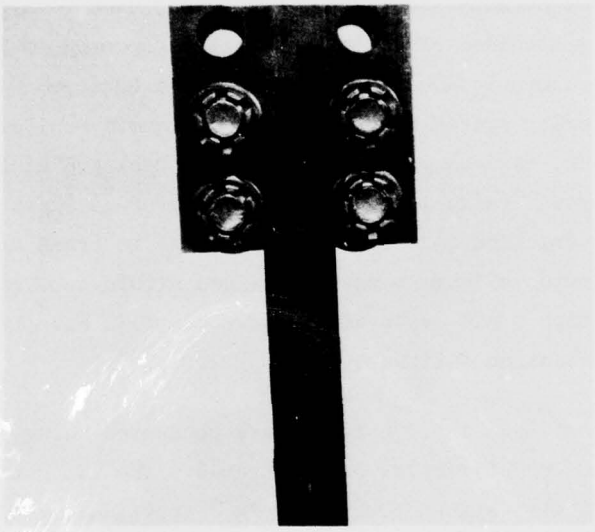


Figure 14. Fatigue Grip

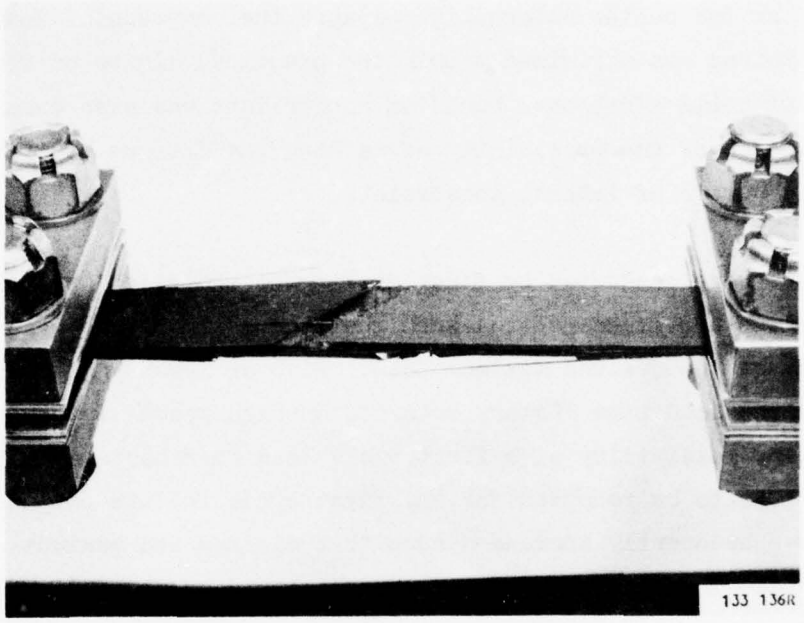


Figure 15. Tension-Tension Fatigue Test Showing Failed Laminate 1 Coupon

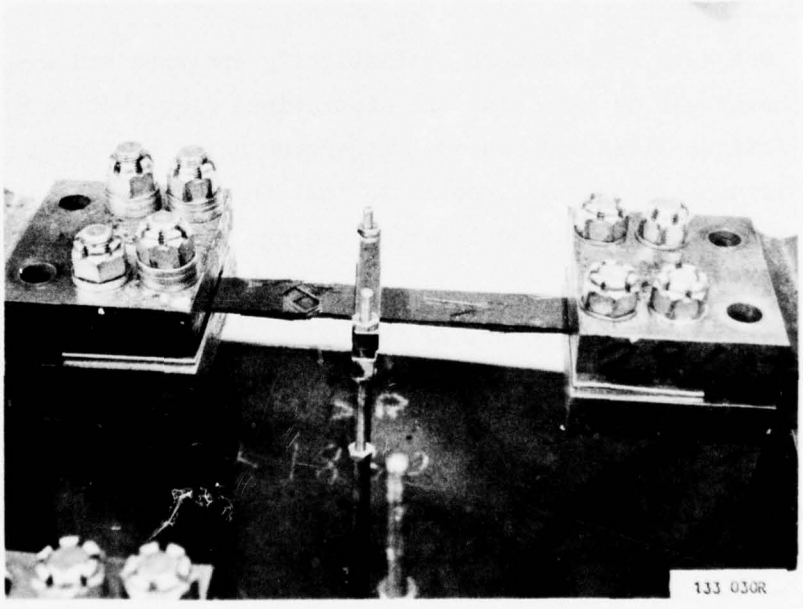


Figure 16. Tension-Compression Fatigue Test Showing Single Buckling Guide

appeared to be the better alternative because the compression load that could be obtained was maximized within the practical limits of the test. The action of using additional buckling constraints was also examined but rejected because of the possibility of masking the fatigue behavior due to an excessive number of lateral constraints.

Fatigue tests were conducted by first dialing to the calculated mean load and setting the amplitude control such that the maximum load was approximately equal to 95% of the desired maximum load. Five or less cycles were then applied and the load time history recorded on high speed visicorders. This eliminated any possibility of a first cycle load overshoot and allowed the load at failure to be recorded for any first cycle failure coupon. The span control was subsequently increased such that minimum and maximum load were those desired. The peak and valley controls shutdown the fatigue loading and returned the load to the mean value if any load deviations beyond 1/2% were detected.

2.6 Data Analysis

All of the test data results were statistically analyzed and compared. Primary emphasis was on examining the statistical distribution of static strengths, fatigue lives and residual strengths using a Weibull [8] distribution. This distribution was chosen so that the correctness of present "wear-out" models [19] could be investigated and further models developed.

For fatigue resistant design, one of the major questions concerning application of damage tolerance concepts is specification of percent levels of probability of survival. This question arises because of the need to translate reliability and confidence measures of data to parallel ones for design requirements [9]. In fatigue, reliability can often be successfully defined in terms of the Weibull survivorship function. The following discussion of Weibull analysis is taken from Reference [9] and was primarily inspired by Dr. G. E. Bowie.

In Weibull's representation of the statistics of fatigue, there are two random variates at each stress test condition. The first of these variates is the ordered sequence of the numbers of cycles to failure for each test result, n_i.

$$n_i: (n_1, n_2, n_3 \ldots . n_N)$$

The second random variate, x, is continuous and is the argument of the Weibull survivorship function, or probability of survival, expressed as

$$P(x) = \exp\left[-((x-e)/(v-e))^k\right], \qquad (1)$$

where $x \geq e$, $v \geq e$, $k > 0$, $P(e) = 1$, $P(v) = 1/\exp(1)$.

The connection between the random variates, n_i and x, is entirely empirical. In practice, numerical procedures are used to derive the three Weibull parameters k, e, and v by means of the approximation

$$P(x) = 1 - i/N \quad \text{when } x = n_i. \qquad (2)$$

For example, when N = 20 and the values n_i are distinct, (N-1) relations can be used in deriving k, e, and v:

$$P(n_1) = 1 - 1/20 = \exp\ ((n_1-e)/(v-e))^k$$
$$P(n_2) = 1 - 2/20 = \exp\ ((n_2-e)/(v-e))^k$$
$$\vdots \qquad\qquad \vdots$$
$$P(n_{19}) = 1 - 19/20 = \exp\ ((n_{19}-e)/(v-e))^k$$

The twentieth relation, $P(n_{20}) = 0$, is not used in deriving the three parameters. The solution of the above equations is by least square analysis where either, R, the correlation coefficient, or FIT, sum of squares of the deviations, can be used to optimize the results [9].

For equation (1), the mean of the sample set is given by [8]:

$$\bar{x} = e + (v-e)\,\Gamma\,(1 + 1/k) \tag{3}$$

the median by:

$$\overset{\circ}{x} = e + (v-e)\,(\log_e 2)^{1/k} \tag{4}$$

and the mode by:

$$\tilde{x} = e + (v-e)\,(1 - 1/k)^{1/k} \tag{5}$$

where Γ indicates the Gamma function.

During the past twenty-five years, a number of names have been applied to the parameters. In general, parameters e and v are scale parameters or factors while the exponent k is a shape parameter. Some confusion has resulted in the literature by referring to scale parameter e as the minimum life estimate. With this choice of words, e is often suggested on physical grounds to be $e \geq 0$. Many authors have reasoned further that since $e << n_i$, $i = 1, 2, 3, \ldots N$, the Weibull survivorship function can be appropriately reduced to dependence on two parameters, k and v, with $e = 0$ arbitrarily. An argument against this practice is given in Reference [8] . Often, the term threshold parameter is applied to parameter e and the term characteristic value to v. In analysis of composite data, k is often denoted by α and v by $\hat{F}$.

The influence of the shape parameter k can be explained as follows. Define a reduced variate Z as

$$Z = (x-e)/(v-e),\ Z \geq 0,\ \text{dimensionless}, \tag{6}$$

and express the probability of survival function as

$$P(x) = \exp\left[-Z^k\right],\ k > 0, \tag{7}$$

where $P(Z) = 1/\exp(1)$ when $Z = 1$,
and $P(Z) = 1$ when $Z = 0$, for all k.

If $k < 1$, this implies the test specimen material develops resistance to fatigue as the number of load cycles is increased. If $k = 1$, the Weibull survivorship function reduces to the constant failure rate relation commonly used in reliability studies. If $k > 1$, one can inquire whether the test specimen material experiences progressive damage as numbers of load cycles are increased.

Figure 17 illustrates the manner in which $P(Z)$ is dependent on the shape parameter k for the range of the reduced variate Z from zero to two. Empirical evidence does not support the interpretation that k might be a smoothly increasing function of stress amplitude. For practical purposes, in the case of structural alloy fatigue, the region of Figure 17 of most interest to designers is bounded as follows:

(a) Above by the limit $P(Z) = 1.0$
(b) Below by the median $P(Z) = 0.5$
(c) On the left by the curve $P(Z) = \exp\left[-Z\right]$
(d) On the right by the curve $P(Z) = \exp\left[-Z^{10}\right]$

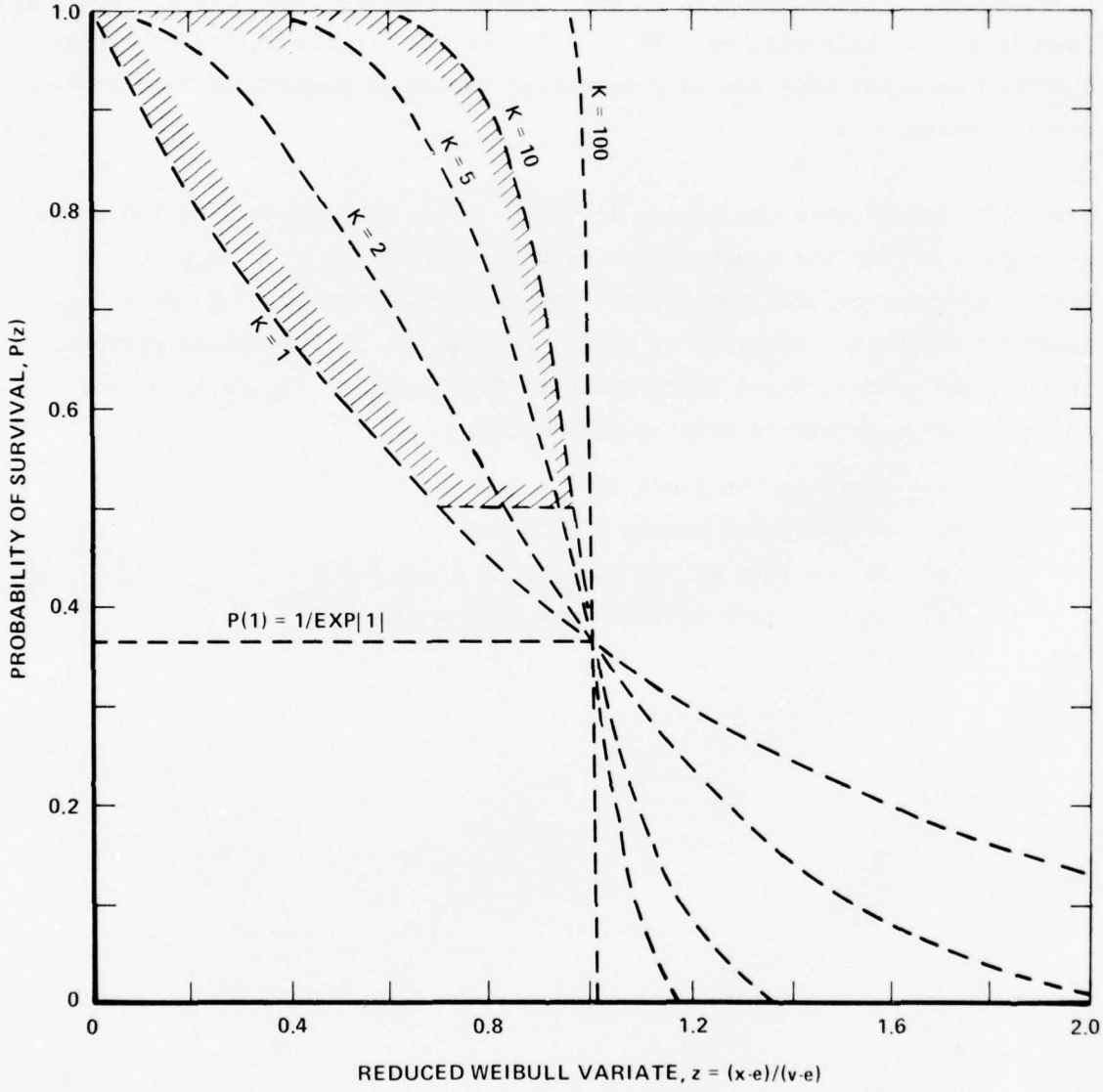


Figure 17. Influence of Shape Parameter k on Probability of Survival

SECTION III

MATERIAL CHARACTERIZATION

The 11 panels of laminate 1 and the four panels of laminate 2 were all fabricated using the procedure of Appendix A and met all of the quality assurance procedures discussed in Section 2.3. Resin, fiber, and void analysis results of laminate 1 panels are given in Table 6 and those of laminate 2 in Table 7.

The fabrication procedure was intended to result in a fiber volume range from 60 to 65%. Notice in Tables 6 and 7 that all but one of the 15 panels fabricated met this specification. Void contents were obtained by standard chemical analysis procedures which unfortunately result in an error of ± 1.6% in void content; i.e., a result of 2% voids can be between 0.4 and 3.6% voids. The error is due to uncertainty in original fiber and matrix density properties and in the amount of absorbed moisture which also affects density. This level of inherent error can, of course, result in physically impossible negative void content determinations. To alleviate this problem, void content determinations were made of three panels using a 1000X light microscope. These results also indicated that void content was extremely low.

In accordance with the fabrication procedure, each panel was non-destructively inspected using an ultrasonic C-scan technique. Results of the C-scan NDI study are shown in Figures 18 to 32. In Figures 18, 19, 21-27, the teflon disks imbedded in the reference panel are clearly visible (see Appendix A for teflon disk sizes and locations within the plies). No significant anomalies were revealed by C-scan of the 10 panels of laminate 1 except for panel 1MJ601 (see Figure 24) where a small surface depression was observed. The coupons from this region of panel 1MJ601 were eliminated from the test program. Similarly, examination of C-scans of the three of the four panels of laminate 2 (Figures 29, 31 and 32) and the last panel of laminate 1 (Figure 28) revealed no significant anomalies. However, Figure 30 shows that numerous indications were observed for panel 1H7699 which were acoustically equivalent to the

TABLE 6

RESIN, FIBER, AND VOID ANALYSIS RESULTS OF LAMINATE 1 PANELS

Panel No.	Resin Content wt. %	Fiber Content wt. %	Resin Content vol. %	Fiber Content vol. %	Void Content V_C % [a]	Void Content V_M % [b]
1HJ 578	31.9	68.1	39.0	61.0	+0.3 [c]	<0.1
580	32.5	67.5	39.7	60.3	-0.6 [c]	
582	29.9	70.1	36.8	63.2	+0.3 [c]	<0.1
583	31.9	68.1	39.0	61.0	-0.1 [c]	
594	28.5	71.5	35.2	64.8	+0.3	
596	29.3	70.7	36.1	63.9	+0.3	
601	27.0	73.0	33.6	66.4	+0.1	
603	28.7	71.3	35.5	64.5	+0.5	<0.1
604	31.3	68.7	38.4	61.6	+0.1	
606	31.3	68.7	38.4	61.6	+0.3	
1NH 693 [d]	32.2	67.8	39.2	60.8	+0.1	

a - V_C, Void content determined by standard chemical analysis procedures

b - V_M, Void content determined by light microscope examination at 1000X

c - Artifact of chemical analysis procedure for void content determination

d - Panel 1NH693 was produced from the same batch of material as that used for laminate 2.

TABLE 7

RESIN, FIBER, AND VOID ANALYSIS RESULTS OF LAMINATE 2 PANELS

Panel No.	Resin Content wt.%	Fiber Content wt.%	Resin Content Vol.%	Fiber Content Vol.%	Void[a] Content V_c %
1NH 696	31.7	68.3	38.6	61.4	0.0
1NH 699	33.0	67.0	40.0	60.0	-0.2[b]
1NH 727	30.1	69.9	36.9	63.1	0.0
1NH 728	30.7	69.3	37.5	62.5	+0.3

a - V_c, Void content determined by standard chemical analysis procedure

b - Artifact of chemical analysis procedure for void content determination.

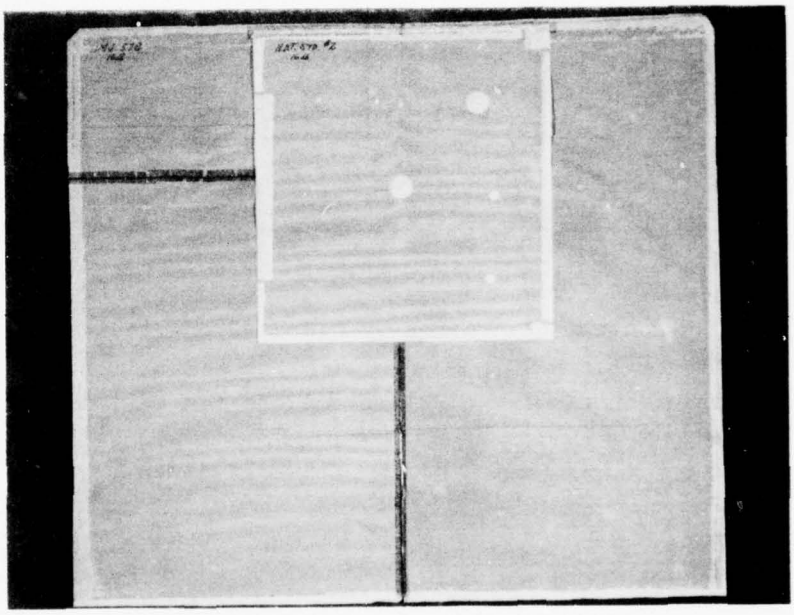


Figure 18. Ultrasonic C-Scan of Laminate 1
Panel 1MJ578

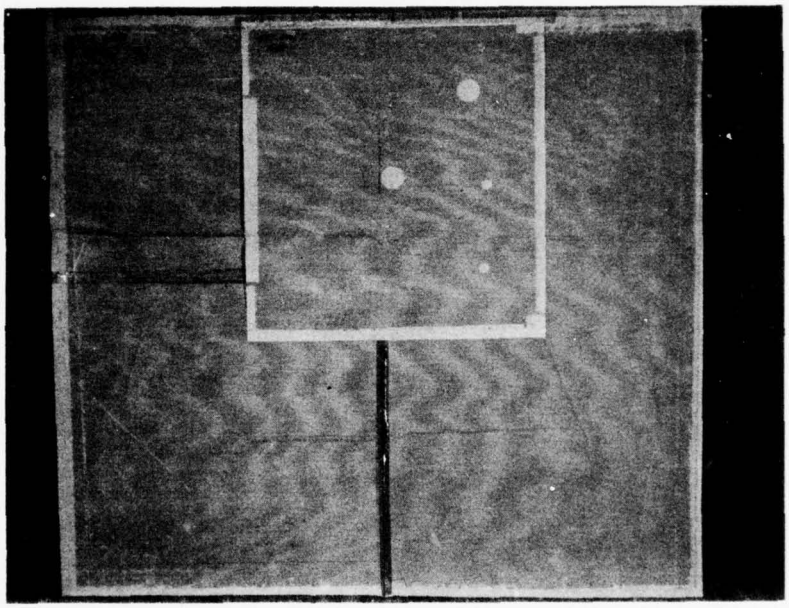


Figure 19. Ultrasonic C-Scan of Laminate 1
Panel 1MJ580

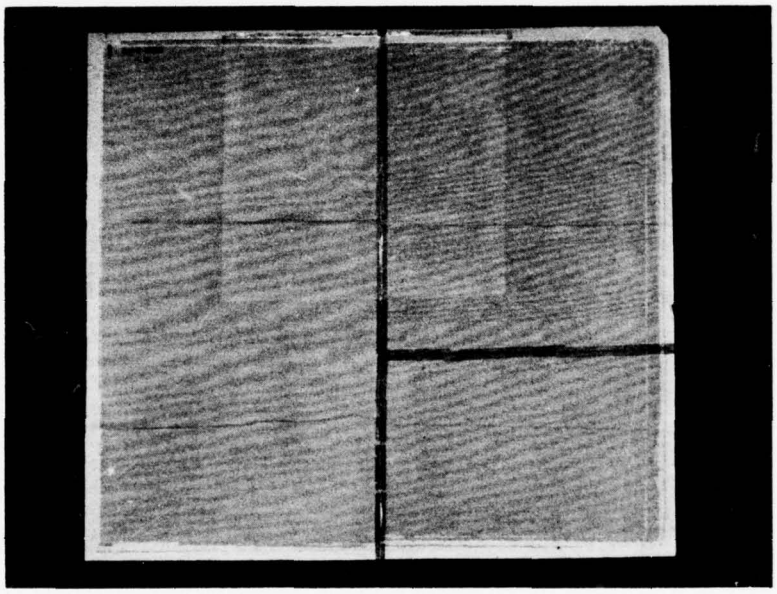


Figure 20. Ultrasonic C-Scan of Laminate 1
Panel 1MJ582

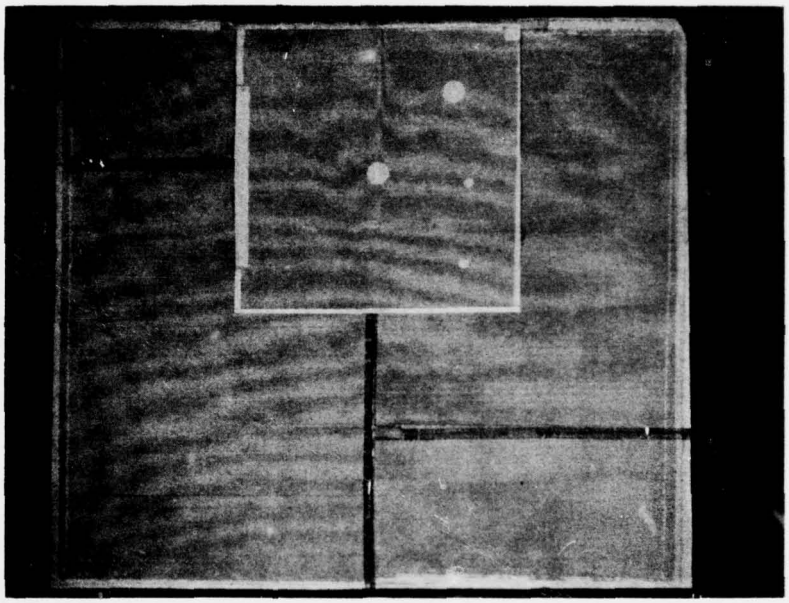


Figure 21. Ultrasonic C-Scan of Laminate 1
Panel 1MJ583

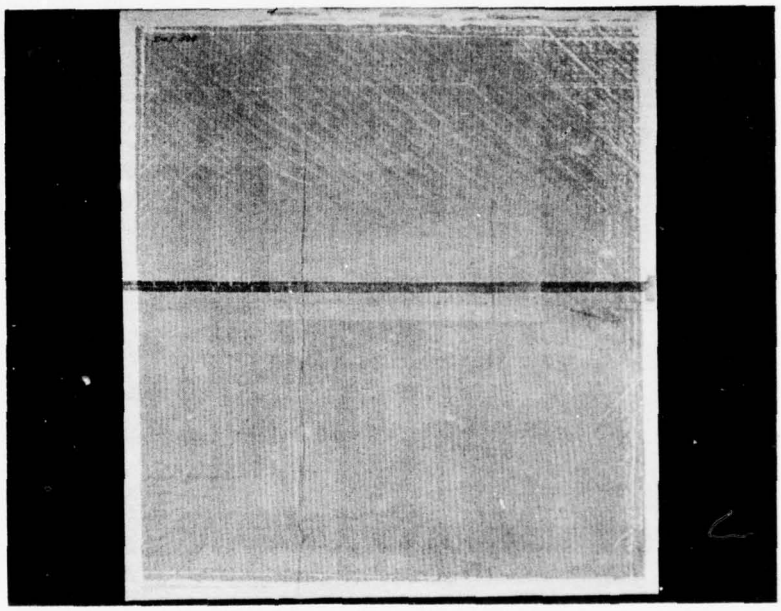


Figure 22. Ultrasonic C-Scan of Laminate 1
Panel 1MJ594

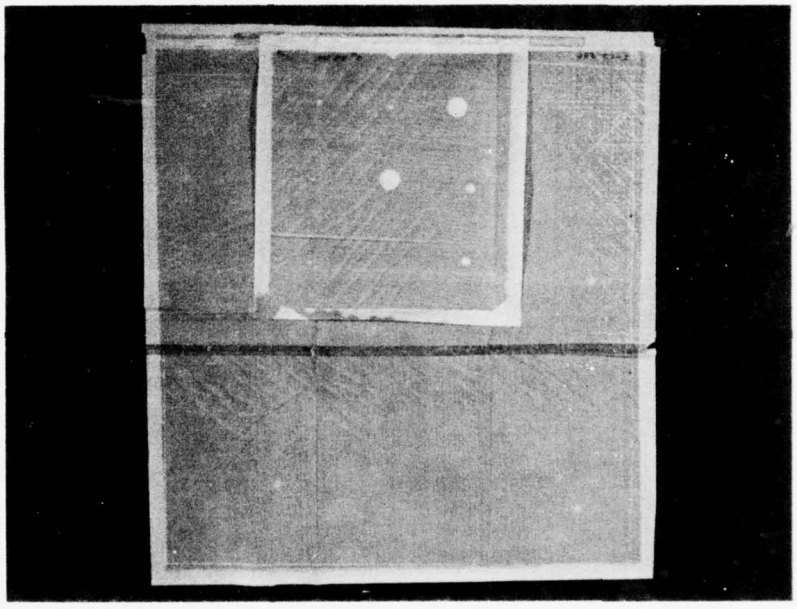


Figure 23. Ultrasonic C-Scan of Laminate 1
Panel 1MJ596

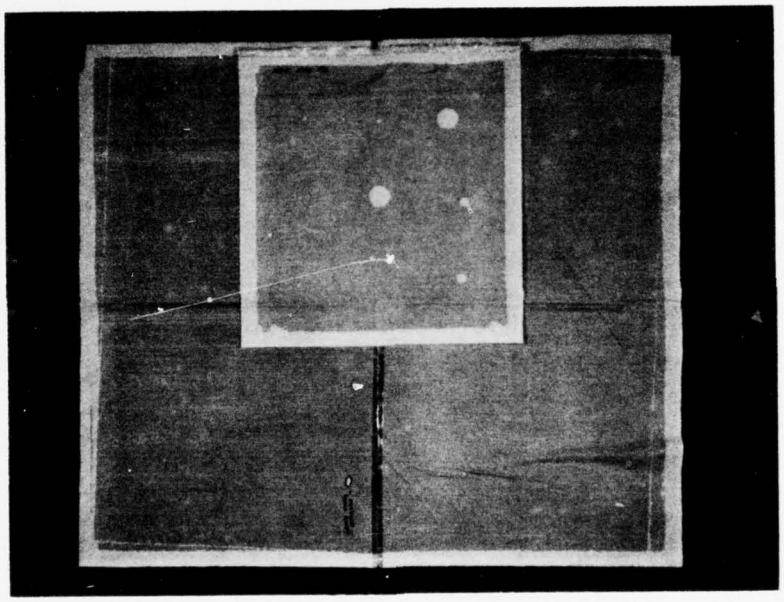


Figure 24. Ultrasonic C-Scan of Laminate 1
Panel 1MJ601

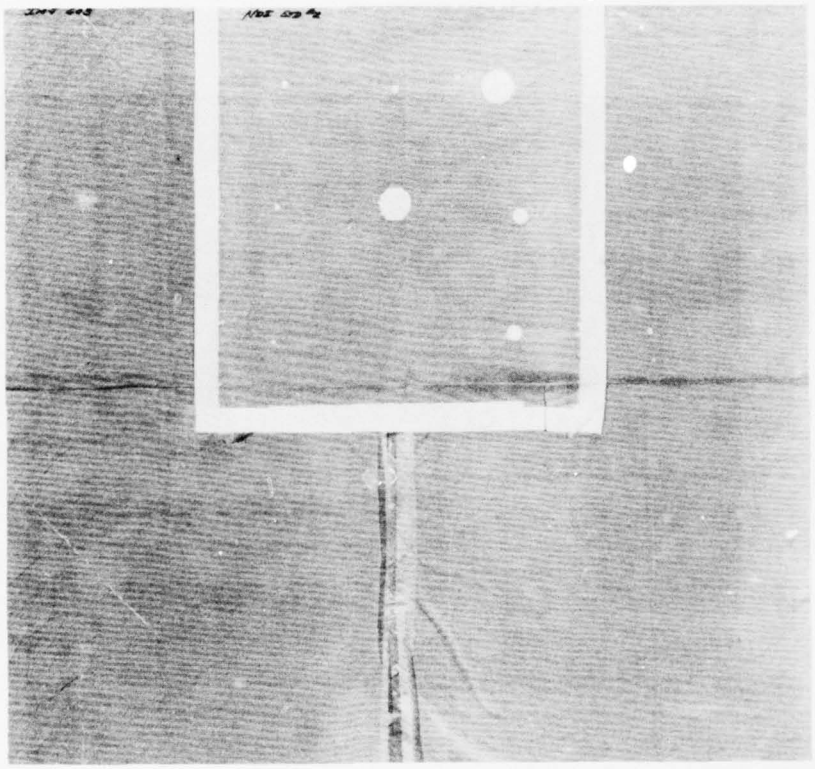


Figure 25. Ultrasonic C-Scan of Laminate 1
Panel 1MJ603

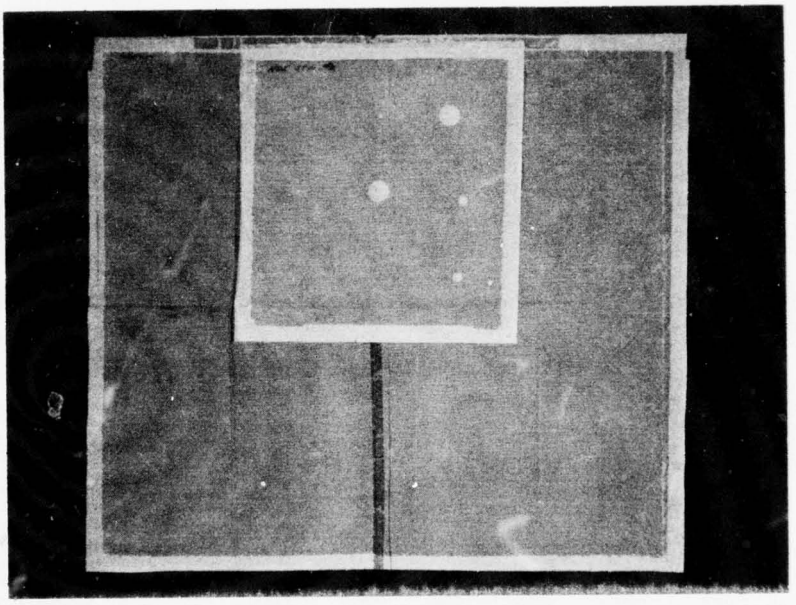


Figure 26. Ultrasonic C-Scan of Laminate 1
Panel 1MJ604

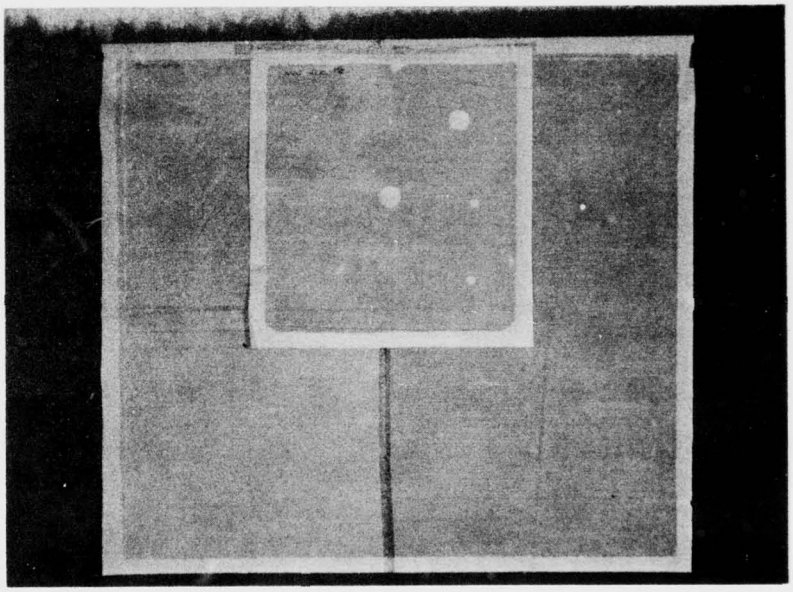


Figure 27. Ultrasonic C-Scan of Laminate 1
Panel 1MJ606

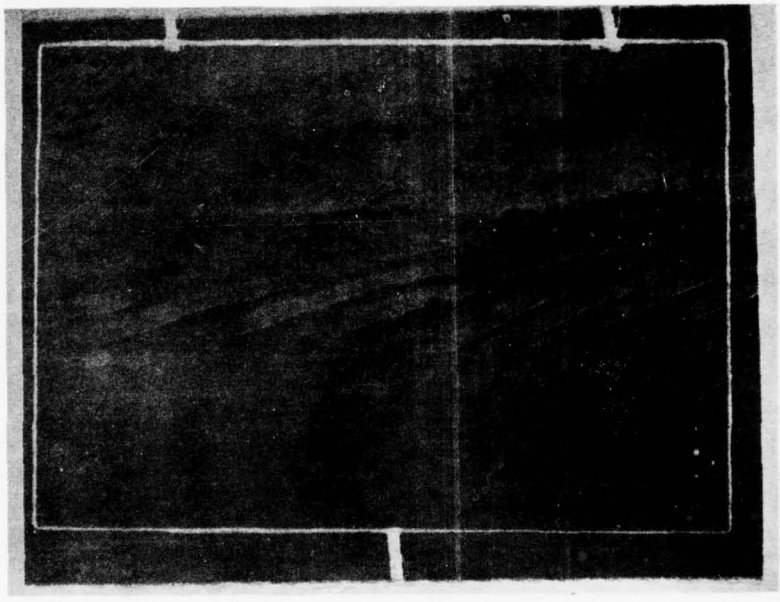


Figure 28. Ultrasonic C-Scan of Laminate 1
Panel 1MJ693

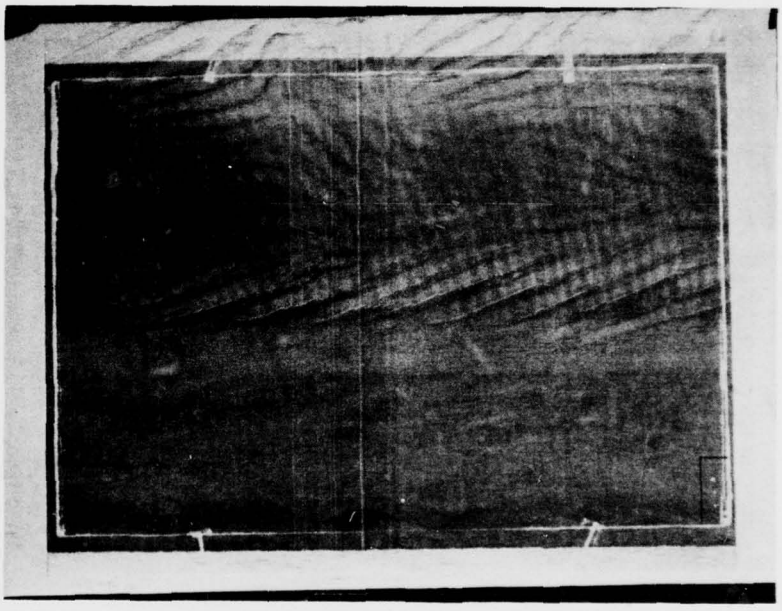


Figure 29. Ultrasonic C-Scan of Laminate 2
Panel 1NH696

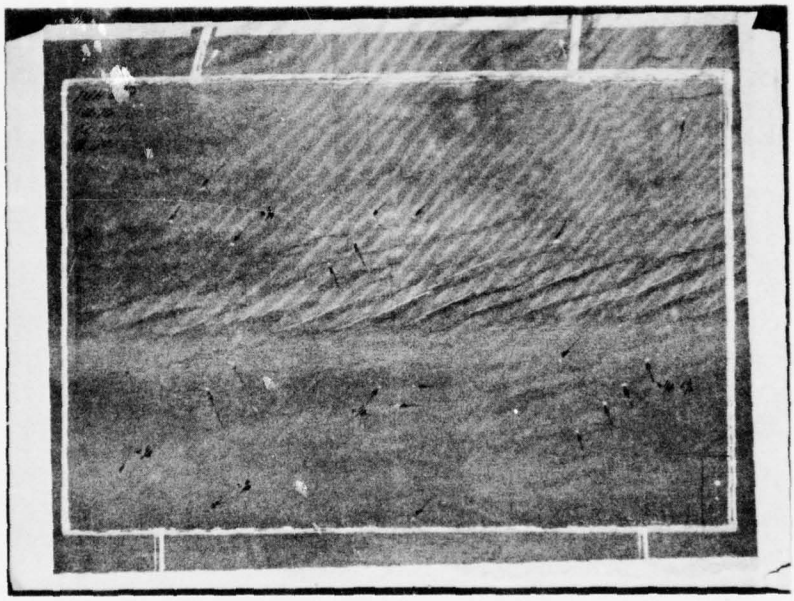


Figure 30. Ultrasonic C-Scan of Laminate 2
Panel 1NH699

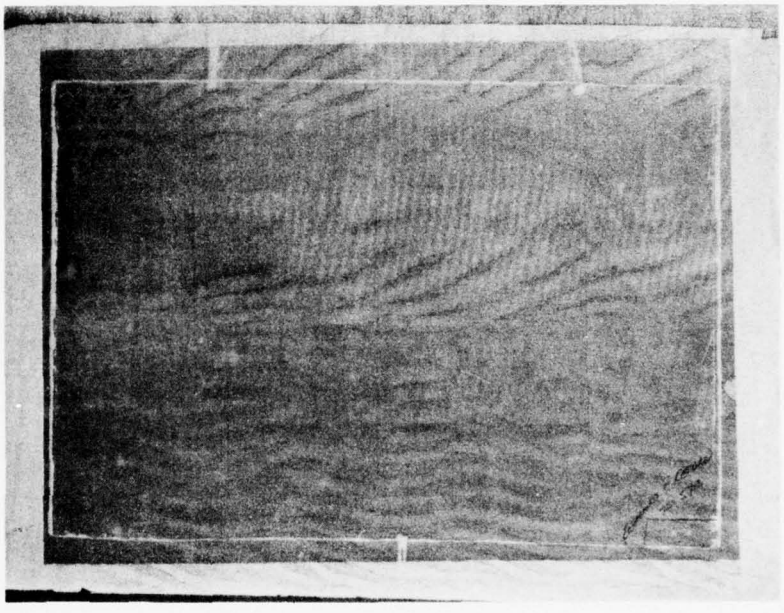


Figure 31. Ultrasonic C-Scan of Laminate 2
Panel 1NH727



Figure 32. Ultrasonic C-Scan of Laminate 2
Panel 1NH728

teflon disk control standards. The meaning of these indications is not known since later coupon post-failure correlation to these positions indicated no apparent abnormal damage.

SECTION IV

STATIC TENSION AND COMPRESSION RESULTS

4.1 Static Tension Test Results

Typical stress-strain curves for static tension tests are shown in Figures 33 and 34 for laminates 1 and 2, respectively. For both laminates all failures were brittle-like without any discernable plastic-like flow at the end of the stress-strain curve. As Figure 33 shows, stress-strain curves of laminate 1 tensile coupons exhibited an initial straight portion with an apparent modulus of elasticity designated as E_{1a}. This straight portion was followed by a short, but not abrupt, change to a straight curve to failure with an apparent modulus designated E_{1b}. In contrast, stress-strain curves of laminate 2 coupons exhibited a nearly linear behavior to failure with an apparent modulus designated E_2.

Figure 35 shows two laminate 1 coupons which failed in static tension and whose failure modes were representative of all laminate 1 coupons. All failures of laminate 1 coupons were within the gage length. Those which failed near the end did not differ in their failure strengths. Figure 36 shows two laminate 2 coupons which failed in static tension in a manner typical of most laminate 2 coupons. However, as shown in Figure 37, despite the large number of 0° plies, two laminate 2 coupons failed along the 45° angle of the 45° plies unlike other coupons which failed in a more haphazard manner at more or less of a 90° angle to the load line. These 45° angle failures indicated that despite the nominally lower failure strength of the 45° plies, they could still dominate the failure mode. In general, failed laminate 1 static tension coupons were observed to have more extensive delamination than laminate 2 coupons.

Static tension test results for the 25 coupons tested from laminate 1 are shown in Table 8 and those for the 20 coupons tested from laminate 2 are shown in Table 9. The two laminate 2 coupons which failed along a 45° angle (699-2A, 699-3B) can be seen from Table 2 to have had two of the highest four

Preceding Page BLANK - FIL

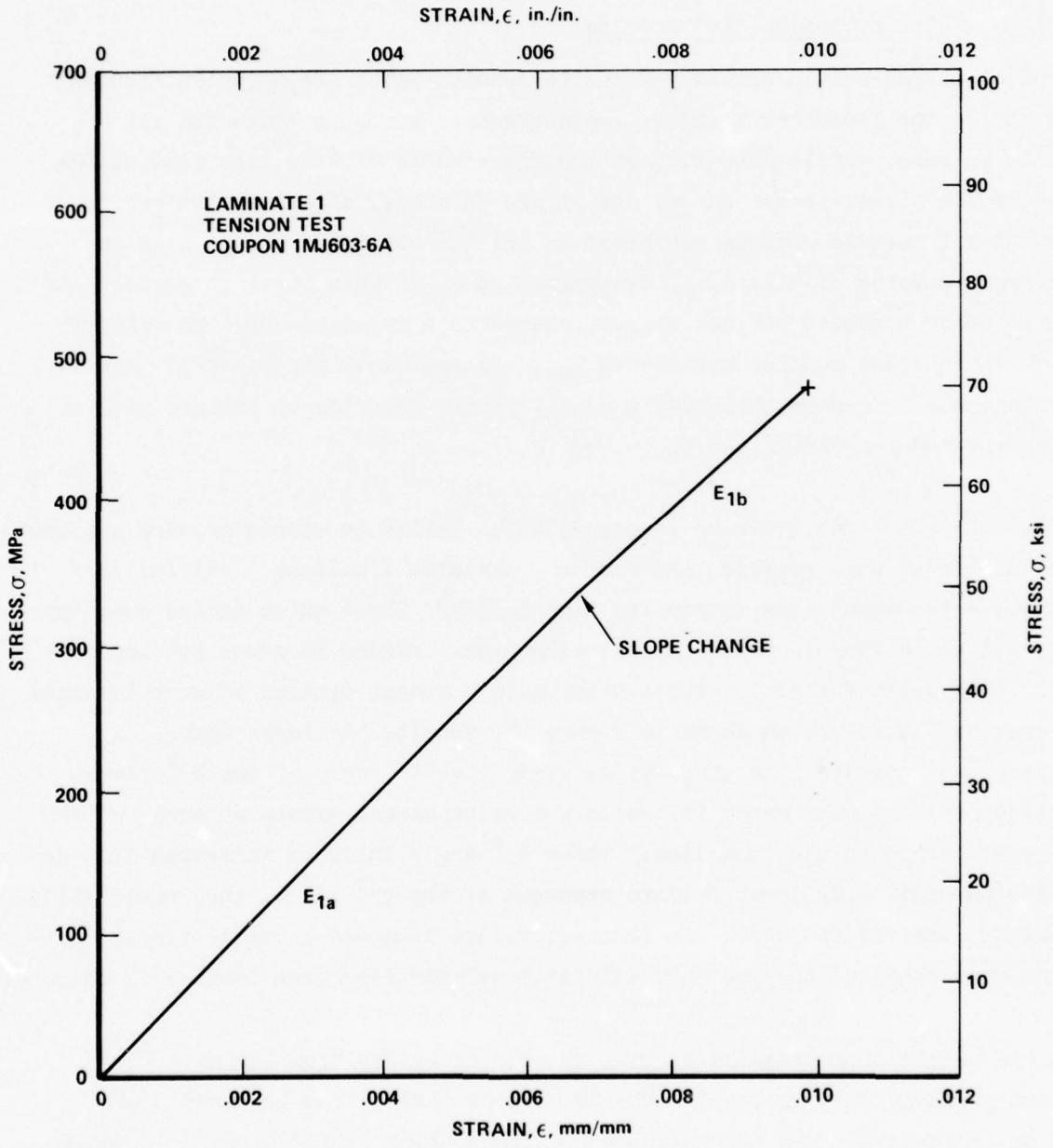


Figure 33. Tension Stress-Strain Curve for Laminate 1 Coupon 1MJ603-6A

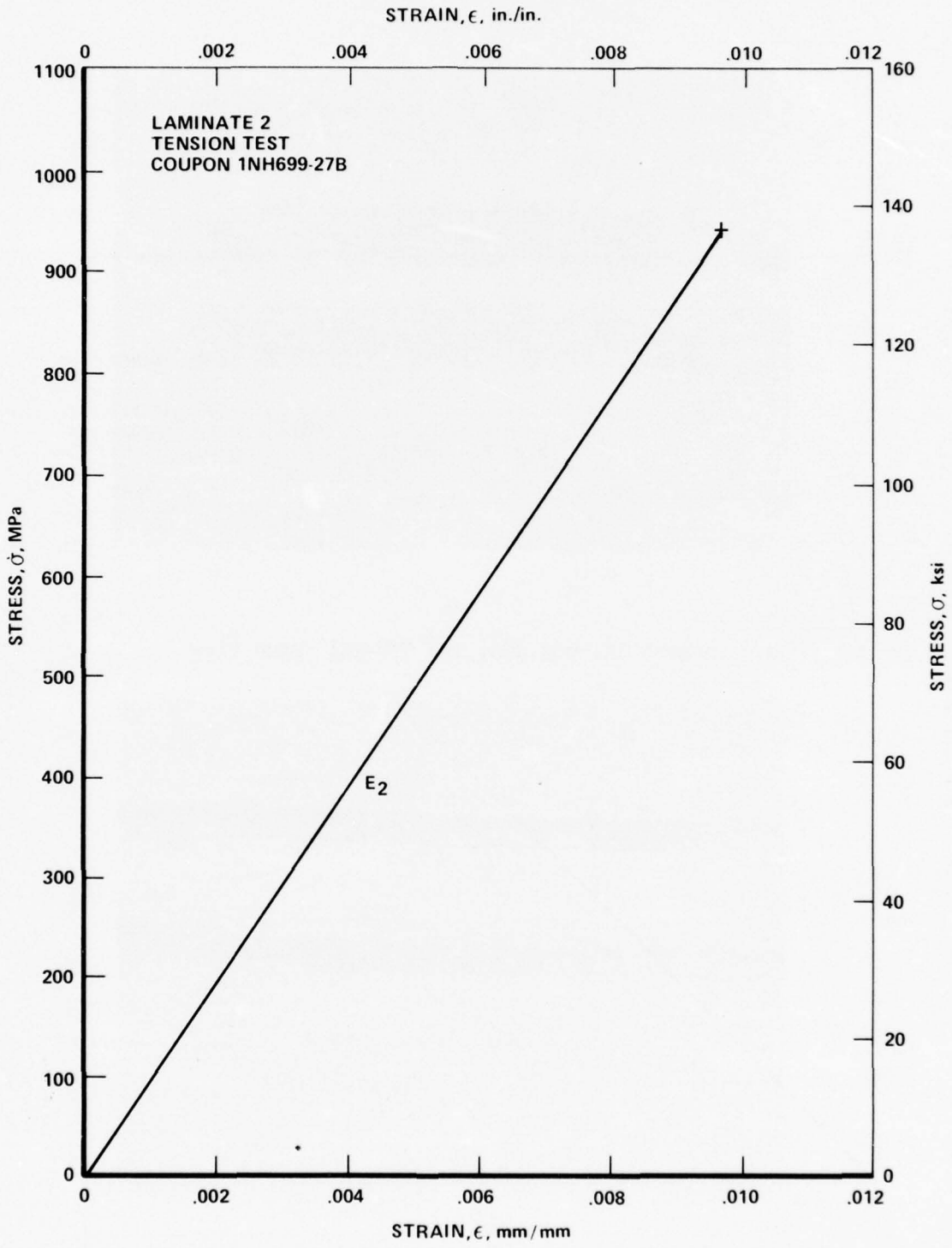
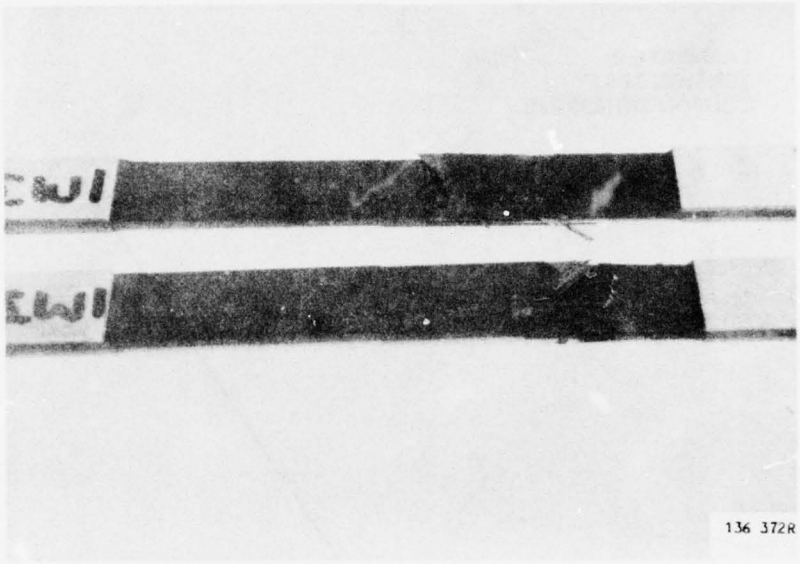
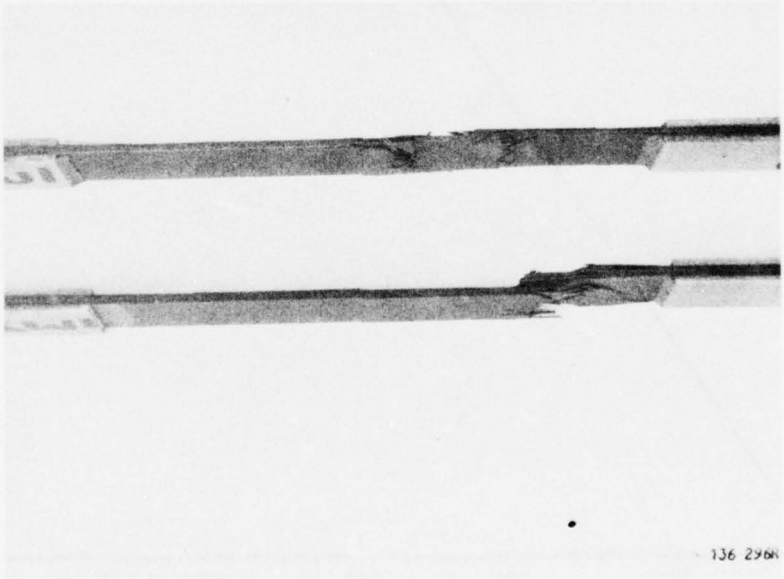


Figure 34. Tension Stress-Strain Curve for Laminate 2 Coupon 1NH699-27B

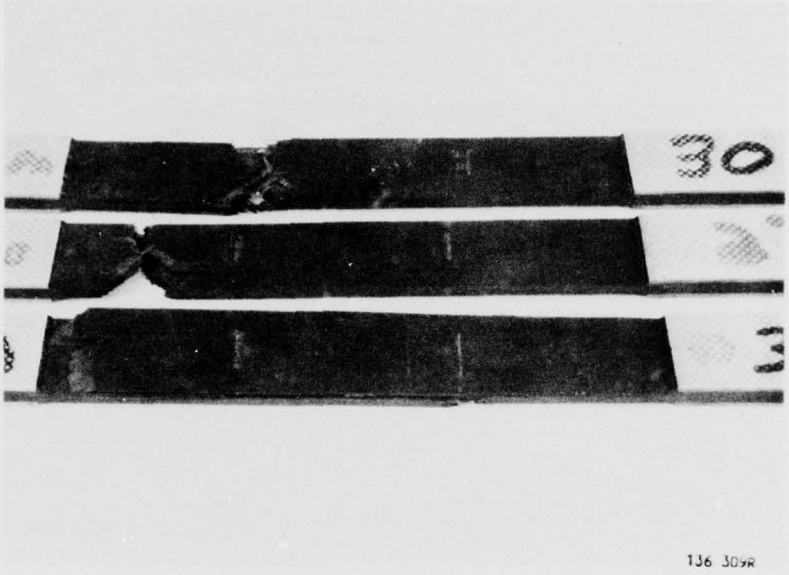


a. Coupons 1MJ 603-25A, 1MJ 578-2A; Side View

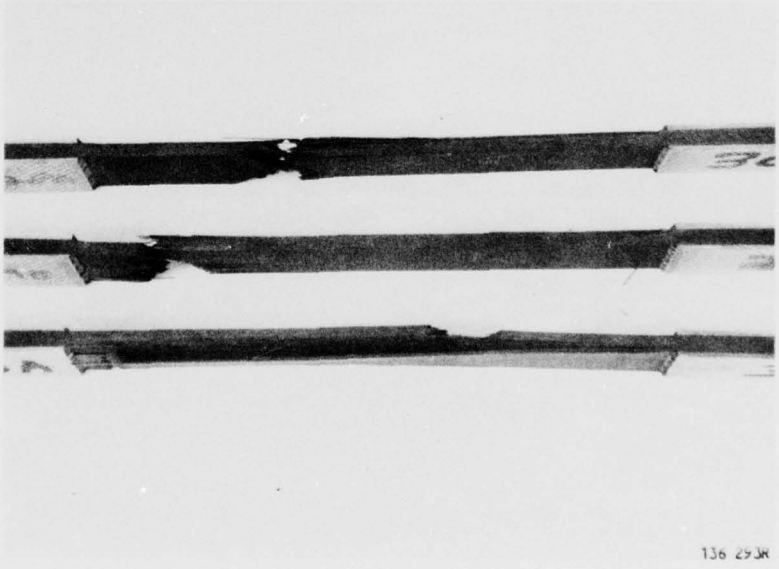


b. Coupons 1MJ 603-25A, 1MJ 578-2A; Edge View

Figure 35. Representative Static Tension Failure Modes of Laminate 1 Coupons

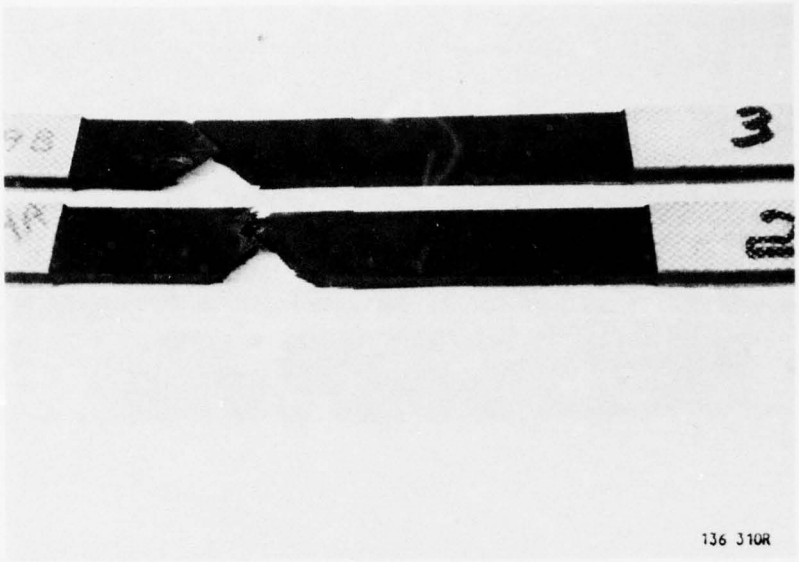


a. Coupons 1NH 728-30A, 1NH 699-27B, 1NH 696-31A; Side View

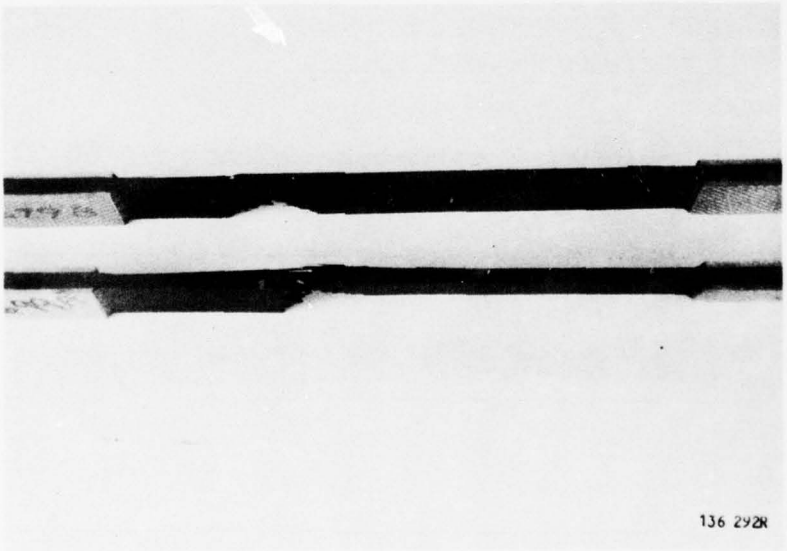


b. Coupons 1NH 728-30A, 1NH 699-27B, 1NH 696-31A; Edge View

Figure 36. Representative Static Tension Failure Modes of Laminate 2 Coupons



a. Coupons 1NH 699-3B, 1NH 699-2A; Side View



b. Coupons 1NH 699-3B, 1NH 699-2A; Edge View

Figure 37. Laminate 2 Coupons Which Failed in Static Tension with Failure Modes Dominated by 45° Plies

TABLE 8A

TENSION TEST RESULTS OF LAMINATE 1 COUPONS (SAMPLE SIZE = 25)

Sample ID	Min. Area, $in.^2$	Ultimate Load, P_{ult}, lbs	Ultimate Stress, σ_{ult}, ksi	Ultimate Strain ε_{ult}, in./in. in 2 in.	Slope Deviation Load, P_y, lbs	Slope Deviation Stress, σ_y, ksi	Slope Deviation Strain, ε_y, in./in. in 2 in.	Initial Apparent Modulus of Elasticity, E_{1a}, psi x 10^6	Final Apparent Modulus of Elasticity, E_{1b}, psi x 10^6
578-23B	.0835	6100	73.0	.0099	4000	47.9	.0062	7.73	6.65
2A	.0837	5800	69.3	.0102	4150	49.6	.0069	7.18	5.97
15A	.0857	5940	69.3	.0107	3750	43.8	.0063	6.95	5.98
580-19B	.0833	5980	71.8	.0097	3780	45.4	.0056	8.10	7.06
18A	.0820	6080	74.2	.0090	3690	45.0	.0055	8.18	7.17
9A	.0827	6240	75.4	.0103	3960	47.9	.0059	8.12	6.72
582-15A	.0840	5680	67.6	.0090	4090	48.7	.0062	7.85	6.61
8B	.0831	5350	64.4	.0088	3640	43.8	.0056	7.82	6.69
20B	.0815	5380	66.0	.0088	3800	46.6	.0059	7.90	6.82
583-24B	.0805	5800	72.0	.0103	3390	42.1	.0054	7.80	6.54
25B	.0821	5960	72.6	.0101	3570	43.5	.0056	7.76	6.41
8A	.0836	5900	70.6	.0099	3950	47.2	.0063	7.50	5.98
594-11A	.0822	5100	62.0	.0086	4100	49.9	.0066	7.56	5.79
10B	.0819	5850	71.4	.0088	4170	50.2	.0064	7.96	6.10
596- 4A	.0820	5790	70.6	.0095	3780	46.1	.0061	7.56	6.78
12B	.0827	5780	69.9	.0100	3650	44.1	.0058	7.61	5.90
601-11B	.0820	5300	64.6	.0093	3800	46.3	.0064	7.24	6.10
6B	.0815	5700	69.9	.0093	4250	52.2	.0066	7.90	6.46
603-25A	.0819	5340	65.2	.0091	3620	44.2	.0058	7.62	6.43
6A	.0821	5740	69.9	.0098	4200	51.2	.0069	7.41	6.77
604- 8B	.0835	5820	69.7	.0099	3150	37.7	.0051	7.40	6.65
22A	.0824	5600	68.0	.0100	3100	37.6	.0051	7.38	6.74
24A	.0817	5280	64.6	.0090	2830	34.6	.0047	7.37	6.80
606-24B	.0804	5300	66.0	.0090	3340	41.5	.0055	7.55	6.56
14A	.0841	6000	71.3	.0101	3800	45.2	.0061	7.41	6.26
Average			69.2	.0096		45.3	.0059	7.64	6.48
			+6.2	+.0011		+ 6.9	+.0010	+0.54	+0.70
			-7.2	-.0010		-10.7	-.0012	-0.69	-0.68

TABLE 8B

TENSION TEST RESULTS OF LAMINATE 1 COUPONS (SAMPLE SIZE = 25)

Sample ID	Min. Area, mm^2	Ultimate Load P_{ult}, kN	Ultimate Stress, σ_{ult}, MPa	Ultimate Strain ε_{ult}, mm/mm in 50.8 mm	Slope Deviation Load, P_y, kN	Slope Deviation Stress, σ_y, MPa	Slope Deviation Strain, ε_y, mm/mm in 50.8 mm	Initial Appar. Modulus of Elasticity, E_{1a}, GPa	Final Appar. Modulus of Elasticity, E_{1b}, GPa
578-23B	53.9	27.1	503	.0099	17.8	330	.0062	53.3	45.8
- 2A	54.0	25.8	478	.0102	18.5	342	.0069	49.5	41.2
-15A	55.3	26.4	478	.0107	16.7	302	.0063	47.9	41.2
580-19B	53.7	26.6	495	.0097	16.8	313	.0056	55.8	48.7
-18A	52.9	27.0	512	.0090	16.4	310	.0055	56.4	49.4
- 9A	53.4	27.8	520	.0103	17.6	330	.0059	56.0	46.3
582-15A	54.2	25.3	466	.0090	18.2	336	.0062	54.1	45.6
- 8B	53.6	23.8	444	.0080	16.2	302	.0056	53.9	46.1
-20B	52.6	23.9	455	.0088	16.9	321	.0059	54.5	47.0
583-24B	51.9	25.8	496	.0103	15.1	290	.0054	53.8	45.1
-25B	53.0	26.5	501	.0101	15.9	300	.0056	53.5	44.2
- 8A	53.9	26.2	487	.0099	17.6	325	.0063	51.7	41.2
594-11A	53.0	22.7	427	.0086	18.2	344	.0066	52.1	39.9
-10B	52.8	26.0	492	.0088	18.5	340	.0064	54.9	42.0
596- 4A	52.9	25.8	487	.0095	16.8	318	.0061	52.1	46.7
-12B	53.4	25.7	482	.0100	16.2	304	.0058	52.5	40.7
601-11B	52.9	23.6	445	.0093	16.9	319	.0064	49.9	42.0
- 6B	52.6	25.4	482	.0093	18.9	360	.0066	54.5	44.5
603-25A	52.8	23.8	450	.0091	16.1	305	.0058	52.5	44.3
- 6A	53.6	25.5	482	.0098	18.7	352	.0069	51.1	46.7
604- 8B	53.9	25.9	481	.0099	14.0	260	.0051	51.0	45.8
-22A	53.2	24.9	469	.0100	13.8	259	.0051	50.9	46.5
-24A	52.7	23.5	445	.0090	12.6	239	.0047	50.8	46.9
606-24B	51.9	23.6	455	.0090	14.9	286	.0055	52.1	45.2
-14A	54.3	26.7	492	.0101	16.9	312	.0061	51.1	43.2
Average			477 + 43 - 49	.0096 +.0011 -.0010		312 + 48 - 74	.0059 +.0010 -.0012	52.7 + 3.7 -4.8	44.7 + 4.8 -4.7

TABLE 9A

TENSION TEST RESULTS
OF LAMINATE 2 COUPONS

(Sample Size = 20)

Sample ID	Average Area, $in.^2$	Ultimate Load, P_{ult}, lbs	Ultimate Stress σ_{ult}, ksi	Ultimate Strain ϵ_{ult}, in./in. in 2.0 in.	Apparent Modulus of Elasticity, E_2, psi x 10^6
727-29A	.1268	18670	147.2	.0095	15.5
8B	.1280	18760	146.6	.0099	14.8
10B	.1303	17800	136.6	.0086	15.9
32B	.1282	19300	150.5	.0092	16.4
12C	.1264	16860	133.4	.0088	15.2
728-30A	.1294	16790	129.8	.0081	16.0
21B	.1310	17620	134.5	.0082	16.4
35B	.1308	18360	140.4	.0093	15.1
29C	.1282	19060	148.7	.0098	15.2
36C	.1301	18320	140.8	.0090	15.6
696-14A	.1252	17680	141.2	.0095	14.9
15A	.1278	17830	139.5	.0098	14.4
31A	.1281	15200	118.7	.0065	18.3
24B	.1264	17200	136.1	.0101	13.5
25C	.1259	18300	145.4	.0094	15.5
699- 2A[a]	.1257	18700	148.8	.0097	15.3
3B	.1258	20360	161.8	.0098	16.5
27B	.1270	17320	136.4	.0097	14.1
15C	.1260	18600	147.6	.0099	14.9
30C	.1278	19190	150.2	.0101	14.5
Average			141.7 + 20.1 - 23.0	.0092 +.0009 -.0027	15.4 + 2.9 - 1.9

a - Coupon failed along a 45° angle

TABLE 9B

TENSION TEST RESULTS

OF LAMINATE 2 COUPONS

(Sample Size = 20)

Sample ID	Average Area, mm^2	Ultimate Load, P_{ult}, kN	Ultimate Stress σ_{ult}, MPa	Ultimate Strain ε_{ult}, mm/mm in 50.8 mm	Apparent Modulus of Elasticity, E_2, GPa
727-29A	81.8	83.0	1015	.0095	107
8B	82.6	83.4	1011	.0099	102
10B	84.1	79.2	942	.0086	110
32B	82.7	85.8	1038	.0092	113
12C	81.5	75.0	920	.0088	105
728-30A	83.5	74.7	895	.0081	110
21B	84.5	78.4	927	.0082	113
35B	84.4	81.7	968	.0093	104
29C	82.7	84.8	1025	.0098	105
36C	83.9	81.5	971	.0090	108
696-14A	80.8	78.6	974	.0095	103
15A	82.4	79.3	962	.0098	99.3
31A	82.6	67.6	818	.0065	126
24B	81.5	76.5	938	.0101	93.1
25C	81.2	81.4	1002	.0094	107
699- 2A[a]	81.1	83.2	1026	.0097	105
3B[a]	81.2	90.6	1116	.0098	114
27B	81.9	77.0	940	.0097	97.2
15C	81.3	82.7	1018	.0099	103
30C	82.4	85.4	1036	.0101	100
Average			977 + 139 - 159	.0092 +.0009 -.0027	106 20 - 13

a - Coupon failed along a 45^{o} angle

failure strengths. The laminate 2 coupon which had the lowest failure strength, 696-31A, was observed to have the largest amount of delamination. A summary of the static tension results comparing the two laminates is shown in Table 10. Data scatter was larger for laminate 2 coupons than for laminate 1 which was anticipated because of the large number of 0° fibers in laminate 2. Notice in Table 10 that the strain to failure of the two laminates differed by less than 5%.

Figures 38 and 39 show comparisons of the predicted versus experimental average stress-strain curves for the two laminates. Predicted moduli of elasticity for laminate 1 were close to the experimental values, however, the 45° ply failure strain was underestimated and the strain to failure overestimated, see Figure 38. For laminate 2, the modulus of elasticity was also accurately predicted and the strain to failure over esimated, see Figure 39. The comparison results were not surprising in view of the derth of ply data on this material available prior to the research program.

Table 11 summarizes the analytically derived Weibull parameters for the static tension test data of the two laminates. Notice that for this static data, the difference between a two or three parameter Weibull function was negligible although as the fit terms indicate, the three parameter function was slightly better. For both laminates, R was quite high and Fit low. In Table 12 the relationship between probability of survival and expected ultimate tensile strength is tabulated for the two laminates while Figures 40 and 41 show the relationship in a plotted format. Those two figures show the accuracy of the three parameter Weibull fit to the data.

An eleventh laminate 1 panel was manufactured from the same batch of material used for and at the same time as laminate 2 panels. Coupons from this panel, in addition to those from the other panels, were used to evaluate the long life fatigue characteristics of laminate 1 under tension-compression fatigue loading. Table 13 shows results of the tension test evaluation of the panel. The average of the five tests was virtually the same as that for the previous

TABLE 10

SUMMARY OF STATIC TENSION TEST RESULTS

	Avg. Ultimate Stress, σ_{ult}, MPa (ksi)	Avg. Ultimate Strain, ε_{ult}, mm/mm in 50.8 mm	Avg. Initial Apparent Modulus of Elasticity, E_A, GPa (psi x 10^6)
LAMINATE 1	477 (69.2)[a] + 43 (6.2), 9% - 50 (7.2), 10%	0.0096 +0.0011, 11% -0.0010, 10%	52.7 (7.64) + 3.7 (0.54), 7% - 4.8 (0.69), 9%
LAMINATE 2	977 (141.7) +139 (20.1), 14% -140 (20.3), 14%	0.0092 +0.0009, 10% -0.0027, 29%	106 (15.4) + 20 (2.9), 19% - 13 (1.9), 12%

a - Based on minimum area

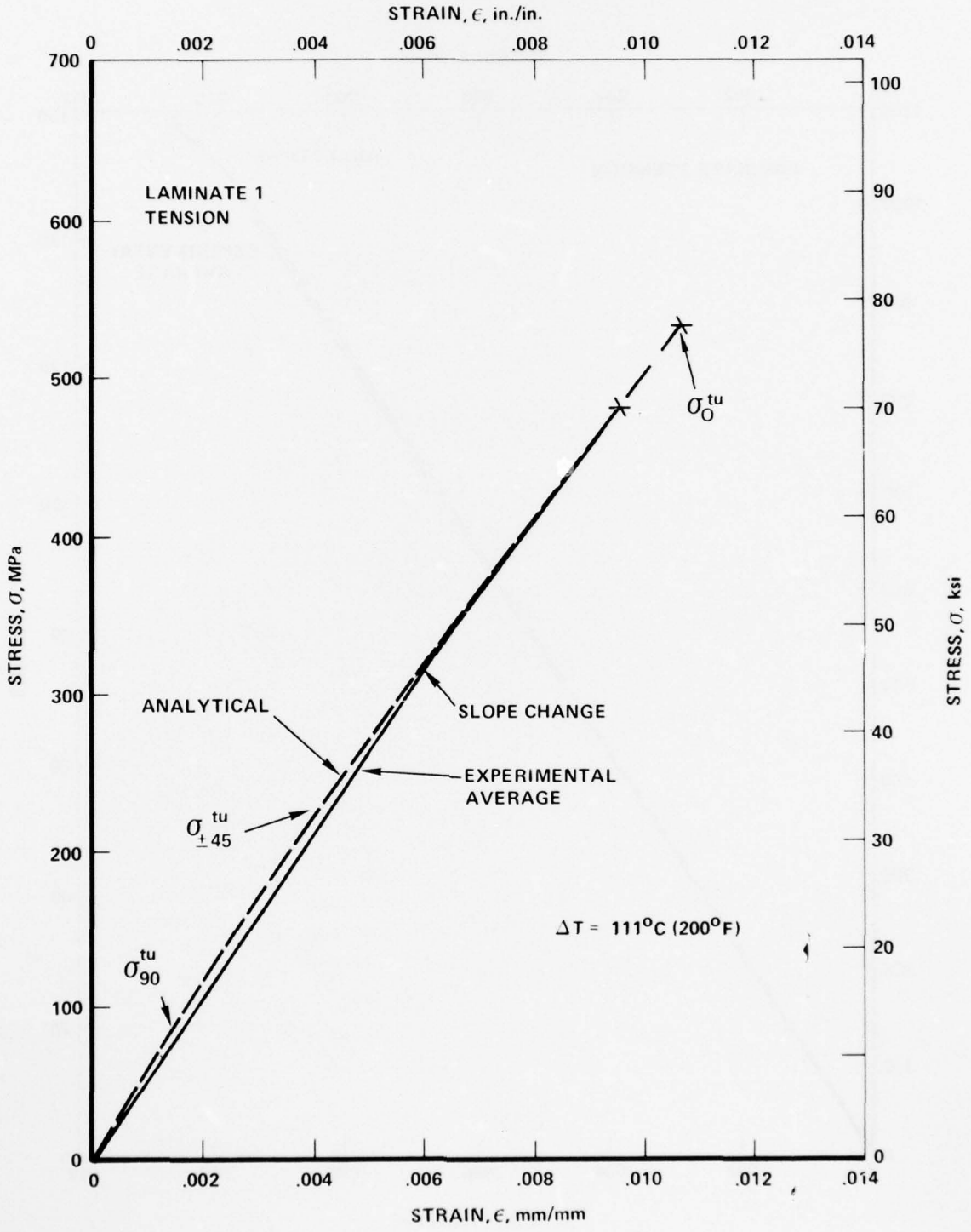


Figure 38. Comparison Between Predicted and Experimental Average Tension Stress-Strain Curves for Laminate 1

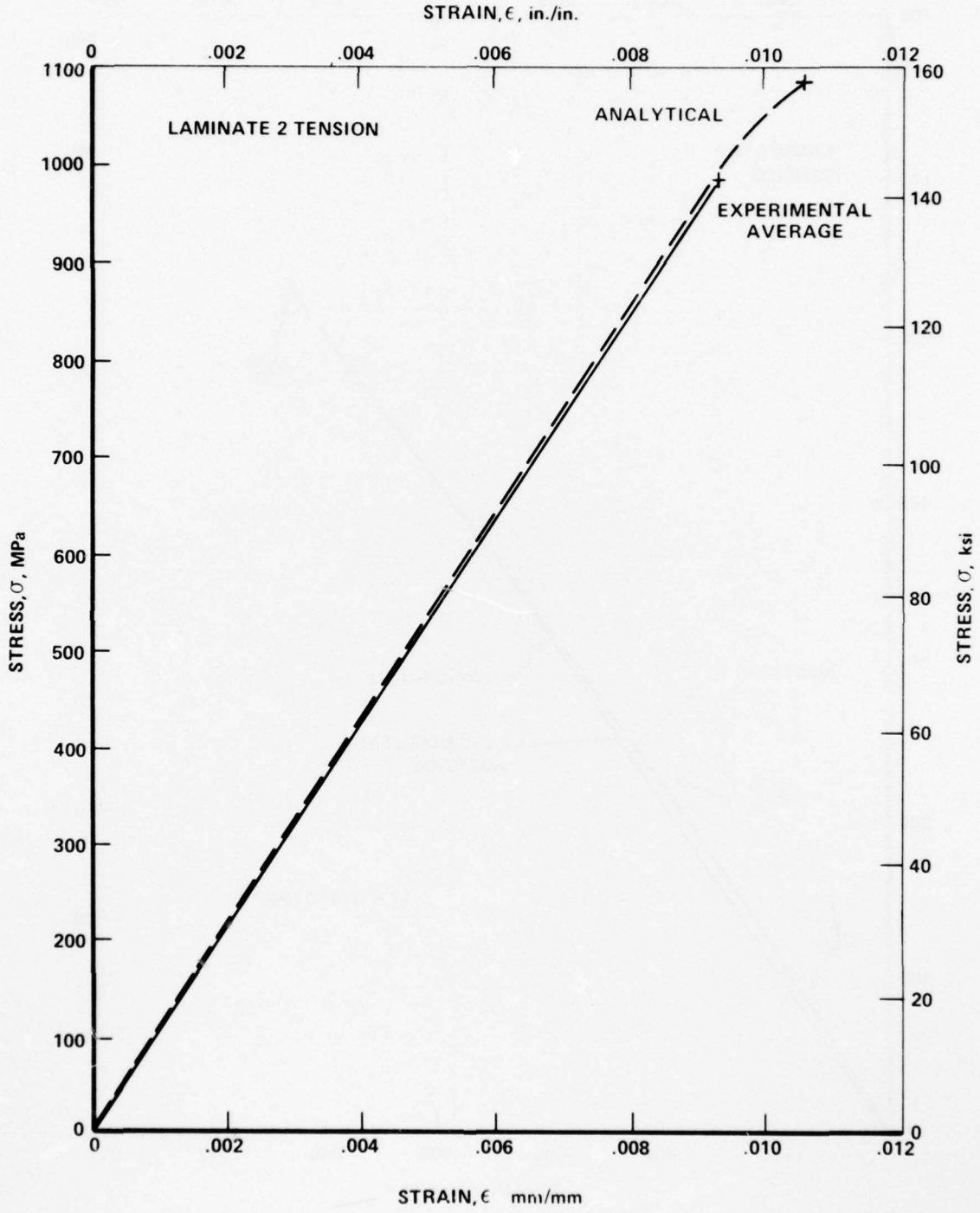


Figure 39. Comparison Between Predicted and Experimental Average Tension Stress-Strain Curves for Laminate 2

TABLE 11

SUMMARY OF STATIC TENSION TEST PARAMETERS

	Number of Weibull Parameters	Weibull Coefficients			Correlation Coefficient, R	Fitting Coefficient, FIT
		k	e	v		
LAMINATE 1	3	24.750	-0.075323	70.500	0.99947	0.00101
	2	24.1227	0	70.571	0.99947	0.00104
LAMINATE 2	3	18.8662	-0.430439	144.407	0.99868	0.00253
	2	18.680	0	144.811	0.99867	0.00268

$$P(x) = \exp\left[-\left(\frac{x-e}{v-e}\right)^{k}\right]$$

FOR 2 PARAMETERS, $\alpha = k$, $\hat{F} = v$

TABLE 12

RELATIONSHIP[a] BETWEEN
PROBABILITY OF SURVIVAL
AND ULTIMATE TENSION STRENGTH

Probability of Survival P(i)	Ultimate Tensile Strength, σ_{ult}, MPa(ksi)	
	Laminate 1	Laminate 2
.99	402 (58.3)	780(113.1)
.95	430 (62.3)	850(123.3)
.9	443 (64.2)	883(128.1)
.8	457 (66.3)	919(133.3)
.7	466 (67.6)	942(136.7)
.6	473 (68.6)	960(139.3)
.5	478 (69.4)	976(141.6)
.4	484 (70.2)	991(143.7)
.3	489 (71.0)	1005(145.8)
.2	496 (71.9)	1021(148.1)
.1	503 (73.0)	1040(150.9)
.05	509 (73.8)	1056(153.1)
.01	518 (75.1)	1080(156.6)

a - Strength values were calculated based on a 3-parameter Weibull Fit to the Data.

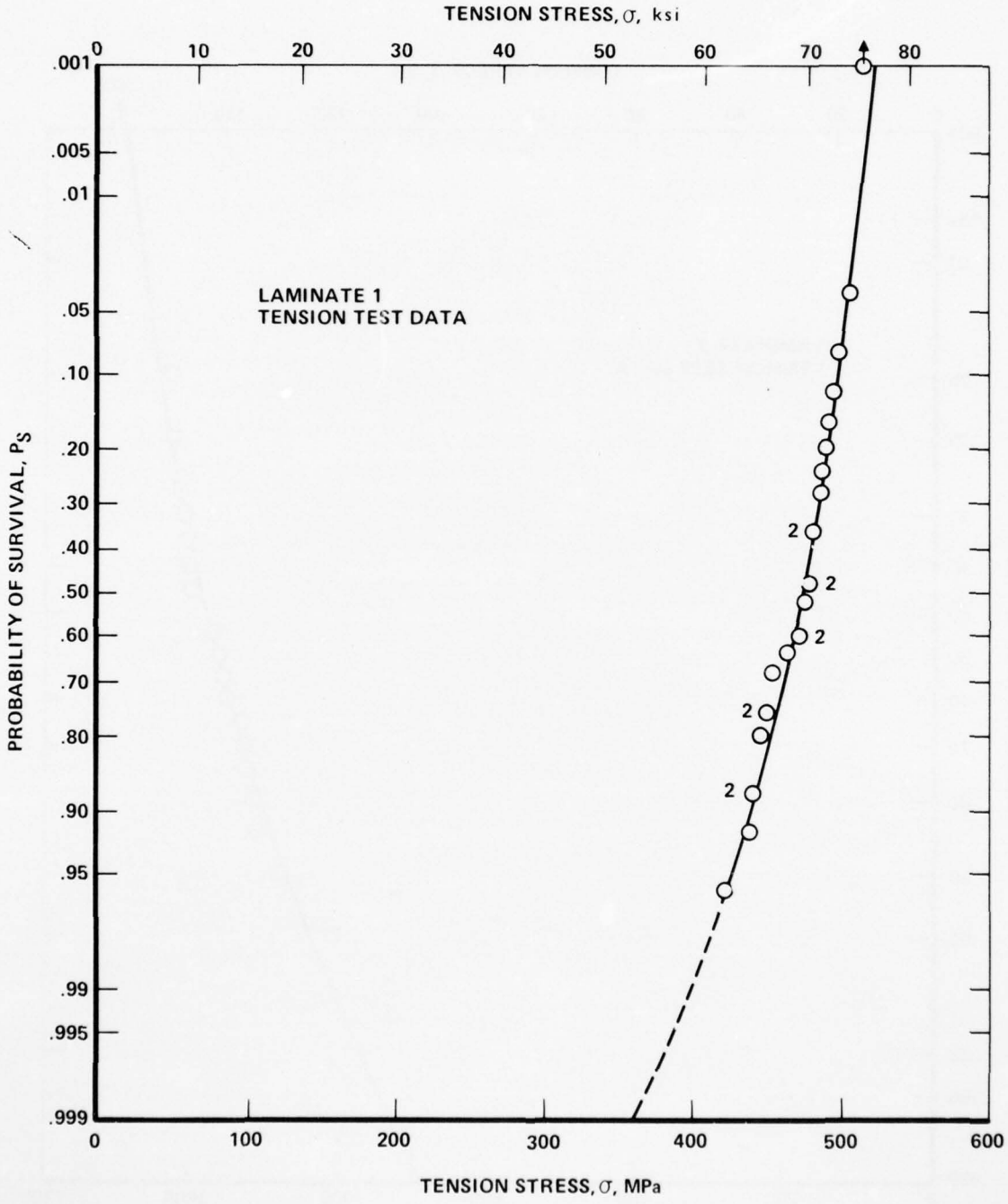


Figure 40. Probability of Survival Versus Ultimate Tension Strength for Laminate 1 Coupons

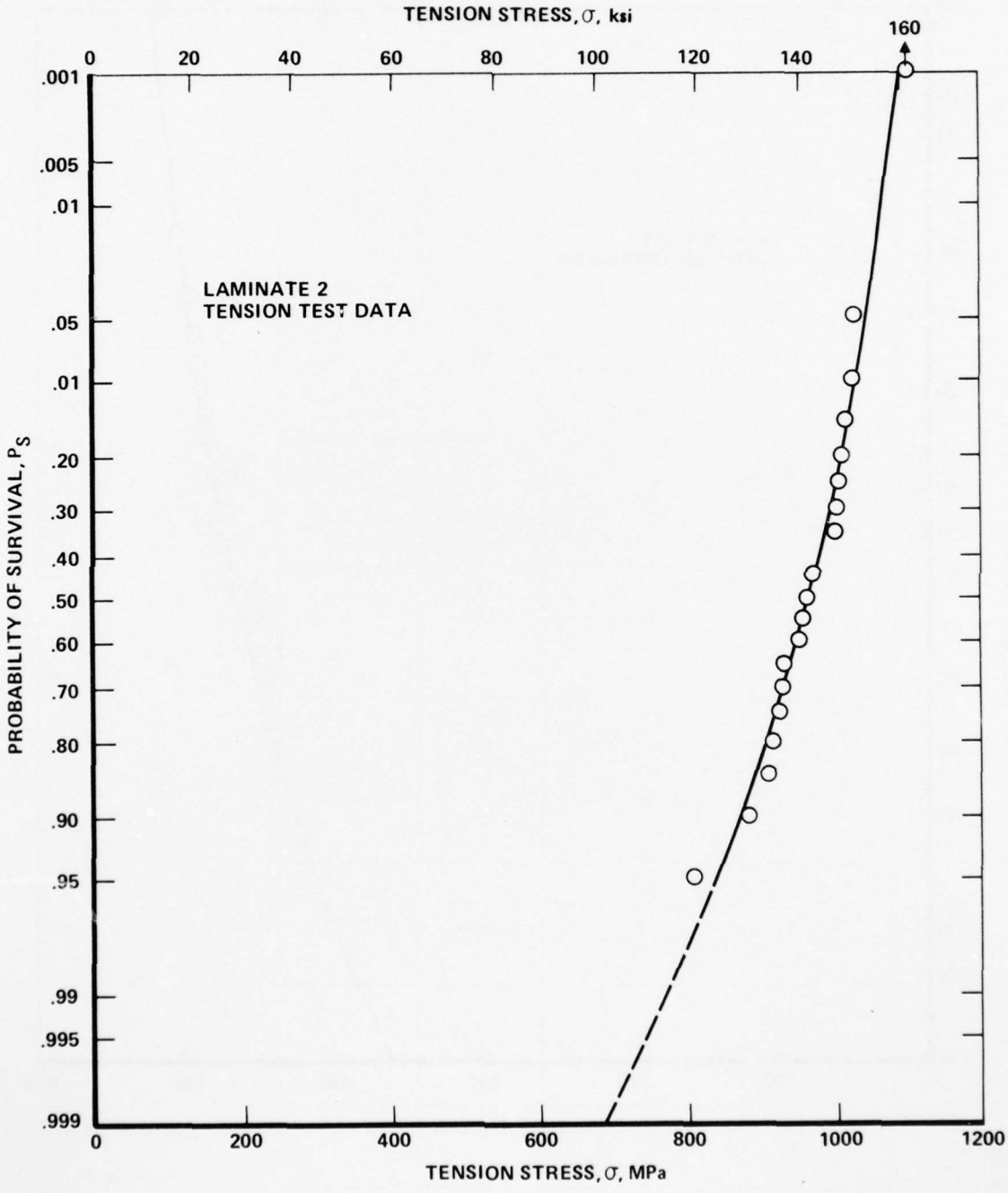


Figure 41. Probability of Survival Versus Ultimate Tension Strength for Laminate 2 Coupons

TABLE 13A

TENSILE TEST RESULTS FOR PANEL 1NH 693, LAMINATE 1

Sample ID	Min. Area $in.^2$	Ultimate Load, P_{ult}, lbs	Ultimate Stress σ_{ult}, ksi	Ultimate Strain, ε_{ult}, in./in. in 2.0 in.	Slope Deviation Load, P_y, lbs	Slope Deviation Stress, σ_y, ksi	Slope Deviation Strain, ε_y, in./in. in 2.0 in.	Initial Appar. Modulus of Elasticity, E_{1a}, psi x 10^6	Final Appar. Modulus of Elasticity, E_{1b}, psi x 10^6
693- 4A	.0852	6740	79.1	.0104	4300	50.5	.0062	7.82	6.18
-11B	.0853	5640	66.1	.0091	3800	45.1	.0056	7.82	6.51
-17B	.0876	5620	64.2	.0089	4500	51.4	.0068	7.61	6.34
- 8C	.0853	5920	69.4	.0090	4300	50.4	.0062	7.33	6.51
-19C	.0861	6100	70.8	.0101	3800	44.1	.0058	7.26	6.11
Average			69.9	.0095		48.3	.0061	7.57	6.33
Panel 693			+ 9.2	+.0009		+ 2.2	+.0007	+0.44	+0.18
			- 5.7	-.0006		- 3.1	-.0003	-0.31	-0.22
Average			69.2	.0096		45.3	.0059	7.64	6.48
Panels 578 to 606			+ 6.2	+.0011		+ 6.9	+.0010	+0.54	+0.70
			- 7.2	-.0010		-10.7	-.0012	-0.69	-0.68

TABLE 13B

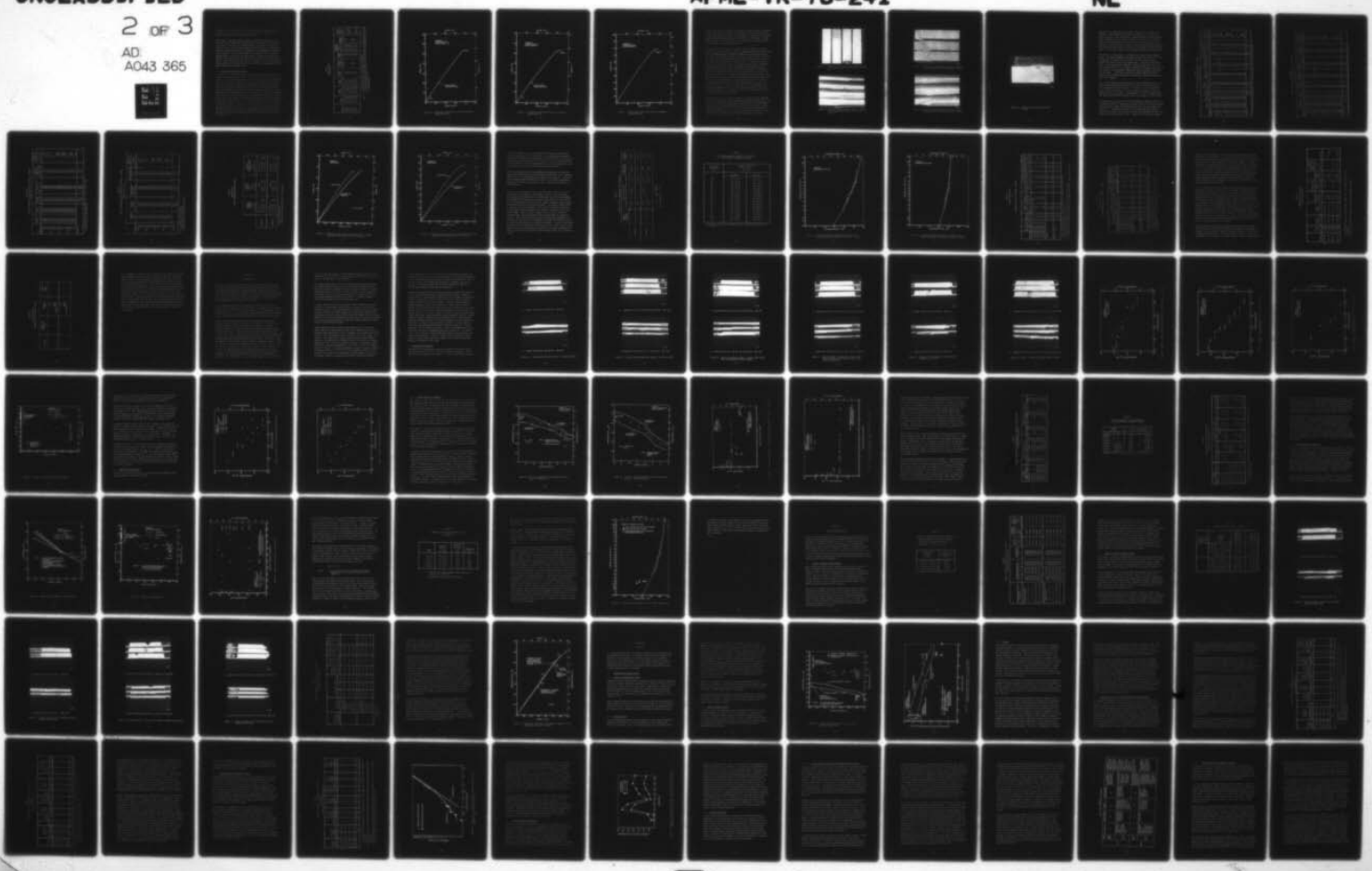
TENSILE TEST RESULTS FOR PANEL 1NH 693, LAMINATE 1

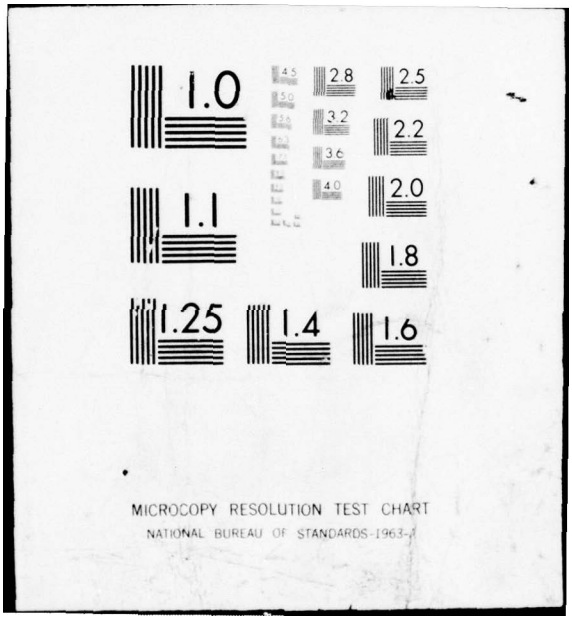
Sample ID	Min. Area mm^2	Ultimate Load P_{ult}, kN	Ultimate Stress, σ_{ult} MPa	Ultimate Strain ε_{ult}, mm/mm in 50.8 mm	Slope Deviation Load, P_y, kN	Slope Deviation Stress, σ_y, MPa	Slope Deviation Strain, ε_y, mm/mm in 50.8 mm	Initial Appar. Modulus of Elasticity, E_{1a}, GPa	Final Appar. Modulus of Elasticity, E_{1b}, GPa
693- 4A	55.0	30.0	545	.0104	19.1	348	.0062	53.9	42.6
-11B	55.0	25.1	456	.0091	17.3	311	.0056	53.9	44.9
-17B	56.5	25.0	443	.0089	20.0	354	.0068	52.5	43.7
- 8C	55.0	26.3	478	.0090	19.1	347	.0062	50.5	44.9
-19C	55.5	27.1	488	.0101	16.9	304	.0058	50.0	42.1
Average			482	.0095		333	.0061	52.2	43.6
Panel 693			+ 63	+.0009		+ 15	+.0007	+ 3.0	+ 1.2
			- 39	-.0006		-21	-.0003	- 2.1	- 1.5
Average			477	.0096		312	.0059	52.7	44.7
Panels 578 to 606			+ 43	+.0011		+ 48	+ .0010	+ 3.7	+ 4.8
			- 50	-.0010		- 74	- .0012	- 4.8	- 4.7

AD-A043 365 LOCKHEED-CALIFORNIA CO BURBANK RYE CANYON RESEARCH LAB F/G 11/4
ASCERTAINMENT OF THE EFFECT OF COMPRESSIVE LOADING ON THE FATIG--ETC(U)
DEC 76 J T RYDER, E K WALKER F33615-75-C-5118

UNCLASSIFIED AFML-TR-76-241 NL

2 OF 3
AD
A043 365




1.0
1.1
1.25
1.4
1.6
1.8
2.0
2.2
2.5
2.8
3.2
3.6
4.0
4.5
5.0
5.6
MICROCOPY RESOLUTION TEST CHART
NATIONAL BUREAU OF STANDARDS-1963-A

10 panels. This good agreement gave some indication of a possible low variability in static tension results from batch-to-batch of prepreg provided panels are manufactured soon after batch receipt.

Eight tension tests were conducted using coupons of both laminates 1 and 2, but with "T" type longitudinal and transverse strain gages. Table 14 lists test results. Note that the apparent moduli of elasticity were the same using the strain gages as those determined previously using an extensometer. However, the strains to failure as recorded by the extensometer did not have precise agreement with the longitudinal strain gages for two of the three coupons tested. The last two columns of Table 14 show that essentially no hysteresis was observed when the coupons were subjected to five repeated load cycles. These results indicated that if the apparent elastic modulus changes during fatigue such a change must be due to a gradual and progressive form of damage throughout the fatigue loading.

4.2 Static Compression Test Results

Figures 42 to 44 show static compression stress-strain curves for particular coupons, but which are representative of the types of curves seen for all test coupons. For laminate 1, stress-strain curves exhibited an initial straight portion of the curve, designated E_{1c} in Figure 42, followed by a continuously curved portion with an average slope approximately 10 percent less than E_{1c}. Just prior to failure of laminate 1 coupons, distinct popping sounds were heard each accompanied by small but noticeable horizontal jumps in the stress-strain curve not observable at the scale of Figure 42. Failure was sudden and "brittle-like", called failure mode 1, for approximately half of the coupons, Figure 42, and "flat topped" followed by brittle failure, called failure mode 2, for the other coupons, Figure 43. Post failure examinations of coupons showed no observable difference between those which failed as in Figure 42, compared to those which failed as in Figure 43. Coupons appeared to fail as soon as some small instability occurred provided some critical load had been reached. The practical differences between the two apparently different failure modes, indicated by their stress-strain diagrams, were considered at this point to be insignificant.

TABLE 14

TENSION TEST RESULTS
USING STRAIN GAGES

Sample ID	Area, mm^2 ($in.^2$)	Ultimate Load P_{ult}, kN(lbs)	Ultimate Stress σ_{ult}, MPa(ksi)	Longitudinal Ultimate Strain ϵ_L, mm/mm	Extensometer Ultimate Long. Strain ϵ_L, mm/mm in 50.8 mm	Transverse Ultimate Strain ϵ_T, mm/mm	Apparent Longitudinal Modulus of Elasticity, E_{AL}, GPa(psi x 10^6)	Number of Hysteresis Loops	Maximum Stress of Hysteresis Loop MPa(ksi)
582-24A[a]	53.2 (.0825)	24.4 (5480)	458 (66.4)	.0092	.0087	-.0028	52.0 (7.55)[b]	None	-
594-15A[a]	53.2 (.0826)	25.6 (5760)	480 (69.7)	.0098	-	-.0031	51.1 (7.41)[b]	5	451 (65.4)[d]
596-11B[a]	54.1 (.0838)	24.3 (5460)	450 (65.2)	.0086	-	-.0024	54.0 (7.84)[b]	5	352 (51.1)[e]
606-1A[a]	52.5 (.0814)	24.1 (5420)	459 (66.6)	.0088	-	-.0022	53.9 (7.82)[b]	5	433 (62.8)[e]
696-34B	81.5 (.1264)	64.8 (14580)	795 (115.3)	.0075	.0075	-.0049	106 (15.4)[c]	None	-
699-17C	83.7 (.1297)	84.2 (18940)	1007 (146.0)	.0098	.0090	-.0063	103 (14.9)[c]	None	-
727-13B	81.6 (.1265)	88.5 (19900)	1084 (157.3)	.0104	-	-.0068	104 (15.1)[c]	5	787 (114.2)[e]
728-7A	83.4 (.1292)	86.2 (19380)	1034 (150.0)	.0102	-	-.0064	101 (14.7)[c]	5	785 (113.9)[e]

Notes:
a - The ultimate stress for these coupons was based on average area
b - Initial Slope for Laminate 1; Previous average of 52.7 GPa(7.64 psi x 10^6), this average 52.7 GPa (7.65 psi x 10^6)
c - Average Slope for Laminate 2; Previous average of 106 GPa (15.4 psi x 10^6), this average 103 GPa (15.0 psi x 10^6)
d - Small amount of apparent hysteresis
e - No apparent hysteresis

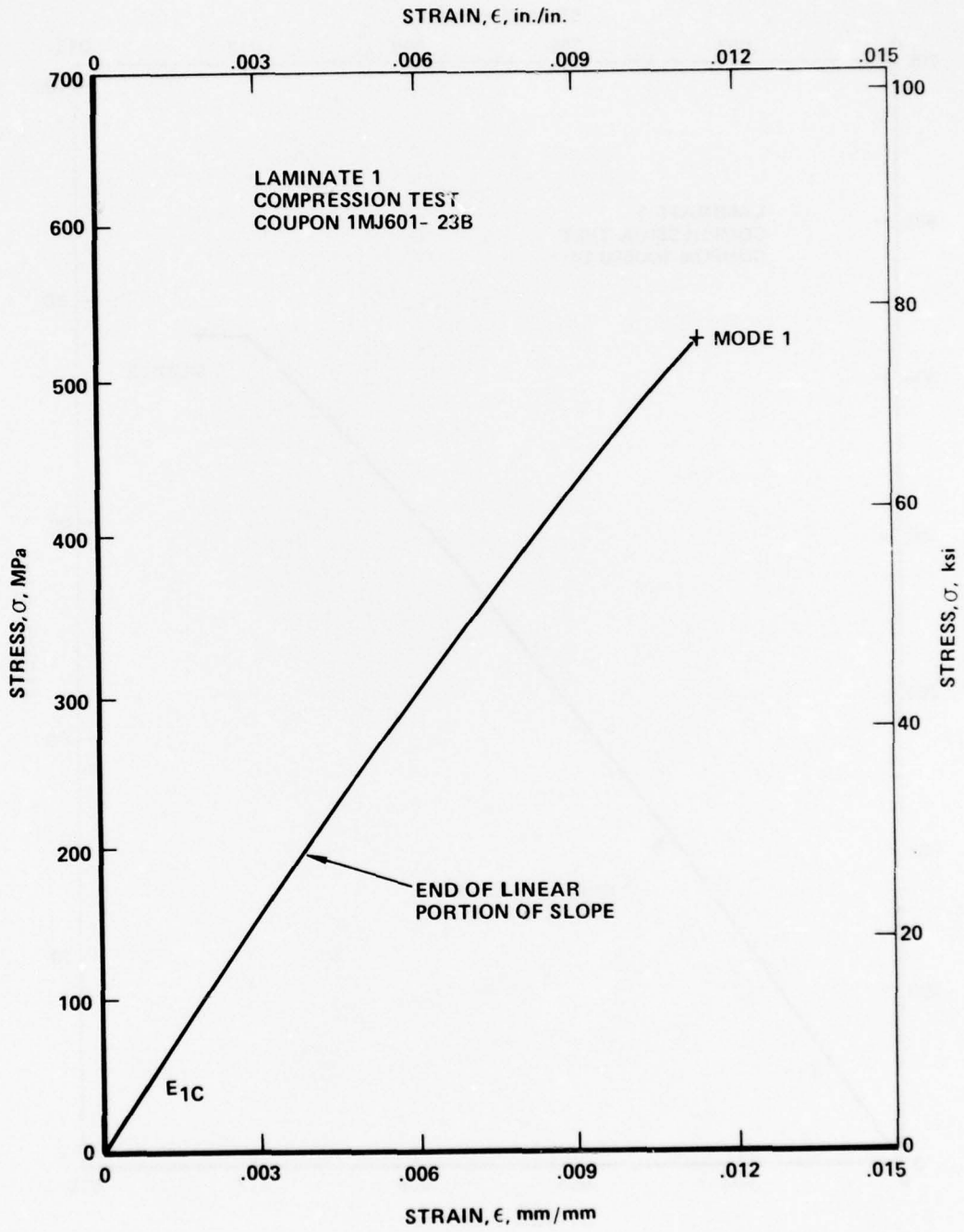


Figure 42. Compression Stress-Strain Curve for Laminate 1 Coupon 1MJ601-23B

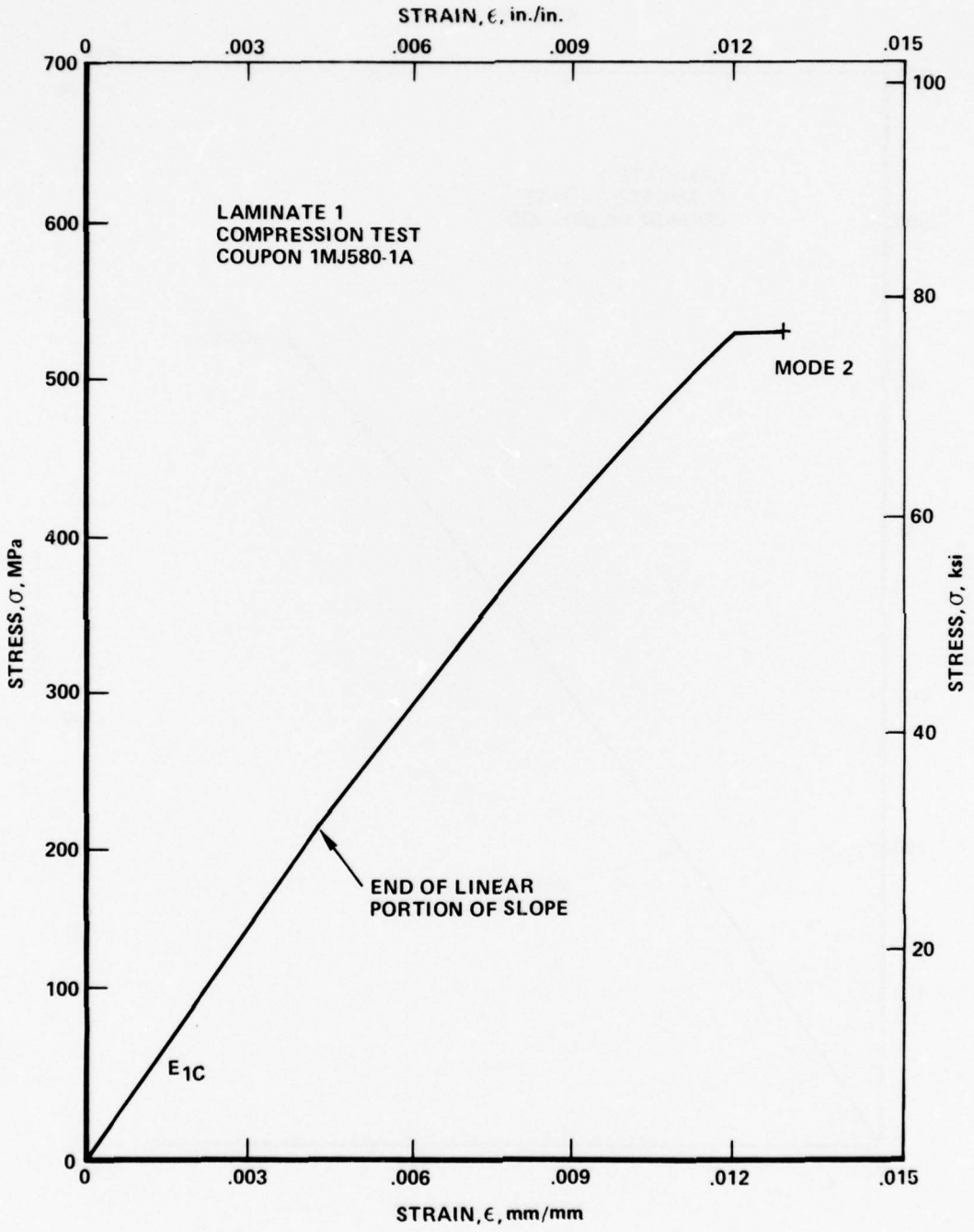


Figure 43. Compression Stress-Strain Curve for Laminate 1 Coupon 1MJ580-1A

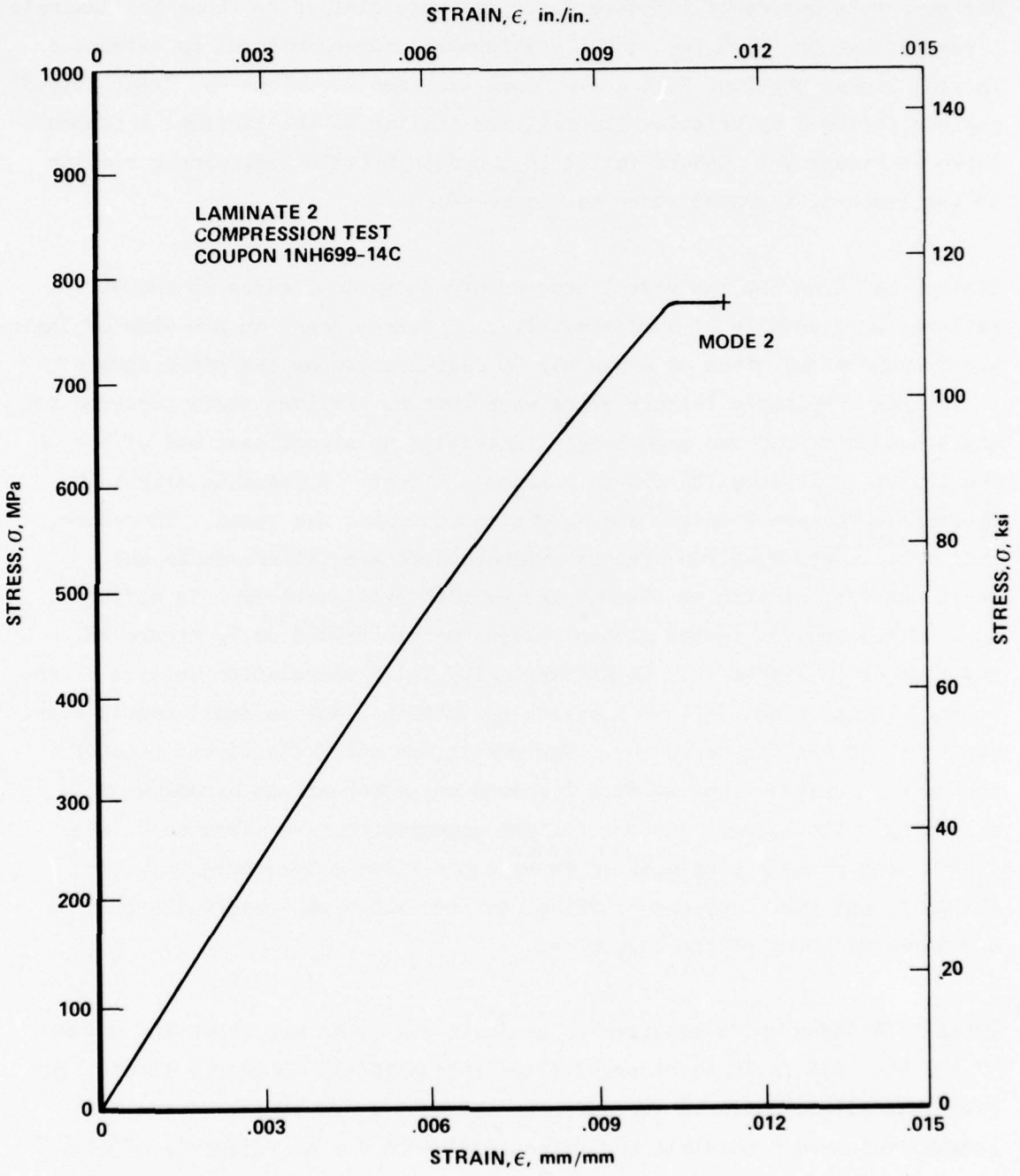


Figure 44. Compression Stress-Strain Curve for Laminate 2 Coupon 1NH699-14C

Stress-strain curves of laminate 2 coupons were similar to those for laminate 1 except that the test record was continuously curved without an extensive initial linear portion, Figure 44. Some laminate 2 coupons had "flat topped" regions followed by brittle-like failures similar to the laminate 1 coupon shown in Figure 43. Others failed in a sudden brittle-like manner similar to the laminate 1 coupon shown in Figure 42.

Typical failures for laminate 1 coupons are shown in Figures 45 and 46. Failures were usually at approximately a 45 degree angle on one side of laminate 1 coupons and often at a roughly 90 degree angle on the other side of the coupon. Multiple failure zones were common. Failure zones occurred at any location within the gage length indicating no significant end effect on the failure zone location due to Poisson's effect. A possible slight influence on failure location due to the extensometer was noted. Therefore, additional tests were run without extensometers and failure modes and locations were similar to coupons tested with extensometers. In addition, some of the coupons tested without extensometers failed as in Figure 42, and some as in Figure 43. No statistically valid correlation between extensometer location and failure location was obtained due to small sample size, but some correlation was noted. The result was not definitive. None of the coupons tested from laminate 1 showed any apparent end brooming or splitting. The lateral support fixture appeared to have adequately prevented such phenomena as well as to have prevented column buckling. An insignificant amount of end crushing occurred which was observable only as a slight smoothing of the coupon end.

Typical failures which occurred in laminate 2 coupons are shown in Figures 47 and 48. All failures occurred along approximately 45 degree lines. The fact that all failures occurred within the bottom 1/2 of the coupon gage length indicated a possible end effect influence due to Poisson's effects. Figure 49, a magnified photo of the end of a typically failed laminate 2 coupon, illustrates that despite a possible Poisson's end effect on failure location, no end brooming or splitting was observed for any coupons.

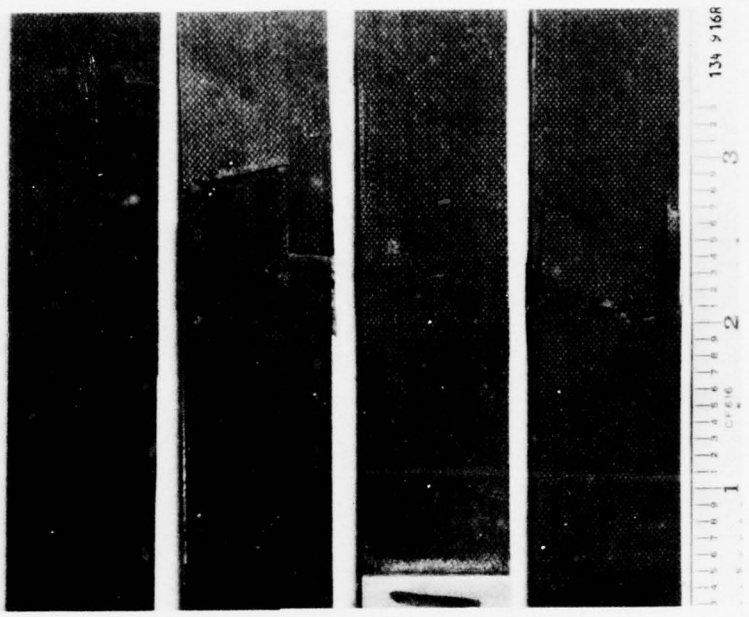


Figure 45. Laminate 1 Failed Coupons; Specimens, Numbered Left to Right, are: 603-26A, 596-2B, 601-17B, 601-5A

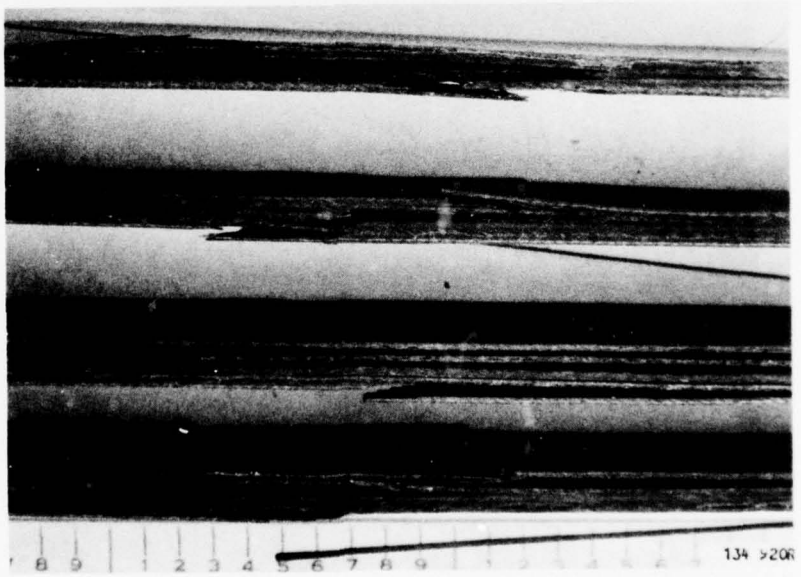


Figure 46. Laminate 1 Failed Coupons; Specimens Numbered Top to Bottom, are: 601-5A, 601-17B, 596-2B, 603-26A

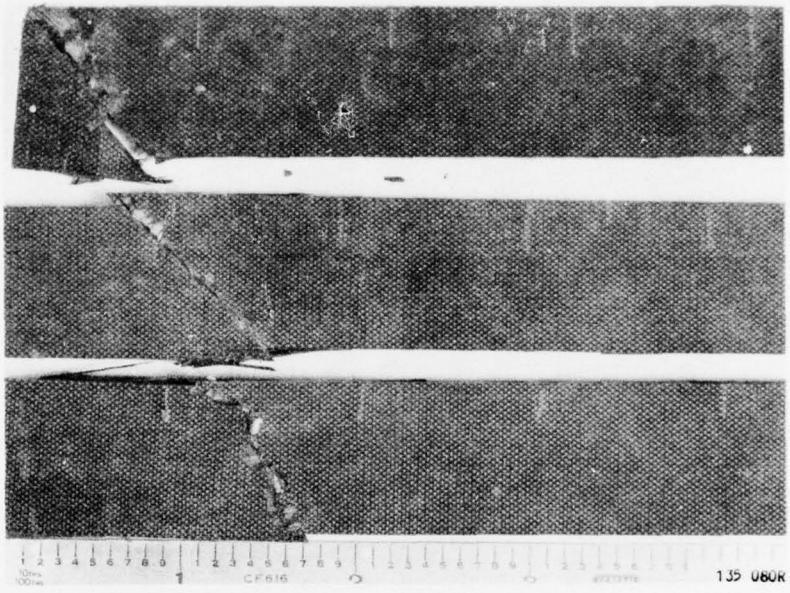


Figure 47. Laminate 2 Failed Coupons; Specimens, Numbered Top to Bottom, are: 727-34A, 699-29C, 728-12B

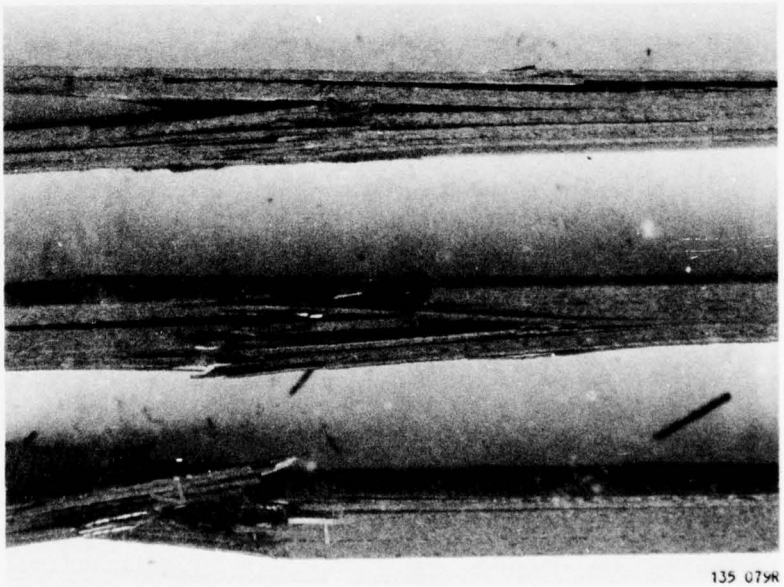


Figure 48. Laminate 2 Failed Coupons; Specimens, Numbered Top to Bottom, are: 728-12B, 699-29C, 727-34A

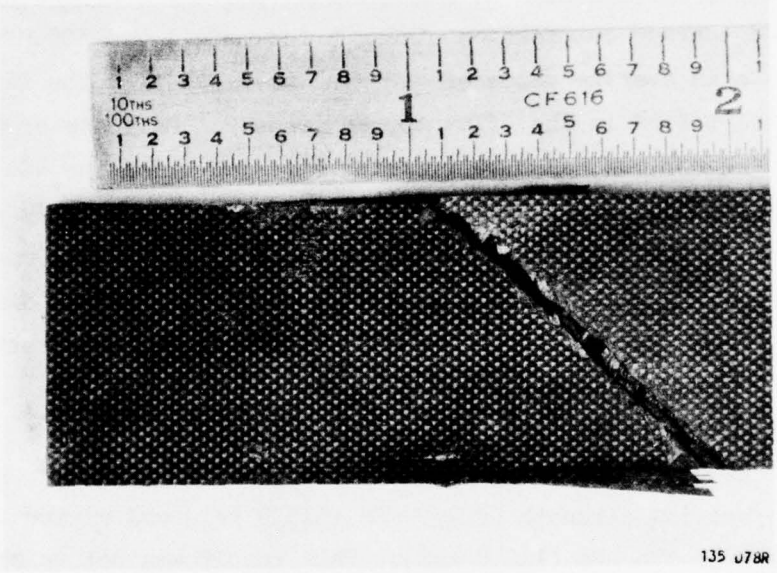


Figure 49. Laminate 2 Failed Coupon; Specimen 728-10B

Tabulated static compression test results. Tables 15 and 16, showed, as expected, a higher compression strength for laminate 2. In Table 15 the stress and strain values for laminate 1 coupons at which the slope deviated from a straight line were somewhat subjective and should not be construed as precise measurements since a best fit-by-eye technique was used. For laminate 2, the slope, being an average value, was again somewhat subjective. The ultimate strains listed are the strain values either to failure (curves without a "flat topped" region) or to the point where the curve became flat.

For laminate 1, failure mode 1. was observed in eleven of the 26 coupons tested. The average compression strength for mode 1 was 505 MPa (73.2 ksi) as opposed to an average value of 463 MPa (67.1 ksi) for the fifteen coupons which failed in the "flat topped" mode 2. Only one of the eleven mode 1 failure coupons had a compression strength below the 481 MPa (69.7 ksi) average value for all 26 coupons. These results strongly suggested that for laminate 1, the compression strength for mode 2 failures was less than that for mode 1. This result indicated a possible physical difference between the failure modes which was not observable in post fracture examination of the coupons.

Nine of the 20 laminate 2 coupons listed in Table 16 failed in mode 1 at an average compression strength of 799 MPa (115.9 ksi) and eleven in mode 2 at an average of 778 MPa (112.8 ksi). This result was not as significant as the result for laminate 1, but again suggested an apparent difference between the two failure modes. Interestingly, 10 of the 20 coupons failed away from the bottom within the gage length and of these 9 failed in mode 2.

The compression test results of the two laminates are compared in Table 17. As expected, laminate 2 coupons were stronger, however, the ultimate stresses and strains may be lower than theoretical because of the test method (see Section 2.4). Comparison of Tables 10 and 17 shows that for laminate 1, scatter in the tension data was less than for the compression data while the reverse was true for laminate 2 data. Figures 50 and 51 show comparisons

TABLE 15A

STATIC COMPRESSION TEST RESULTS OF LAMINATE 1 COUPONS

(Sample Size = 26)

Sample ID	Min. Area, $in.^2$	Ultimate Load, P_{ult}, lbs	Ultimate Stress σ_{ult}, ksi	Ultimate Strain ε_{ult}, in./in. in 2.0 in.	Load at Initial Curve Deviation, P_{CD}, lbs	Stress at Initial Curve Deviation, σ_{CD}, ksi	Strain at Initial Curve Deviation, ε_{CD}, in./in. in 2.0 in.	Initial Apparent Modulus of Elasticity, E_{IC}, psi x 10^6	Amount of Strain at Ultimate Load, ε, in./in. in 2.0 in.
578-10B	.0828	6750	81.5	.0128	3260	39.4	.0056	7.09	0[a]
18A	.0856	6650	77.7	.0130	2870	33.5	.0048	6.98	.0006
9A	.0840	6180	73.6	.0120	3000	35.7	.0051	7.00	0
580-25A	.0824	5180	62.9	.0099	2660	32.3	.0048	6.73	.00045
1A	.0828	6360	76.8	.0118	2460	29.7	.0042	7.07	.0006
582-19B	.0823	6410	77.9	.0132	3010	36.6	.0056	6.59	0
10A	.0824	6340	76.9	.0123	σ-ε record continuous curve				.0006
583- 5A	.0824	5360	65.0	.0098	3330	40.4	.0057	7.09	.0018
4A	.0824	6070	73.7	.0113	2420	29.4	.0048	6.12	.0006
18A	.0860	6230	72.4	.0117	3130	36.4	.0052	6.93	0
16B	.0849	6560	77.3	.0128	3250	38.3	.0056	6.90	0
594-21B	.0813	5790	71.1	.0108	2800	34.4	.0050	6.96	.0006
14B	.0830	5660	68.2	.0108	1630	31.7	.0045	7.04	.00045
596-19A	.0809	5260	65.0	.0112	2760	34.1	.0050	6.82	.0006
25B	.0813	4890	60.2	.0106	2520	31.0	.0044	6.81	.0012
3B	.0820	5370	65.5	.0100	2670	32.6	.0045	7.24	.00045
601-23B	.0811	6280	77.4	.0114	3080	38.0	.0052	7.23	0
6A	.0819	5720	69.8	.0106	3150	38.5	.0057	6.75	0
603- 5A	.0822	6000	73.0	.0116	2520	30.7	.0045	6.81	0
14B	.0828	5380	65.0	.0100	2540	30.9	.0044	7.10	.0003
13B	.0819	5720	69.8	.0106	3150	38.5	.0057	6.75	0
604-20B	.0832	5300	63.7	.0102	2380	28.6	.0042	6.81	0
26B	.0816	4700	57.6	.0086	3180	39.0	.0054	7.22	.0006
19B	.0833	4820	57.9	.0085	3360	40.3	.0057	7.08	.0003
606-20A	.0829	5260	63.4	.0099	2780	33.5	.0046	7.21	.0006
23A	.0806	5580	69.2	.0102	3090	38.3	.0052	7.37	0
Average			69.7	.0110		34.9	.0050	6.95	
			+11.8	+.0022		+5.5	+.0007	+0.42	
			-12.1	-.0025		-8.5	-.0008	-0.83	

a - A zero denotes that the coupon failed without a flat topped region prior to failure, see Figure 43.

TABLE 15B

STATIC COMPRESSION TEST RESULTS OF LAMINATE 1 COUPONS

(Sample Size = 26)

Sample ID	Minimum Area, mm^2	Ultimate Stress σ_{ult}, MPa	Ultimate Strain ε_{ult}, mm/mm in 50.8 mm	Stress at Initial Curve Deviation, σ_{CD}, MPa	Strain at Initial Curve Deviation ε_{CD}, mm/mm in 50.8 mm	Initial Apparent Modulus of Elasticity E_{IC}, GPA	Amount of Strain at Ultimate Load ε, mm/mm in 50.8 mm.
578-10B	53.4	561.9	.0128	271.6	.0056	48.9	0[a]
18A	56.0	535.7	.0130	231.0	.0048	48.1	.0006
9A	54.9	507.4	.0120	246.1	.0051	48.3	0
580-25A	53.9	433.7	.0099	222.7	.0048	46.4	.00045
1A	54.2	529.5	.0118	204.8	.0042	48.7	.0006
582-19B	53.8	537.1	.0132	252.3	.0056	45.4	0
10A	53.9	530.2	.0123	σ - ε record continuous curve			.006
583- 5A	53.9	448.2	.0098	278.5	.0057	48.9	.0018
4A	53.9	508.1	.0113	202.7	.0048	42.2	.0006
18A	56.2	499.2	.0117	251.0	.0052	47.8	0
16B	55.5	533.0	.0128	264.1	.0056	47.6	0
594-21B	53.2	490.2	.0108	237.2	.0050	48.0	.0006
14B	54.3	470.2	.0108	218.6	.0045	48.5	.00045
596-19A	52.9	448.2	.0112	235.1	.0050	47.0	.0006
25B	53.2	415.1	.0106	213.7	.0044	47.0	.0012
3B	53.6	451.6	.0100	234.8	.0045	49.9	.00045
601-23B	53.0	533.6	.0114	262.6	.0052	49.8	0
6A	53.6	481.2	.0106	265.4	.0057	46.5	0
603- 5A	53.8	503.3	.0116	211.7	.0045	47.0	0
14B	54.2	448.2	.0100	213.0	.0044	49.0	.0003
13B	53.6	481.2	.0106	265.4	.0057	46.5	0
604-20B	54.4	439.2	.0102	197.2	.0042	47.0	0
26B	53.3	397.1	.0086	268.9	.0054	49.8	.0006
19B	54.5	399.2	.0085	277.8	.0057	48.8	.0003
606-20A	54.3	437.1	.0099	231.0	.0046	49.7	.0006
23A	52.7	477.2	.0102	264.1	.0052	50.8	0
Average		480.6	.0110	240.6	.0050	47.9	
		+81.3	+.0022	+37.9	+.0007	+2.9	
		-83.5	-.0025	-43.4	-.0008	-5.7	

a--0 denotes that the coupon failed without a flat topped region prior to failure, see Figure 43.

TABLE 16A

STATIC COMPRESSION TEST RESULTS OF LAMINATE 2 COUPONS
(Sample Size = 20)

Sample ID	Average Area, $in.^2$	Ultimate Load, P_{ult}, lbs	Ultimate Stress, σ_{ult}, ksi	Ultimate Strain, ε_{ult}, in./in. in 2.0 in.	Apparent Modulus of Elasticity, E_A, psi x 10^6	Amount of Strain at Ultimate load, ε, in./in. in 2.0 in.
696-20A	.1295	13950	107.7	.0096	11.0	.0003
21A	.1303	14100	108.2	.0091	11.7	0[a]
28A	.1283	14300	111.4	.0088	12.3	.0011
11B	.1276	15125	118.5	.0101	11.6	0
14C	.1281	15050	117.5	.0102	11.0	.0008
699- 7A	.1303	13550	104.0	.0087	11.6	0
18A	.1286	15100	118.2	.0105	11.4	0
19B	.1277	15150	118.6	.0102	11.1	0
14C	.1281	15050	117.5	.0106	11.2	.0009
29C	.1273	14000	110.0	.0089	12.2	.0008
727-12A	.1262	14250	112.9	.0099	11.2	0
27A	.1234	14000	113.4	.0095	11.4	.0009
20B	.1281	14500	113.2	.0093	12.2	.0009
7C	.1277	15100	118.2	.0101	11.6	.0006
15C	.1290	15000	116.3	.0101	11.5	0
728-23A	.1322	15550	117.6	.0102	11.6	0
10B	.1322	15750	119.1	.0102	11.5	.0009
12B	.1294	13850	107.0	.0096	11.1	.0011
3C	.1289	16650	129.2	.0112	11.4	0
20C	.1319	14000	106.1	.0087	11.8	.0011
Average			114.2 + 15.0 - 10.2	.0098 +.0014 -.0011	11.5 + 0.8 - 0.5	

a - A 0 denotes that the coupon failed with a flat topped region prior to failure, see Figure 44.

TABLE 16B

STATIC COMPRESSION TEST RESULTS OF LAMINATE 2 COUPONS

(Sample Size = 20)

Sample ID	Average Area, mm^2	Ultimate Stress, σ_{ult}, MPa	Ultimate Strain ε_{ult}, mm/mm in 50.8 mm	Appar. Modulus of Elasticity E_A, GPa	Amount of Strain at Ultimate Load ε, mm/mm, in 50.8 mm
696-20A	84.7	742.6	.0096	75.8	.0003
21A	85.3	746.0	.0091	80.7	0[a]
28A	83.9	768.1	.0088	84.8	.0011
11B	83.5	817.0	.0101	80.0	0
14C	83.8	810.0	.0102	75.8	.0008
699- 7A	85.2	717.0	.0087	80.0	0
18A	84.1	815.0	.0105	78.6	0
19B	83.5	817.7	.0102	76.5	0
14C	83.8	810.1	.0106	77.2	.0009
29C	83.3	758.4	.0089	84.1	.0008
727-12A	82.6	778.4	.0099	77.2	0
27A	80.7	781.9	.0095	78.6	.0009
20B	83.8	780.5	.0093	84.1	.0009
7C	83.5	815.0	.0101	80.0	.0006
15C	84.4	801.9	.0101	79.3	0
728-23A	86.5	810.8	.0102	80.0	0
10B	86.5	821.2	.0102	79.3	.0009
12B	84.6	737.7	.0096	76.5	.0011
3C	84.3	890.8	.0112	78.6	0
20C	86.3	731.5	.0087	81.4	.0011
Average		787.4	.0098	79.3	
		+103.4	+.0014	+5.5	
		-70.4	-.0011	-3.5	

a - A 0 denotes that the coupon failed without a flat topped region prior to failure, see Figure 44.

TABLE 17

COMPARISON OF

STATIC COMPRESSION TEST RESULTS

	AVERAGE ULTIMATE STRESS, σ_{ult}, MPa (ksi)	AVERAGE ULTIMATE STRAIN, ε_{ult}, mm/mm in 50.8 mm	AVERAGE APPARENT MODULUS OF ELASTICITY, E_{avg}, GPa (psi x 10^6)
LAMINATE 1	481 (69.7)[a] +81 (11.8), 17% -82 (12.1), 17%	0.0110 +0.0022, 20% -0.0025, 23%	47.9 (6.95)[b] +2.0 (0.29), 4% -5.7 (0.83), 12%
LAMINATE 2	787 (114.2) +103 (15.0), 13% -70 (10.2), 9%	0.0098 +0.0014, 14% -0.0011, 11%	79.3 (11.5) +5.5 (0.8), 7% -3.4 (0.5), 4%

a - Based on minimum area

b - Average Initial Apparent Modulus of Elasticity

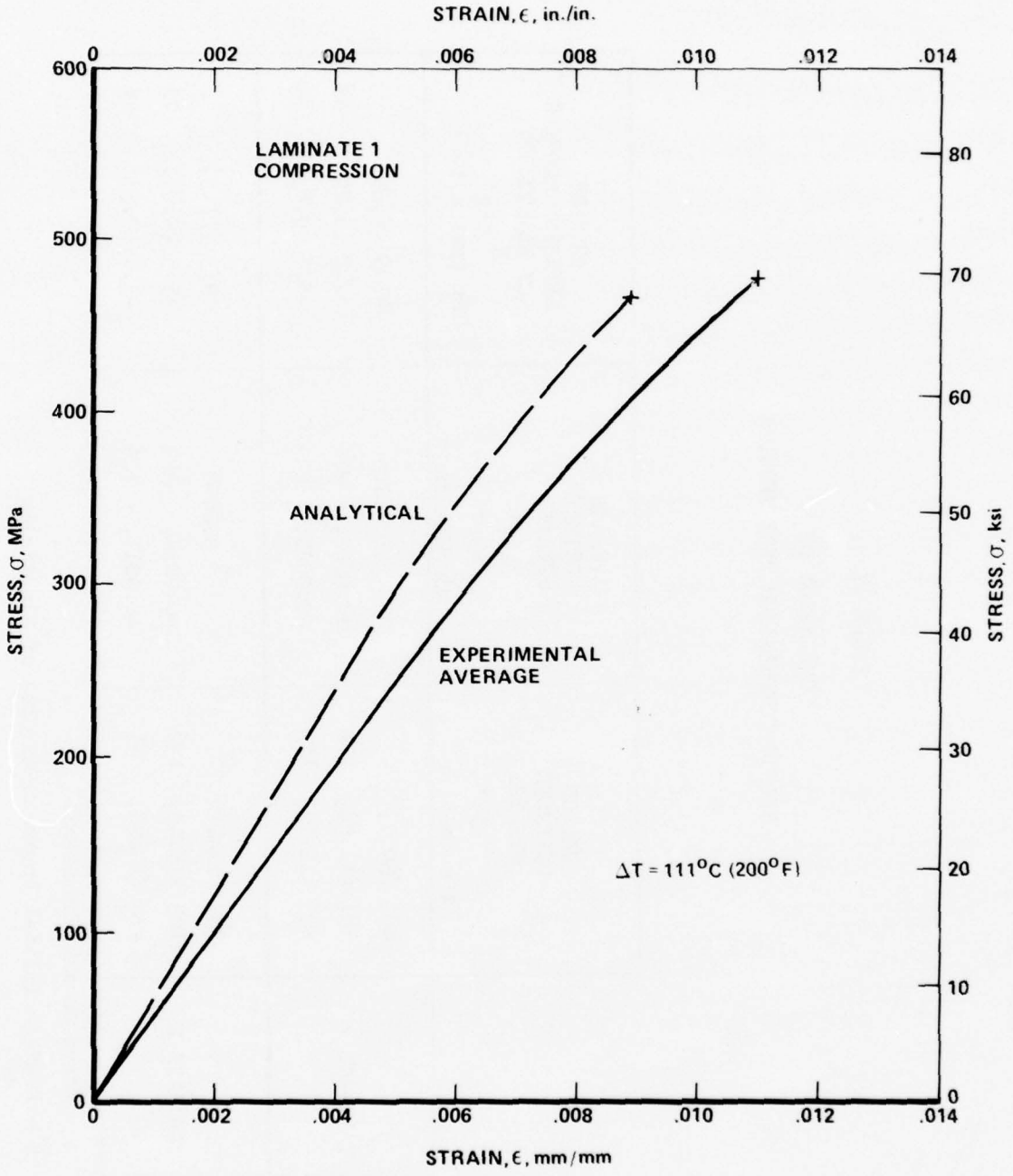


Figure 50. Comparison Between Predicted and Experimental Average Compression Stress-Strain Curves for Laminate 1

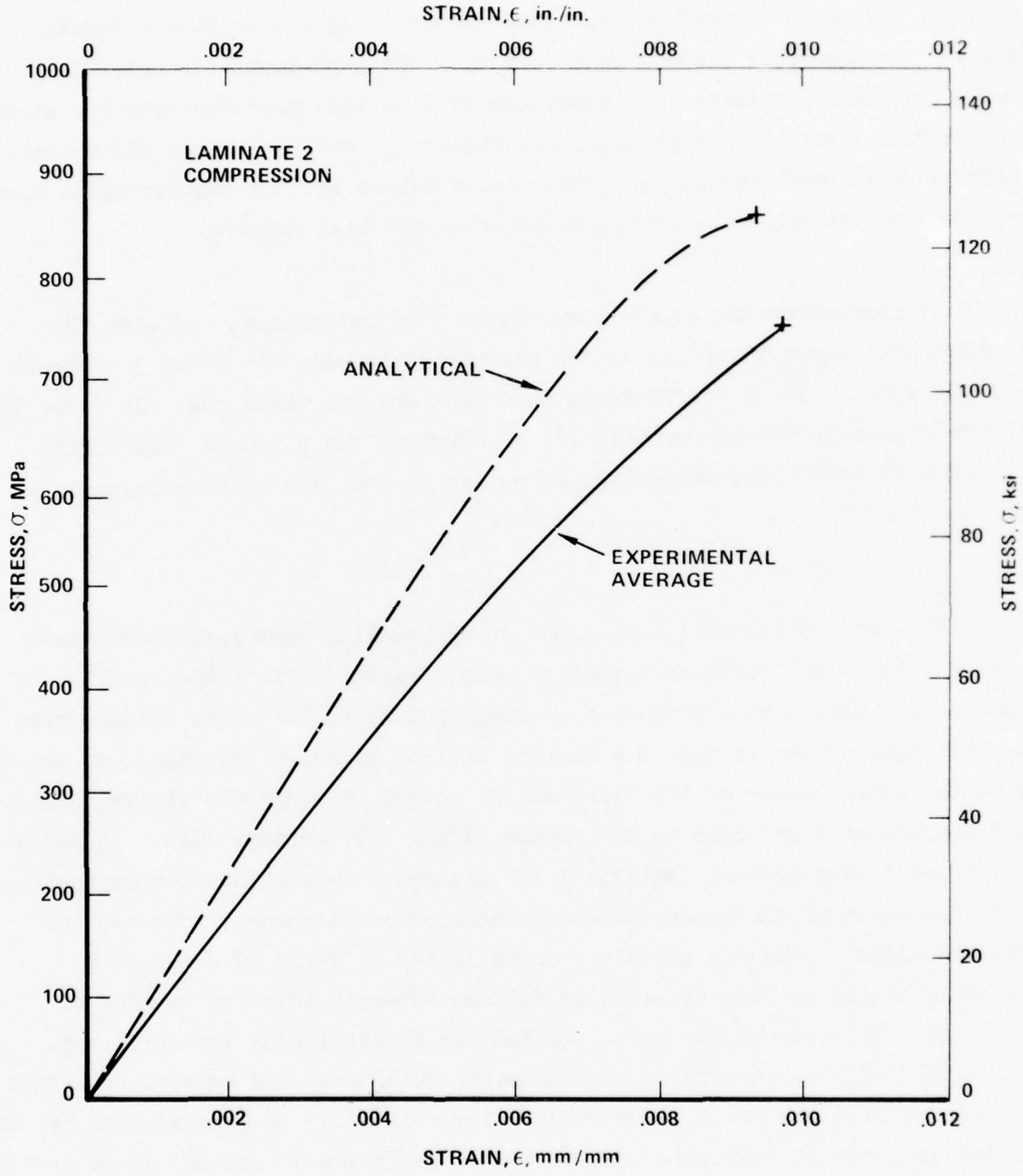


Figure 51. Comparison Between Predicted and Experimental Average Compression Stress-Strain Curves for Laminate 2

between the predicted and average experimental compression stress-strain curves for laminates 1 and 2 respectively. The experimentally determined modulus of both laminates was considerably less than predicted and the strain to fracture considerably greater, see Figures 50 and 51. These differences between predicted and actual stress-strain curves are not surprising in view of the derth of ply data available prior to the test program.

Table 18 summarizes the static compression test parameters, and like the tension data shows there was little difference between the 2 and 3 parameter Weibull fits. The R coefficients were high and Fit terms low. In Table 19 the relationship between probability of survival and ultimate compression strength is tabulated, while Figures 52 and 53 show the relationships in a plotted format.

The effect of extensometer attachment on compression test results was explored using a few laminate 1 test coupons. Table 20 lists the results. Two coupons were tested without the extensometer; two with the extensometer on the edges of the coupon, but bearing on tabs glued on the edge; and two with the extensometer on the sides of the coupon, through the fixture holes, and bearing on tabs glued to the coupon sides. All coupons listed in Table 20 failed in the typical laminate 1 failure modes indicating that neither the attachment of the extensometer or location of attachment affected the failure modes. However, the six coupons listed in Table 20 did have a slightly higher average compression failure strength than the coupons of Table 15. This result was quite limited and statistically insignificant, but indicated that the type of extensometer attachment and subsequent effect on failure strength needs to be further investigated. In general, the results listed in Table 20 indicated that test data in Tables 15 and 16 can be safely compared because test procedures were identical, but precise comparisons to other test results using different strain measuring devices must be made with caution.

TABLE 18

SUMMARY OF STATIC COMPRESSION TEST PARAMETERS

	NUMBER OF WEIBULL PARAMETERS	WEIBULL COEFFICIENTS			CORRELATION COEFFICIENT, R	FITTING COEFFICIENT, FIT
		k	e	v		
LAMINATE 1	3	12.089	-0.457164	72.194	0.99730	0.00578
	2	11.940	0	72.534	0.99727	0.00632
LAMINATE 2	3	25.018	-0.259155	115.821	0.99888	0.00211
	2	24.905	0	116.074	0.99888	0.00220

$$P(x) = \exp\left[- \left(\frac{x-e}{v-e}\right)^{k} \right]$$

FOR 2 PARAMETERS, $\alpha = k$, $\hat{F} = v$

TABLE 19

RELATIONSHIP BETWEEN PROBABILITY OF SURVIVAL
AND ULTIMATE COMPRESSION STRENGTH[a]

Probability of Survival P(i)	Ultimate Compressive Strength, σ_{ult}, MPa (ksi)	
	Laminate 1	Laminate 2
.999	280 (40.6)	605 (87.8)
.995	320 (46.4)	646 (93.7)
.99	339 (49.2)	664 (96.3)
.95	389 (56.4)	709 (102.8)
.90	412 (59.8)	729 (105.8)
.80	439 (63.7)	752 (109.1)
.70	457 (66.3)	766 (111.1)
.60	471 (68.3)	777 (112.7)
.50	483 (70.0)	787 (114.1)
.40	494 (71.7)	796 (115.4)
.30	505 (73.3)	805 (116.7)
.20	518 (75.1)	814 (118.0)
.10	534 (77.4)	826 (119.8)
.05	545 (79.1)	834 (121.0)
.01	565 (82.0)	849 (123.1)
.005	578 (83.9)	854 (123.8)
.001	585 (84.8)	863 (125.1)

a - Strength values were calculated based on a 3-parameter Weibull fit to the data.

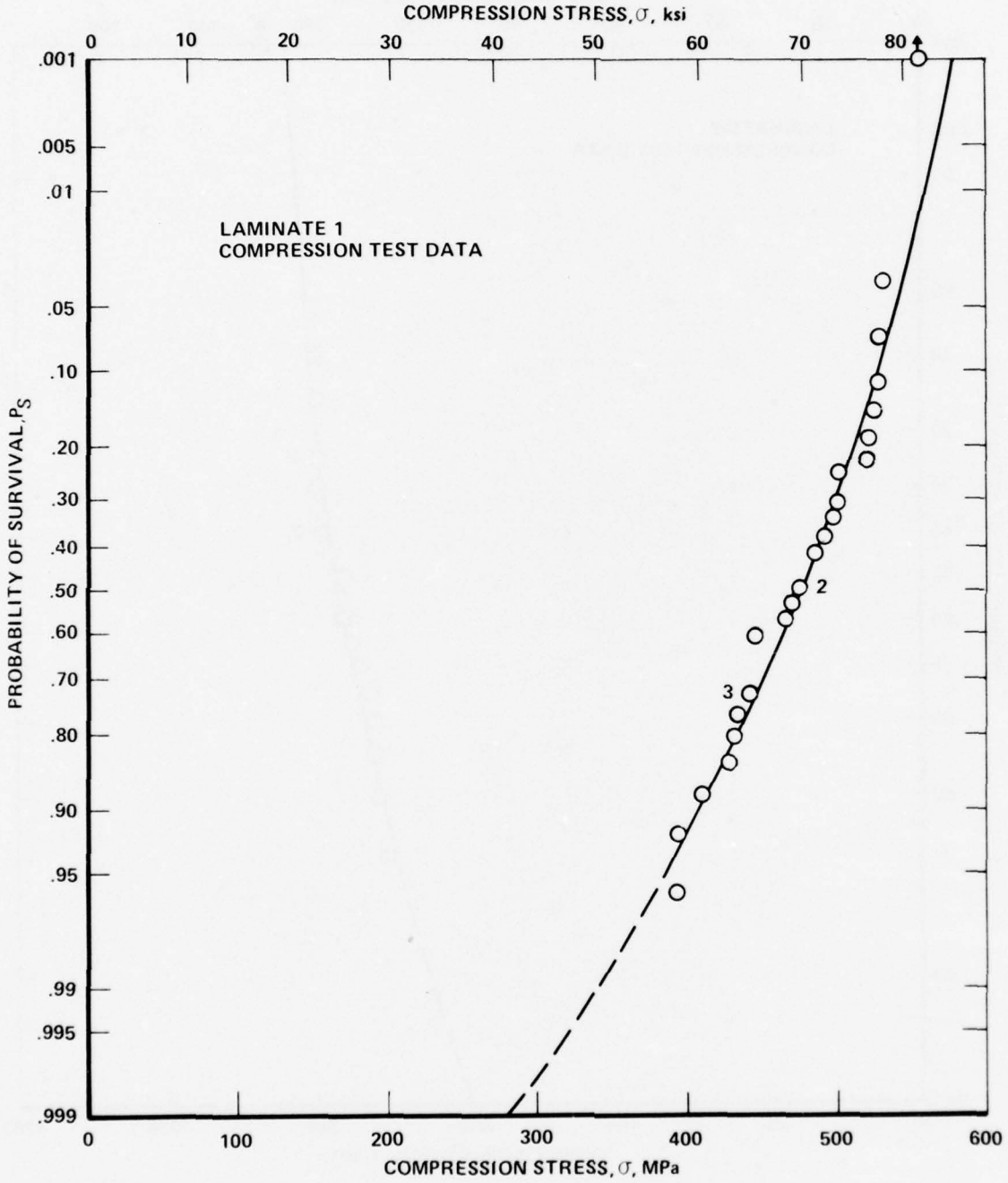


Figure 52. Relationship Between Probability of Survival and Ultimate Compression Strength for Laminate 1 Coupons

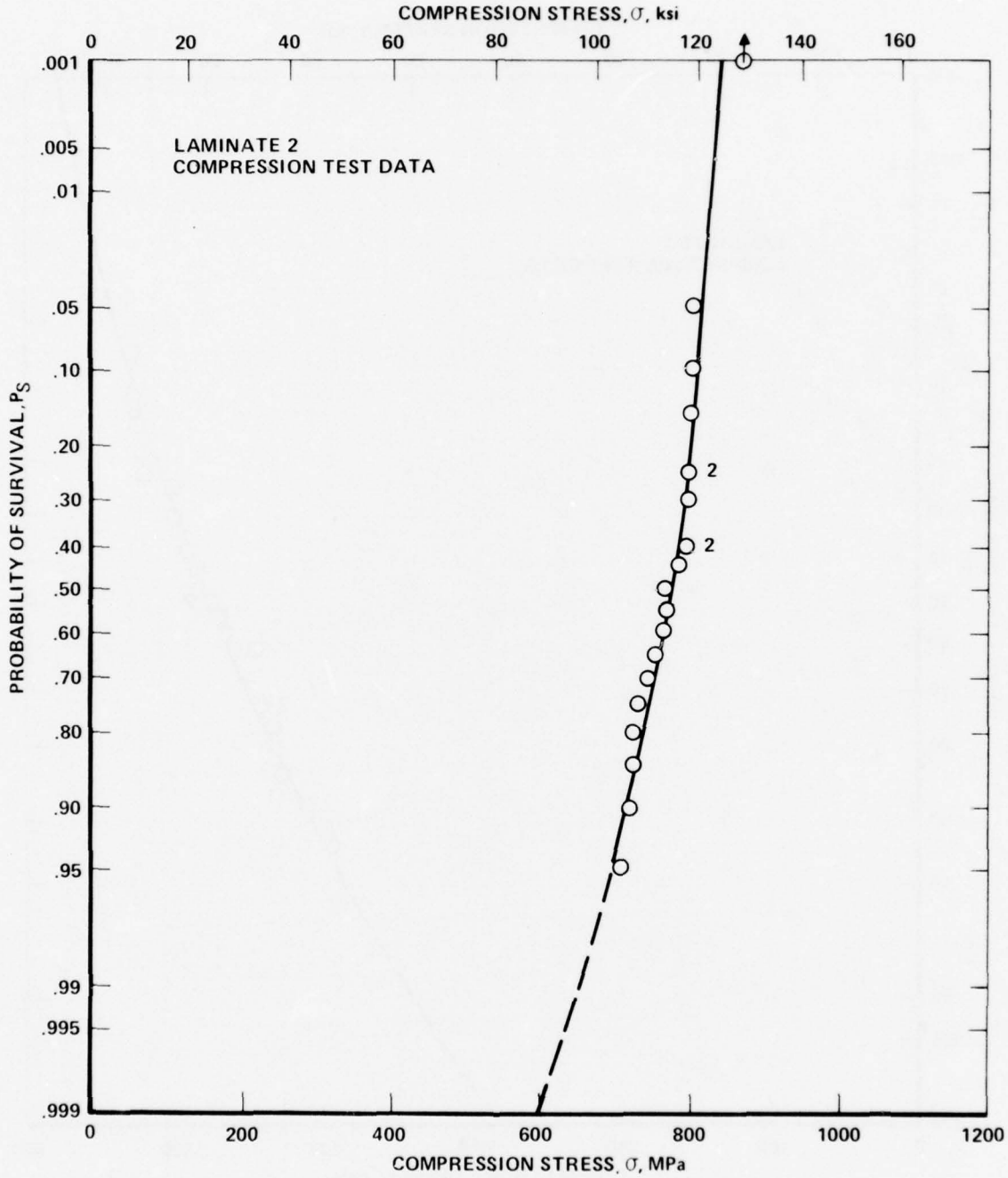


Figure 53. Relationship Between Probability of Survival and Ultimate Compression Strength for Laminate 2 Coupons

TABLE 20A

EFFECT OF TEST DETAIL

ON

COMPRESSION RESULTS OF LAMINATE 1 COUPONS

Sample ID	Min. Area, $in.^2$	Ultimate Load, P_{ult}, lbs	Ultimate Stress, σ_{ult}, ksi	Ultimate Strain, ϵ_{ult}, in./in. in 2.0 in.	Load at Initial Curve Deviation, P_{CD}, lbs	Stress at Initial Curve Deviation, σ_{CD}, ksi	Strain at Initial Curve Deviation, ϵ_{CD}, in./in. in 2.0 in.	Apparent Modulus of Elasticity E_{1C}, psi x 10^6	Amount of Strain at Ultimate Load, ϵ, in./in. in 2.0 in.
582-12A[a]	.0819	6330	77.3	Curve Not Recorded					
594-12A[a]	.0826	5290	64.0	.0093	3100	37.5	.0050	7.51	0[d]
582-20A[b]	.0822	6230	75.8	.0111	3800	46.2	.0066	7.00	.0009
603-15B[b]	.0824	5800	70.4	-	3400	41.3	.0063	6.56	-
580-6A[c]	.0823	6680	81.2	.0132	3550	43.1	.0059	7.31	.0012
583-26B[c]	.0816	5940	72.8	.0120	3200	39.2	.0056	7.00	.0015
Average			73.6	.0114		41.5	.0059	7.08	
			+7.6	+.0018		+4.7	+.0007	+0.43	
			-9.6	-.0021		-4.0	-.0003	-0.52	
Previous Average			69.7	.0110		34.9	.0050	6.95	
			+11.8	+.0022		+5.5	+.0007	+0.42	
			-12.1	-.0025		-8.5	-.0008	-0.83	

a - Tests run with graphite tabs glued on coupon edges, extensometer on coupon edges.

b - Tests run with extensometer on coupon faces.

c - Tests run with extensometer on coupon faces with tabs glued on coupon.

d - A 0 denotes that the coupon failed without a flat topped region prior to failure, see Figure 43.

TABLE 20B

EFFECT OF TEST DETAIL

ON COMPRESSION RESULTS OF LAMINATE 1 COUPONS

Sample ID	Min. Area, mm^2	Ultimate Stress, σ_{ult}, MPa	Ultimate Strain, ϵ_{ult}, mm/mm in 50.8 mm	Stress at Initial Curve Deviation, σ_{CD}, MPa	Strain at Initial Curve Deviation, ϵ_{CD}, mm/mm in 50.8 mm	Apparent Modulus of Elasticity, E_{1C}, GPa	Amount of Strain at Ultimate Load, ϵ, mm/mm in 50.8 mm
582-12A[a]	52.8	533.0	Curve Not Recorded				
594-12A[a]	53.3	441.3	.0093	258.6	.0050	51.8	0[d]
582-20A[b]	53.0	522.6	.0111	318.5	.0066	48.3	.0009
603-15B[b]	53.2	485.4	-	284.8	.0063	45.2	-
580- 6A[c]	53.1	559.9	.0132	297.2	.0059	50.4	.0012
583-26B[c]	52.6	501.9	.0120	270.3	.0056	48.3	.0015
Average		507.4	.0114	286.1	.0059	48.5	
		+52.5	+.0018	+32.4	+.0007	+3.0	
		-66.1	-.0021	-27.7	-.0003	-3.6	
Previous Average		480.6	.0110	290.6	.0050	47.9	
		+81.3	+.0022	+37.9	+.0007	+2.9	
		-83.5	-.0025	-43.4	-.0008	-5.7	

a - Tests run with graphite tabs glued on coupon edges, extensometer on coupon edges.

b - Tests run with extensometer on coupon faces.

c - Tests run with extensometer on coupon faces with tabs glued on coupon.

d - A 0 denotes that the coupon failed without a flat topped region prior to failure, see Figure 43.

Table 21 lists four coupons, two of each laminate, which were tested using strain gages to record strain. All gages were placed on each specimen at the same location; under the top fixture holes, see Figure 13. One coupon of each laminate had strain gages on both sides of the coupon at the same location to allow specimen misalignment to be studied. Two of the coupons also had an extensometer attached to the coupon sides as indicated in Table 21. All gages were "T" type and thus both longitudinal and transverse strains were recorded. Experimentation conducted for a Lockheed-California Company funded test program indicated that strain gages must be attached to areas where the outer layer of epoxy has been carefully removed if reliable readings are to be obtained. All gages used in this limited study were attached using this procedure.

Table 21 shows that, for either laminate, this testing procedure provided near perfect alignment, as indicated by the ultimate longitudinal strain readings of the two coupons with two "T" type gages. The two longitudinal and transverse strain gages of these coupons had nearly identical values throughout the tests. In addition, Table 21 shows that extensometer strain and longitudinal strain gage readings agreed within 1-1/2 percent, which gave confidence in the extensometer strain results of Tables 15 and 16. The possible effect of the extensometer on the ultimate failure strength is also indicated in Table 21 and shows that, for both laminates, the coupon with attached extensometer and strain gage had a lower compression ultimate strength than the coupon with strain gages only. This result was suggestive only, with no statistical significance, and needs to be further investigated. However, the test result cautions against comparison between test results unless all testing procedures are identical.

Table 22 shows the results of the experimental determination of Poisson's ratio based on a limited number of strain gaged tension and compression coupons. For each laminate, Poisson's ratio was determined to be the same in tension and compression. The average Poisson's ratio for laminate 2 was approximately 0.63 as opposed to that for laminate 1 which was approximately

TABLE 21

COMPRESSION TEST RESULTS

USING STRAIN GAGES

Sample ID	Area, mm^2 ($in.^2$)	Ultimate Load, P_{ult}, kN(lbs)	Ultimate Stress σ_{ult}, MPa(ksi)	Longitudinal Ultimate Strain, ε_L, mm/mm	Extensometer Ultimate Longitudinal Strain, ε, mm/mm in 50.8 mm	Transverse Ultimate Strain ε_T, mm/mm	Average Apparent Longitudinal Modulus of Elasticity, E_A, GPa (psi x 10^6)	Remarks
596-19B[a]	53.5 (.0830)	24.1(5420)	450 (65.3)	.0098	.0099	.0024	-	
603- 7B[a]	54.0 (.0837)	32.0(7200)	593 (86.0)	.0129[c] .0133	-	.0036[b] .0035	-	2 "T" Gages
696-17C[b]	83.5 (.1295)	65.3(14700)	783 (113.5)	.0090	.0089	.0055	85.5(12.4)	
727- 6C[b]	80.9 (.1254)	72.1(16200)	891 (129.2)	.0106[c] .0106	-	.0065[b] .0068	85.5(12.4)	2 "T" Gages

a - The ultimate stress for these coupons (Laminate 1) was based on average area.

b - Laminate 2

c - Gages on both sides read similar values indicating good alignment

TABLE 22

TEST RESULTS FOR

DETERMINATION OF POISSON'S RATIO

Laminate	Tension or Compression (T,C)	Poisson's Ratio	Number of Coupons
1	T	0.29	4
	C	0.26	2
		Average 0.28	
2	T	0.64	4
	C	0.62	2
		Average 0.63	

0.28. Therefore, if the end effect influenced failure location, the effect would be expected to be more important for the laminate with the higher Poisson's ratio. This assumption was supported by the large variation in failure location for laminate 1; hence, there was no apparent end effect due to Poisson induced restraint. However, for laminate 2 the end effect was apparently large enough that, if the end was not sufficiently stabilized, failure occurred at the end. If sufficient end stabilization existed, the failure zone shifted towards the center of the gage length, for reasons explained in Section 2.5.2, and observed for exactly half of the laminate 2 failed coupons. Therefore, these test results appear to support the assumption that compression tests conducted with a stabilizing end guide cannot solve an inherent end effect for high Poisson ratio laminates, but would merely shift the failure location. This shift in failure location towards the center of the gage length does not necessarily imply an increase in test validity.

SECTION V

FATIGUE RESULTS

The fatigue study was divided into two major sub-tasks. In the first task, the general stress-life characteristics of the two laminates were developed under both tension-tension and tension-compression loading. This S-N scan was conducted by testing three coupons at each of several maximum stress levels. Subsequent to determining the general characteristics of the S-N behavior, the extent of fatigue scatter was determined by conducting 20 or more tests of several specifically chosen maximum stress levels.

A major consideration prior to the fatigue test program was which of the loading variables pertinent to fatigue should be held constant. The variables considered were: load ratio, R; maximum stress, σ_{max}; stress range $\Delta\sigma$; and minimum stress, σ_{min}. Any one of these variables could have been held constant and two others allowed to vary while the effect of the fourth was evaluated.

Coupled with the considerations of loading variables was the practical problem that these laminates acted like thin columns, thus limiting the maximum compression that could be reached without buckling. A laminate 1 coupon was loaded in a fatigue test machine in compression using one central buckling restraint and a second coupon loaded using two constraints spaced 50.8 mm (2 in.) apart. A laminate 2 coupon was also loaded in compression using two restraints. For these tests buckling was defined as 0.0254 mm (0.001 in.) deflection out-of-plane anywhere within the gage length. For laminate 1 with one restraint, this criterion limited the maximum compression stress in fatigue to - 68.9 MPa (-10 ksi) and for two restraints to - 110 MPa (-16 ksi). Laminate 2 with two restraints was limited to - 207 MPa (-30 ksi). Based on the practical test restraint of buckling, fatigue tests conducted at constant R values were considered impractical because stress ranges would be severely restricted. All fatigue tests were thus conducted at a constant minimum stress (0, -68.9, -110 MPa (0, -10, -16 ksi) for laminate 1 and 0 and -207 MPa

(0 and -30 ksi) for laminate 2) and the maximum stress was allowed to vary. This procedure permitted direct comparison of results based on σ_{max} or $\Delta\sigma$ as well as a limited study of the effect of R.

For tension-tension tests, failure was defined as breakage of the coupon; for tension-compression tests, failure was defined as coupon breakage or inability to sustain compression load due to severe delamination. Investigation showed that if the latter failure definition was used, breakage of the specimen could be forced by the addition of a few more cycles. Only four tension-compression specimens of laminate 1 and none of laminate 2 failed due to inability to sustain compression load.

A primary observation was that significant visible delamination often did not occur in tension-tension testing prior to failure, but when such delamination did occur, the remaining cycles to failure could be either small or large. However, for tension-compression testing when delamination was noted prior to failure, normally 90% or more of the coupon life was exceeded. Therefore, in the future delamination may possibly be a more useful definition of failure in tension-compression fatigue while coupon breakage may be more useful for tension-tension fatigue.

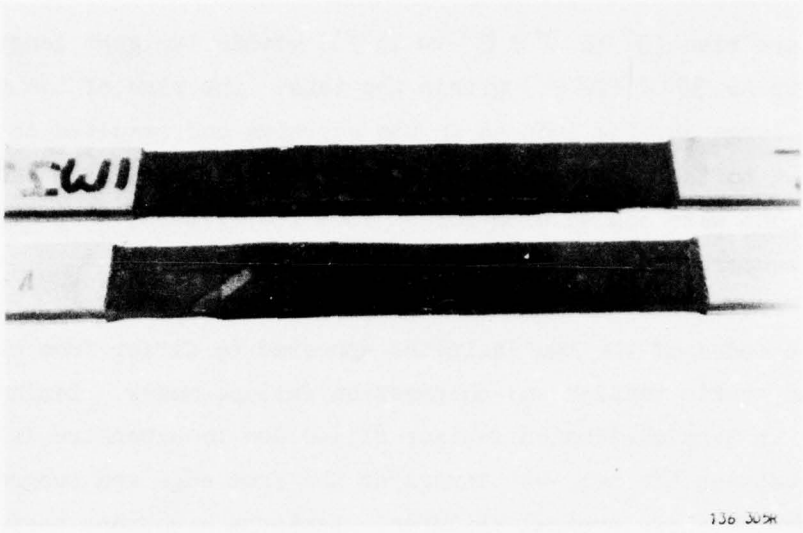
Another problem of major concern was the possibility of an increase in coupon temperature during fatigue cycling. Both laminates were studied by measuring coupon temperature at the tab midpoint; on the coupon surface near each tab; and on the coupon surface at the center of the gage length. For laminate 1, the temperature of tension-tension fatigue coupons remained constant at the laboratory air temperature until a cycle count was reached approximately equal to when delamination was noted. At this point, temperature quickly increased approximately 4° to 8°C (8° to 15°F) and remained constant to failure. The tension-compression coupons of laminate 1 exhibited a temperature rise of 4° to 8°C (8° to 15°F) immediately after test commencement, but afterwards the temperature remained constant until failure. In contrast, laminate 2 coupons tested under both conditions exhibited a

small temperature rise (3° to 8°C (5° to 15°F)) within the gage length, but a large rise (up to 39°C (70°F)) within the tabs. The rise of tab temperature was due to the large strains induced in the adhesive and resulted in creep of the tab relative to the coupon and tab pull-off. Therefore, grip ends of laminate 2 coupons were cooled with forced room temperature, shop air to keep the grip temperature near room air temperature.

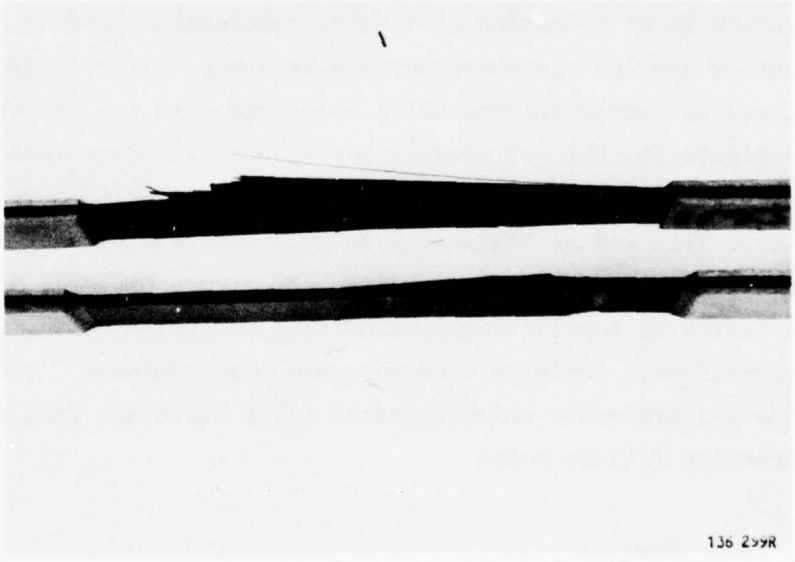
Fatigue failure modes of the two laminates appeared to differ from each other as well as from static tension and compression failure modes. Laminate 1 coupons tested in tension-tension fatigue failed due to extensive delamination which started between the two -45° layers at the free edge and progressed inwards. Figure 54 shows typical failures. Laminate 1 coupons tested in tension-compression fatigue failed similarly to those tested in tension-tension, but large out-of-plane buckling of the outer four plies also occurred reducing fatigue life after the onset of delamination. Typical failures are shown in Figure 55. Laminate 2 coupons sustained no early delamination during fatigue under either tension-tension or tension-compression loading. Fatigue damage in laminate 2 coupons was characterized by outer 0° fiber shredding eventually followed by sudden failure which sometimes resulted in massive delamination, see Figure 56, but not always, see Figure 57. Some laminate 2 fatigue failures were dominated by the 45° plies, see Figure 58. Tension-compression fatigue failures of laminate 2 coupons also exhibited plies with sharp breaks due to the accompanying buckling, see Figure 59. All laminate 1 and 2 coupons tested in tension-compression fatigue failed during the compression load excursions. Laminate 1 coupons and most laminate 2 coupons displayed fatigue failure modes which appeared quite different from static tension or compression failure modes.

5.1 Stress-Life Scan Results

The results of the stress-life study used to determine the general form of the fatigue behavior of the two laminates are shown in Figures 60 - 62 for laminate 1 and in Figure 63 for laminate 2. The data shown for the tension-

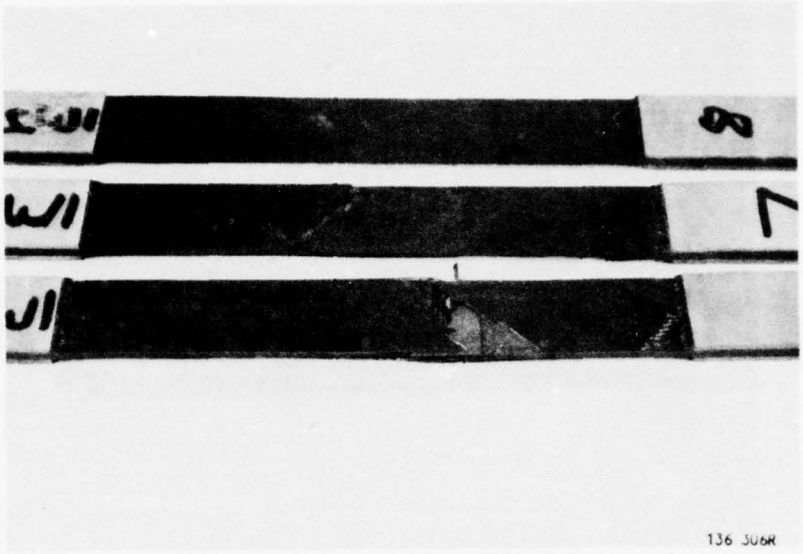


a. Coupons 1MJ 599-21A, 1MJ 601-19A; Side View

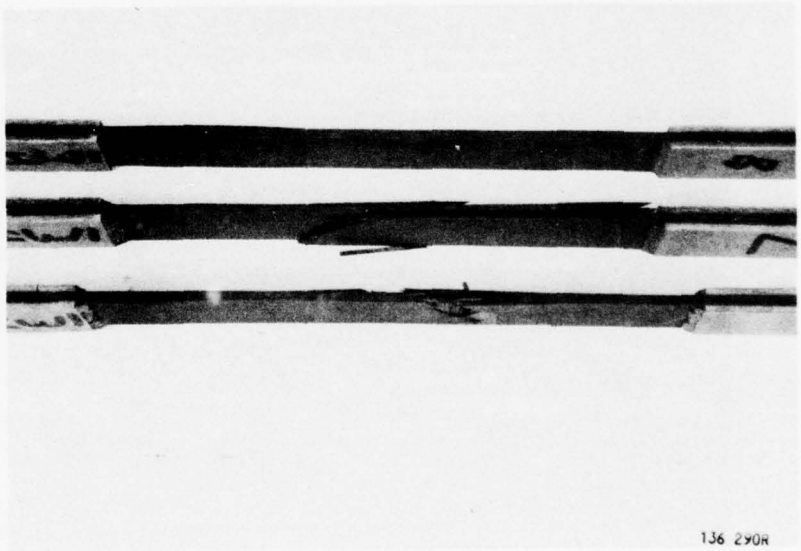


b. Coupons 1MJ 599-21A, 1MJ 601-19A; Edge View

Figure 54. Typical Tension-Tension Laminate 1 Fatigue Failures

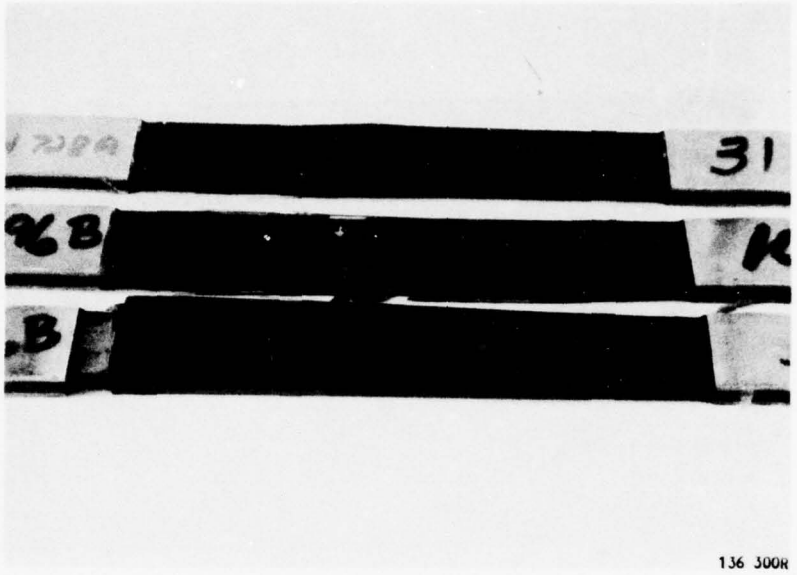


a. Coupons 1MJ 578-8A, 1MJ 604-7A, 1MJ 580-24B; Side View

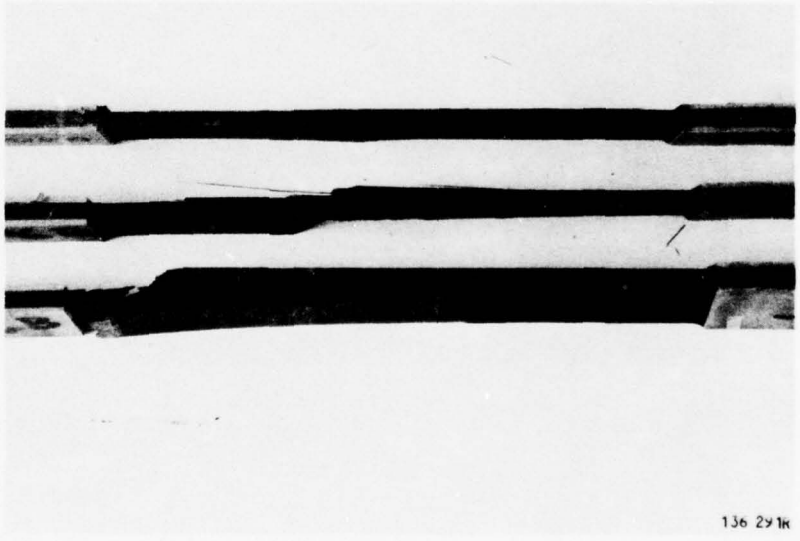


b. Coupons 1MJ 578-8A, 1MJ 604-7A, 1MJ 580-24B; Edge View

Figure 55. Typical Tension-Compression Laminate 1 Fatigue Failures

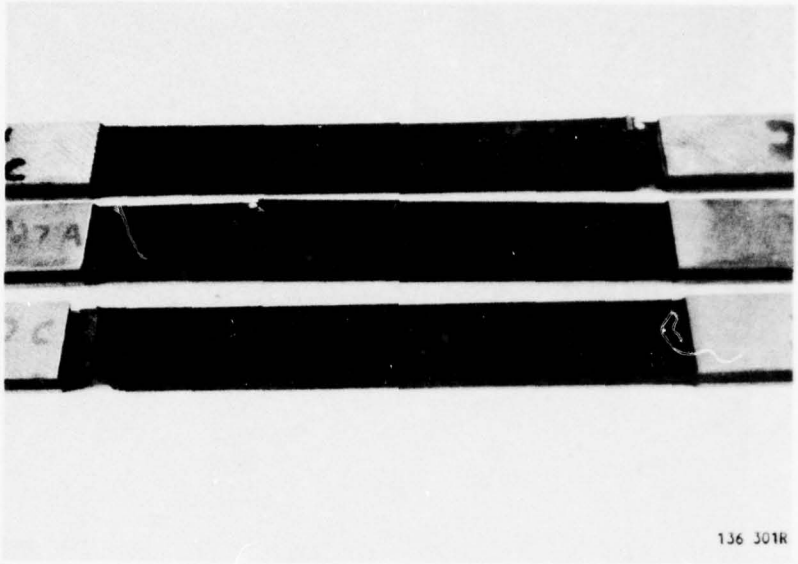


a. Coupons 1NH 728-31A, 1NH 696-10B, 1NH 696-5B; Side View

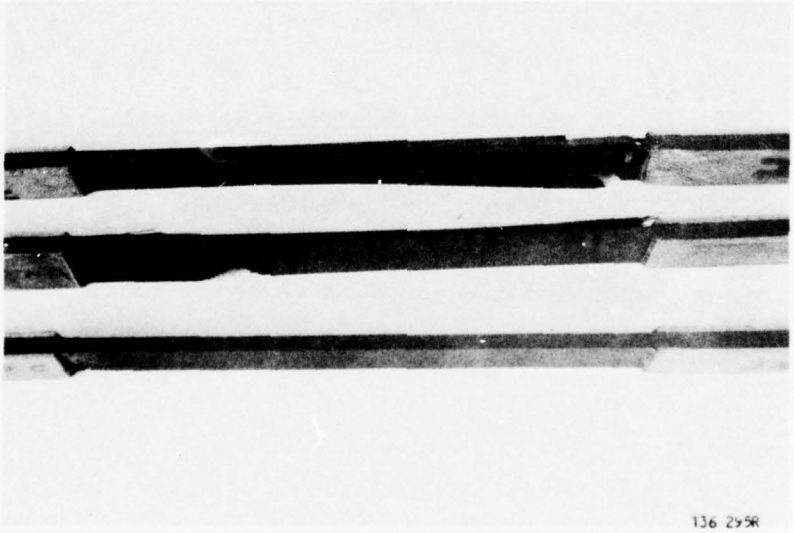


b. Coupons 1NH 728-31A, 1NH 696-10B, 1NH 696-5B; Edge View

Figure 56. Typical Delaminated Laminate 2 Coupons Which Failed Under Tension-Tension Fatigue Loading.

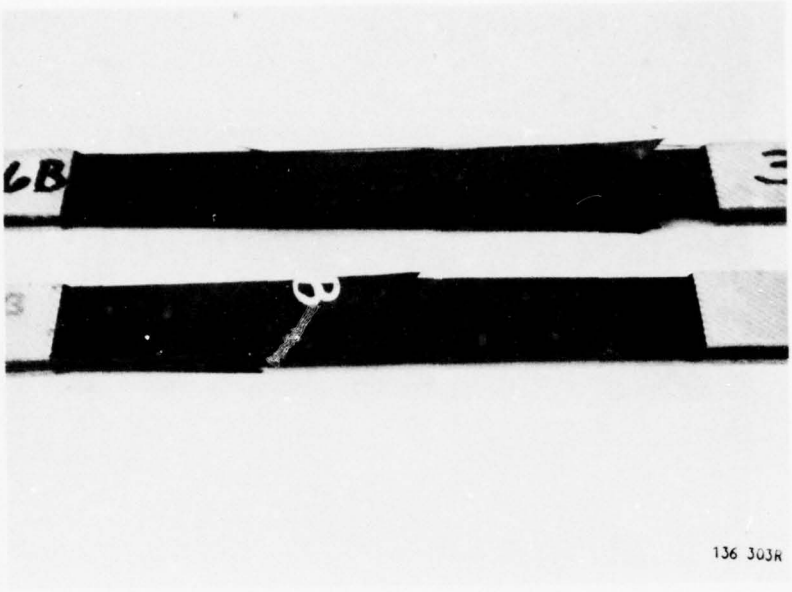


a. Coupons 1NH 728-27C, 1NH 727-15A, 1NH 727-36C; Side View

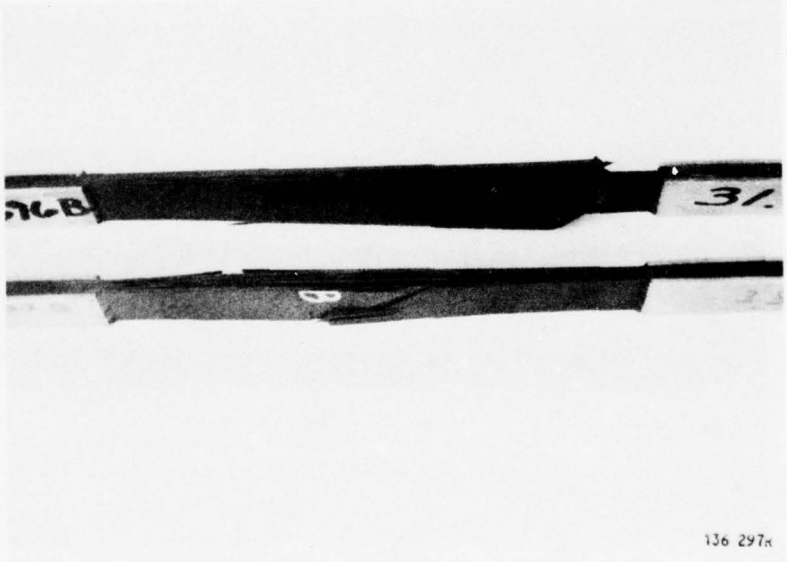


b. Coupons 1NH 728-27C, 1NH 727-15A, 1NH 727-36C; Edge View

Figure 57. Typical Laminate 2 Coupons Which Failed Under Tension-Tension Fatigue Loading Without Significant Delamination.

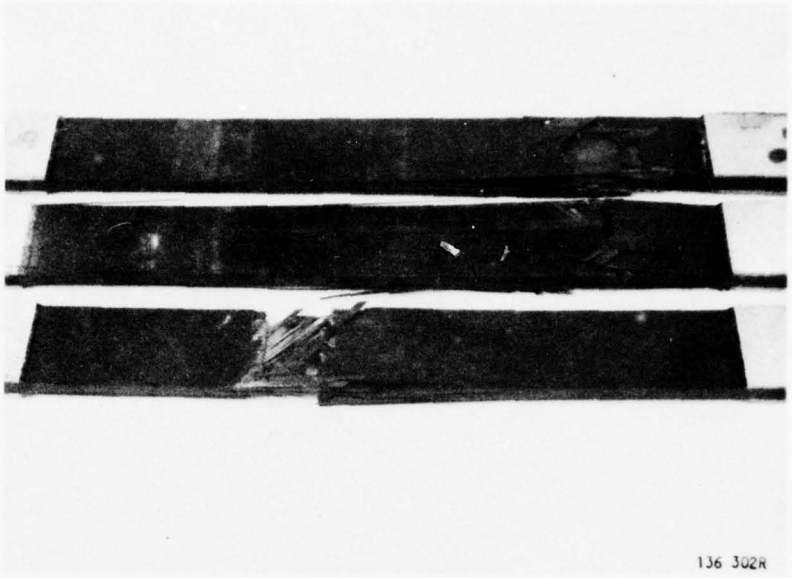


a. Coupons 1NH 696-31B, 1NH 727-35B; Side View

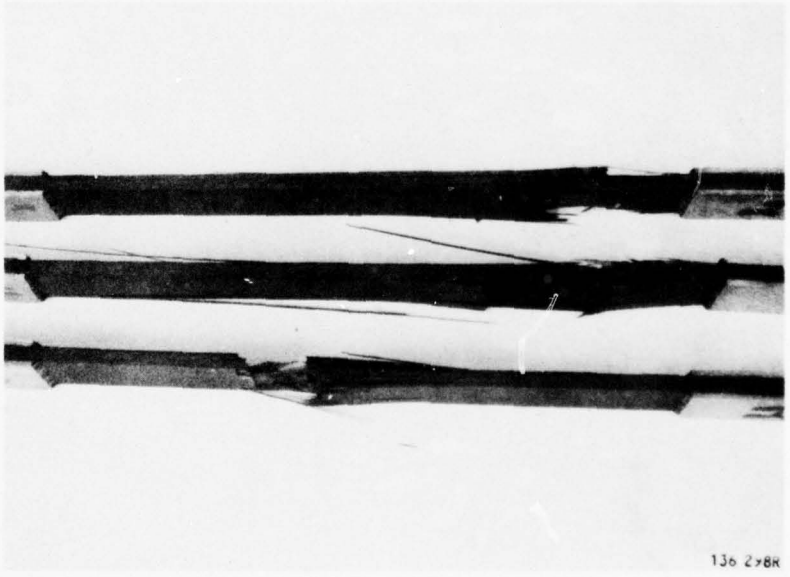


b. Coupons 1NH 696-31B, 1NH 727-35B; Edge View

Figure 58. Laminate 2 Tension-Tension Fatigue Failures Dominated by 45° Plies



a. Coupons 1NH 728-24A, 1NH 727-16C, 1NH 728-20A; Side View



b. Coupons 1NH 728-24A, 1NH 727-16C, 1NH 728-20A; Edge View

Figure 59. Laminate 2 Tension-Compression Fatigue Failures

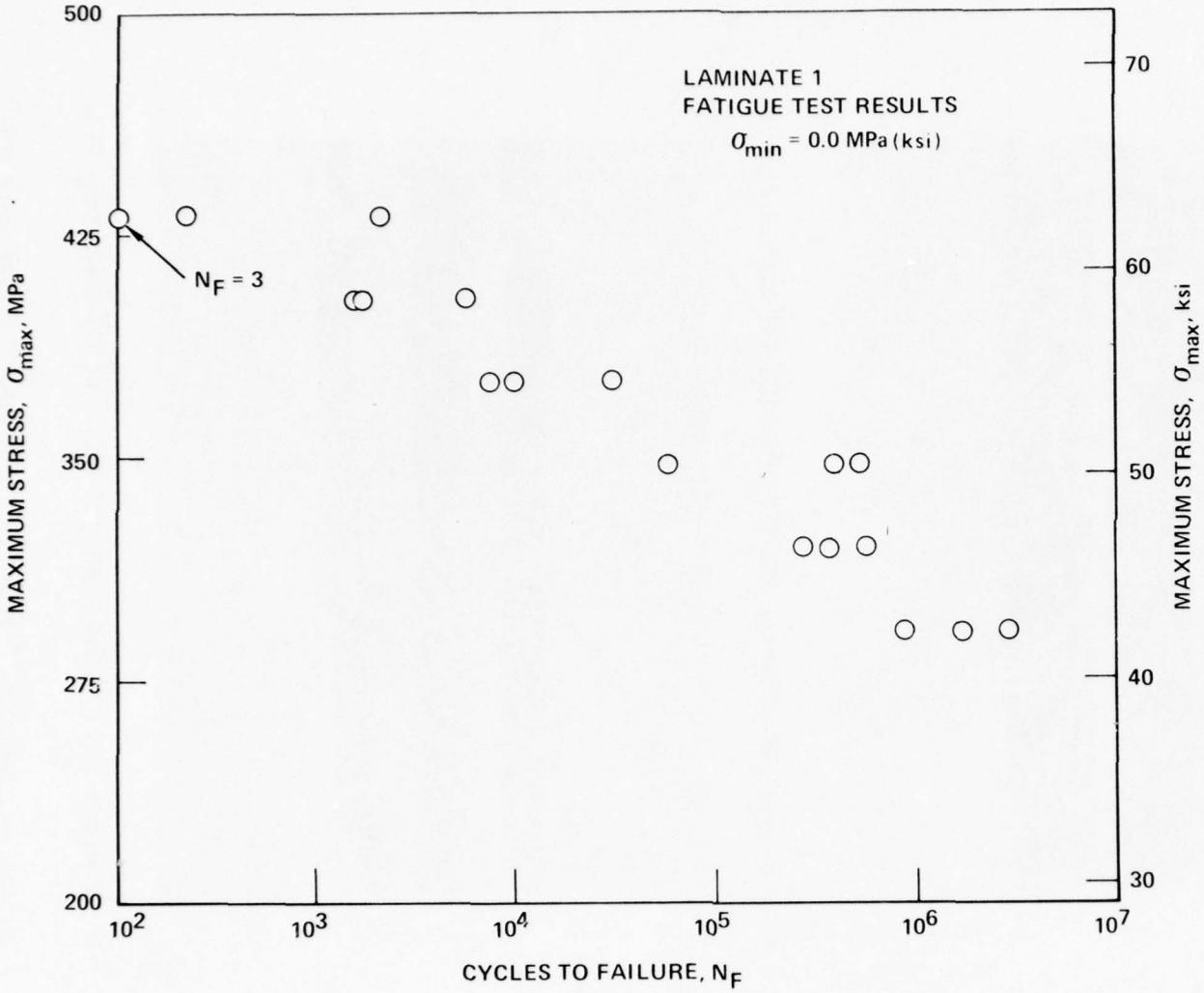


Figure 60. Laminate 1 Tension-Tension Fatigue Stress-Life Scan Results at σ_{min} = 0.0 MPa (ksi)

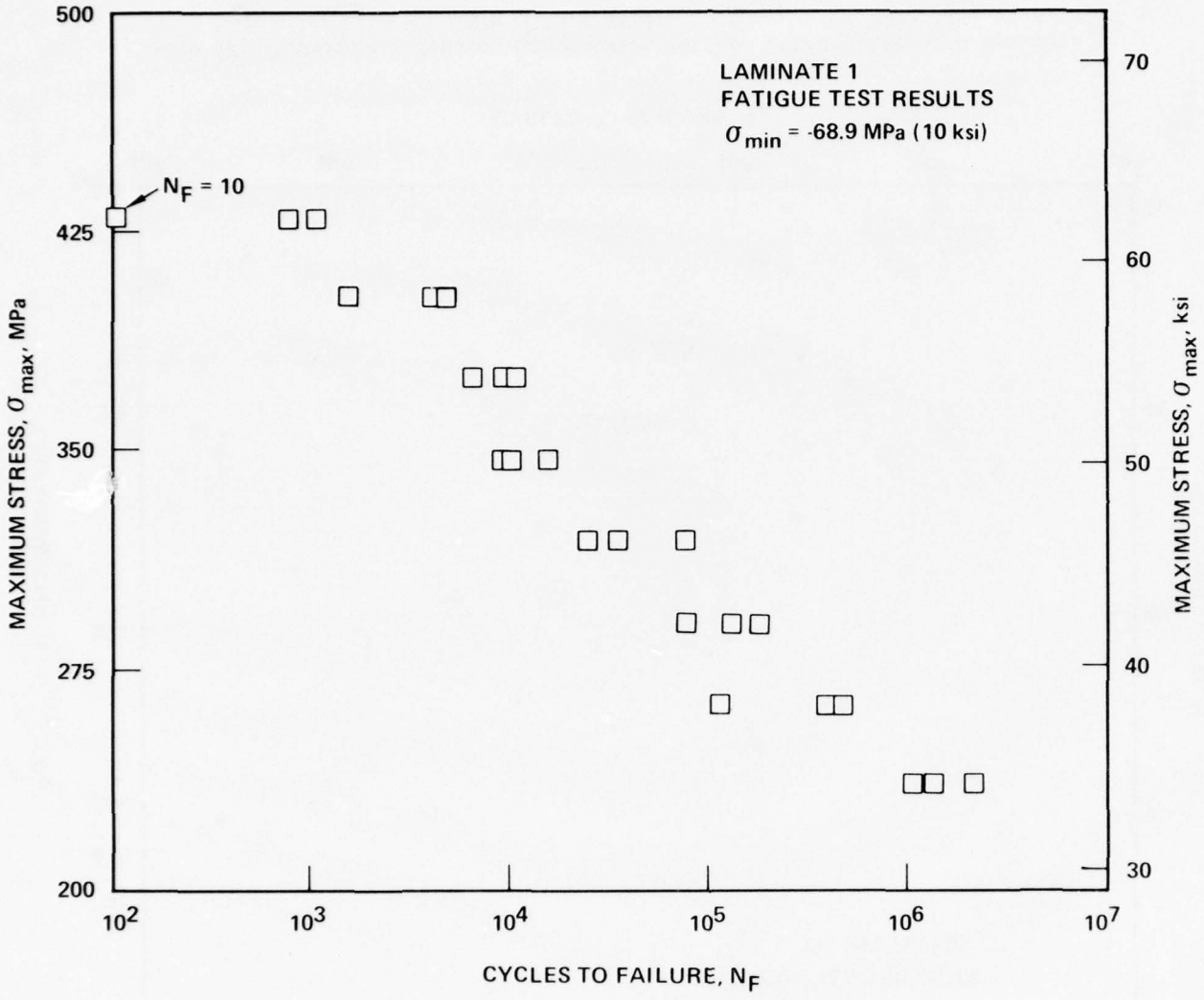


Figure 61. Laminate 1 Tension-Compression Fatigue Stress-Life Scan Results at σ_{min} = -69 MPa (10.0 ksi)

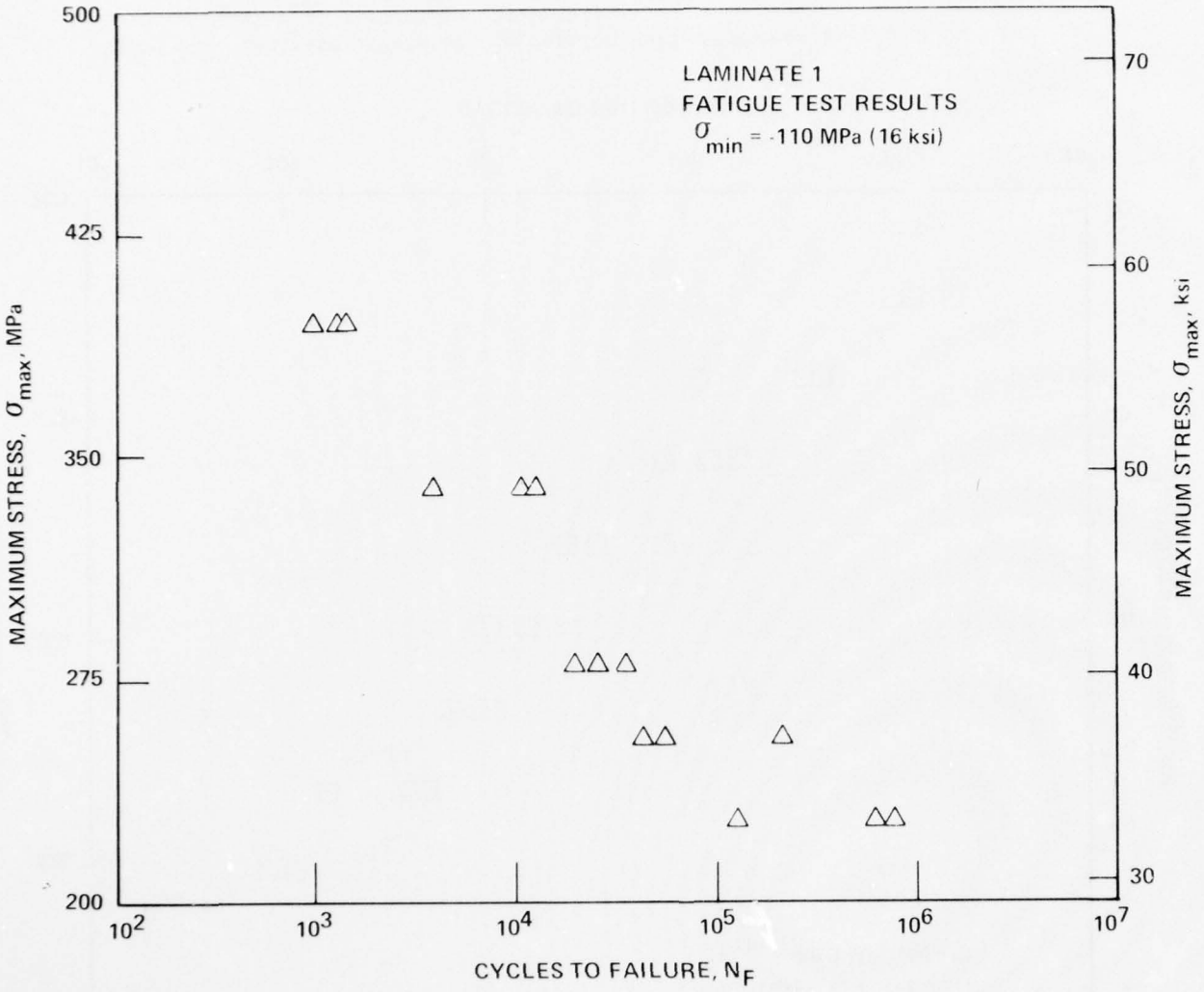


Figure 62. Laminate 1 Tension-Compression Fatigue Stress-Life Scan Results at σ_{min} = -110 MPa (16.0 ksi)

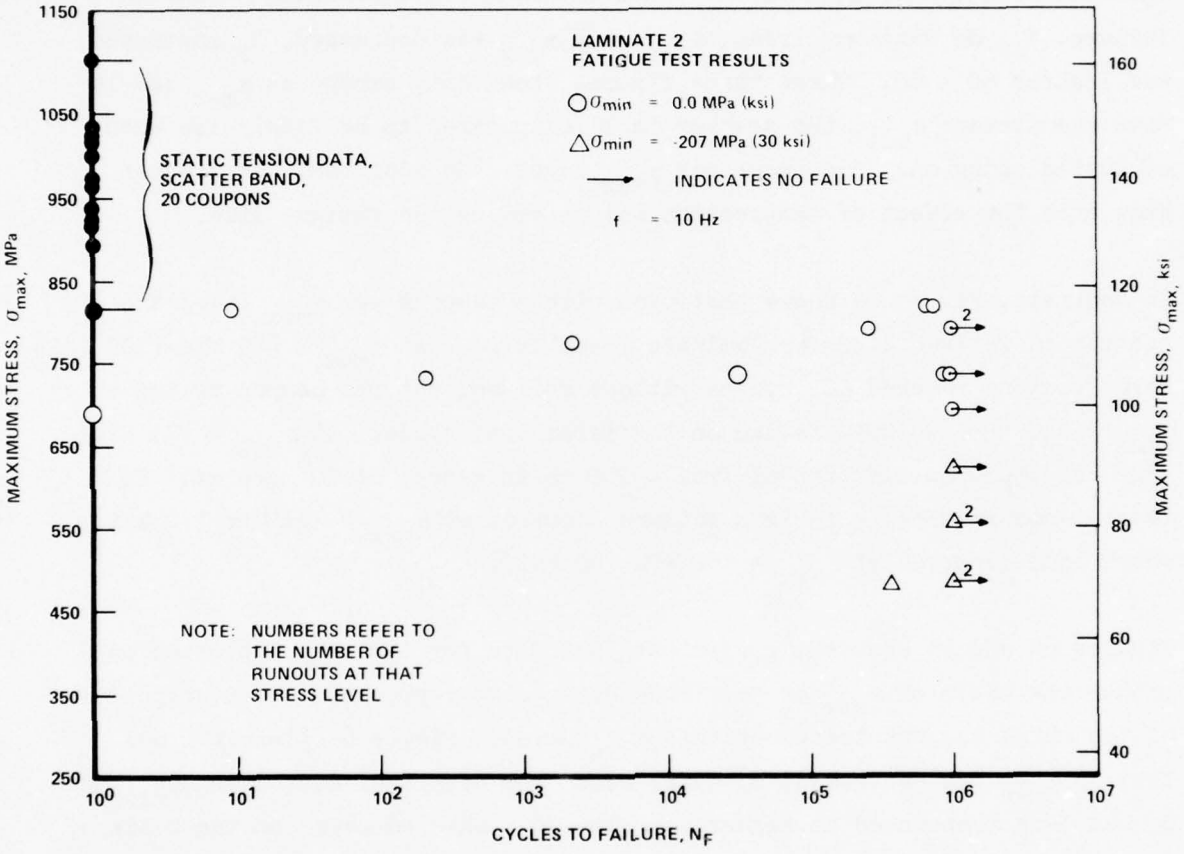


Figure 63. Laminate 2 Fatigue Stress-Life Scan Results

compression results for laminate 2 were limited because all but one coupon tested above 620 MPa (90 ksi) maximum stress failed due to tab adhesive failure. The data used in Figures 60-63 are given in Appendix B.

The fatigue behavior of laminate 1 was a simple dependence of cycles to failure, N_F, on maximum stress, σ_{max}. As σ_{max} was decreased, N_F increased, see Figures 60 - 62. These three figures show that, except at σ_{max} levels near the average σ_{ult}, the scatter in life appeared to be fairly low when evaluated using only 3 coupons per σ_{max} level. In addition, the figures show that the effect of compression was to reduce the fatigue life.

In contrast, Figure 63 shows that even with 3 coupons per σ_{max} level the scatter in fatigue life for laminate 2 was large. At σ_{max} = 689 MPa (100 ksi), three coupons reached 10^6 cycles without failure, but the coupon tested at σ_{max} = 648 MPa (94 ksi) failed on the first load cycle. At σ_{max} = 731 MPa (106 ksi), coupon life ranged from $\sim$ 200 to in excess of 10^6 cycles. In tension-compression, a fatigue failure occurred at σ_{max} = 483 MPa (70 ksi) where none occurred at σ_{max} = 552 MPa (80 ksi).

Figures 64 and 65 show the preliminary S-N data for laminate 1 plotted on either the basis of σ_{max} or $\Delta\sigma$. Each data point represents the average life of the three coupons tested at that σ_{max} level. Figure 64 clearly shows that as σ_{min} was decreased, N_F decreased. The effect of decreasing σ_{min} on N_F was less pronounced at higher σ_{max} levels. When compared on the basis of $\Delta\sigma$, Figure 65, the effect of σ_{min} on N_F decreased at lower $\Delta\sigma$ levels. Therefore, a tentative conclusion was made that for laminate 1, N_F was dominated by the effect of σ_{max} at high σ_{max} levels (above $\sim$ 345 MPa (50 ksi)) and by $\Delta\sigma$ at low σ_{max} levels.

5.2 Extent of Fatigue Scatter

Based on the S-N results, specific σ_{max} stress levels were chosen to determine the extent of fatigue life scatter.

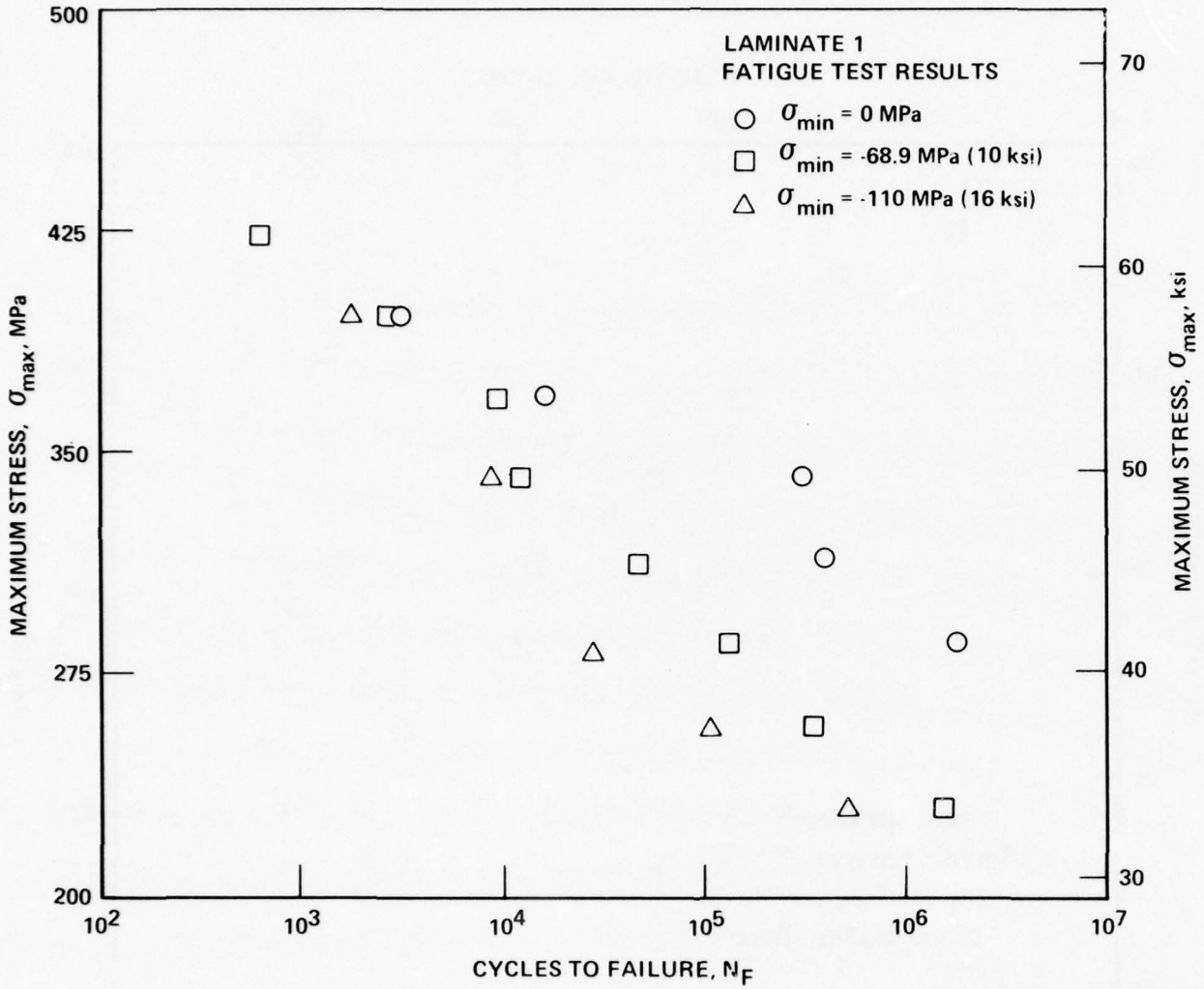


Figure 64. Laminate 1 Fatigue Stress-Life Scan Results for σ_{max}

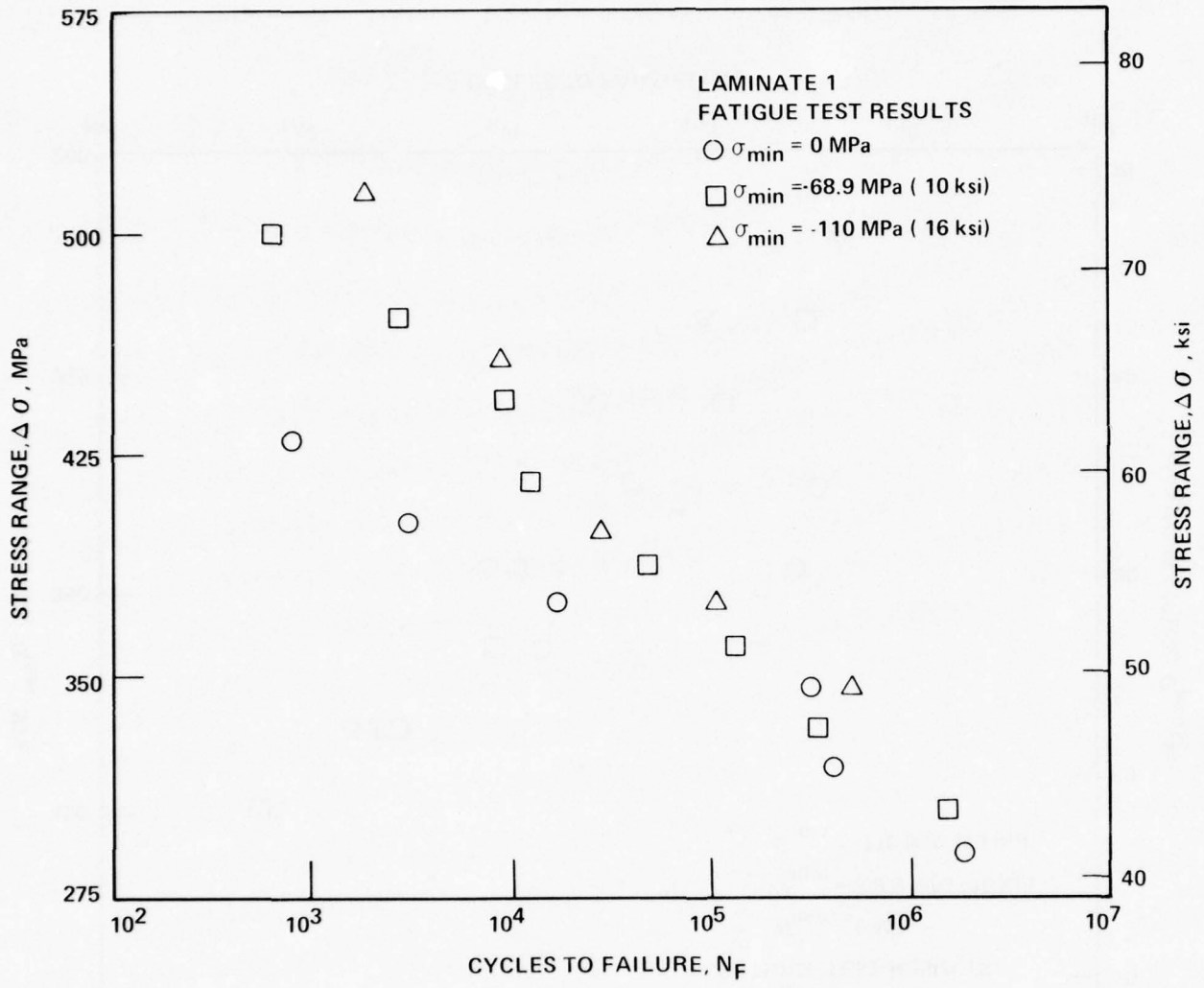


Figure 65. Laminate 1 Fatigue Stress-Life Scan Results for $\Delta\sigma$

5.2.1 Fatigue Behavior - Laminate 1

For laminate 1, three stress levels, 400, 345 and 290 MPa (58, 50 and 42 ksi), were chosen to define the scatter of the tension-tension and tension-compression fatigue curves. The highest stress level was chosen as representative of the life region where the maximum stress dominated the fatigue curve while the lowest stress level was chosen as representative of the life region where stress range was more predominant. A stress level of 345 MPa (50 ksi) appeared to be about the life at which maximum stress and stress range were equally important. At each of these three stress levels, twenty coupons were fatigue cycled, including the original three, to failure under tension-tension loading and twenty under tension-compression loading.

For laminate 1, the extent of fatigue scatter can be clearly seen in Figures 66 and 67. Each data point represents a single test point while the dashed lines indicate 95% and 5% probability of survival ($P_{.95}$ and $P_{.05}$) limits based on the 20 point data sets. The vertical lines in Figures 66 and 67 indicate the limits of the data at each stress level. Question marks indicate that the shape of an extrapolated curve was unknown as was the exact position of the $P_{.95}$ and $P_{.05}$ curves at all stress levels. The data used in Figures 66 and 67 are given in Appendix B.

In general, the data for a sample size of 20 scattered over approximately two orders of magnitude in life at any σ_{max} level. The data appeared to indicate that a type of endurance limit may exist at lower σ_{max} levels. This was especially indicated for the tension-tension data when none of the coupons tested at σ_{max} = 179 or 231 MPa (26 or 33.5 ksi) failed up to the maximum life tested. The possibility of a practical endurance limit was also supported when the data were replotted on a linear life scale as shown in Figures 68 and 69. These two figures show that no coupons under either tension-tension or tension-compression loading survived 10^6 cycles until σ_{max} was reduced to 345 MPa (42 ksi) (tension-tension) or 179 MPa (26 ksi) (tension-compression). Below σ_{max} = 290 MPa (42 ksi), tension-tension fatigue lives appeared to dramatically increase. The possibility of a practical endurance limit fatigue life for this laminate must be investigated in a future study.

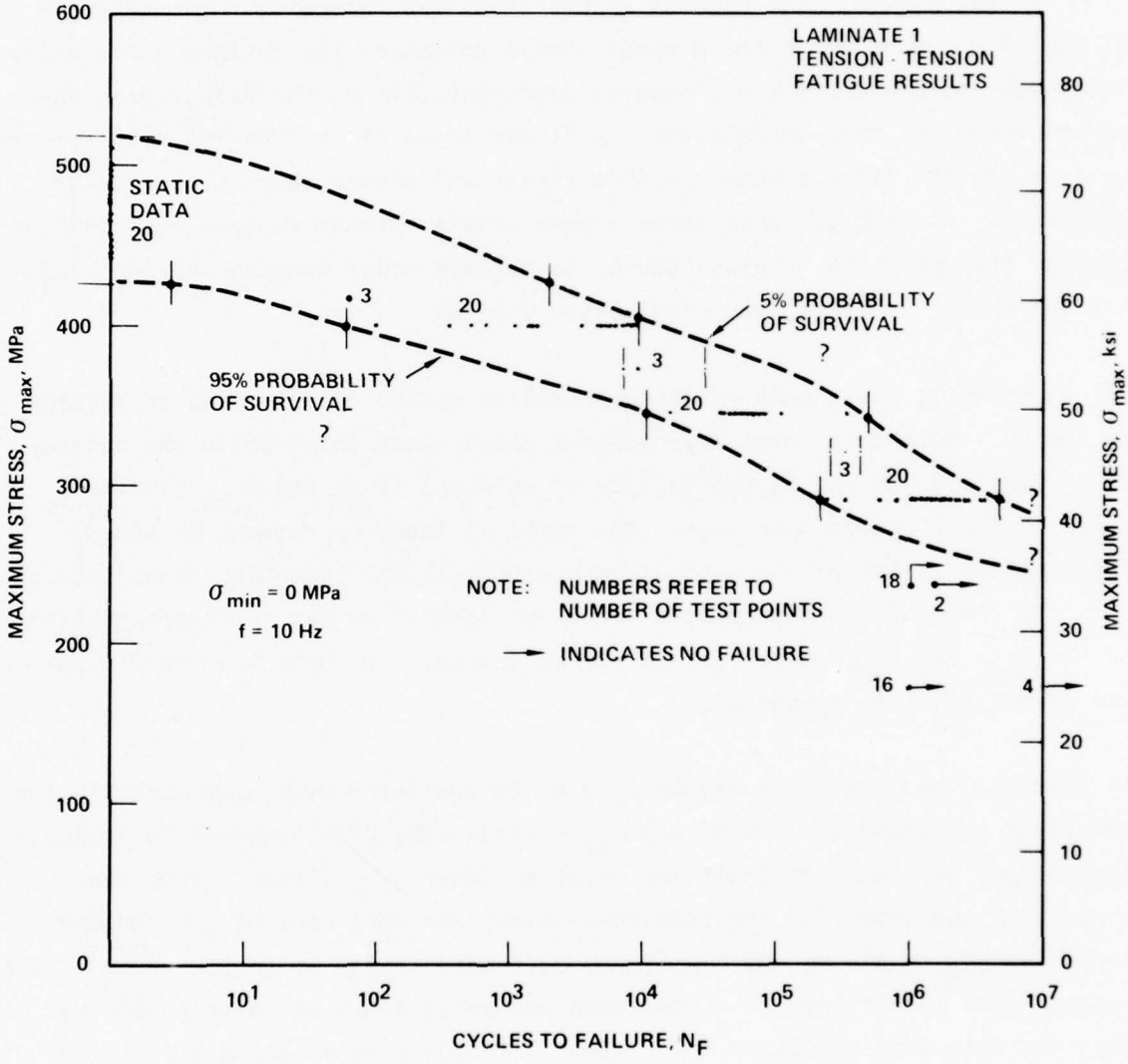


Figure 66. Laminate 1 Tension-Tension Fatigue Results at σ_{min} = 0.0 MPa (ksi)

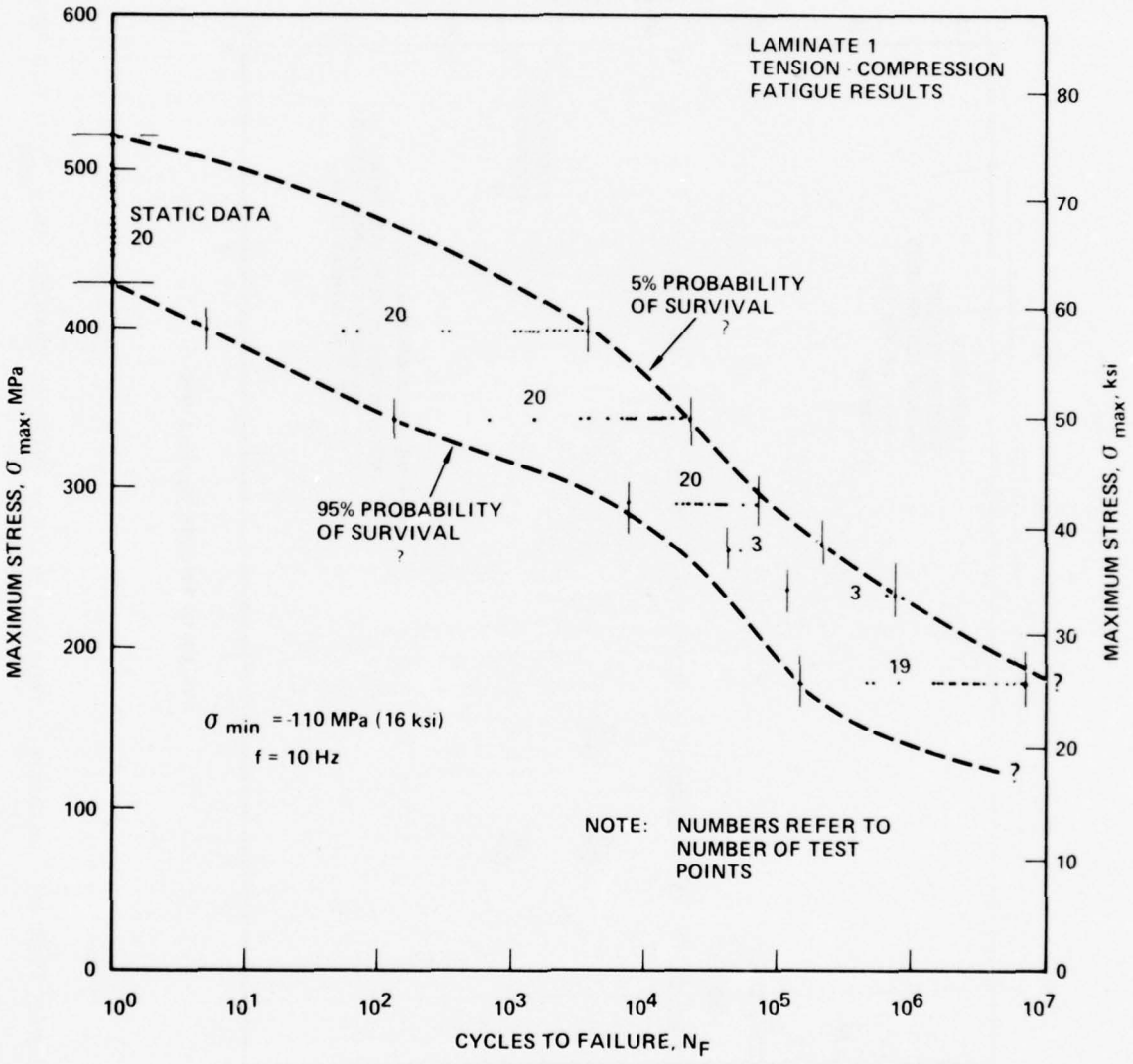


Figure 67. Laminate 1 Tension-Compression Fatigue Test Results at σ_{min} = -110 MPa (16.0 ksi)

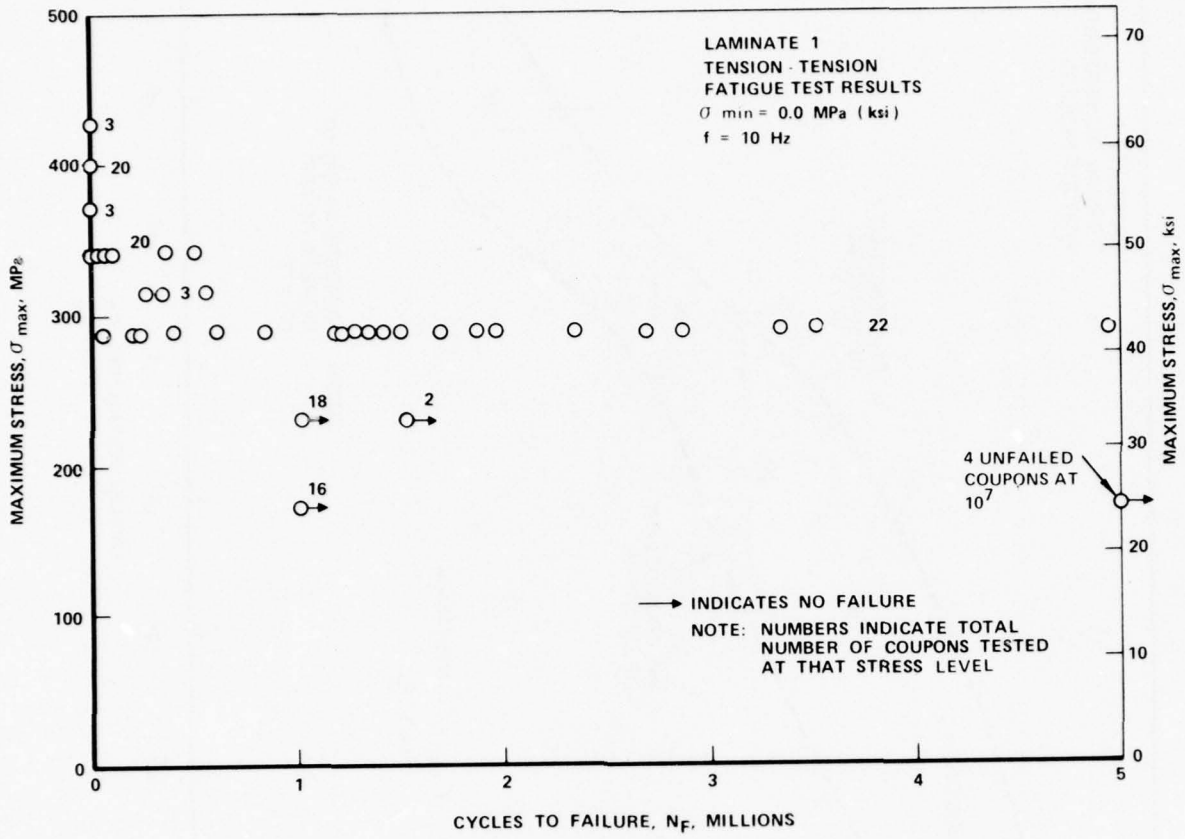


Figure 68. Linear Plot of Laminate 1 Tension-Tension Fatigue Results at σ_{min} = 0.0 MPa (ksi)

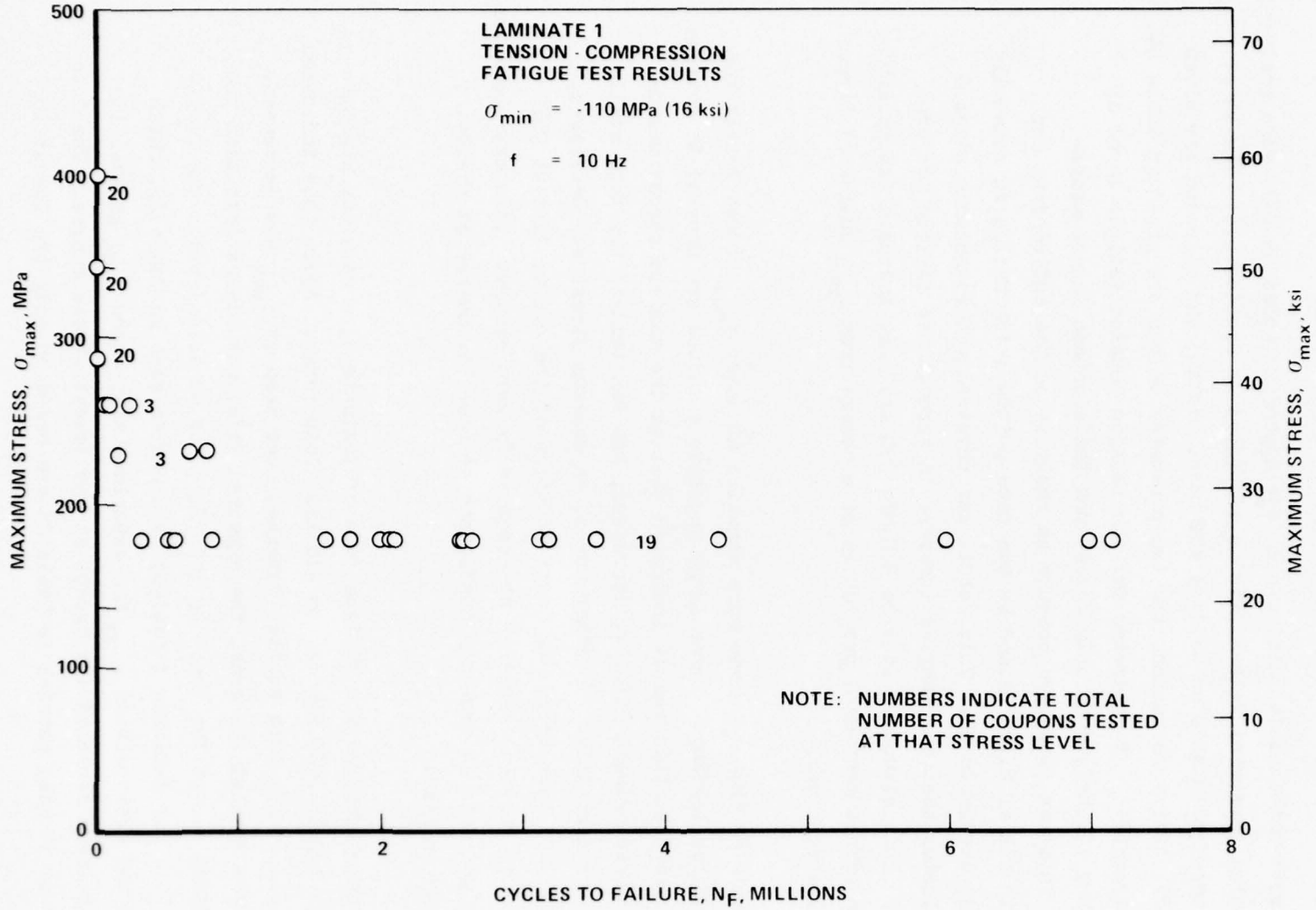


Figure 69. Linear Plot of Laminate 1 Tension-Compression Fatigue Results at σ_{min} = -110 MPa (16.0 ksi)

The data sets obtained for laminate 1 (see Appendix Tables 5B-13B) were analyzed using a three parameter Weibull fit as disucssed in Section 2.6. The k, e, v values were calculated as well as the mean, median, and mode and are given in Table 23. For information, the two parameter values are given in Table 24. Weibull parameters and estimates for the tension-tension fatigue level of 0 to 345 MPa (50 ksi) were only based upon the eighteen lowest sample entries. This was necessary because an analysis of the entire data set resulted in a k of 0.195 caused by two data points which failed at unusually long lives, see Table 6B. This result was physically unreasonable since a $k < 1$ indicates that the samples increase in strength as fatigue cycling continues. This situation at 0 to 345 MPa (50 ksi) may indicate the possible transition effect mentioned previously of a change from σ_{max} dominated lives to $\Delta\sigma$ dominated lives.

Note in Table 23 that e became more negative at lower σ_{max} stress levels for tension-tension loading. These large negative e values are unusual in fatigue data. In essence, this result indicated that as the maximum stress was decreased, characteristic life, v, increased, but the tail of the data still extended near zero life. In other words, as maximum stress was decreased, the average life increased, but extrapolation of the cyclic life at 99% probability of survival remained at essentially zero cycles. This extrapolation of the fatigue data is probably inadequate at some low number of cycles, a few thousand or less.

For the tension-compression fatigue data of laminate 1, e remained negative except at the 179 to -110 MPa (26 to -16 ksi) load range. Again this indicated that the tail of the data scatter remained near zero as σ_{max} was decreased. Note in Table 23 that the mode, the expected life, was always less than the mean or median except for the 0 to 345 MPa (0 to 50 ksi) level. The implication of this for laminate 1 fatigue data can be seen in Table 25, which shows that the extrapolated $P_{.99}$ and experimentally based $P_{.95}$ probability of survival lives remained low except at the lowest stress ranges. The 0 to 345 MPa (0 to 50 ksi) entries in Table 25 are based on only the lowest 18

TABLE 23

WEIBULL PARAMETERS AND ESTIMATES FOR LAMINATE 1 FATIGUE DATA
(20 Coupons/Stress Level)

Stress MPa (ksi)		Weibull Coefficients			Estimated Cycles to Failure		
max	min	k	e	v	Mean	Median	Mode
400(58)	0	1.988	- 2,030	4,899	4,007	3,660	2,868
345(50)	0	4.564	- 20,711	64,621	57,224	58,036	60,119
290(42)	0	1.846	-280,781	1,900,898	1,657,169	1,508,046	1,148,930
400(58)	-110(-16)	2.409	- 1,015	1,979	1,639	1,556	1,381
345(50)	-110(-16)	2.796	- 4,973	10,964	9,217	9,006	8,630
290(42)	-110(-16)	2.915	- 3,040	33,806	29,822	29,452	28,860
179(26)	-110(-16)	1.214	+ 74,246	2,892,580	2,717,625	2,138,043	748,300

TABLE 24.

WEIBULL PARAMETERS FOR TWO PARAMETER FIT
TO FATIGUE DATA OF LAMINATE 1 COUPONS

Stress MPa (ksi)		Weibull Coefficients	
max	min	k	v
400(58)	0	1.523	5,910
345(50)	0	3.159	71,374
290(42)	0	1.639	1,992,588
460(58)	-110(-16)	1.684	2,300
345(50)	-110(-16)	1.936	12,380
290(42)	-110(-16)	2.536	33,880
179(26)	-110(-16)	1,234	2,861,394

TABLE 25

FATIGUE LIVES AT VARIOUS PROBABILITIES
OF SURVIVAL FOR LAMINATE 1

Stress MPa (ksi)		Probability of Survival					
max	min	0.99	0.95	0.90	0.50	0.1	0.01
				Cycles N			
400 (58)	0	~ 0[a]	~ 0	~ 0	3,661	8,575	12,986
345 (50	0	10,430	23,800	31,404	58,036	81,731	98,535
290 (42)	0	~ 0	155,784	364,000	1,508,000	3,147,000	4,709,000
231 (33.5)	-110 (-16)	-[b]	>1,000,000	-	-	-	-
179 (26)	-110 (-16)	-	>1,000,000	-	-	-	-
460 (58)	-110 (-16)	~ 0	~ 0	162	1,557	3,218	4,629
345 (50)	-110 (-16)	~ 0	536	2,153	9,006	16,503	22,546
290 (42)	-110 (-16)	4,564	10,261	13,986	29,452	46,011	59,179
179 (26)	-110 (-16)	137,937	318,177	515,633	2,138,043	5,677,060	9,991,962

a - 0 indicates that the number of cycles to failure at that P(x) was essentially zero.

b - Indicates no entry.

sample lives of Table 6B. Even for tension-tension fatigue testing at 0 to 290 MPa (0 to 42 ksi) the $P_{.99}$ probability of survival cycles remained near zero. This result is, from a design viewpoint, clearly unacceptable. However, at 0 to 231 MPa (0 to 33.5 ksi) the $P_{.95}$ life dramatically increased as did the $P_{.95}$ life at 179 to -110 MPa (26 to -16 ksi). This result again indicated the possibility of a fatigue endurance limit for laminate 1.

The average lives of all of the fatigue data obtained for laminate 1 are plotted in Figure 70. Although the tail of data scatter is of more importance, these average values show that stress range was, at best, a poor parameter for relating fatigue life under tension-tension and tension-compression fatigue testing. In Figure 70, the fatigue behavior below $\Delta\sigma$ = 290 MPa (42 ksi) is clearly shown to be unknown. An endurance limit was only one of two possibilities the other being a continual linear extrapolation of $\Delta\sigma$ versus N_F. If this latter possibility is true, the implications for using composites like laminate 1 in certain helicopter design applications are adverse.

5.2.2 Fatigue Behavior - Laminate 2

Because of the distinctly different fatigue response of laminate 2, the same procedure for choosing σ_{max} levels to define the fatigue life scatter could not be used as was used for laminate 1. Therefore, for tension-tension loading 20 coupons (including the original three) were fatigue cycled to failure at σ_{max} = 772 MPa (112 ksi) while at σ_{max} = 689 MPa (100 ksi), coupons were fatigue cycled until at least 40 unfailed coupons were obtained which had been subjected to 10^6 load cycles. Tension-compression tests were conducted only at a maximum stress of 483 MPa (70 ksi) due to the temperature induced adhesive breakdown problem discussed previously. Testing of coupons was continued until 40 coupons were obtained which had survived 10^6 cycles.

Results of the fatigue tests of laminate 2 coupons are tabulated in Appendix B and are plotted as σ_{max} versus log (N_F) in Figure 71. The data are also plotted as σ_{max} versus linear N_F in Figure 72. The main conclusion that can

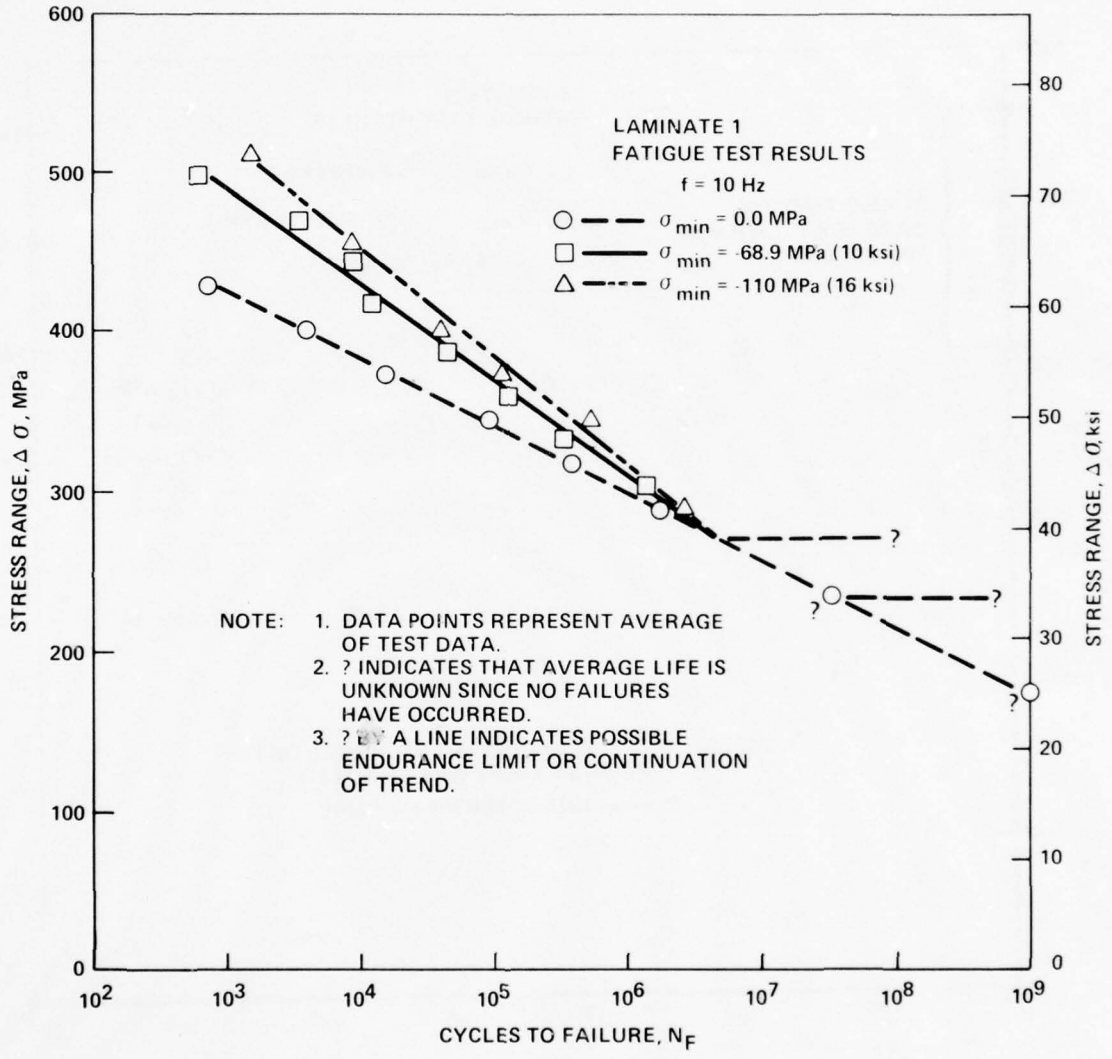


Figure 70. Combined Plot of Laminate 1 Fatigue Results

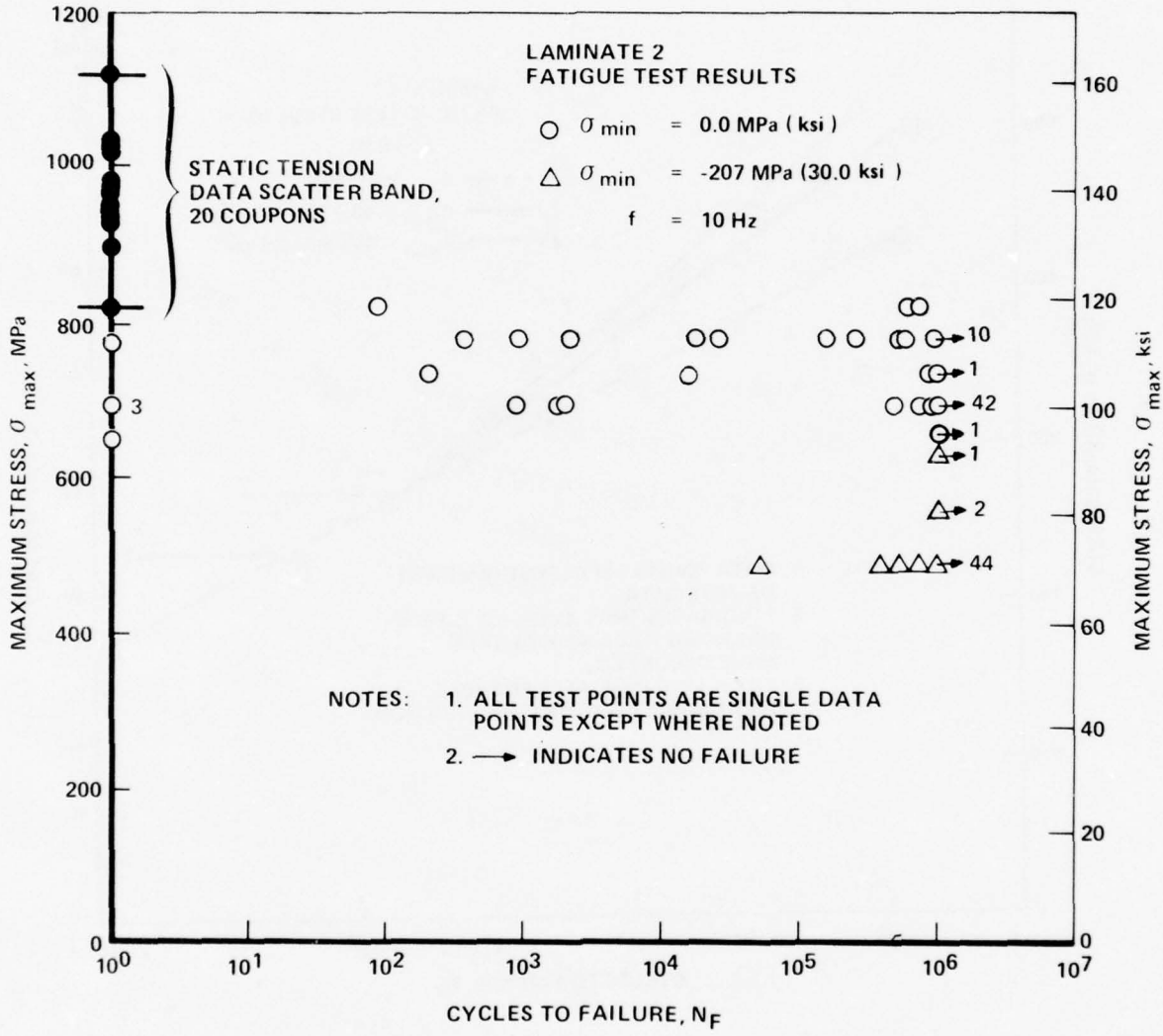


Figure 71. Laminate 2 Fatigue Results

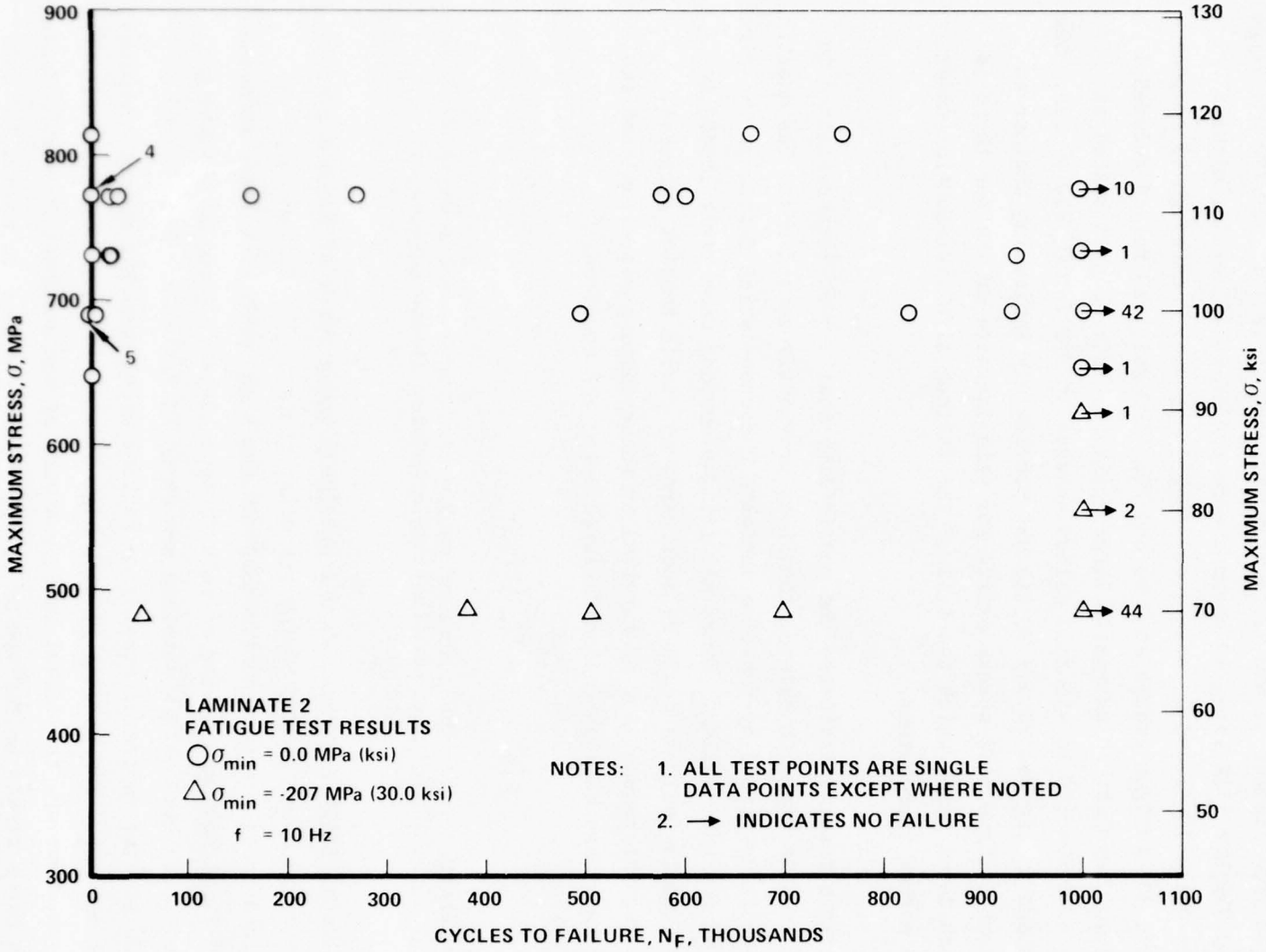


Figure 72. Linear Plot of Laminate 2 Fatigue Results

be drawn from Figures 71 and 72 is that the scatter in fatigue life was large. At 0 to 772 MPa (112 ksi), 10 coupons were cycled to 10^6 cycles without failure while 10 failed between 1 and 599,330 cycles. Although 43 coupons survived 10^6 fatigue cycles at 0 to 689 MPa (100 ksi), 10 failed between 1 and 930,000 cycles, an extremely large scatter. Four coupons tested at 483 to -207 MPa (70 to -30 ksi) failed between 58,090 to 696,420 cycles. The data shown in Figures 71 and 72 did not provide any indication whether an endurance fatigue life stress exists for this laminate or whether there is a stress level below which the tail of the fatigue life distribution undergoes a marked improvement.

The fatigue results indicated the possibility that a much larger scatter in static tensile strength existed than that previously considered. The question was especially raised by the five laminate 2 coupons which failed on the first cycle of fatigue loading. Since all fatigue coupons were first loaded in tension, these failures could be considered as static tension failures. Therefore, the probability of survival of these coupons was calculated assuming they were static tension failures using the equation:

$$P(x) = 1 - {}^{1}/_{n}$$

where n = the number of static or fatigue coupons whose maximum first cycle tension stress equaled or exceeded x

The value of failure stress, x, was precisely known for 4 of the 5 early failure coupons and within 5% for the other coupon. The failure load was determined using the permanent records of the high speed visicorder recorded for the first few load cycles of each fatigue coupon. Based on the above procedure, the P(x) values obtained are shown in Table 26. Also listed in Table 26 are the estimated strains to failure based upon the average apparent tensile modulus. The modulus at such high strain rates may have been slightly different, however, the lowest failure stress of the original 20 static failure coupons had a strain to failure of 0.0065 mm/mm; the same as coupon 728-19B

TABLE 26

SUMMARY OF FIRST CYCLE FATIGUE FAILURES
OF LAMINATE 2

Coupon ID	Ultimate Stress at σ_{ult}, MPa (ksi)	Estimated[a] Strain to Failure, ε_{ult}, mm/mm	Probability of Survival, P(x)
728-19B	687 (99.7)	.0065	.989
727-1C	633 (91.8)	.0060	.99
699-1B	543 (78.8)	.0051	.9906
699-28C	540 (78.3)	.0051	.99065
699-34B	483 (70)[b]	.0045	.994

a - Based on the average apparent tensile modulus of 106 GPa (15.4 x 10^6 psi)

b - Estimated at 483 MPa (70 ksi) within 5%

which failed on the first load cycle. Three of the five coupons of Table 26 were from panel 1NH699 which may be significant considering the C-scan record for that panel.

Figure 73 shows the estimated distribution of static tensile strength data for laminate 2. The distribution indicates the possibility of an extended tail in the static strength data. The low static strength data could have been caused by any of four possibilities; (1) a strain rate effect, (2) a material defect, (3) a geometric variation in the coupon, (4) an error in testing.

1) The strain rate during static tensile testing was approximately 0.0015 mm/mm/min. while that during the first cycle of a fatigue test was approximately 6.0 mm/mm/min. or $\sim$ a 10^3 faster rate. This high strain rate may have caused a coupon to be more sensitive to any small local defect. However, as will be shown in Section 6 by the static residual tension strength data, this effect is unlikely because no degradation in residual strength of the unfailed coupons was observed. 2) Possibly rare, but not unique unobserved defects in the coupons caused the five first cycle fatigue failures particularly in the case of those from panel 699. If this was true, such defects were not larger than the coupon gage length area because coupons which were situated in the panels above or below or on either side of the failed coupons had long fatigue lives or high static tension strengths. 3) Extremely small variations in the tab geometry ($\pm$ 0.0254 mm (0.001 in.)) may have caused load introduction problems and resultant early failure. 4) One possibility for an error in testing was an excessive torque on the grip bolts. Although this could have occurred, bolts on each laminate 2 coupon were uniformly tightened to 181 N·m (1600 in.·lbs) thus any variation would have to have been due to the specific load transfer caused by the particular geometry of each bolt. The possibility of an inadvertent coupon overload was prevented by maximum and minimum peak and valley detectors used on all tests which would have tripped if the load exceeded the preset maximum fatigue load. Additionally, visicorder records revealed no load overshoots.

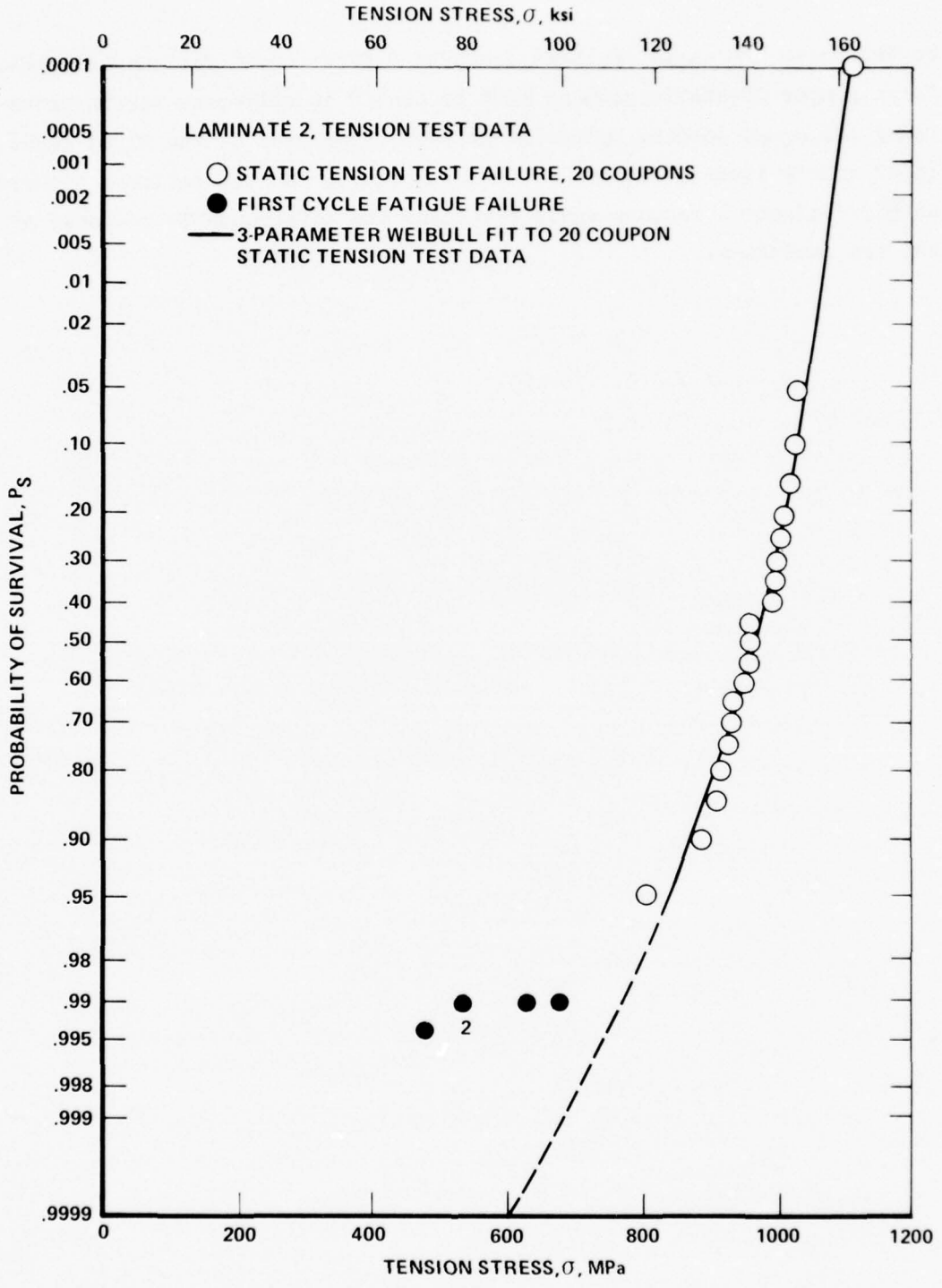


Figure 73. Distribution of Laminate 2 Static Tension Strength Data

To determine the cause of these laminate 2 first cycle fatigue failures, a large number of static coupons must be tested at different strain rates using uniformly loading hydraulic grips. Regardless of the final cause (most likely items 1, 2, and 3, in that order), no such failures occurred within laminate 1 coupons again revealing the difference in response of the two laminates.

SECTION VI

RESIDUAL STRENGTH RESULTS

Due to the different fatigue life scatter behaviors of the two laminates, the residual strength degradation study was designed differently for each laminate. For laminate 1, coupons were fatigue cycled to a life chosen equivalent to a probability of survival equal to $P_{.90}$ at each σ_{max} level. Coupons were fatigue cycled until 40 unfailed samples were obtained. Coupons which failed during fatigue were replaced. For laminate 2, coupons were fatigue cycled at 0 to 689 MPa (100 ksi) and at 483 to -207 MPa (70 to -30 ksi) until at least 40 unfailed coupons after 10^6 cycles were obtained at each maximum stress level. Half of all unfailed coupons of both laminates were subsequently tested in static tension and half in static compression.

6.1 Laminate 1 Residual Strength Results

Table 27 shows the number of cycles equivalent to $P_{.90}$ at each σ_{max} level to which 40 coupons were fatigue cycled for the residual strength study of laminate 1 coupons. The cycles listed in Table 27 are equal to a probability of survival of $P_{.90}$ based on a 3-parameter fit at the tabulated fatigue stress levels. Appendix C contains the static tension and compression residual strength data for the coupons fatigue tested to the cycles shown in Table 27. Included in Appendix C are the coupons which failed during fatigue cycling together with their respective cycles to failure.

Table 28 lists a summary of all of the residual strength data for laminate 1. The essential equivalence of the two and three parameter Weibull fits to the static data is clearly evident in Table 28. The average ultimate stress, ultimate strain and apparent initial modulus of the tension or compression residual strength coupons increased with the severity of the fatigue stress range. This result implied that fatigue cycling at more severe stress ranges screened more coupons by early failure and that the nature of the obvious strength degradation was not simple.

TABLE 27

NUMBER OF FATIGUE CYCLES TO WHICH LAMINATE 1 RESIDUAL STRENGTH COUPONS WERE SUBJECTED (The number of cycles is equivalent to a Probability of Survival of $P_{.90}$)

Fatigue Stress Level MPa (ksi)	Number of Fatigue Loading Cycles
290 to 0 (42 to 0)	364,000
345 to 0 (50 to 0)	31,400
290 to-110 (42 to -16)	14,400
345 to-110 (50 to -16)	2,150

TABLE 28

SUMMARY OF RESIDUAL STRENGTH TESTS FOR LAMINATE 1
(20 Coupons/Test Condition)

Fatigue Stress Levels, MPa (ksi)	Weibull Parameters			Correlation Coefficient, R	Average Ultimate Stress, σ_{avg}, MPa (ksi)	Average Ultimate Strain, ϵ_{avg}, mm/mm in 50.8 mm	Average Apparent Modulus, E_{avg}, GPa ($psi \times 10^6$)
	k	e	v				
Tension Test Results Before Fatigue	24.18	-0.0753	70.50	0.9995	477(69.2)	0.0096	52.7(7.64)
	24.12	0	70.57	0.9995			
290 to 0 (42 to 0)	12.12	-0.6276	64.52	0.9958	430(62.4)	0.0090	47.2(6.84)
	11.88	0	65.04	0.9957			
345 to 0 (50 to 0)	12.85	-0.1688	67.31	0.9987	449(65.1)	0.0093	48.3(7.01)
	12.78	0	64.45	0.9987			
290 to -110 (42 to -16)	18.51	-0.0608	68.43	0.9995	463(67.2)	0.0094	49.4(7.17)
	18.48	0	68.49	0.9995			
345 to -110 (50 to -16)	18.34	-0.1326	69.26	0.9992	467(67.7)	0.0095	49.2(7.13)
	18.27	0	69.38	0.9992			
Compression Test Results Before Fatigue	12.09	-0.4572	72.19	0.9973	480(69.7)	0.0110	47.9(6.95)
	11.94	0	72.53	0.9973			
290 to 0 (42 to 0)	7.22	-0.6574	60.15	0.9962	394(57.2)	0.0098	43.9(6.37)
	7.07	0	60.52	0.9961			
345 to 0 (50 to 0)	13.02	-0.2053	65.62	0.9988	439(63.7)	0.0111	45.8(6.64)
	12.94	0	65.79	0.9988			
290 to -110 (42 to -16)	12.54	-0.2387	67.26	0.9982	450(65.3)	0.0108	45.9(6.66)
	12.46	0	67.45	0.9982			
345 to -110 (50 to -16)	14.74	-0.5418	70.34	0.9969	473(68.6)	0.0110	45.9(6.66)
	14.52	0	70.82	0.9969			

Throughout the residual strength analysis for laminate 1 results, coupons which failed during fatigue were not included in the static data analysis. The procedure and associated implications will be discussed further in Section 7.4. They were excluded because of the apparent difference in failure modes between static and fatigue failures and because the static residual strength distributions did not appear to directly relate to coupons which failed during fatigue. The latter point is illustrated in Table 29 which shows that for the tension results, the strength of the weakest tensile coupon was significantly above the maximum fatigue stress. Figures 74 and 75 show typical failure modes for tension and compression residual strength coupons, respectively. These failure modes were similar to previous static failure modes and less similar to fatigue failure modes.

6.2 Laminate 2 Residual Strength Results

For laminate 2, residual strength tests were conducted on coupons cycled to 10^6 cycles either under tension-tension loading from 0 to 689 MPa (100 ksi) or from 483 to -207 MPa (70 to -30 ksi) under tension-compression loading. Forty unfailed coupons at each σ_{max} level were tested, half in tension and half in compression. The detailed results of these tests are given in Appendix C.

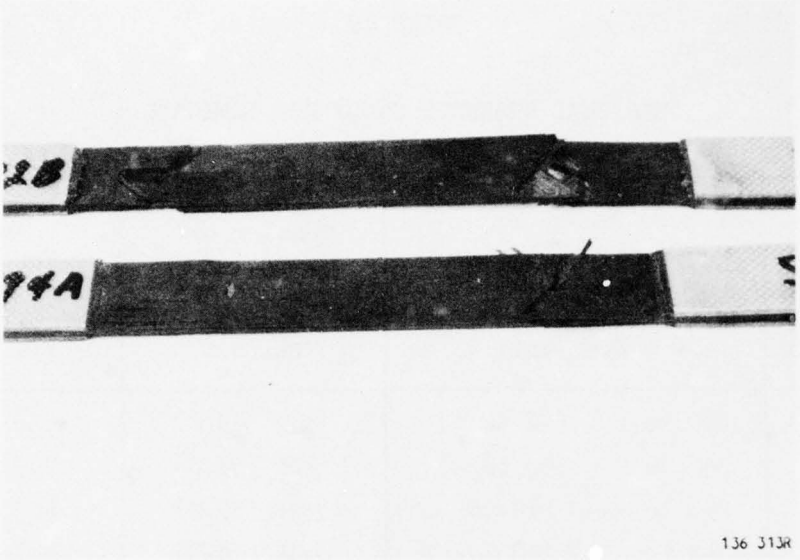
The only difference in failure modes between the original tensile tests and the tensile residual strength tests was that most of the static tensile residual strength stress-strain curves had a short "flat-topped" region prior to fracture. Figure 76 shows similar tension failure modes as those noted previously on the initial tensile tests. Compression residual strength stress-strain curves and failure modes, see Figure 77, were also similar to the initial unfatigued static compression data.

Table 30 summarizes the results of the laminate 2 residual strength study. The tension residual strength results were virtually identical in all properties to the original tension results even though 9 of 52 coupons tested in fatigue at 0 to 689 MPa (100 ksi) failed. In contrast to laminate 1 data, there was no tension residual strength degradation after 10^6 cycles at the stress levels

TABLE 29

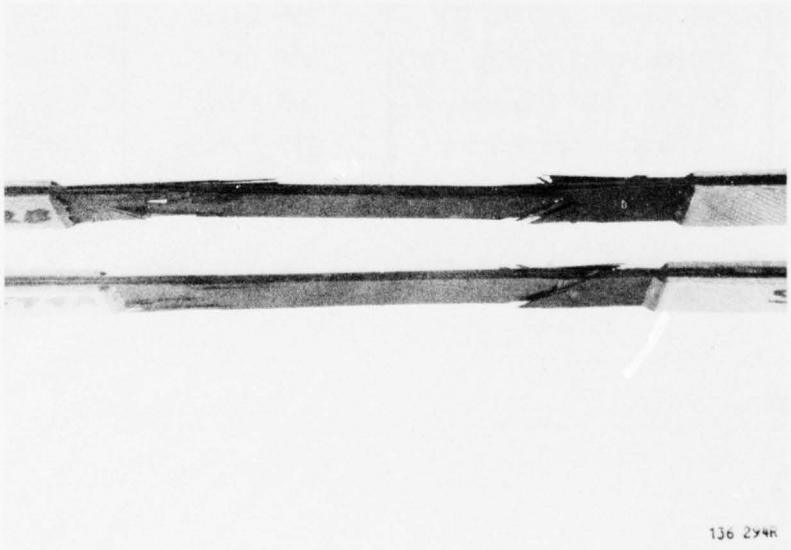
RESIDUAL STRENGTH STUDY FOR LAMINATE 1

Type of Test T-Tension, C-Compression	Fatigue Stress Level, MPa (ksi)	Lowest Tension or Compression Failure Stress, MPa (ksi)	Average Tension or Compression Strength, MPa (ksi)
T	290 to 0 (42 to 0)	339 (49.2)	430 (62.4)
	345 to 0 (50 to 0)	376 (54.6)	449 (65.1)
	290 to -110 (42 to -16)	407 (59.0)	463 (67.2)
	345 to -110 (50 to -16)	402 (58.3)	467 (67.7)
	Static Tension	427 (62.0)	477 (69.2)
C	290 to 0 (42 to 0)	285 (41.4)	394 (57.2)
	345 to 0 (50 to 0)	356 (51.6)	439 (63.7)
	290 to -110 (42 to -16)	362 (52.5)	450 (65.3)
	345 to -110 (50 to -16)	390 (56.5)	473 (68.6)
	Static Compression	397 (57.6)	481 (69.7)



136 313R

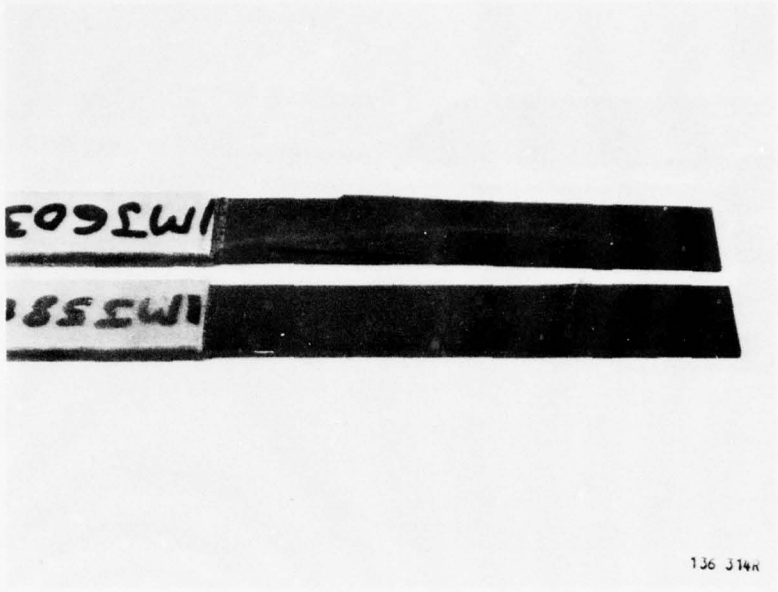
a. Coupon 1MJ 582-6B, 1MJ 594-10A; Side View



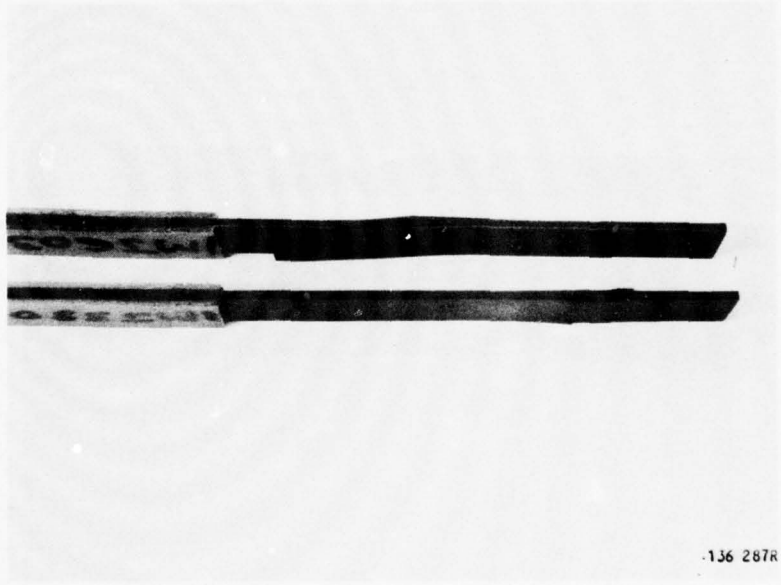
136 294R

b. Coupon 1MJ 582-6B, 1MJ 594-10A; Edge View

Figure 74. Typical Laminate 1 Static Tension Residual Strength Failure Modes

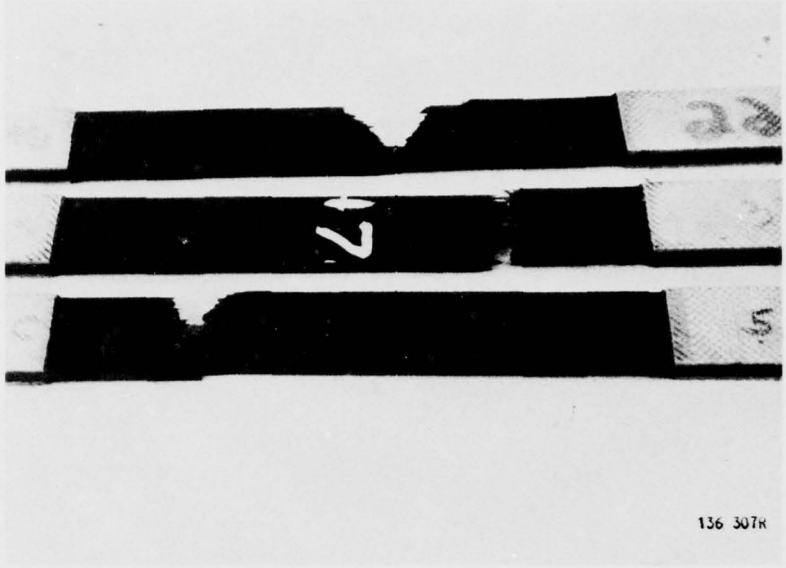


a. Coupons 1MJ 603-5A, 1MJ 580-1A; Side View

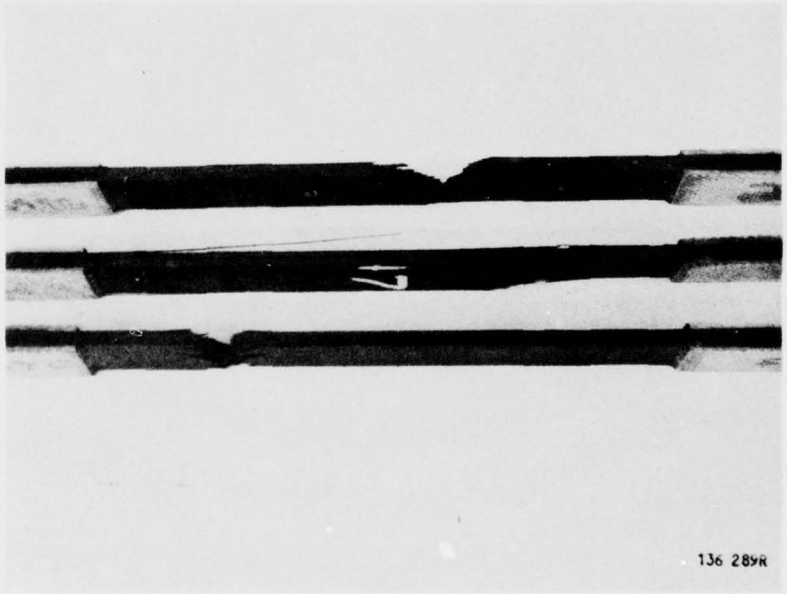


b. Coupons 1MJ 603-5A, 1MJ 580-1A; Edge View

Figure 75. Typical Laminate 1 Static Compression Residual Strength Failure Modes

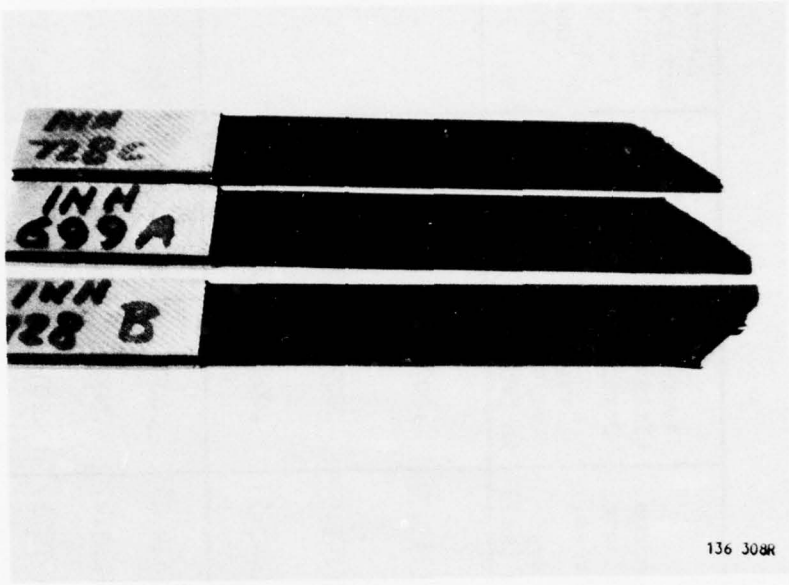


a. Coupons 1NH 699-22B, 1NH 728-37A, 1NH 727-5C; Side View

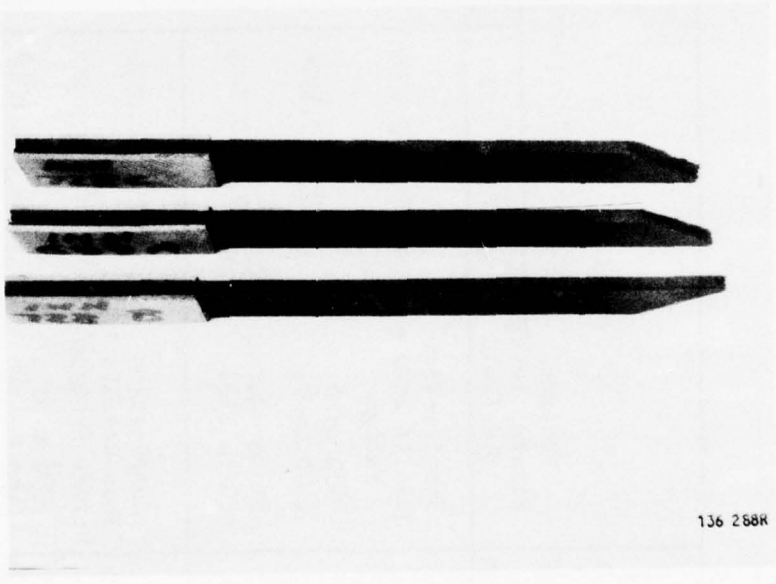


b. Coupons 1NH 699-22B, 1NH 728-37A, 1NH 727-5C; Edge View

Figure 76. Typical Laminate 2 Static Tension Residual Strength Failure Modes



a. Coupons 1NH 728-31C, 1NH 699-27A, 1NH 728-35B; Side View



b. Coupons 1NH 728-31C, 1NH 699-27A, 1NH 728-35B, Edge View

Figure 77. Typical Laminate 2 Static Compression Residual Strength Failure Modes

TABLE 30

SUMMARY OF RESIDUAL STRENGTH TESTS FOR LAMINATE 2

(20 Coupons/Test Condition)

Type of Static Test, T-Tension C-Compression	Fatigue Stress Level, MPa (ksi)	Weibull Parameters			Average Ultimate Stress, σ_{avg}, MPa (ksi)	Average Ultimate Strain, ε_{avg}, mm/mm in 50.8 mm	Average Apparent Modulus, E_{avg}, GPa (psi x 10^6)	Secant Modulus at 483 MPa (70 ksi) E_{sec}, GPa (psi x 10^6)
		k	e	v				
T	Tensile Test Results Before Fatigue	18.87	-0.4304	144.41	977(141.7)	.0092	106 (15.4)	-
	689 to 0 (100 to 0)	17.19	-0.3926	146.81	989(143.5)	.0092	108 (15.7)	-
	483 to -207 (70 to -30)	21.57	-0.1409	146.42	991(143.7)	.0094	105 (15.3)	-
C	Compression Test Results Before Fatigue	25.02[a]	-0.2592	115.82	787(114.2)	.0098	79.3 (11.5)	86.2(12.50)
		19.79[b]	-0.4902	115.97	782(113.4)	.0093	83.4 (12.1)	91.0(13.21)
	689 to 0 (100 to 0)	9.30	-1.6398	103.07	665(99.3)	.0078	87.6 (12.7)	92.9(13.46)
	483 to -207 (70 to -30)	9.32	-4.8439	102.60	681(98.8)	.0079	86.7 (12.6)	92.9(13.50)

a - Tested 3-76

b - Tested 10-76

investigated. However, this was not true for the compression residual strength tests. Table 30 shows the degradation which occurred in σ_{ult} and in ε_{avg}. The degraded compression residual strength results were virtually identical to each other, but drastically different from the original compression data. Note the large decrease in the exponent k for the residual compression results.

Because the average apparent modulus increased for the compression residual strength coupons and because the residual strength results resembled each other more than the initial distribution of unfatigued static coupons, the initial tests of unfatigued compression coupons were duplicated using 20 new coupons. In addition, due to the subjective nature of the apparent modulus the secant modulus from 0 to 483 MPa (70 ksi) was measured for all 80 coupons. The results of the new compression tests of unfatigued coupons are also summarized in Table 30 and tabulated in Table 13C of Appendix C. Table 30 clearly shows that σ_{avg} was unchanged, but that ε_{avg} decreased and E_{avg} and E_{sec} increased. This result gave confidence in the original tests as well as supported the observed increase in E_{avg} for the residual strength coupons. The conclusion was that E_{avg} actually increased for the compression residual strength coupons as supported by the four sets of test results for E_{avg} and the non-subjective E_{sec}. Additionally, the compression residual strength properties did degrade, but the effects of the T-T and T-C load ranges were identical.

The cause of the increase in apparent modulus of the compression residual strength coupons was hypothesized to be due to two effects. First, an increase in moisture due to longer shelf storage prior to testing could decrease strain to failure and increase the modulus as supported by the observations for the two sets of unfatigued coupons (see Table 30) and predicted theoretically for this layup as shown in Figure 78. This figure also shows that the same effect, though less observable, should occur in a different matrix. Second, fatigue cycling may redistribute residual stresses by inducing matrix cracking and thus allow the modulus to increase.

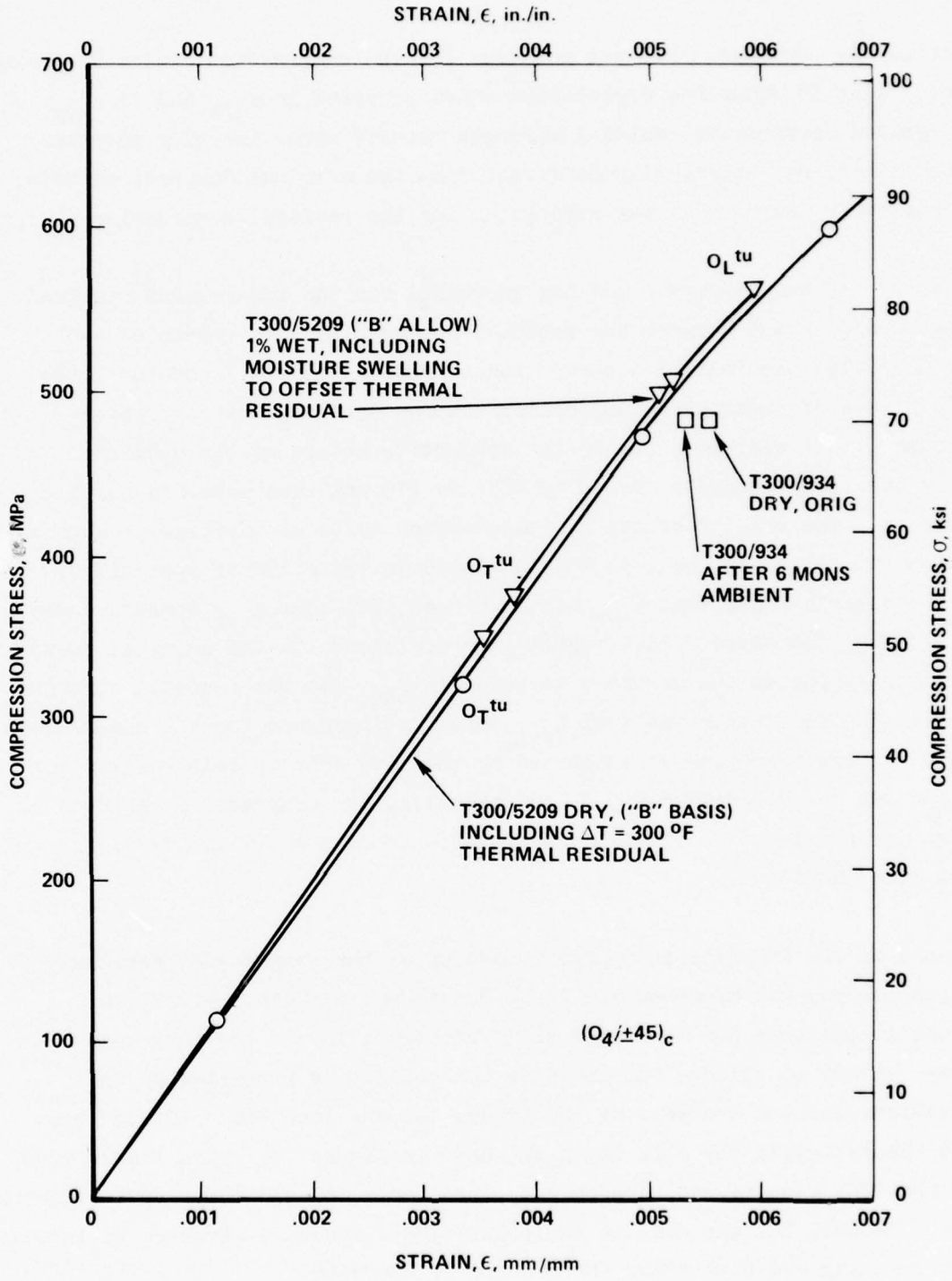


Figure 78. Theoretical Prediction of the Effect of Moisture on the Compression Strength of Laminate 2

SECTION VII

DISCUSSION

In this section differences and comparisons between the test results of the two laminates will be drawn. In addition, the effects on data analysis and modeling of a data sample set due to using either a 3- or 2- parameter Weibull fit will be discussed as well as the minimum sample size needed to extrapolate predictions. Finally, the applicability of one commonly used formulation of the "wear-out" type analytical model for predicting residual strength degradation will be discussed.

7.1 Comparison of Laminate Results

7.1.1 Tension and Compression Results

Although the static tension ultimate strengths and apparent moduli of elasticity of the two laminates were greatly different, their strains to failure were quite similar and, in fact, similar to that of the 0° fibers alone. Thus, the particular layup essentially only affected the apparent modulus of elasticity while the change in ultimate strength appeared to be a reflection of this modulus change. The layup also affected Poisson's ratio: laminate 1 $\sim$ 0.28, laminate 2 $\sim$ 0.63.

Static compression moduli for both laminates were lower than their respective tension moduli and the strains to failure did not agree as well as the tension strains to failure. The scatter in the compression data was greater than in the tension data for laminate 1, but this situation was reversed for laminate 2.

7.1.2 Fatigue Results

The primary difference between the two laminates in their fatigue properties, besides the difference due to relative strength, was the apparent larger scatter of the laminate 2 data. The tension-tension fatigue response of the

two laminates is compared in Figure 79 which shows the large difference observed. For equivalent fatigue lives, σ_{max} was higher for laminate 2 than for laminate 1, however, this was primarily a reflection of the higher static strength of laminate 2. The scatter in fatigue lives was noted to be less for laminate 1 than that for laminate 2. A more pronounced slope, i.e., dependence of N_F on σ_{max} of the laminate 1 data compared to laminate 2 data appeared possible. However, Figure 80 shows the tension-tension fatigue data replotted as $\sigma_{max}/\sigma_{ult}$ versus log N_F and indicates that the shape of the laminate 2 curve may be similar to that of laminate 1, but was possibly masked by the large laminate 2 data scatter. To settle the question of the S-N curve shape for laminate 2, more data would be needed at σ_{max} levels below 689 MPa (100 ksi). Note in Figure 80 that the first cycle laminate 2 fatigue failures were not plotted because of lack of knowledge as to the true cause of their failure.

Laminate 2 also appeared to respond to fatigue loading differently from laminate 1 as supported by the first cycle failures of some laminate 2 coupons. The cause of these early failures is unknown, however, the fact remains that no laminate 1 coupons experienced such a phenomenon.

The tension-tension fatigue response of the two laminates shown in Figure 80 is essentially plotted on the basis of average failure strain because strains at failure were similar. Perhaps in the future, strain should be used as a common variable instead of stress.

7.1.3 Residual Strength Results

The static tension and compression residual strengths and moduli of laminate 1 coupons degraded with application of fatigue loading. In contrast, only the static compression residual strength of laminate 2 degraded. Because the amount of observed degradation in the laminate 1 residual strength properties appeared to decrease with an increase in severity of the fatigue loading, the degradation was probably not as simple as the "wear-out" type of degradation normally assumed.

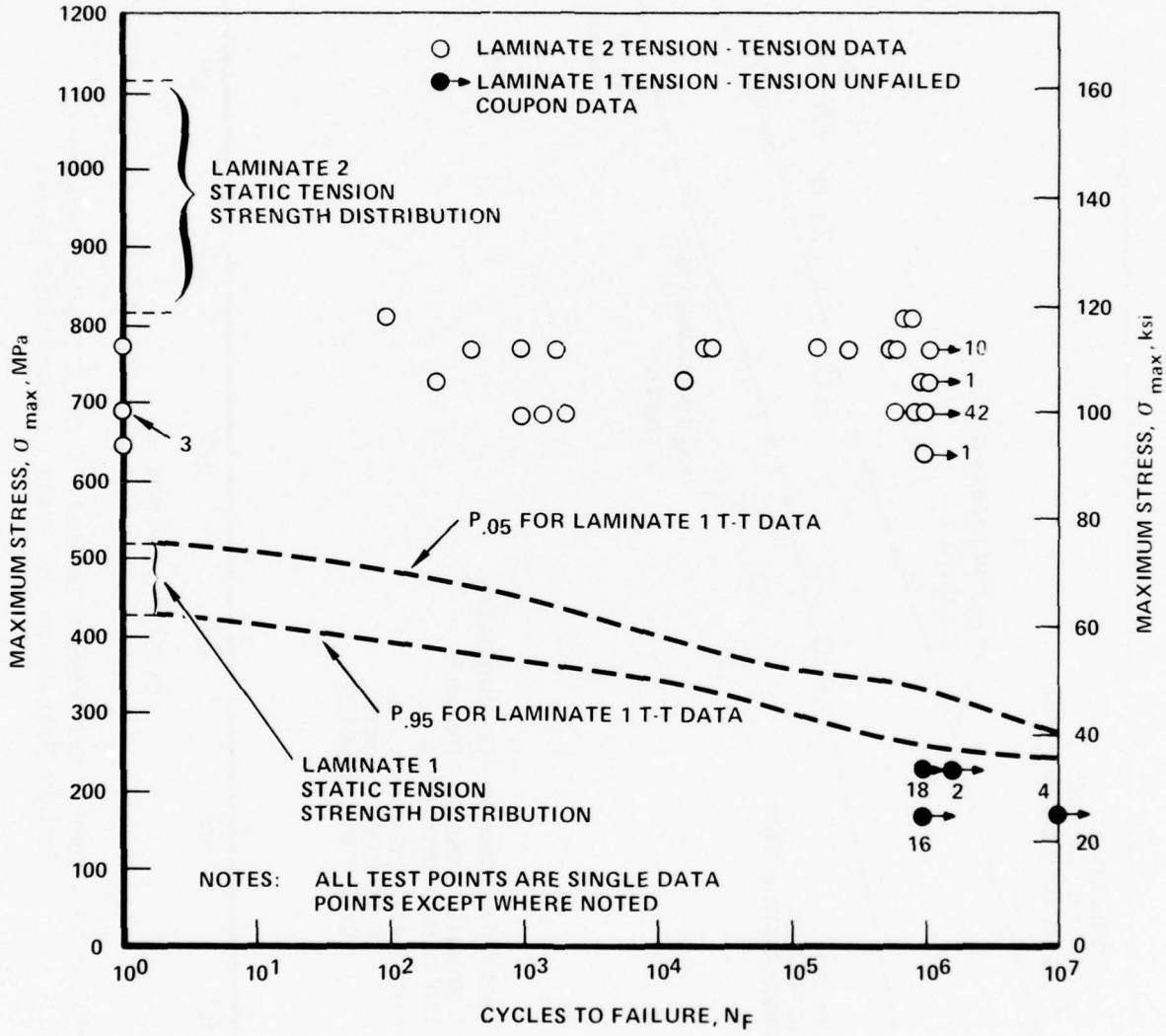


Figure 79. Comparison between Laminate 1 and 2 Tension-Tension Fatigue Results

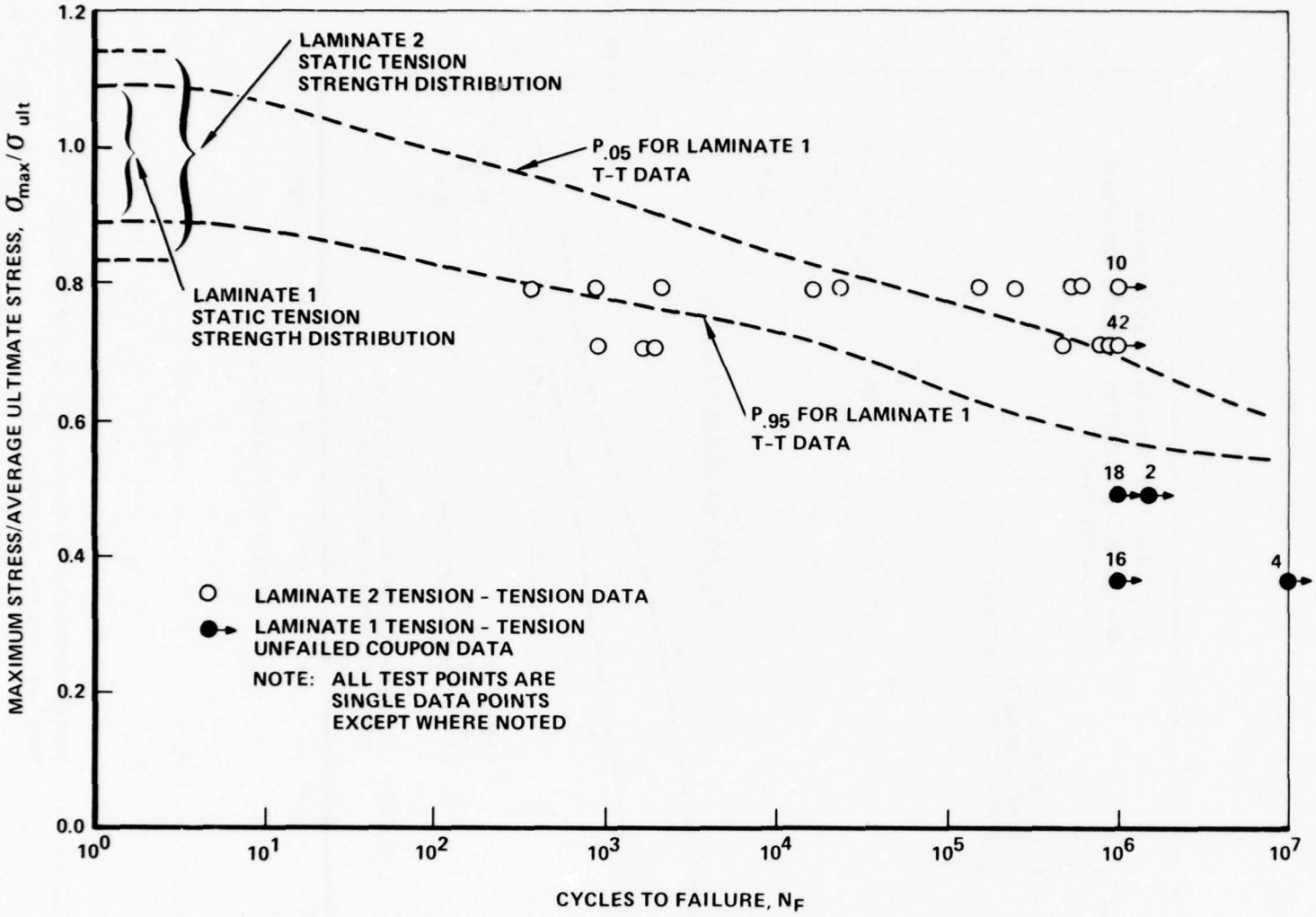


Figure 80. Comparison Between Laminate 1 and 2 Tension-Tension Fatigue Results on the Basis of Normalized Stress

7.1.4 Summary

The mechanical behavior test results of the two laminates were, in general, strikingly different. A major conclusion appears to be that a significant number of different stacking sequences and/or layups may have to be fully and independently evaluated for response to mechanical testing prior to drawing any general conclusions. This appears to be true in spite of the fact that different layups are made of the same material. Without such an evaluation, prediction of laminate properties, especially fatigue and residual strength, will require considerable test data on laminates of interest until greater experience in the use of composite materials is developed. Perhaps relating properties of different layups on the basis of strain will prove fruitful. The scatter in fatigue properties was especially disturbing, particularly the existence of a long tail in the data. The cause of this scatter needs to be determined and reduced.

At first glance, the conclusion regarding the large differences in mechanical response of the two laminates and the extent of their data scatter appears to present a formidable challenge to future structural use of composites. Though the challenge is real, the situation for all metal alloys was no different in the past, and for many alloys still is today, than the situation for graphite/epoxy composites.

The large differences in mechanical response of these two laminates made of the same material are similar to those found for different heat treatments of the same metal alloy. Possibly, different layups of the same material are as different as two different heat treatments of the same metal alloy while the effect of different stacking sequences of the same laminate may be like the more subtle effects of small differences in some heat treatments of one metal alloy. In metals, as the strength of an alloy is increased, the scatter in properties increases like that of laminate 2 data compared to laminate 1. Carrying the analogy further, metals, especially titanium, often have fatigue scatter in the range of two orders of magnitude in life if special care is not given to alloy manufacture and extreme care to preventing cold work and surface degradation during machining. The scatter in composites may possibly

be reduced by attention to the same type of details. For metals, special care must be given to furnace cool-down rate to minimize microcracking, a situation undoubtedly analogous in composites concerning autoclave cool-down rates. However, in metals slow cool-down rates, though at first glance, advantageous, can result in other problems; also a likely possibility in composites.

In summary, though the difference in mechanical response between different layups of the same composite material was large, the situation is analogous to metal alloys. The physical principles appear to be the same although the details of their application differ due to the nature of fibrous directionally reinforced materials. Difficulties in applying the details of physical and mechanical principles to composites appear to be no greater than applying them to metals. The problem of data scatter for composites appears to be formidable and yet the same problem of a similar magnitude has been solved for many metal alloys. The problem of wide scatter may, of course, be far less severe for notched coupons. The development of better understanding of property trends and quality control of composites may prove to be difficult and costly, but most likely is no worse than that already accomplished for many metal alloys. Similar analogies can also be made for the special problems that may exist in the testing of composite materials.

7.2 Comparison of 3- and 2- Parameter Weibull Analysis Results

To investigate differences between the accuracy of fitting fatigue data with a 2- or 3- parameter Weibull equation, the data of laminate 1 was more extensively analyzed. Based on the original fatigue sample size at each fatigue level, an extrapolation was made for each stress level based on a 3-parameter Weibull fit. This extrapolation was compared to the actual large sample sets at each stress level which consisted of the original 20 coupons plus the first fatigue coupons used for static residual strength testing before any failures were replaced. This procedure allowed for a comparison between predicted and actual fatigue failure rates for a large sample size (60) based on the analysis of a smaller sample size (20). In addition, the same procedure was used based on a 2-parameter Weibull equation so that direct comparisons could be drawn

between 2- and 3- parameter Weibull fits. This was especially important in light of the observed large scatter in fatigue data since the 3-parameter fit would be expected to predict the extrapolated short life tail better than the 2-parameter fit. Results of this life prediction study are shown in Tables 31 and 32.

To explain the significance of the results listed in Tables 31 and 32, consider the results for the fatigue stress level, 0 to 290 MPa (42 ksi). According to Table 31 and based on a 3-parameter fit to the original 20 coupon sample set of Section 5.2.1, the life equal to that at which 90% of the coupons would survive, $P_{.90}$, was calculated as 364,000 cycles compared to 504,860 cycles calculated at $P_{.90}$ for a 2-parameter fit, see column (2) of Table 31.

Two of the original 20 coupons should have failed at a cycle life equal to or less than the number of cycles equivalent to a 90% probability of survival, $P_{.90}$, regardless of whether the calculated cycles were based on a 2- or 3-parameter fit. As can be seen in column 5 of Table 31, 3 coupons of the 20 actually failed below the predicted life of 364,000 cycles (3-parameter fit) as did 3 at less than 504,860 cycles (2-parameter fit). Column (6) shows that 40 coupons were fatigue cycled before failed coupons were replaced for the residual strength study while column (7) shows that at $P_{.90}$, 4 would, of course, be expected to fail. Column (8) shows that actually 5 of the 40 coupons of column (7) failed below the life corresponding to $P_{.90}$ based on a 3-parameter fit. The accuracy of the 2-parameter fit could not be evaluated in column (8) because coupons were not cycled beyond a life equivalent to $P_{.90}$ predicted by the 3-parameter fit (364,000 cycles). Columns (9 and 10) show that the total sample size was 60 with 6 expected to fail below $P_{.90}$, and column (11) shows that 8 failed below the calculated life at $P_{.90}$ based on a 3-parameter fit.

The sample size at any one stress level in Table 31 was not large enough to judge the accuracy of the 2- or 3-parameter Weibull fits. Therefore, in the bottom row results were summed, since the accuracy of the fits to their respective data sets were essentially equivalent. The total row shows that

TABLE 31

SUMMARY OF EXPECTED AND OBSERVED FAILURE RATES AT $P_{.90}$

FOR LAMINATE 1
(BASED ON WEIBULL ANALYSIS)

(1)	(2)		(3)	(4)	(5)		(6)	(7)	(8)	(9)	(10)	(11)
Fatigue Stress Range, MPa (ksi)	Number of Cycles to Failure at $P_{.90}$ [a]		Initial Sample Size [b]	Number of Expected Failures Below $P_{.90}$	Number of Failed Coupons Below $P_{.90}$		Sample Size Fatigue Tested Prior to Residual Strength Tests	Number of Expected Failures Below $P_{.90}$	Number of Failed Coupons Below $P_{.90}$ [c]	Total Sample Size	Total Number of Expected Failures Below $P_{.90}$	Total Number of Failed Coupons Below $P_{.90}$
	3 Parameter	2 Parameter			3 Parameter	2 Parameter			3 Parameter			3-Parameter
0 to 290 (0 to 42)	364,000	504,860	20	2	3	3	40	4	5	60	6	8
0 to 345 (0 to 50)	31,400	35,000	20	2	2	2	40	4	4	60	6	6
290 to -110 (42 to -16)	14,000	13,950	20	2	1	1	40	4	4	60	6	5
345 to -110 (50 to -16)	2,150	3,870	20	2	3	4	40	4	1	60	6	4
TOTAL			80	8	9	10	160	16	14 [d]	240	24	23 [d]

a - $P_{.90}$ means that 90% of the samples are expected to survive the number of equivalent fatigue cycles and 10% to fail

b - These were the sample sets which were fitted by Weibull analysis used to estimate the cycles at $P_{.90}$

c - These coupons were replaced for the residual strength study

d - 2-parameter data could not be calculated because coupons were not fatigue cycled to the cycle life based on 2-parameters.

TABLE 32

SUMMARY OF EXPECTED AND OBSERVED FAILURE RATES AT $P_{.95}$

LAMINATE 1

(BASED ON WEIBULL ANALYSIS)

(1)	(2)		(3)	(4)	(5)		(6)	(7)	(8)		(9)	(10)	(11)	
Fatigue Stress Range, MPa (ksi)	Number of Cycles to Failure at $P_{.95}$[a]		Initial Sample Size[b]	Number of Expected Failures Below $P_{.95}$	Number of Failed Coupons Below $P_{.95}$		Sample Size Fatigue Tested Prior to Residual Strength Tests	Number of Expected Failures Below $P_{.95}$	Number of Failed Coupons Below $P_{.95}$		Total Sample Size	Total Number of Expected Failures Below $P_{.95}$	Total Number of Failed Coupons Below $P_{.95}$	
	3 Parameter	2 Parameter			3 Parameter	2 Parameter			3 Parameter[c]	2 Parameter			3 Parameter	2 Parameter
0 to 290 (0 to 42)	155,780	325,430	20	1	0	2	40	2	3	5	60	3	3	7
0 to 345 (0 to 50)	23,800	27,870	20	1	2	2	40	2	3	3	60	3	5	5
290 to -110 (42 to -16)	10,260	10,500	20	1	1	1	40	2	2	2	60	3	3	3
345 to -110 (50 to -15)	540	2,670	20	1	1	3	40	2	0	1	60	3	1	4
TOTAL			80	4	4	8	160	8	8	11	240	12	12	19

a - $P_{.95}$ means that 95% of the samples are expected to survive the number of equivalent fatigue cycles and 5% to fail.

b - These were the sample sets which were fitted by Weibull analysis used to estimate the cycles at $P_{.95}$

c - These coupons were replaced for the residual strength study

80 coupons were in the initial sample set (column 3), 8 were expected to fail below the cycles equal to $P_{.90}$ and that 9 failed below the calculated life based on the 3-parameter fit while 10 failed below the calculated life based on 2-parameter fit, see column (5). This limited result indicated a possible preference for the 3-parameter fit for extrapolation of the tail of the fatigue lives. Continuing on in the total row of Table 31, 160 coupons were tested for residual strength of which 16 should fail below $P_{.90}$ while according to a 3-parameter fit, 14 failed below the $P_{.90}$ calculated life, see column (8). The total sample size was 240, column (9), the total expected failures was 24, column (10); and the number of failures below the calculated cycles equivalent to $P_{.90}$, based on a 3-parameter fit, was 23, column (11). This result showed the apparent accuracy of the 3-parameter Weibull fit for extrapolating the tail of the fatigue data to 60 coupons based on 20 coupons.

To more fairly compare failure rate extrapolations based on a 2-parameter fit *versus a 3-parameter fit*, the exercise of Table 31 was repeated at a probability of survival of 95%, $P_{.95}$, as shown in Table 32. Considering the total row, column (3) shows the 80 coupons in the initial sample set; column (4) the expected 4 failures at $P_{.95}$; column (5) shows that 4 failures actually occurred below the calculated $P_{.95}$ life based on the 3-parameter fit while 8 failed below the calculated $P_{.95}$ life based on the 2-parameter fit. Column (6) of Table 32 lists the 160 coupons fatigue tested for the residual strength study and column (7) the 8 expected to fail of the 160 while column (8) shows that 8 coupons failed below the calculated $P_{.95}$ life based on the 3-parameter fit while eleven failed below the calculated $P_{.95}$ life based on the 2-parameter fit. Finally, column (9) shows the 240 coupons of the total sample set; column (10) the 12 expected failures; and column (11) the fact that 12 failed below the calculated $P_{.95}$ life based on the 3-parameter fit, but 19 failed below the calculated $P_{.95}$ life based on the 2-parameter fit. In summary, the 2 parameter fit was dangerously unconservative in extrapolating the initial 80 coupon set to 240 coupons for calculating the expected life at $P_{.95}$ since only 12 of 240 coupons should have failed below the calculated $P_{.95}$ life based on 2-parameter fit, but 19 actually failed.

In Table 33, a comparison between calculated and actual number of failures at $P_{.90}$ and $P_{.95}$ in the 160 sample size residual strength set based on the 80 sample size initial data set is summarized for the 3-parameter fit. The accuracy of the calculations is apparent.

7.3 Extrapolation of Fatigue Life Results

Although the previous section showed the apparent superiority of the 3-parameter Weibull fit over the 2-parameter fit for predicting the $P_{.95}$ fatigue cycle life of a fatigue data is illustrated in Figure 81 which is a plot of the probability of failure versus log cycles to failure for the given data set. If 20 fatigue test points are analyzed, prediction of $P_{.95}$ for a larger data set will be accurate using a 3-parameter Weibull fit, but how many test points are needed to predict $P_{.99}$ or $P_{.999}$. This question is of extreme importance for presently used composites if they are to be used in aerospace structural applications because of the large data scatter presently inherent in such materials. Thus, predicting the tail or low life regime of the data is of utmost concern.

The accuracy of a 3-parameter Weibull fit for predicting the tail or low cycle life of the fatigue data is illustrated in Figure 81 which is a plot of the probability of failure versus log cycles to failure for the fatigue data obtained from tension-tension testing laminate 1 coupons at σ_{max} = 290 MPa (42 ksi). Open circles are the original baseline twenty point data set. The filled circles are failures which occurred in the first forty coupons subjected to fatigue cycling for subsequent residual strength tests. The accuracy of the 3-parameter fit to the baseline data compared to the 2-parameter fit is well illustrated in Figure 81. The dashed line is an extrapolation of the 3-parameter fit to the 98% probability of survival, $P_{.98}$, level. The accuracy of extrapolating the 3-parameter fit to $P_{.98}$ is apparent. Unfortunately, extrapolation of the data to $P_{.99}$ did not appear to be possible because of the large data scatter.

TABLE 33

SUMMARY OF EXPECTED AND OBSERVED FAILURE RATES

FOR LAMINATE 1

(BASED ON THREE PARAMETER WEIBULL FIT)

Fatigue Stress Levels, MPA (ksi)	Calculated Number of Cycles		Initial[c] Sample Size	Number of Expected Failures Below		Number of Failed Coupons Below		Sample Size Fatigue Tested Prior to Residual Strength Tests	Number of Expected Failures Below		Number of Failed Coupons[d] Below	
	$P_{.90}$[a]	$P_{.95}$[b]		$P_{.90}$	$P_{.95}$	$P_{.90}$	$P_{.95}$		$P_{.90}$	$P_{.95}$[d]	$P_{.90}$	$P_{.95}$
0 to 290 (0 to 42)	364,000	155,780	20	2	1	3	0	40	4	2	5	3
0 to 345 (0 to 50)	31,400	23,800	20	2	1	2	2	40	4	2	4	3
290 to -110 (42 to -16)	14,400	10,260	20	2	1	1	1	40	4	2	4	2
345 to -110 (50 to -15)	2,150	540	20	2	1	3	1	40	4	2	1	0
TOTAL			80	8	4	9	4	160	16	8	14	8

a - $P_{.90}$ means that 90% of the samples are expected to survive the number of equivalent fatigue cycles and 10% to fail.

b - $P_{.95}$ means that 95% of the samples are expected to survive the number of equivalent fatigue cycles and 5% to fail.

c - This is the sample set which was fitted by Weibull analysis used to estimate the $P_{.90}$ and $P_{.95}$ cycles.

d - These failed coupons were replaced for the residual strength tests.

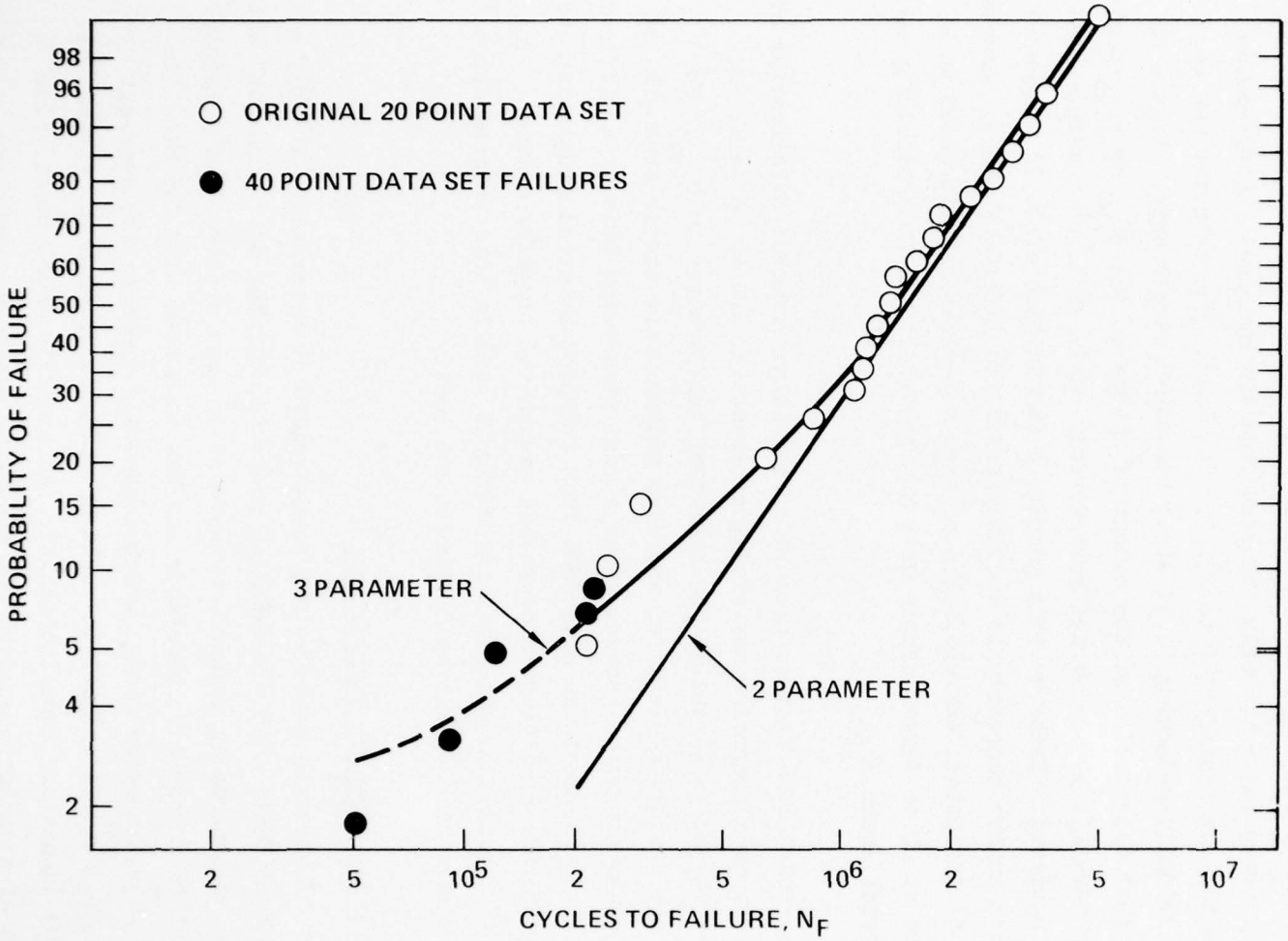


Figure 81. Probability of Failure for Laminate 1 Tension-Tension Fatigue Results at σ_{max} = 290 MPa (42.0 ksi)

In Figure 82 the effect of sample size on probability of survival is illustrated. The data displayed in the figure were obtained by calculating the results for three tests randomly selected from the original twenty coupon fatigue sample set tested at 0 to 290 MPa (42 ksi). The exercise was repeated by randomly selecting 5, 7, etc., sub-sized sample sets. Figure 82 indicates that calculation of the number of cycles at the $P_{.90}$ or $P_{.95}$ probability of survival levels varied considerably until at least a sample size of 15 was achieved. Based on this result, a sample size of 20 is suggested as a minimum number necessary to reliably establish fatigue scatter. However, as Figure 81 indicates, extrapolation of even a 3-parameter fit based on a sample size of 20 to larger sample sets may be unreliable at probability of survival rates above $P_{.98}$.

The primary conclusion is that because of the large inherent data scatter of the presently used composite materials, at least 15, and to be safe, 20, coupons are needed to establish the extent of that scatter to $P_{.95}$. To establish the fatigue cycle life, and also probably the static strength, at $P_{.99}$, 100 coupons must be tested. From a cost standpoint this is a difficult conclusion. Improvement can only come from improved material processing and coupon manufacture resulting in decreased mechanical property scatter. In light of the fabrication and machining controls used in this program, such improvement will most likely be difficult and costly.

7.4 Residual Strength Degradation

The concept of strength degradation, as described in References [24-28], refers to an hypothesis that a mechanical property degrades or "wears-out" with time due to an externally induced environment or load spectrum. In general, this concept is physically reasonable and has long been used for metallic materials. A mathematical model which accurately predicts the wear-out properties of advanced composites would be valuable to both the structural designer and laboratory experimentalist. An accurate model might allow formulation of a design procedure for employing advanced composites in aircraft structures similar to that outlined for metallic materials in MIL-STD 1530 [29].

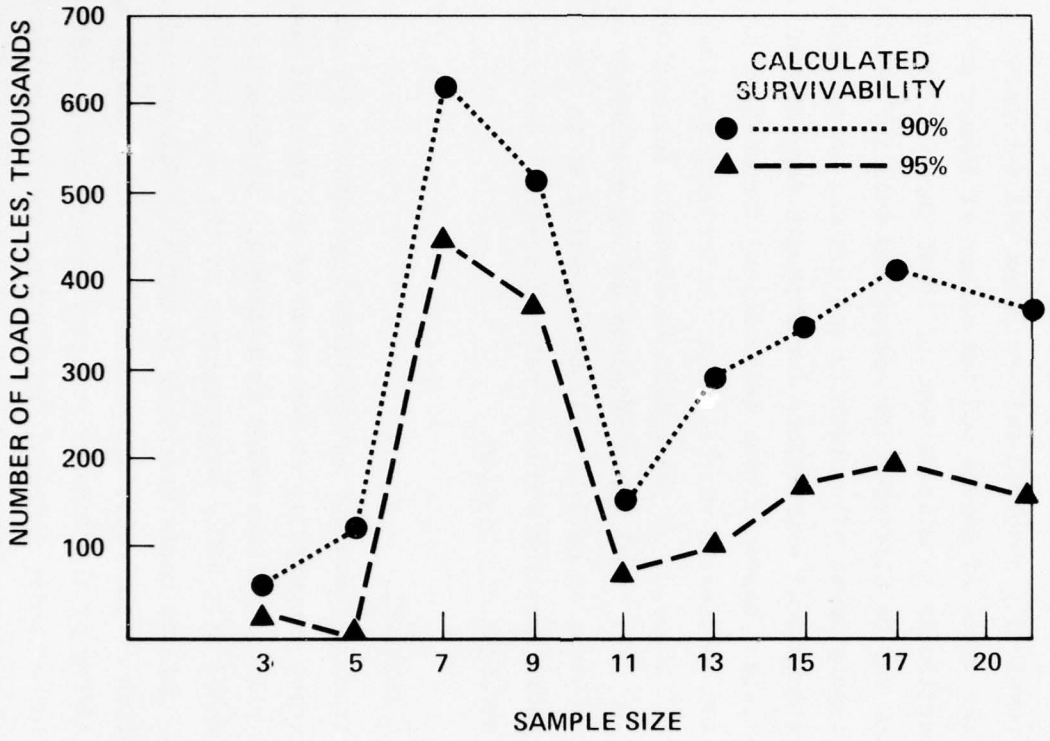


Figure 82. Effect of Sample Size on the Number of Fatigue Cycles at Specific Probability of Survivals (Laminate 1 Data at 0 to 290 MPa (42.0 ksi))

Essentially, development of a model representative of strength degradation consists of making three assumptions: 1) the nature of the degradation rate; 2) the criterion of failure; 3) the relationship between failure modes which occur under static to those resulting from dynamic loads. Fundamental to mathematically formalizing these assumptions into engineering practice is an awareness of the physically observed failure modes and determination and understanding of the types of damage and the nature of damage growth. One purpose of this section is to discuss some of these physical principles, especially how they may be different for composites than for metals, to ascertain the necessary level of complexity and general format which may be required of the mathematical expressions for strength degradation. A second purpose is to evaluate a commonly used mathematical formulation of composite strength degradation to discern whether or not underlying physical principles are satisfied and if accuracy of prediction is adequate for engineering purposes. Based upon the conclusions obtained during discussion of the above described purposes, an outline will be suggested as to the direction of future experimental research and mathematical analysis necessary to accurately predict strength degradation.

7.4.1 Physical Principles

In order to successfully formulate mathematical expressions for strength degradation in fibrous composites, an awareness of the physical nature of damage growth and related failure modes is required. Experimental data on observed failure modes will allow comprehension of the relationship between static and fatigue failure modes necessary to define a failure criterion. Similarly description of the cause and nature of growth of damage zones allows an understanding of the form of required damage growth expression. Lastly, a comparison of these physical descriptions for composites to those for metals will allow determination of the level of mathematical complexity required for expression of composite strength degradation.

7.4.1.1 Damage Growth and Failure Modes Observed in this Program

Although no obvious damage was visible to the eye prior to coupon separation, the stress-strain curves, and analysis and data results found in the literature such as in Reference [30], suggest that the 90° and 45° plies of laminate 1 coupons failed during static tension loading before final coupon fracture. Observation of the failed laminate 1 static tension coupons (see Figure 35) revealed only minor amounts of delamination essentially confined to the fracture region. Multiple fracture locations sometimes occurred. As expected, the 90° and 45° plies failed in the matrix while the fibers in the 0° ply were fractured. This mode of failure was observed to be essentially the same for the static tension residual strength coupons except for those which also had extensive delamination due to the prior fatigue loading (see Figure 74).

Laminate 1 static compression coupons exhibited no obvious damage prior to fracture although the stress-strain curve often was flat just prior to failure indicating internal damage. Coupons usually failed at one location with the outer plies in the fracture region buckled out of plane in a symmetrical pattern with respect to the axis of the coupon, see Figures 45 and 46. Extensive delamination occurred, but was limited over approximately 25 to 50 mm (1 to 2 in.) of the gage length in the vicinity of the fracture region. Fractures appeared on the outer surface of the coupon along a 45° angle to the loading or along an irregular line approximately 90° to the loading direction. The static compression failure mode of coupons previously tested in fatigue was similar to that of the unfatigued coupons except that the amount of delamination was often more extensive due to the delamination which occurred during fatigue loading, see Figure 75.

In contrast to damage which occurred in the static tests, laminate 1 coupons tested in fatigue displayed damage prior to fracture in the form of extensive delamination. The amount of observed delamination was dependent on stress level, the lower stressed coupons having more extensive delamination. Regardless of whether the coupon was tested in tension-tension or

tension-compression fatigue, delamination started at the free edge, at one or more locations, primarily between the two -45° plies and propagated towards the center of the coupon and along the free edge. Local out-of-plane buckling of the outer four plies often occurred in various localized regions of delamination. These regions did not necessarily extend to the coupon edge and occurred under both T-C and T-T loading, but were more pronounced under T-C fatigue. Delamination often developed early in the life of T-T coupons while T-C coupons usually failed soon after the delamination was observed. The final fracture of coupons tested in T-T was due to tensile overload of unbroken 0° fibers and 45° and 90° plies with the failure location usually confined to one region. The damage zone could be quite extensive, see Figures 54 and 55. Final failure of T-C coupons which only occurred during a compression load excursion was also usually confined to one region, but was caused by fracture of the plies which were buckled out of plane.

Like laminate 1 coupons, laminate 2 coupons exhibited different failure modes and damage growth depending on the type of loading. In static tension, regardless of whether coupons had experienced prior T-T or T-C fatigue loading, the failure mode was typified by one localized failure region dominated by 0° fiber breaks, 45° ply matrix failures and extensive delaminations over a large portion of the coupon usually between the outer 0_2 and -45 plies, see Figures 36 and 76. Sometimes the failure regions were dominated by breakage of the 0° fibers along a line 45° to the load line direction, see Figure 37. In essense, the failure in these coupons was dominated by the 45 plies. The coupons which failed along a 45° line sustained much less delamination than the coupons which failed along 90° lines. Typically static compression failures of laminate 2 coupons, whether or not they had been exposed to the fatigue loading, were along a predominately 45° line to the loading direction with delamination confined primarily to the failure region and with broken plies buckled out of plane in a symmetrical fashion about the coupon centerline, see Figures 47, 48 and 77. Under either static tension or compression loading, no damage was visually observed prior to fracture.

Tension-tension and tension-compression fatigue coupons of laminate 2 exhibited delamination damage during the last portion of the coupon life. Unlike laminate 1 coupons, this damage did not necessarily start at free edges and was confined in extent. Delamination, during fatigue cycling which was more extensive under T-C loading, consisted of shredded and broken single fibers or small groups of fibers from the outer 0° plies. Damage zones appeared to grow by out-of-plane localized buckling of the delaminated plies. Failures of T-T coupons usually, but not always, showed extensive internal delamination usually between the 0° and -45° plies, see Figures 56 and 57. The failure zones were dominated by either 0° fiber fractures at 90° to the load line and 45° ply matrix failures or sometimes by 0° fiber fractures at 45° to the load line which showed the large influence of the 45° plies, see Figure 58. The primary difference between the static tension and tension-tension fatigue failure mode appearances was in the failure region which for the static loading was much more confined and far less ragged in appearance. Failure of T-C coupons occurred only during a compression load excursion and appeared to be caused by local breakage of delaminated fibers while buckling out-of-plane, see Figure 59. Only single location fracture regions were observed for both T-T and T-C coupons.

The specific types of damage growth and failure modes observed for the two laminates and four different types of loading are summarized in Table 34. Essentially four different types of failure modes were observed. Damage growth between static and dynamic loading was quite different, but more similar between T-T and T-C fatigue loading. Damage growth during fatigue was different for each laminate layup. The most similar failure modes were those seen for laminate 2 coupons tested in static tension and in T-T fatigue, though even for these two cases differences were evident. The fact that the laminate 2 residual static tension strength was identical to the original strength after exposure to T-T fatigue levels which caused 9 failures out of 51 coupons suggests that the static and fatigue damage mechanisms were indeed significantly different.

TABLE 34

SUMMARY OF OBSERVED DAMAGE GROWTH AND FAILURE MODES

	Test Type	Static Tension	Static Tension Residual Strength	Static Compression	Static Compression Residual Strength	T-T Fatigue	T-C Fatigue
Laminate 1	Damage Growth During Test	None	None	None	None	Delamination between the two -45° plies starting at free edge progressing along edge and toward center.	a. Delamination between the two -45° plies starting at free edge progressing along edge and toward center. b. More pronounced out-of plane buckling of delaminated plies than in T-T.
	Failure Mode	a. Small amounts of Delamination confined to fracture region b. 90° & 45° ply matrix fractures c. 0° fiber fracture d. Occasional Multiple Fracture region	a. Similar to static tension failures b. Some coupons had extensive delamination due to prior fatigue loading	a. Extensive localized delamination b. Fracture of outer plies due to out-of-plane buckling c. Outer surface fractures along 45° line or irregular 90° line to load direction d. Occasional Multiple fracture region	a. Similar to static compression failures b. Some coupons had extensive delamination due to prior fatigue loading	a. One failure location often quite extensive b. Large amount of delamination especially between two -45° plies c. Many 0° fiber fractures, mostly matrix fractures in 45° & 90° plies.	a. One failure location often quite extensive b. Large amount of delamination especially between two -45° plies c. Many 0° fiber fractures, mostly matrix fractures in 45° and 90° plies d. Fractured outer 4 plies buckled out-of plane
Laminate 2	Damage Growth	None	None	None	None	Random localized delamination of fibers and fiber bundles from the outer surface 0° plies, not usually occurring at free edges, late in coupon life.	Similar to T-T coupons but with more extensive delamination
	Failure Mode	a. Extensive delamination usually between 0°_2 and 45° plies b. One failure location c. 0° fiber fracture and 45° ply matrix fracture d. Several coupons with 0° fibers fractured along a 45° line to load direction	a. Similar to static tension coupons	a. Localized delamination b. Fracture of coupon along a 45° line to load direction c. Fractured plies buckled symmetrically out-of-plane	a. Similar to static compression failures b. Some coupons had extensive delamination due to prior fatigue loading	a. Usually extensive delamination regions often between 0°_2 and 45° plies b. Rugged fracture regions dominated by 0° fiber fractures essentially at 90° to the load line and 45° ply matrix fracture c. Some coupons with 0° fiber fractures running at 45° to the load line	a. Usually extensive delamination regions often between 0°_2 and -45° plies b. Plies fractured out-of-plane due to buckling and fracture during compression load excursion

7.4.1.2 Comparisons Between Composites and Metals

To understand the practical problems of developing a model for strength degradation in composites a short review of the nature of damage growth in metals will be discussed. The purpose of this review is to explain the reasons for the success, albeit a limited one, of relatively simple damage growth models for metals and why this fortuitous situation should not necessarily be expected to occur in continuous fiber composites.

In metals, regardless of whether loading is static or dynamic, damage consists [31], simplifying a complex situation, of the pile up of dislocations, generation of dislocation tangles, slip, and twinning which results in inelastic deformation and the generation and propagation of cracks or crack-like defects. In ductile materials, only large cracks affect static failure load which is primarily due to plastic or tensile instability. Materials which are more brittle generally exhibit failure loads sensitive to the presence of cracks.

During fatigue, numerous micro-sized crack-like defects develop and propagate, (especially around holes or notches). The dominance of these cracks, regardless of whether the metal is brittle or ductile, is dependent on stress level (or, better, strain range). At very high stresses or strains, large plastic flow occurs leading to tensile instability and short life and unless the material contains a large sharp notch or crack, the effect of the flaw is not obviously manifested. At lower, but still high stresses, a predominant crack (or cracks) develops early in life resulting in damage and failure due to crack growth at an intermediate life. If the stress is still lower, fatigue life can become long, many microcracks develop and grow, but a predominant flaw does not occur until late in fatigue life.

This outline of damage growth in metals indicates that, in most cases, formulation of relatively simple expressions, which include the crack, for damage growth and the failure criterion would be quite difficult. In fact, only for brittle materials have such simple expressions been developed, and even then only when they are subjected to fatigue loading at the intermediate stress

levels where a dominant flaw can develop. Even in this relatively restricted case large complications arise [32]. This is not to say that strength degradation or flaw growth does not occur in the other materials, but only that the analysis of such flaw growth is extremely onerous due to the associated extensive plasticity. Only in recent years has analysis of flaws and flaw growth in a large scale plastic field been undertaken with, to date, limited success.

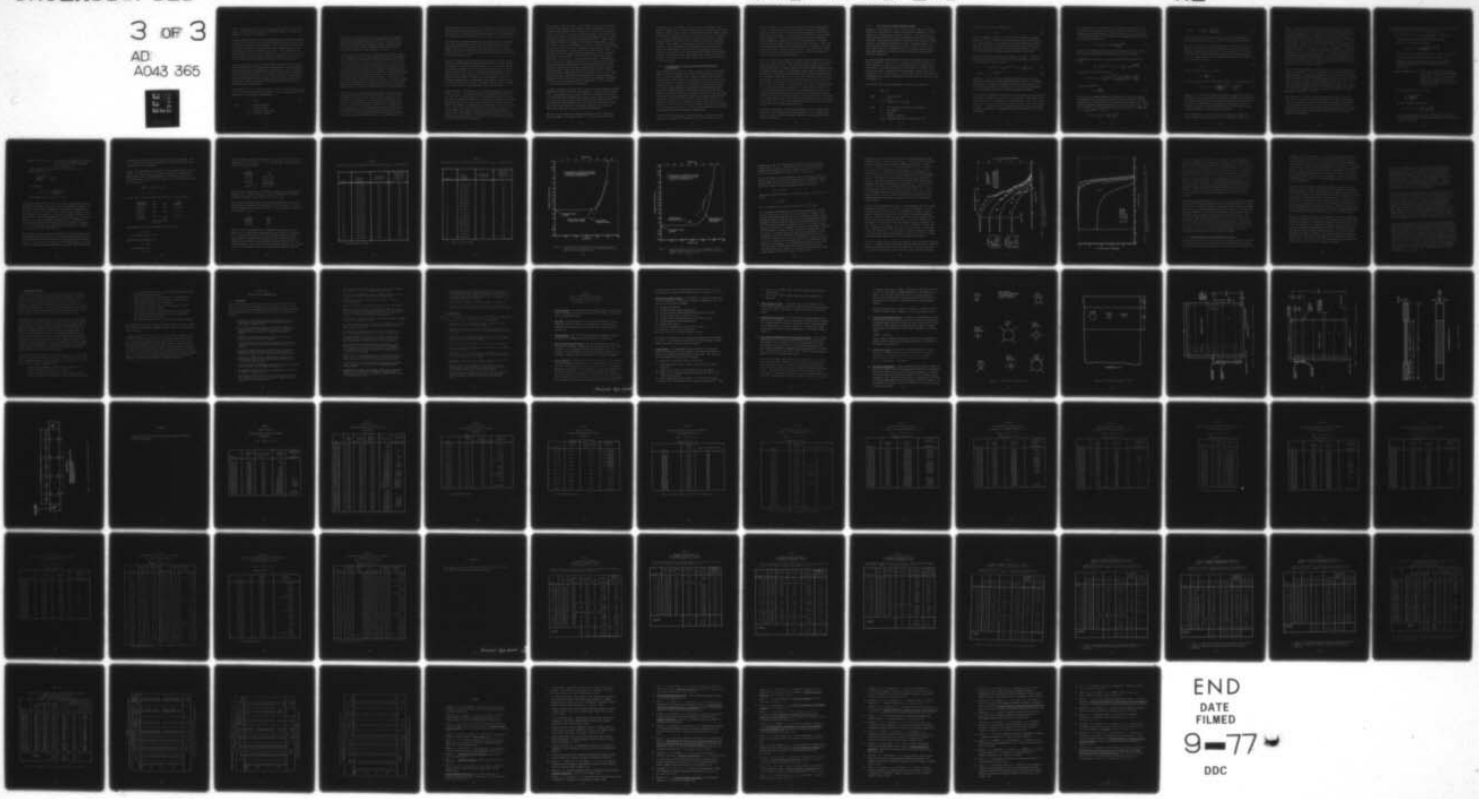
In the situations where flaw growth can be analyzed, the reasons which make the analysis possible are due to the nature and scale of the metallic microstructure. In a crude sense, a metal consists of a crystallographic arrangement of the principal elements with the structure containing substitial and interstitial elements and colonies of the other constituent elements. This crystallographic structure is arranged into grains (subregions of like orientation) and often has two phases (such as in steel or titanium) within a grain. Within these grains and along their boundaries, cracks form and propagate. Although there are numerous exceptions, grain size is usually of the order of .025 to .25 mm (.001 to .01 in.) while the secondary subgrain structure (called "platelets" in titanium) is even smaller. Based on this general microstructural scheme, one can understand the reasons for the small number of situations for which relatively simple crack growth expressions can be formulated.

At the level of the grain or subgrain, crack growth is necessarily complex for as the crack grows all sorts of changes in the crystal structure, element type, and strain field are met. These changes encountered by the moving crack tip result in a rather tortuous crack path. At the microscopic level, the effects of the nucleating and growing cracks can be manifested in three essentially different, though hardly distinct ways. If the remote stress (or strain) is high, plastic flow within the grains is large and the resultant crack growth is complex and no one flaw is likely to be dominant. If stresses are lower, one or a few cracks will propagate to a length beyond that which is grossly affected by the microstructure which allows for the possibility of applying a relatively simple crack growth expression. At still lower stresses, none of the cracks nucleate or propagate quickly which restricts macrostructural damage

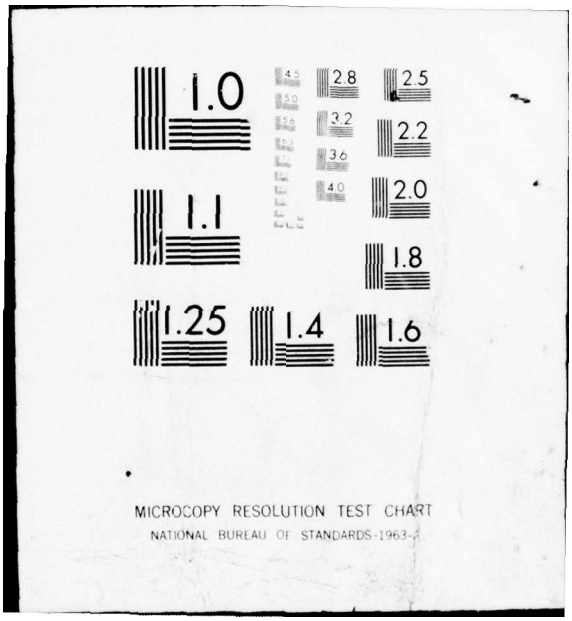
AD-A043 365 LOCKHEED-CALIFORNIA CO BURBANK RYE CANYON RESEARCH LAB F/G 11/4
ASCERTAINMENT OF THE EFFECT OF COMPRESSIVE LOADING ON THE FATIG--ETC(U)
DEC 76 J T RYDER, E K WALKER F33615-75-C-5118

UNCLASSIFIED AFML-TR-76-241 NL

3 OF 3
AD
A043 365



END
DATE
FILMED
9-77
DDC


1.0
1.1
1.25
1.4
1.6
1.8
2.0
2.2
2.5
2.8
3.2
3.6
4.0
4.5
5.0
5.6
MICROCOPY RESOLUTION TEST CHART
NATIONAL BUREAU OF STANDARDS-1963-A

to the accumulated effect of many small cracks locked within the local grain region. In this latter case and in the first case, simple crack growth expressions are difficult to formulate.

The above described three cases are the same regardless of whether the material is "brittle" or "ductile". Of course, the distinction between the three cases and between brittle and ductile is diffuse. Only if the material is relatively brittle can the second case frequently occur in service and one or a few cracks become dominant on a macrostructural level. In all other cases, the macrostructurally observed damage is dominated by the microstructure. Even for the more brittle materials, simple growth rate expressions are not possible until the scale of the crack dominates the scale of the microstructure.

One can see that the success of the expressions is dependent upon the microstructure being such that macrostructural damage growth and failure criterion are not dominated by the microstructural discontinuities. For the restricted class of metal applications where the material is more "brittle" and stresses are such that flaws can develop of a size which dominates the microstructure, analytical expressions for crack (damage) growth and failure criterion have been derived. These expressions come under the general heading of linear elastic fracture mechanics, LEFM.

The assumption is made in LEFM that the metal alloy in static tension or fatigue will fail when the crack-like defect grows to a critical length defined by the expression (see, for example, Reference [33]):

$$K = \sigma f_g \sqrt{a} \tag{8}$$

where K = fracture toughness

σ = far field stress

a = crack-like defect length

f_g = function of geometry

Equation (8) is assumed to hold for a metal that is essentially responding in a linear-elastic fashion regardless of whether the load is applied only once as in static tension or repeatedly as in fatigue. The term f_g can be and often is extremely complex. Expressions similar to Equation (8) have been developed to allow limited handling of the situation where greater plasticity occurs (see for example References [34, 35, 36]).

In order to predict the life of a metal component subject to fatigue, Equation (8) is combined with a suitable rate equation of which many have been proposed [32]. The solution to predicting cyclic life prior to failure under fatigue loading is in principle quite simple using Equation (8) and the selected rate equation: the initial flaw size prior to fatigue loading is assumed; the value of K is obtained from static tests and Equation (8); the critical crack length, a_c, for the part is calculated; the life is determined by integrating the selected rate equation until the crack length reaches a_c. The procedure is assumed to work despite the fact that the manner in which a_c was reached is quite different for a static load as opposed to fatigue loads. In the static case, a_c is the defect size of any notch present prior to loading. Under fatigue loading, a_c is reached by propagation of an initial crack to that size. This outlined procedure is more or less accurate depending on the relative accuracy of the individual steps. The procedure has proven successful in many applications [32].

Equation (8) and the selected associated rate equation, are only valid for the restricted class of metals described above where: the fatigue failure is dominated by a crack-like defect; linear elasticity applies; the values of K obtained from a static test are applicable to the dynamic case. The last point, the major assumption which allows the failure criterion to have practical utility, does not appear to be strictly true. Calculation of K, using Equation (8), at the crack length present when failure occurred often leads to higher values than the value calculated in the static case [37]. This problem is not greatly important because normally the time between when the crack reaches the critical crack length, a_c, calculated using a static

toughness value and the actual value of a_c which occurs in fatigue is usually short compared to previous component life. This fact is equivalent to saying that for metals the distribution of residual strengths can be expressed with the fatigue failures included without an undue amount of conservativeness.

At first glance, one might conclude that the limited number of situations meeting the restrictions described above where simple rate equations and failure criteria can be formulated for metals would be small. In fact, however, many practical problems in metal structural applications meet the restricted conditions. For this reason, simple expressions such as Equation (8) have found great utility.

Now that the reasons for the limited success of relatively simple failure criteria and damage growth expressions for metals are understood, the probable situation in composites can be analyzed. In a general sense, damage in composites consists of: fiber fractures and matrix cracks and crazing (within and between the plies). Graphite/epoxy composites have two component materials, fiber and epoxy, both of which respond to load in an essentially brittle fashion. However, as the stress-strain curves of an unnotched composite show, the response of the composite loaded to failure is non-linear and highly inelastic. The reason for this inelastic response is due to the nature of the microstructure and damage processes.

Roughly speaking, the microstructure of a composite consists of the fibers, matrix, and plies. The fibers and matrix are analogous to the two phases of a metal such as titanium except that the strength and elastic moduli of the phases are drastically different. A single ply is analogous to a metallic grain except the scale is large. Within and between the plies cracks can nucleate and propagate. The low modulus of elasticity of the brittle matrix allows a local stress field change due to the fracture of one fiber to be easily redistributed without a significant concomitant macrostructural strength loss. This property of stress redistribution which is much like plasticity allows the two brittle constituents of a graphite/epoxy composite to have metal-like inelastic response.

Keen awareness of how cracks act at the microstructural level in metals can now help in understanding their expected response in composites. A crack in a graphite/epoxy composite should propagate in a highly torturous complex fashion because of the two phase nature of the material. This form of propagation is observed and is similar to the form of propagation seen in a metal (especially a 2-phase alloy) at the microstructural level. Unlike a metal, the "grains" (plies) of a composite are macrosized and therefore we would expect that for a single flaw to dominate the failure response, flaw dimensions would have to be much larger than required in metals. This, in fact, is exactly the situation observed. Flaws in brittle metal alloys can be as small as the order of grain size before complex expressions for failure criterion or growth rate need be written. Thus successfully analyzable flaws can be quite small (.2 mm (.01 in.) or in some cases even less). For composites, the flaw must be of a magnitude similar to that of the ply ("grain") dimension before simple expressions for failure criterion would be successful. Research investigations have strongly supported this contention under both static and dynamic loading (see for example References [38 to 46]) which effectively implies damage zones must be larger than ~25 mm (1.0 in.). This does not imply that linear elastic fracture mechanics cannot be applied to composites, but only that the range of utility will be strongly restricted. In fact, much of the information given in References [38 to 46] may prove to be quite useful when more fully developed.

The above discussion by no means implies that crack (damage) growth or strength degradation concepts are not true for composites. The conclusions are simply that: 1) expressions for these concepts should not be expected to be simple; 2) failure modes under different loading should not be expected to be constant. The latter conclusion is made because different loading types will lead to quite different distributions of fiber and matrix cracks and matrix crazing whose interactional effect will be greatly influenced by the large ply (grain) size resulting in different strength distributions.

The above two conclusions are strongly supported by the data generated in this test program. For example laminate 1, T-T fatigue coupon lives were

dominated by σ_{max} at high stress levels, but by $\Delta\sigma$ at low stress levels. These data suggest that the rate of damage growth is determined by both strain range and maximum strain. Laminate 2 static tension residual strength coupons showed no loss in strength after being subjected for 10^6 cycles to either T-T or T-C fatigue loadings which resulted in many fatigue failures. However, these same fatigue load levels caused a reduction in residual compression strength. These laminate 2 data indicate that the same amount of damage can result in quite different effects depending on the type of loading. Finally, one should expect large scatter in the mechanical property data, especially in the fatigue data, for composites when compared to many metals because of the highly irregular damage growth pattern caused by the microstructure. The expected large scatter, especially in fatigue, was observed in this test program.

7.4.1.3 Nature of Required Failure and Damage Growth Expressions for Composites

The microstructure of a metal has a great influence upon the rate of damage growth and upon the response of the material to environmental influences (see as one example Reference [47]). However, microstructural details in metals are not always manifested macroscopically to the extent that a dominant flaw theory is invalidated. For this reason, linear elastic fracture mechanics has had a limited, albeit extremely valuable, success in metals. In contrast, fibrous composites are materials in which microstructural details are manifested directly at the macrostructural level and thereby intimately control the defect growth process. This fact renders the development of simple useful expressions for growth and failure criteria difficult to develop. Similarly, the fact that the macrostructural influence and growth of a damage zone in a composite is strongly affected by the plies ("grains"), and thus also by the layup, invalidates the practical assumption of a constant mode of fracture or at least the easy expression of the manner in which the fracture mode changes with loading type.

The above described, admittedly disturbing problem, naturally raises the question as to whether or not the problem is true for notched as well as

unnotched components. The failure of a constant failure mode assumption and the loss of simple expressions for damage growth and failure criterion for unnotched composites is not necessarily of great importance if the system of assumptions and expressions can be shown to have reasonable validity for most notched components. However, limited investigations into the response of notched coupons would suggest that, at best, the hypothesis of a constant failure mode may have only limited validity for specific layups. Static tests of notched coupons strongly imply that large notches are required if a simple equation for failure criterion is needed [38-46]. Such notched data, whether or not the notch is a circular hole or thin slit, appear to be better correlated with other types of formulations [48].

The static tension failure modes of such notched coupons, regardless of layup appear to be dominated by the stress concentrations at the hole and the induced localized damage at the hole. Failure modes of notched coupons in tension-tension fatigue appear to possibly depend on the layup and/or loading direction. For example, damage growth in quasi-isotropic layups appears to consist of the extension of a damage region from the notch equal to the notch width, consisting of broken 0° fibers and 45° and 90° ply matrix cracking, to the end of the gage length in a plane parallel to the loading direction [49-51]. The failure mode of such a notched damaged coupon would be quite different from that observed under static loading. In layups with no 90° plies and a high percentage of 0° plies, damage appears to progress in a limited zone in an apparently through thickness plane perpendicular to the loading direction [49-51]. The problem is even more complex in that different failure modes under the same fatigue load cycle and loading direction can apparently occur in the same layup of a notched composite [52]. Even different frequencies can result in different failure modes [53]. Fatigue investigations [54,24] even indicate that residual strength can first increase before decreasing.

The general conclusion is that predicting composite residual strength degradation will require possibly quite complex expressions. At a minimum they will be of a quite different form than those used in linear elastic fracture mechanics for metals.

7.4.2 Evaluation of a Strength Degradation Model

Because of the conclusions reached as to the required nature of successful mathematical formulations for strength degradation in composites, a detailed analysis of one proposed formulation was undertaken. This formulation was chosen because of the relatively simple mathematical expressions and assumptions used. The analysis was expected to show whether or not the conclusions reached in the foregoing discussion were valid. In essence, despite the logic which led to the conclusions, can the simple model be shown to have at least enough accuracy for engineering utility. The particular formulation chosen for analysis will be shown to lead to an inadequate representation of strength degradation.

One model of strength degradation or "wear-out" for composites is well formulated in References [24-28 and 55-57]. Because much of the discussion in these references is similar as are the data presented, the following outline of the model is based upon Reference [24] which contains a complete presentation of the model. Throughout the discussion which follows, the notation of Reference [24] will be maintained. This notational choice allows for easier comparison of the equations as presented here to the manner in which they appear in Reference [24].

In this model, the rate of damage growth is assumed to be defined as:

$$\frac{dc}{dt} = MC^r \tag{9}$$

where C = damage zone size

t = time

$M \propto$ constant $\cdot W^r \simeq AD^r F_{max}^{2r}$

where W = far field work inputted by the environment

r = rate exponent

A = constant

D = effective compliance

F_{max} = maximum stress level of the external load

The criterion for failure is assumed to be:

$$K = F\sqrt{C} \tag{10}$$

where K = toughness. Equations (9) and (10) are analogous to equations formulated in linear elastic fracture mechanics for metallic materials [58, 33]. Because Equation (10) is assumed to apply regardless of the cause of degradation or loading, the corollary assumption is made to join the two equations, namely that the mode of fracture remains constant. This is, of course, similar to the assumption made for Equation (8) for metals.

Based on these three assumptions, the strength at any time, t, for the i^{th} member of a population can be found by integrating Equation (9) with the aid of Equation (10) which results in:

$$F_i(t)^{2(r-1)} = F_i(t_o)^{2(r-1)} - (r-1)\, A_4\, F_{max}^{2r}\, (t-t_o) \tag{11}$$

where

$$A_4 = AD^r K^{2(r-1)} \tag{12}$$

Equations (9) and (10) and the associated corollary form the basis of a formulation for modeling strength degradation while Equation (11) describes the strength of a coupon or component at some future time. Equation (11) will have accurate predictive capability if the forms of the equations for rate of degradation and failure criterion were correctly assumed.

At this point, no assumption has been made as to the manner in which the initial and residual strengths, $F(t_o)$ and $F(t)$, are distributed. Their manner of distribution is not of real importance to formulation of the model. Any distribution could be used, such as Normal or Weibull, provided the data are properly described. A 2-parameter Weibull distribution was chosen because the static strength distribution of a composite material could apparently be accurately represented.

The 2-parameter Weibull distribution can be combined with Equation (11) and used to derive an equation which, hopefully, accurately predicts the future (residual) strength distribution. Using the 2-parameter Weibull distribution and following Reference [24], the initial static strength distribution, $F(t_o)$, is assumed to be modeled by:

$$P\left[F > F_i(t_o)\right] = \exp\left| - \left(\frac{F}{\hat{F}(t_o)}\right)^{\alpha_o}\right| \tag{13}$$

Equation (13) represents the static strength distribution at time t_o where $\hat{F}(t_o)$ is the characteristic strength and α_o is the shape parameter.

The probability that $F(t) > F$ is just the probability that Equation (11) holds:

$$F(t_o) > \left| F(t)^{2(r-1)} + (r-1)\, A_4\, F_{max}^{2r}\, (t-t_o)\right|^{\frac{1}{2(r-1)}} \tag{14}$$

By Equation (13), this probability is:

$$P\left[F(t) > F\right] = \exp\left\{ - \left[\frac{F(t)^{2(r-1)} + (r-1)\, A_4 F_{max}^{2r}\, (t-t_o)}{\hat{F}(t_o)^{2(r-1)}} \right]^{\alpha_f} \right\} \tag{15}$$

where α_f is defined as:

$$\alpha_f = \frac{\alpha_o}{2(r-1)} \tag{16}$$

If the cause of strength degradation is fatigue, as in this investigation, the highest value of probability which can occur for the residual strength distribution is that calculated for the maximum fatigue stress, F_{max}. Effectively the residual strength distribution, $F(t)$, is truncated by F_{max}. Therefore, assuming F_{max} is significantly less than $F(t_o)$, that $t_o = 0$, and that $t \to \infty$, then $F(t)^{2(r-1)} \to 0$ and:

$$P\left[\, F(t) > F_{max}\right] = \exp\left[- \frac{t}{\hat{t}_b} \right]^{\alpha_f} \tag{17}$$

where $$\hat{t}_b \, F_{max}^{2r} = \frac{\hat{F}(t_o)^{2(r-1)}}{(r-1)\, A_4} \tag{18}$$

and where $\hat{t}_b$ is the characteristic fatigue life for the distribution of fatigue lives obtained at F_{max} and α_f is the fatigue life shape parameter.

Equation (17) implies [24], since a constant mode of fracture was assumed, an approximate fixed fatigue life shape parameter, α_f, independent of load history, environment, and scale effects. The parameter α_f is related to α_o by Equation (16) and both parameters are assumed to be material variables [24]. If a constant loading rate is assumed during the static strength tests, α_o can be written as [24]:

$$\alpha_o = 2r + 1 \tag{19}$$

and, thus, by Equation (16), α_f becomes:

$$\alpha_f = \frac{2r + 1}{2(r-1)} \tag{20}$$

Because t_o is usually taken as time zero, Equation (15) can be rewritten as:

$$P\,[F(t) > F] = \exp\left\{-\left[\left(\frac{F(t)}{\hat{F}(t_o)}\right)^{2(r-1)} + \frac{t}{\hat{t}_b}\right]^{\alpha_f}\right\} \tag{21}$$

Equation (21) is the basic equation of the model with predictive capability because the equation describes the distribution of strength at a future time. The equation is based on the assumed rate equation and failure criterion as well as on a 2-parameter Weibull distribution. Expressions similar to Equation (21) could be derived, of more or less validity, if other distributions describing the static strength were assumed.

If the formulation of a model for wear-out as expressed in Equation (21) is valid, a powerful tool is available for use in engineering design. For

example, in theory the characteristic static strength, $\hat{F}(t_o)$, and shape parameter, α_o, (and by Equation (16), r) for the static strength distribution of a particular composite could be determined as well as the characteristic life, $\hat{t}_b$, and shape parameter α_f, at a particular maximum fatigue stress, F_{max1}. Using Equation (18), A_4 could be determined using $\hat{t}_{b1}$ and F_{max1} and therefore, from the same equation, $\hat{t}_b$ at any other maximum fatigue stress, F_{max2}, could be calculated. Equation (21) could be used to calculate the distribution of static strength at any time t for any other F_{max}. Therefore, a limited amount of fatigue testing at a few stress levels would allow prediction of strength degradation caused by any other stress level. In theory, this procedure could be extended to complex fatigue loading and a full scale structure [24]. Because of the potential value of the model, the validity of Equations (18) and (21), and thus, by implication, the assumed growth rate and failure criterion, Equations (9) and (10), will be assessed.

To prove the applicability of this formulation of the wear-out process and the associated Equations (15) or (21), both necessary and sufficient conditions must be satisfied. The necessary conditions are actually mathematical boundary conditions while the sufficient conditions are the specific physical predictions which must be met accurately. Three boundary conditions and at least five separate, although related, sufficient conditions can be formulated. Proof that the boundary conditions are met is not adequate, contrary to the practice [24] used in the composite literature, to prove the validity of the model as formulated in Equations (9) and (10).

This question of necessary and sufficient conditions is not just esoteric. Proof that the necessary or boundary conditions are met proves that Equation (21) has been correctly derived and is internally consistent, a requirement of any mathematical formulation. Proof that the sufficient conditions are met proves that Equation (21) has value to the practicing engineer; in essence, proves that the mathematical formulation actually describes the mechanical properties of composites.

The necessary or boundary conditions consist of the restriction that Equation (21) must be internally valid. The boundary conditions are:

Boundary Condition 1 (BC1): At $t = 0$, Equation (21) must reduce to Equation (13).

This boundary condition can easily be shown to be true.

Setting $t = 0$, Equation (21) becomes:

$$P\left[F(0) > F\right] = \exp\left[-\left(\frac{F(0)}{\hat{F}(0)}\right)^{\alpha_f 2(r-1)}\right]$$

which is the same as Equation (13) since $t_o = 0$ and $\alpha_f = \alpha_o/2(r-1)$.

Note that since BC1 is met, this implies that for $t \ll \hat{t}_b$, Equation (21) should fairly accurately predict the residual strength distribution since little strength degradation will have occurred.

Boundary Condition 2 (BC2): The truncated maximum level of probability of survival of the residual strength distribution, $P\left[F(t) > F\right]$, must closely approximate the correct value for the spectrum and associated F_{max} level used to calculate α_f and $\hat{t}_b$.

BC2 is met because for $F(t) \ll \hat{F}(t_o)$:

$$\frac{t}{\hat{t}_b} \gg \left[\frac{F(t)}{\hat{F}(t_o)}\right]^{2(r-1)}$$

and thus Equation (21) reduces to:

$$P\left[F(t) > F\right] \simeq \exp\left[-\left(\frac{t}{\hat{t}_b}\right)^{\alpha_f}\right]$$

which is just the original fatigue distribution and at any time, t, will give essentially the correct, although not precise, truncated value of $P\left[F(t) > F\right]$.

Boundary Condition 3 (BC3): At any time, t, the probability of survival for the residual strength distribution must → 0 for $F(t) \gg F$.

This condition can be shown by the fact that for $F(t) \gg F$, then in Equation (21).

$$\left(\frac{F(t)}{\hat{F}(t_o)}\right)^{2(r-1)} \gg \frac{t}{\hat{t}_b}$$

and therefore,

$$P\left[F(t) > F\right] \simeq \left| -\left(\frac{F(t)}{\hat{F}(t_o)}\right)^{\alpha_o} \right|$$

This equation does → 0 for $F(t) \gg \hat{F}(t_o)$.

The sufficient conditions which must be satisfied to completely prove this particular formulation of the wear-out model, as expressed in Equation (21), are, listed in their order of importance: 1) prediction of probability of survival, $P\left[F(t) > F\right]$, must be correct over the entire range of P for the data obtained at the original F_{max} levels; 2) prediction of both the truncated value of P and all intermediate values at any other F_{max} level must be correct; 3) the residual strength distribution must be smooth when the failures which occurred during fatigue testing are included; 4) Equations (16), (19), and (20) must give essentially the same damage rate exponent, r; 5) failure modes must remain constant.

Now that the specifics of one common formulation of the wear-out model have been expressed, the data of this report and that contained in others can be used to assess the validity of the rate and failure assumptions (Equations 9 and 10). Recall that the analysis of the data should show that the three boundary conditions (necessary conditions) are satisfied and that this does

not constitute proof of the above outlined expression of the theory. Only if the sufficient conditions are satisfied can the hypothesis be reasonably considered to have been confirmed.

Consider the quasi-isotropic data for the T300/934 material obtained in this program. The question arises as to how well Equation (21) models the observed static tensile strength degradation. For this layup and using a 2-parameter Weibull fit and the data of Tables 10 and 11, the static tensile data for laminate 1 is:

$$F(\hat{t}_o) = 487 \text{ MPa } (70.57 \text{ ksi})$$

$$\alpha_o = 24.1$$

and from Table 24 for the fatigue data, also using a 2-parameter fit:

Stress Range MPa (ksi)	t_b min	α_f	F_{max} MPa (ksi)
0 to 400 (0 to 58)	9.58	1.52	400 (58)
0 to 345 (0 to 50)	119.0	3.16	345 (50)
0 to 290 (0 to 42)	3321	1.64	290 (42)
	Average $\overline{\alpha_f}$	=2.11	

Using Equation (16), the rate exponent, r, is found to be:

$$r = 6.71$$

and, therefore $2(r-1) = 11.42$

However, based on Equation (19)

$$r = 11.55$$

and by Equation (20)

$$r = 2.35$$

Since the different methods of determining r do not agree, Equation (16) will be used and r will be taken as r = 6.71. Using Equation (18), the following values of A_4 can be obtained:

F_{max} MPa (ksi)	A_4
400 (58)	4.965 x 10-5
345 (50)	3.012×10^{-5}
290 (42)	1.120×10^{-5}
Average $\overline{A_4}$ =	3.032×10^{-5}

The term A_4 can be seen not to be a constant contrary to the implications of Equation (18). In order to continue, A_4 must be considered as a constant therefore the average value of 3.032×10^{-5} will be used.

To evaluate the formulated model, the strength distribution at the two lower stress levels as represented by Equation (21) will be compared to the actual residual strength data discussed in Section 6. The time values at probability of survival of $P_{.90}$ are:

F_{max} MPa (ksi)	t, min
345 (50)	52.3
290 (42)	606.7

Tables 35 and 36 and Figures 83 and 84 compare the distribution given by Equation (21), to the nominal distribution based on Equation (2) of Section 2.6. In both Tables 35 and 36, only the data from the first 20 coupons fatigue tested to determine static tension residual strength were used. Failures which occurred during the fatigue tests were included as per the modeling procedure. Note in these tables and figures, that for F_{max} = 345 MPa (50 ksi), the calculated values of P_s determined using Equation (21) were

TABLE 35

PREDICTED AND ACTUAL PROBABILITY OF SURVIVAL VALUES AT F_{max} = 345 MPa (50 ksi)

Index	Failure Stress, MPa (ksi)	Probability of Survival P_s	Probability of Survival, Based on Equation (21) P_s
1	345 (50.0)[a]	0.95	.824
2	376 (54.6)	0.90	.799
3	398 (57.7)	0.85	.763
4	399 (57.9)	0.80	.759
5	407 (59.0)	0.75	.739
6	412 (59.8)	0.70	.722
7	418 (60.6)	0.65	.701
8	425 (61.6)	0.60	.670
9	444 (64.4)	0.55	.548
10	444 (64.4)	0.55	.548
11	455 (66.0)	0.45	.451
12	456 (66.2)	0.40	.437
13	462 (67.0)	0.35	.381
14	465 (67.5)	0.30	.344
15	478 (69.3)	0.25	.207
16	482 (69.9)	0.20	.165
17	492 (71.4)	0.15	.076
18	494 (71.7)	0.10	.063
19	494 (71.7)	0.10	.063
20	501 (72.6)	0.00	.032

a - Coupon failed in Fatigue

TABLE 36

PREDICTED AND ACTUAL PROBABILITY OF SURVIVAL VALUES AT F_{max} = 290 MPa (42 ksi)

Index	Failure Stress, MPa (ksi)	Probability of Survival P_s	Probability of Survival, Based on Equation (21) P_s
1	290 (42.0)[a]	0.95	.972
2	290 (42.0)[a]	0.95	.972
3	339 (49.2)	0.85	.967
4	367 (53.2)	0.80	.959
5	401 (58.2)	0.75	.928
6	403 (58.5)	0.70	.925
7	404 (58.6)	0.65	.924
8	409 (59.4)	0.60	.913
9	410 (59.5)	0.55	.912
10	417 (60.5)	0.50	.895
11	418 (60.7)	0.45	.891
12	427 (62.0)	0.40	.860
13	427 (62.0)	0.40	.860
14	440 (63.8)	0.30	.798
15	468 (67.9)	0.25	.521
16	474 (68.8)	0.20	.433
17	476 (69.0)	0.15	.413
18	480 (69.6)	0.10	.350
19	490 (71.1)	0.05	.199
20	499 (72.4)	0.00	.095

a - Coupon failed in Fatigue

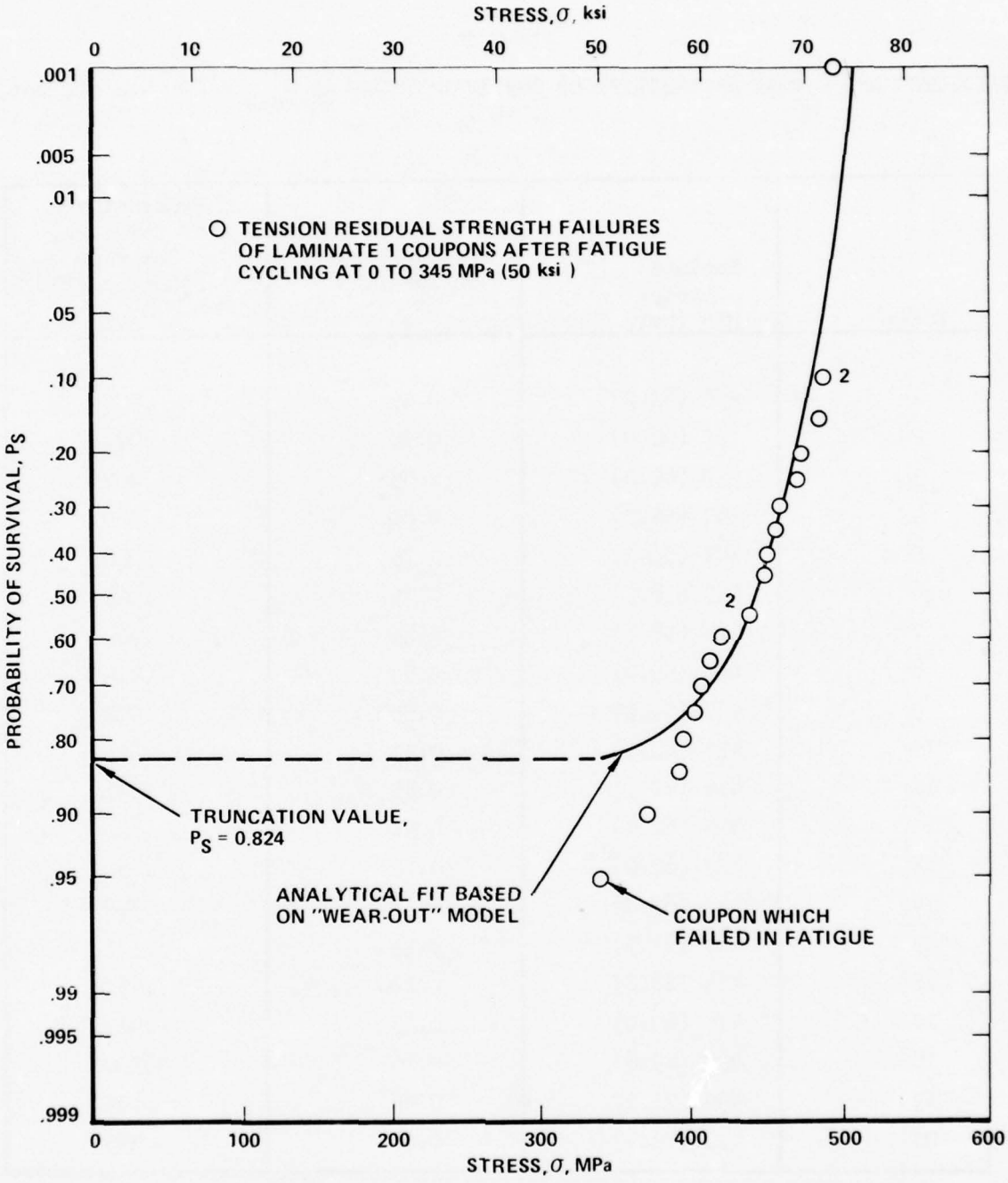


Figure 83. Comparison Between Analytical Fit and Laminate 1 Static Tension Residual Strength Data for Specimens Prior Fatigue Tested at 0 to 345 MPa (50.0 ksi)

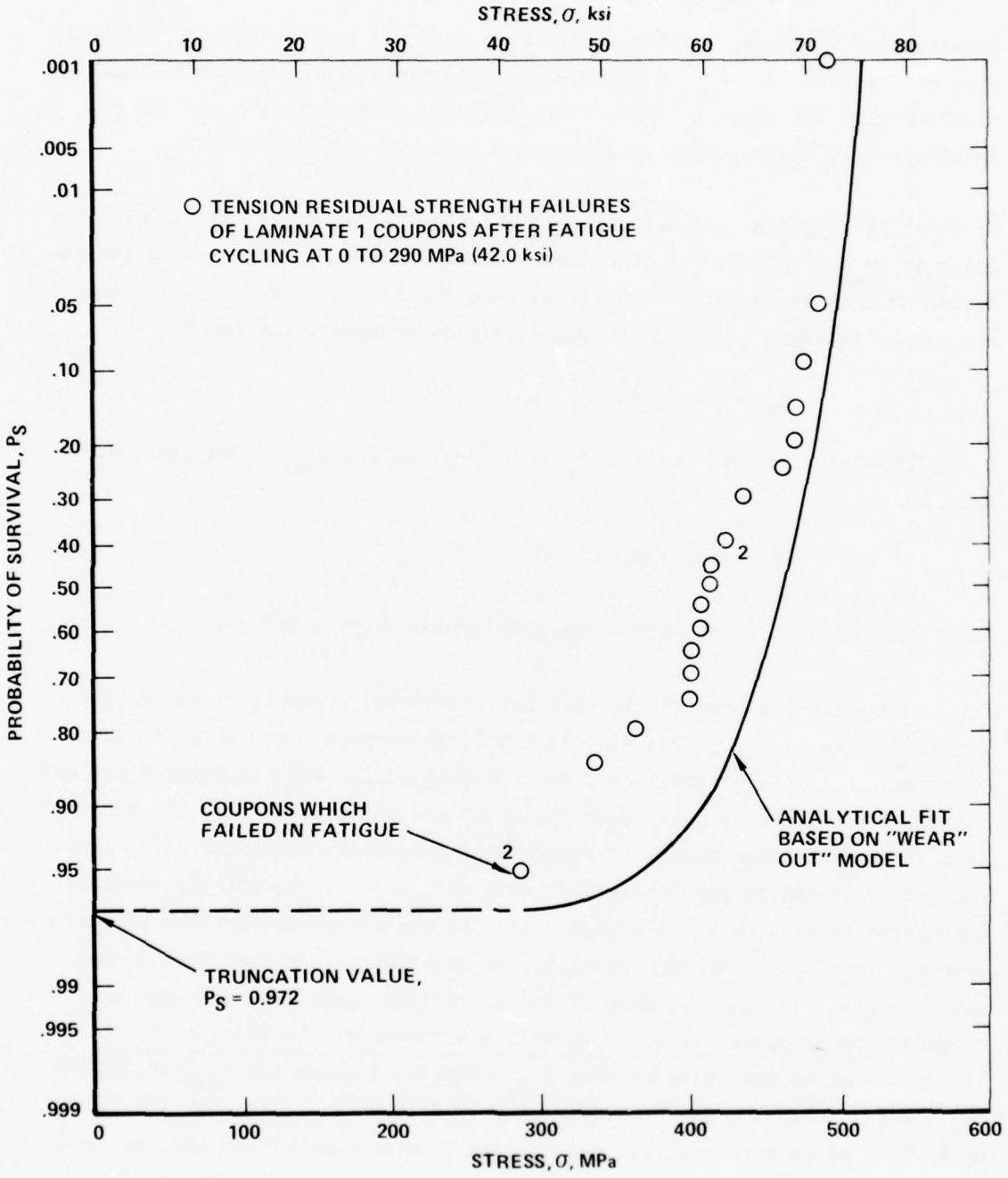


Figure 84. Comparison Between Analytical Fit and Laminate 1 Static Tension Residual Strength Data for Specimens Prior Fatigue Tested at 0 to 290 MPa (42.0 ksi)

conservative at first, but were reasonably accurate for the higher residual strength values. For F_{max} = 290 MPa (42 ksi) data, the reverse situation occurred with the first P_s value being slightly unconservative and the remaining values increasingly in error, see Table 36 and Figure 84.

To check if Equation (21) has any predictive value for other F_{max} levels, the value of F_{max} = 231 MPa (33.5 ksi) was chosen because 20 coupons were fatigue tested at this level to 10^6 cycles and none failed. In this case, t = 1667 min and by Equation (18) and the previously determined value for $\bar{A}_4$:

$$\hat{t}_b = 44371 \text{ min}$$

Using Equation (21), the value of P_s at 10^6 cycles for F_{max} = 231 MPa (33.5 ksi) is:

$$P_s = 0.999006$$

For P_s to reduce to 0.95, t must be 10849 min or 6.51×10^6 cycles.

Let us consider the possibility that this predicted probability of survival for 10^6 cycles at F_{max} = 231 MPa (33.5 ksi) is correct. As Tables 35 and 36 showed, sufficient condition 1 was not met; sufficient condition 2 was not satisfied for Table 35 data; both Tables 35 and 36 indicate that the residual strength data are not smooth if failures are included; Equations (16), (19) and (20) resulted in completely different values of r; and finally previous discussion in Section 7.4.1.1 suggested that the static and fatigue failure modes were not constant. Further, evaluation of Equation (17) showed that A_4 was not constant. In summary, none of the sufficient conditions were met and therefore no credence can be given to the accuracy of the value of P_s at 10^6 cycles or to the value of t at $P_{.95}$ calculated above for F_{max} of 231 MPa (33.5 ksi). Guessing at the values of $P_{.90}$ or t at $P_{.95}$ from the S-N curve appears to be as reasonable as calculating them in view of the lack of correlation between the experimental data and that predicted by the model. This latter point can, of course, only be proven by actually testing a large coupon sample size to failure at F_{max} = 231 MPa (33.5 ksi).

To explore the last question more fully, one can inquire whether the data obtained at F_{max} = 400 MPa (58 ksi) and F_{max} = 345 MPa (50 ksi) can be used to predict the known residual strength distribution for F_{max} = 290 MPa (42 ksi). In this case, α_f = 2.34 and by Equation (16) r = 6.15, and $\bar{A}_4$ is 3.9885×10^{-5}. From Equation (18), $\hat{t}_b$ for F_{max} = 290 MPa (42.0 ksi) is calculated to be 587 min which is unrealistically low compared to the actual value of 3321 min. The calculated truncated value of P_s corresponding to t = 606.7 min is 0.336 which is much lower than the actual value of 0.95. This lack of consistency is not unexpected since the sufficient conditions were not met and because the data above F_{max} = 345 MPa (50 ksi) were previously noted to be apparently dominated by σ_{max} while at lower stress levels, $\Delta\sigma$ was dominant. The lack of correlation at F_{max} = 290 MPa (42 ksi) between the actual probability of survival value, 0.95, and the predicted value, 0.336, is a further indication of the inadequacy of the present formulation of the model to correctly describe the data obtained in this program.

In view of these disappointments, one is led to reconsider how well the data presented in Reference [24] actually fit the model formulation. The data of Reference [24], Figures 9 and 10, are reproduced in Figures 85 and 86. Figure 85 appears to indicate that, as expected, the boundary conditions were met. Between the limits of P_s, the predicted residual strength distribution fits the actual data, at best, poorly. The data of Figure 85 do not support the formulation of the wear-out model as given by Equation (21). The values of r = 5.64 and α_o = 12.3 are given in Reference [24] for these data. Therefore, from Equation (20), α_f can be found to be 1.32 which also checks with Equation (16). No indication is given in Reference [24] whether or not the failure modes remained constant or whether the residual strength distributions were smooth when the fatigue failures were included.

The data in Figure 85 again indicate, as expected, that the boundary conditions are met. As discussed above, that these conditions were met does not constitute sufficient support for the accuracy of Equation (21). Between the extremes of P_s, the fit of the model curve to the data appears to be reasonably good

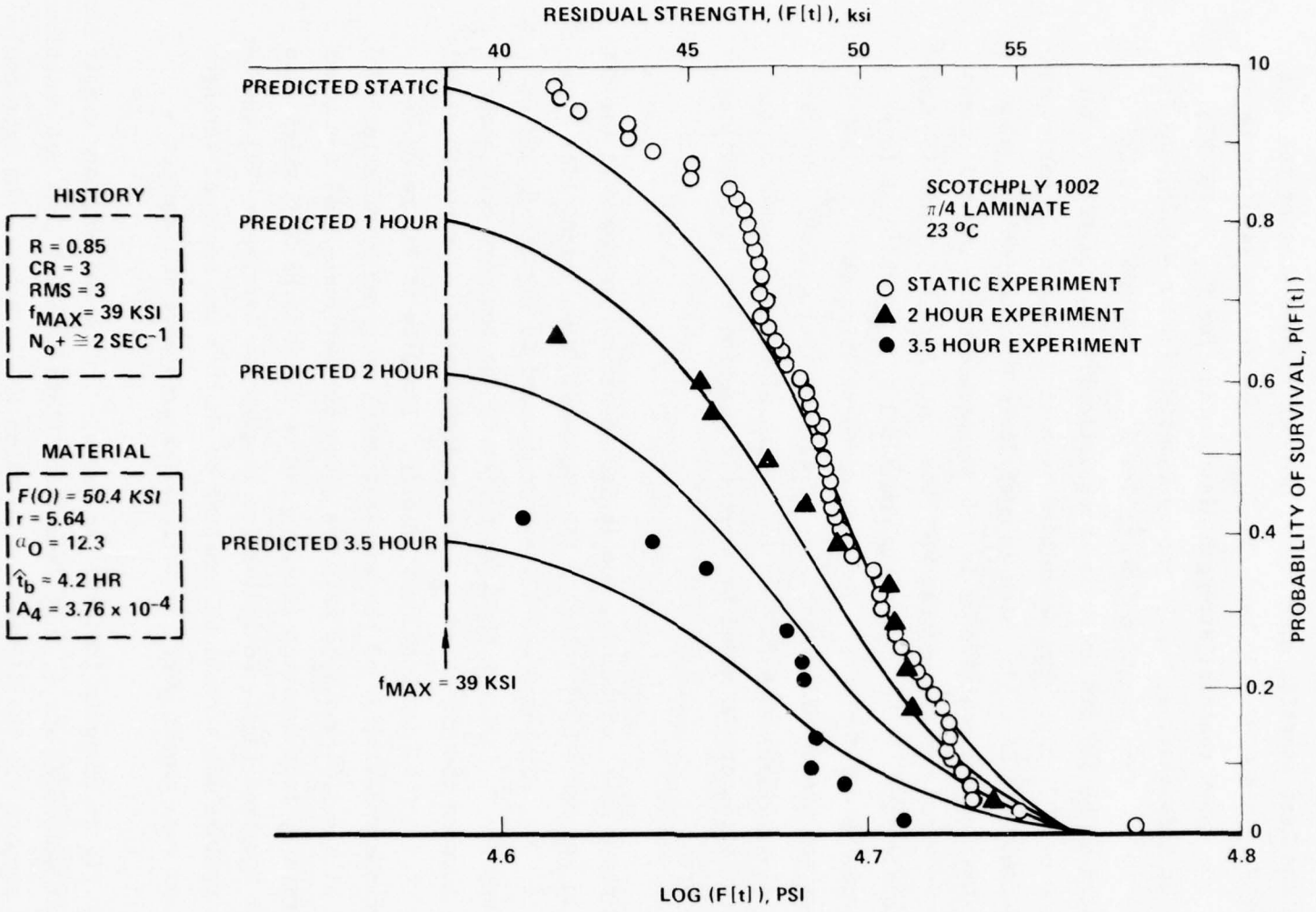


Figure 85. Residual Strength Degradation with Time for a Composite Material; Comparison Between Theory and Experiment (Figure Duplicates Figure 9 of Reference 24)

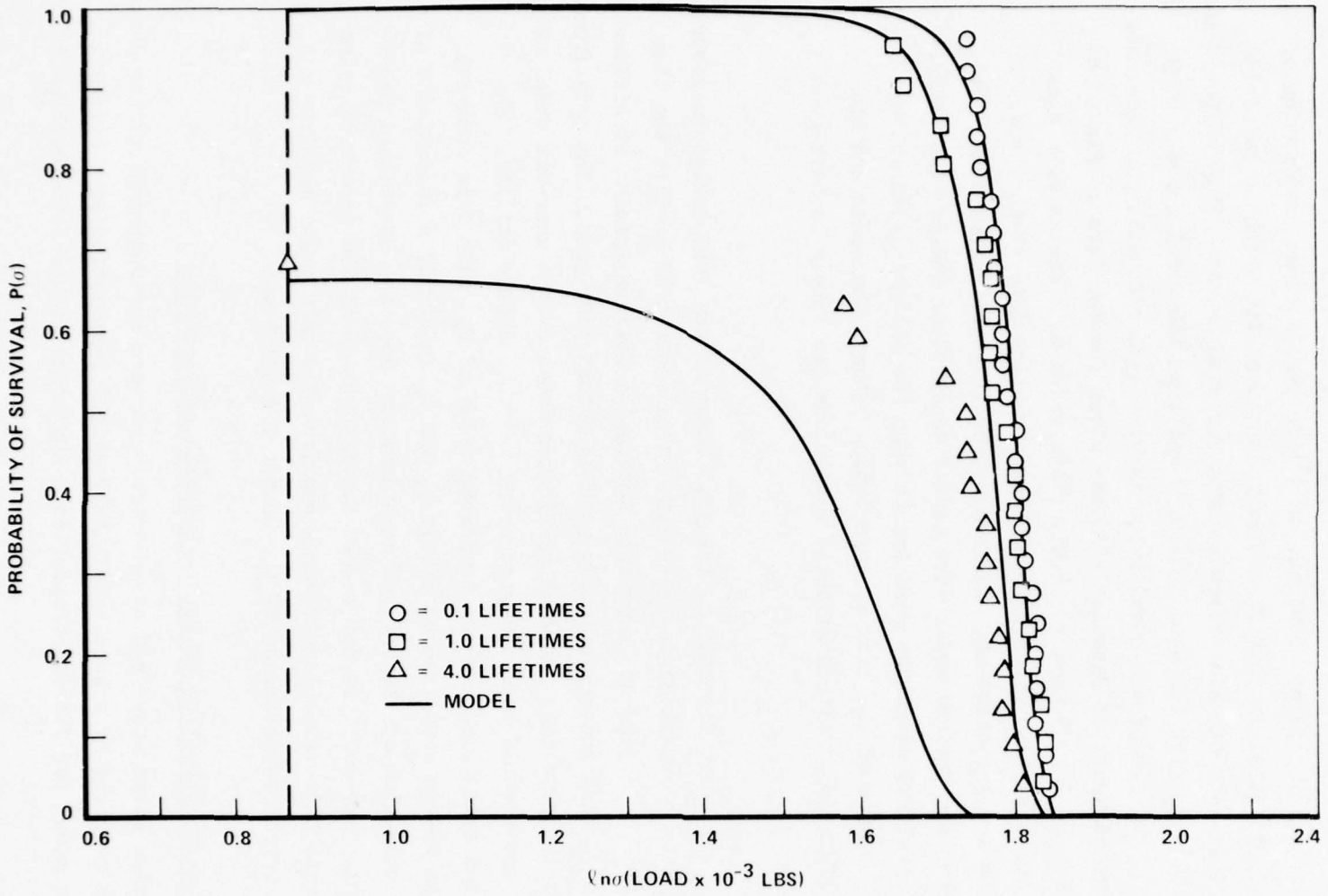


Figure 86. Residual Strength Degradation and Truncation with Time for a Bonded Joint; Comparison of Theory and Experiment (Figure Duplicates Figure 10 of Reference 24)

for the 0.1 lifetime data. However, at 1 lifetime, a close examination of the data as presented in this figure reveals a poor fit which is partially masked by this form of data presentation. For example, at $\sim$ 26.9 kN (6050 lbs) ($\ln \sigma = 1.80$), P_s from the data is $\simeq 0.39$ and from the model curve $\simeq 0.09$. At 4 lifetimes, the fit of the model curve is clearly inadequate. In Reference [24] the coefficients of Equation (21) are given for the data of Figure 86 as $\alpha_o = 32.5$, $\alpha_f = 4.35$, and $r = 4.73$. This value of r checks with Equation (16), but Equation (19) gives $r = 15.75$ and Equation (20) gives $r = 1.45$. These values are inconsistent. No information is given in Reference [24] as to whether the failure modes were indeed constant or whether the distributions of residual strengths were smooth when the fatigue failures were included. In view of the lack of correlation between the model and the data, see Figure 86, neither of these conditions are likely to have been satisfied.

Summarizing the above discussion, the real value of any formulation to describe the wear-out or strength degradation rate is to accurately predict the time to first failure of coupons or components undergoing fatigue loading at different levels of F_{max} than those previously used to obtain life data. The data from this report indicate that any such prediction based on the wear-out model as formulated above would have a low accuracy and thus little utility. The fact that the model predicts the truncated value of P_s, with fair accuracy, for the data set or sets used to obtain α_f and $\hat{t}_b$ is simply a fulfillment of a boundary condition of the derived equations and does not constitute proof of the model. The model is not needed for prediction of the truncated value of P_s, because this value is already known from the data. The model is inadequate beyond satisfaction of the boundary conditions.

7.4.3 Summary; Direction of Future Research and Analysis

The discussion given above had as an overall purpose ascertainment of the characteristics required of a successful mathematical formulation of a strength degradation model for fibrous composites. Any model requires the mathematical

expression of three assumptions: 1) the nature of the degradation rate; 2) the criterion of failure; 3) the relationship between failure modes under static and dynamic loading. In order to discern the required complexity of the model an outline of physical observations and principles was described which included: distribution of damage growth and failure modes in unnotched coupons; a determination of the microstructural reasons for the limited success of strength degradation models in metals; description of the nature of the fibrous composite microstructure and comparison to metals; and a short investigation of the complexity of observed damage growth and failure modes in notched composites.

The discussion of the physical principles underlying composite strength degradation led to a number of expected mechanical responses for a composite which were observed in this research program. The general conclusion of this study is that the form of the mathematical expressions necessary for successful prediction of strength degradation in composites should be expected to be quite complex. The reason for this is due to the fact that damage zone sizes of practical consideration will usually be significantly smaller than the dominant microstructural detail which is the ply. Essentially, damage growth and failure properties are macrostructurally complex in composites requiring the development of relatively complicated rate and failure formulations.

Because of the disturbing nature of this general conclusion for engineering analysis and component life prediction, one proposed relatively simple model of strength degradation was appraised to discern if the conclusion was indeed valid. The appraisal of the simple model strongly showed that the form of this model for strength degradation was inadequate for engineering utility. Although other simple strength degradation models [59] were not assessed, they should be carefully evaluated in the light of physical principles discussed here and the results of the appraisal of the degradation model of Reference [24]. Most likely, other such simple models will show superficial success which will not stand up to rigorous examination.

Because of the conclusions reached in this discussion section, the question naturally arises as to what can be substituted for simple models of strength degradation in composites. One must recognize three basic points before this question can be answered: 1) no successful formulation is likely to be simple or even general; 2) development of new formulations will be difficult; 3) no viable solutions are presently available as substitutes. In view of these three points, life and strength degradation prediction for composites will have to rely in the near future on experimentally generated static and fatigue data just as is true for most metal components.

Over the longer term, this discussion section has indicated the considerations necessary for successful analyses and mathematical formulations, namely; emphasize the macroscopically inhomogeneous nature of fibrous composites; consider in detail the general characteristics of damage growth; carefully observe, describe and record failure modes. Analytical derivations which carefully consider the above described considerations will lead to phenomenological explanations of fatigue life and fracture strength prediction rather than more general degradation models such as those in References [24-28 and 55-57]. Numerous attempts at developing such phenomenological explanations and theories, using finite elements, linear elastic fracture mechanics, and other concepts, have been considered some of which are listed in References [38-46, 52, and 60-64].

Unfortunately, none of these attempts are adequate, because the derived mathematical formulations contain two or more experimentally based parameters without real physical significance. The formulations, which are in many cases relatively complex, are primarily curve fitting procedures which only apply to a restricted set of experimental results (see Reference 65 for a more complete discussion of this point). What is needed is a mathematical model with predictive and extrapolative capability which incorporates the various micromechanical failure processes [65]. The model developed by Kannenen, Rybicki and Griffith [66] attempts to solve the problems raised in this discussion section by treating the material as heterogenous where microstructural effects predominate and as a homogenous anisotropic continum where they are not. Perhaps their paper best indicates the direction for future effort.

7.5 Applications to Design

All of the results discussed in this report apply only to narrow unnotched coupons. The major question for the application of composites to aerospace structural usage is whether test results on small laboratory coupons can be directly or indirectly applied to structural analysis and design. The situation for composites is analogous to that of metals where the application of laboratory coupon results to practical design questions remains a problem. However, within reasonable limitations, several procedures have been successfully applied in metals to scale-up laboratory coupon test results.

Two problems are of major concern when considering the data of this report. First, because only unnotched coupons were used, the data must be used with caution because in practical application fatigue failures originate in the region of notches. Second, the question arises as to whether fatigue or static test results for narrow coupons are the same for wide panels. In regard to the second problem, because of the apparent differences in the two fatigue failure modes for the two laminates considered in this program, test results for wide panels compared to narrow coupons are expected to be different for the two laminates. Scaling to wide panels from narrow coupons is probably laminate dependent. Future composite research must be oriented, in part, towards ascertaining the extent of the difference in mechanical behavior between wide panels and narrow coupons.

In regards to employing insights into material properties gained from programs such as this one, the reference by Anthony [67] is pertinent. Anthony made a number of observations in 1972 most of which have been confirmed by this program. Quoting at length, Anthony observed:

1. The fracture of composites and the fatigue of both metals and composites appears to be statistical in nature.
2. Of prime importance in statistically defining material behavior is the low probability of failure tail of the strength distribution.

3. A large number of statistical distribution functions are available for defining material behavior.
4. Despite the availability of many mathematical expressions or distribution functions, it is difficult to accurately define property distributions in the tail regions.
5. The extensive data generation required to improve the definition of tail regions is expensive.
6. Since there are usually a number of possible failure locations the allowable probability of failure at any one location is lower than that for the aircraft.
7. For composites some relatively low loads have a degrading effect.

His proposed solution to the problem of handling the tail of the data distribution is interpolation from a threshold strength rather than extrapolation from a curve fit.

A research question which should be of future interest is whether or not a threshold for fatigue failures exists in a practical sense. Since at most of the stress levels examined in this study, scatter in the fatigue data was large, the question of the existence of a practical threshold should be of major interest to the designer. Possibly, potential service failures due to fatigue can be prevented by restricting ultimate strains below the threshold value. This concept is similar to that proposed [67] for static strength values. The concept of a threshold seems to be of far more value to the designer of aircraft than the concept of strength degradation.

SECTION VIII

CONCLUSIONS AND RECOMMENDATIONS

8.1 Conclusions

Based on the results of this program, several major conclusions have been drawn. Conclusions pertain specifically to narrow width coupons of a type similar to that used in this research program. However, with proper concern for complexity scale-up, the conclusions are believed to have some general validity.

- Consistent well-controlled coupons were manufactured with low variability in geometry and material characteristics such as void content and fiber volume.
- The tensile stress-strain response of laminate 1 coupons was linear followed by a curved region prior to a brittle-like failure while that of laminate 2 was essentially linear to failure.
- Laminate 1 coupons exhibited more delamination after static tensile failure than laminate 2 coupons.
- In some laminates, off-axis plies can dominate the failure mode even though they make up only one-third of all plies in the laminate.
- The static tensile strength and apparent modulus of laminate 2 coupons were higher than laminate 1 coupons and exhibited slightly more scatter, but the strains to failure were similar.
- Variation in tensile strength among the same laminates made from different batches of the same material manufactured early in batch shelf life was small.
- The static compression strength and modulus of laminate 2 exceeded that of laminate 1 and had somewhat less scatter.
- The Poisson's ratio of laminate 2 was approximately 0.63 and that of laminate 1 approximately 0.28.
- Both laminates showed large data scatter during fatigue loading and a dependence of fatigue life on maximum stress. This was especially noticeable for laminate 1.

- Compression markedly reduces fatigue life with a greater reduction corresponding to a larger compression load excursion.

- The effect of compression can not be reliably correlated over all stress levels on either stress range or maximum stress.

- A fatigue life endurance limit appears to exist, but is not definitively proven.

- Fatigue data scatter was greater for laminate 2 than for laminate 1.

- Laminate 2 coupons subjected to fatigue are susceptible to first cycle failures at strain levels significantly below that necessary for static failure. This response was not true of laminate 1 coupons. The cause of this effect remains unknown.

- The tensile and compressive residual strengths of laminate 1 coupons degraded due to fatigue cycling.

- The tensile residual strength of laminate 2 coupons did not degrade after 10^6 fatigue load cycles at stress levels at which other coupons failed in fatigue.

- The compressive residual strength of laminate 2 coupons at the stress range studied degraded after 10^6 fatigue load cycles.

- The apparent modulus of elasticity of laminate 2 coupons under compressive loading increased. This was most likely due to moisture absorption and redistribution of residual stresses.

- The difference in mechanical response between laminate 1 and laminate 2 was large. The nature of the difference appeared to be similar to that observed in different heat treatments of a metal alloy and thus there is hope that such differences can be analyzed and understood.

- Differences in the mechanical response of composite laminates may possibly be more easily correlated on the basis of the average strain to failure as opposed to the average ultimate stress.

- A 3-parameter Weibull fit to fatigue data appears to be significantly superior to a 2-parameter fit at high probability of survival levels.

- Extrapolation of fatigue (and possibly static) data to the most important region of concern to aerospace designers, namely in excess of $P_{.99}$, appears to be, at present, inadequate even using a 3-parameter Weibull fit.

- The recommended minimum number of coupons needed to describe the extent of fatigue scatter inherent in presently used composites is 20. However, even this number only allows calculation to a probability of survival level equivalent to $P_{.95}$. To determine $P_{.99}$, 100 coupons may have to be tested.

- Present models of residual strength degradation are inadequate.

- A major question remains as to whether test results obtained using small coupons can be extended to large coupons or structural panels.

8.2 Recommendations

Based on the conclusions listed in Section 8.1, the following recommendations for future research work in composite materials are suggested.

- Determine whether the mechanical response of wider and larger coupons is the same as for narrow coupons.

- Investigate the techniques needed to improve prepreg, panel fabrication, and machining quality such that mechanical property scatter is reduced.

- Investigate those material properties which can result in fatigue failure of some coupons under loading conditions which do not degrade the properties of other coupons.

- Determine the cause of laminate 2 first cycle fatigue failures.

- Further investigate the possibility of using strain as a comparison parameter instead of stress.

- Investigate the effect of environment and temperature upon the scatter of the data and the response of the material to compressive load excursion during fatigue loading.

- Investigate the effect of holes and notches under similar loading conditions as those used in the research program.

- Extend analytical and experimental investigations into the phenomenological characteristics of damage growth and failure for developing strength and life prediction models.

- Investigate whether a threshold for fatigue failure exists in a practical sense and determine whether or not the threshold value for different layups can be related on the basis of strain.

APPENDIX A

T300/934 GRAPHITE/EPOXY LAMINATE AND

TEST SPECIMEN FABRICATION PROCEDURE

AFML Contract F33615-75-C-5118

1. Material Storage - All material shall be stored in sealed moisture-proof bags in refrigerators maintained at -18 ± 12°C (0 ± 10°F). Storage time shall not exceed six months.

2. Open Time - All material shall be laid up and cured within a total cumulative time of 72 hours out of refrigerators. Material shall be removed from refrigerators for at least one hour before removal from covering bag.

3. Receiving Tests - Each batch of prepreg shall be sampled and tested in accordance with Lockheed Material Specification C-22-1379/111.

4. Tool and Caul Plates for Curing - All tool plates used for curing laminates shall be aluminum. Thickness of the caul plate shall be 12.7 mm (0.500 in.) with a tolerance of ± 0.08 mm (± 0.003 in.), flat and parallel. Caul plates used on top surface of laminate under the vacuum bag shall be aluminum sheet (1.62 mm (0.064 in.) standard thickness).

5. Lay-Up Procedure - Panels shall be laid up using 305 mm (12 in.) wide prepreg graphite/epoxy (T300/934) tape as the base material. Tape shall be laid with a gap tolerance of 0 to 0.8 mm (0 to 0.031 in.). A check-off system shall be used by the lay-up operator to assure proper orientation of the tape edge (within ± 2° of an oriented template) and stacking sequence of each ply in the laminate. All panels shall be laid up oversize to allow for 25.4 mm (1.0 in.) trim minimum on all edges of the panel to avoid edge taper and resin content variables of panels as laminated.

Preceding Page BLANK

Laminate 1 panels shall be approximately 610 x 660 mm (24 in. x 26 in.) while Laminate 2 panels shall be approximately 965 x 1372mm (38 x 54 in.).

6. Bleeding and Bagging Procedure - The bleeding and bagging materials used for curing laminates 16 plies thick are listed in sequence starting from surface of curing plate as follows:

(1) Release film (Teflon)
(2) Two plies Mochburg CW1850 Bleeder paper
(3) One ply of porous Teflon-coated glass cloth (duPont Armalon)
(4) Graphite/epoxy laminate (Laminate 1 or 2)
(5) One ply porous Teflon-coated glass cloth (duPont Armalon)
(6) Two plies Mochburg CW1850 bleeder paper
(7) Release film (Teflon)
(8) Caul plate (aluminum 1.62 mm (0.064 in.) thick).
(9) Glass boat cloth (vacuum distribution)
(10) Nylon bag (Vac-Pac 0.076 mm (0.003 in. thick))

The nylon bag is sealed to the cure plate with sealing putty (Presstite No. CS12-4). The bag seal and bag shall be carefully checked for leaks under vacuum before the cure cycles are started.

7. Cure Procedure - The thermocouple shall be placed on the caul plate adjacent to the laminate and the complete time-temperature history of each laminate monitored and recorded on a strip chart. The cure cycle used for T300/934 material shall be as follows:

(1) Apply full vacuum 88-98 x 10^3 Pa (26-29 in.Hg)
(2) Raise temperature to 121°C (250°F) at average of 1-2°C (3-4°F) per minute
(3) Dwell at 121°C (250°F) for 15 minutes with vacuum pressure
(4) Apply 0.69 MPa (100 psi) pressure plus vacuum and hold at 121°C (250°F) for 45 minutes
(5) Raise temperature to 177°C (350°F) at 2-3°C (3-5°F) per minute
(6) Hold at 177°C (350°F) and 0.69 MPa (100 psi) plus vacuum for 2 hours

(7) Cool to 82.2°C (180°F) under vacuum and pressure while recording cool-down rate

(8) Cool to 65.6°C (150°F) under vacuum only while recording cool-down rate.

8. Resin Content and Voids - The average resin and void content of each panel fabricated shall be determined. Resin content shall be maintained at 28-31 wt.% (60-65 vol.% fiber). Void content shall be 2.0% max. by volume.

9. Non-Destructive Inspection - Each panel shall be inspected using ultrasonic C-scan techniques. Results for Laminate 1 panels shall be compared to a reference panel standard containing known voids at specified depths and of specified sizes as shown in Figure 1A. For Laminate 2 panels, results will be compared to known voids placed in each panel as shown in Figure 2A.

10. Fabrication and Bonding of Glass Fabric/Epoxy Grip Tabs - Grip tab sheet material shall be fabricated by laminating eight plies of 1581 glass/fabric/epoxy to make a laminate 1.65-1.78 mm (0.065-0.070 in.) thick. The material to be used is Fiberite Corp. MXB-7701/1581 glass fabric/epoxy prepreg conforming to Lockheed material specification LCM C22-1032/131. This material is to be cured at 121°C (250°F) for one hour under a pressure of 0.34 MPa (50 psi) plus vacuum.

The glass fabric/epoxy laminate shall be cut into 76.2 mm (3 in.) wide strips to be located on graphite panels in preparation for bonding as shown in Figures 3A and 4A. After all preliminary machining is done, glass tabs shall be thoroughly cleaned by wiping with methyl-ethyl-ketone solvent. The adhesive film shall then be cut to size and applied to glass/epoxy tab strips which are located on the test laminate with 1.59 mm (0.0625 in.) rivets placed in pre-drilled holes in trim area on the panel.

The adhesive used shall be American Cyanamid Co. FM-137 film 0.96 Kg/m^2 (0.06 lb/ft^2) conforming to Lockheed Specification LCM 30-1085 Type II, Grade A. Spacers used between tabs next to curing plate shall be constructed of the same glass fabric epoxy sheet used for fabricating tabs using 0.127 mm (0.005 in.) Teflon film next to graphite/epoxy laminate.

The laid up panels shall be bagged and cured in an autoclave at 121°C (250°F) for one hour with a pressure 0.34 MPa (50 psi) plus vacuum.

11. Panel and Coupon Identification - All panels and coupons shall be clearly marked before and after application of tabs to indicate the bag side of the graphite/epoxy laminate as originally cured. Panels shall be identified with a number including material code and autoclave run number. Coupons shall be identified with panel number from which cut and dash numbers.

Example: ILY 556-1A

Coupons shall be numbered consecutively as they are cut from panels to indicate relative location in the panel (see Figure 3A for Laminate 1 and Figure 4A for Laminate 2).

12. Machining of Coupons - Coupons of the configuration shown in Figure 5A shall be machined from each panel as per Figure 3A or Figure 4A. Coupons shall be machined dry using a 152.4 mm (6 in.) diameter, 40 tooth carbide cutter at 250 ± 10 rpm and at a feed rate of 304.8 ± 25.4 mm/min (12 ± 1 in./min).

13. Performance Requirements - Laminate panels shall be rejected if review of fabrication records reveals that prepreg did not meet Item 3 and laminates did not meet Items 9 and 10 of this fabrication procedure. In addition, finished coupons shall be measured for width in four (4) places and for thickness in eight (8) places as per Figure 6A. Coupons shall be rejected if all width measurements are not 22.22 ± 0.07 mm (0.875 ± 0.003 in.) and if thickness is not within ± 0.05 mm (± 0.002 in.) of the average of eight thickness measurements.

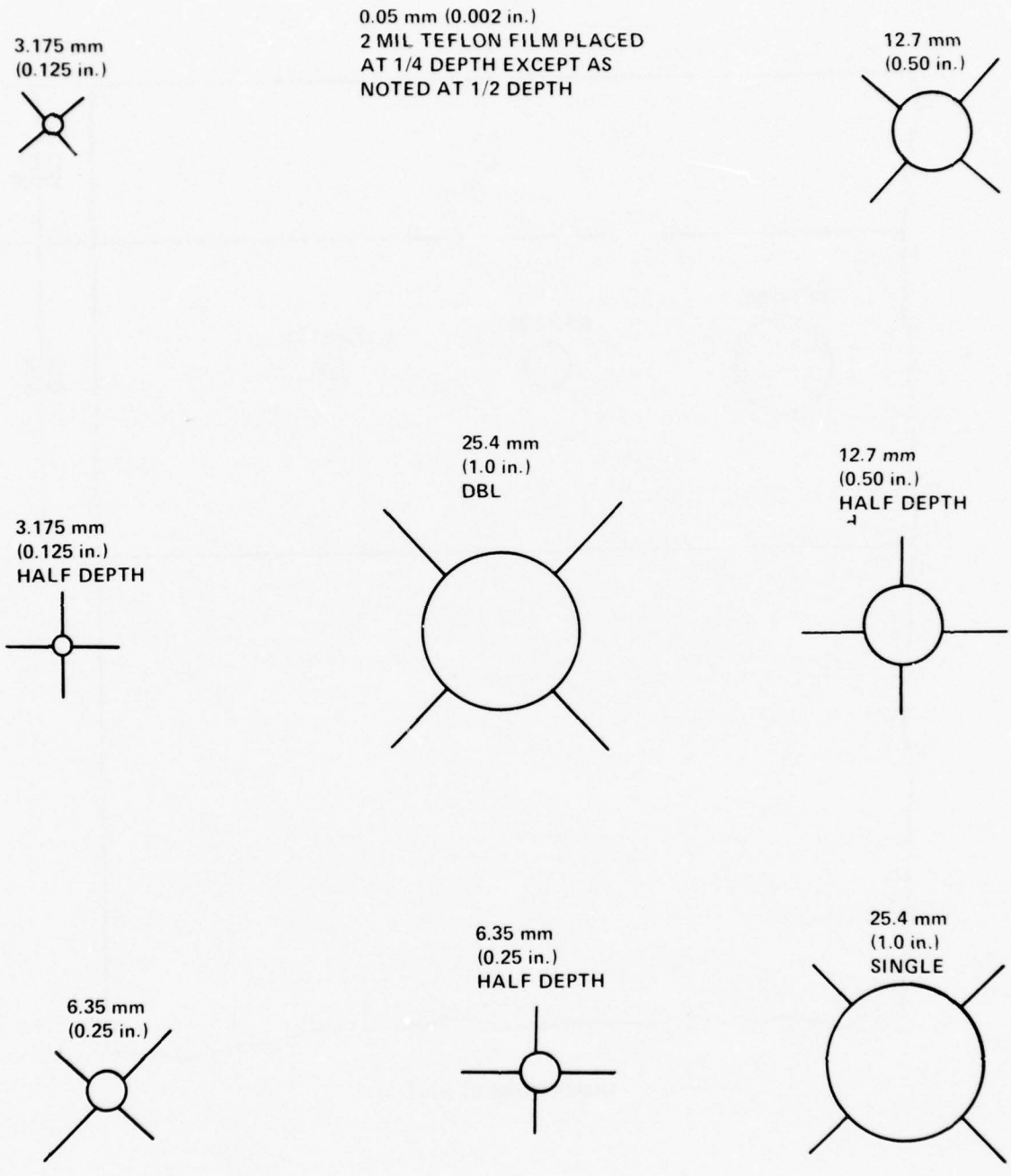


Figure 1A. Template for Laminate 1 Panels

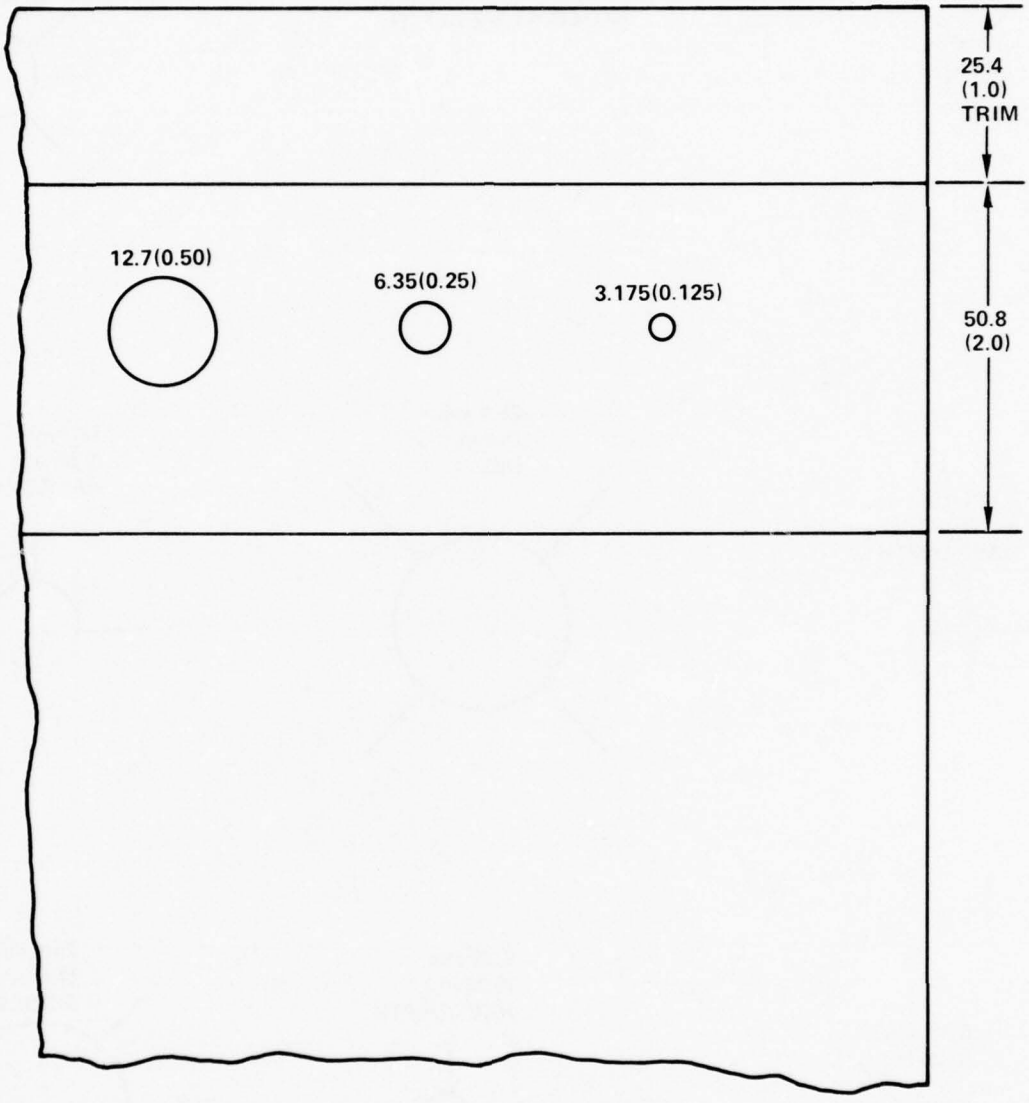


Figure 2A. Template for Laminate 2 Panels

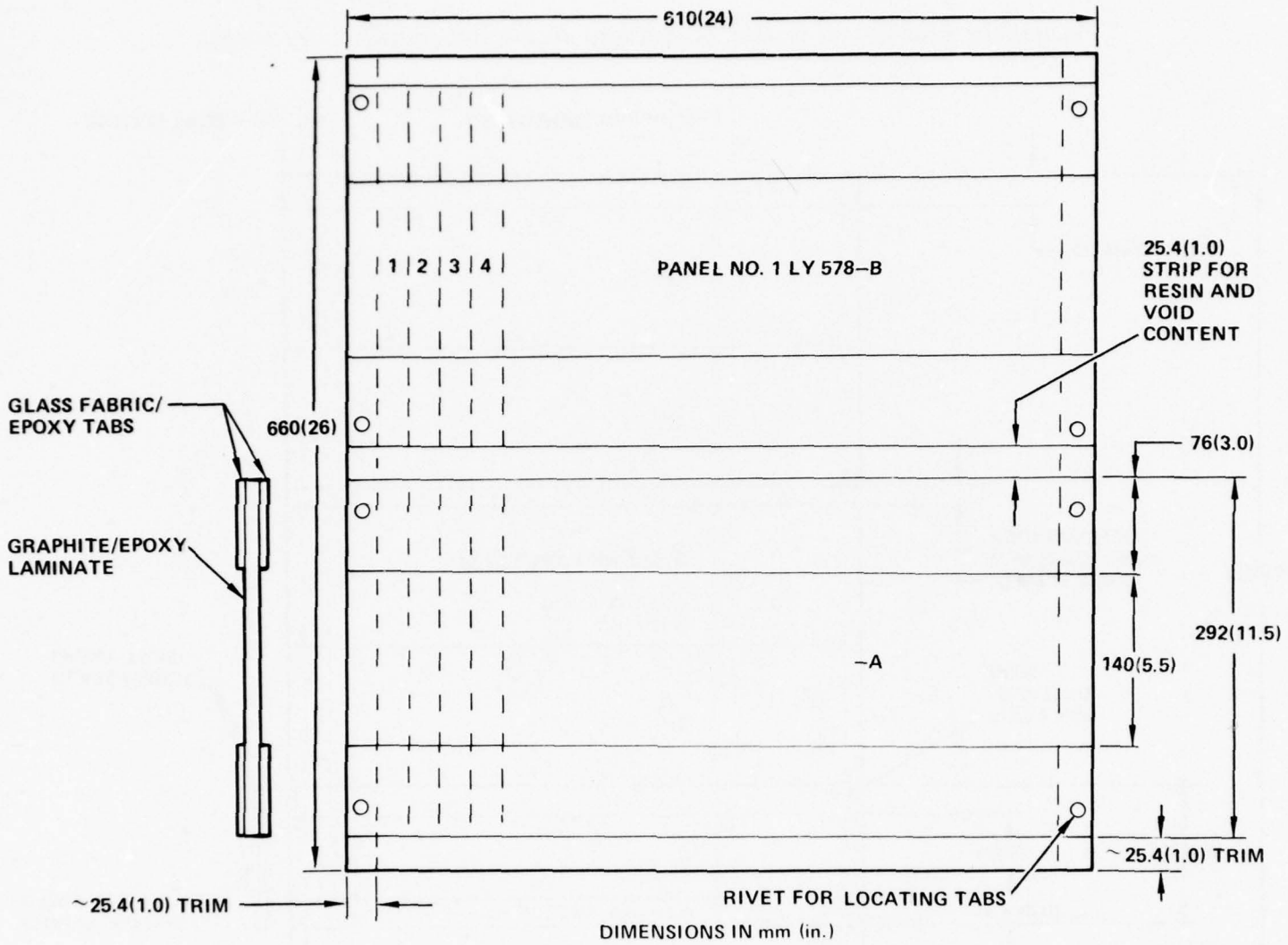


Figure 3A. Identification of Laminate 1 Panels and Coupon Locations

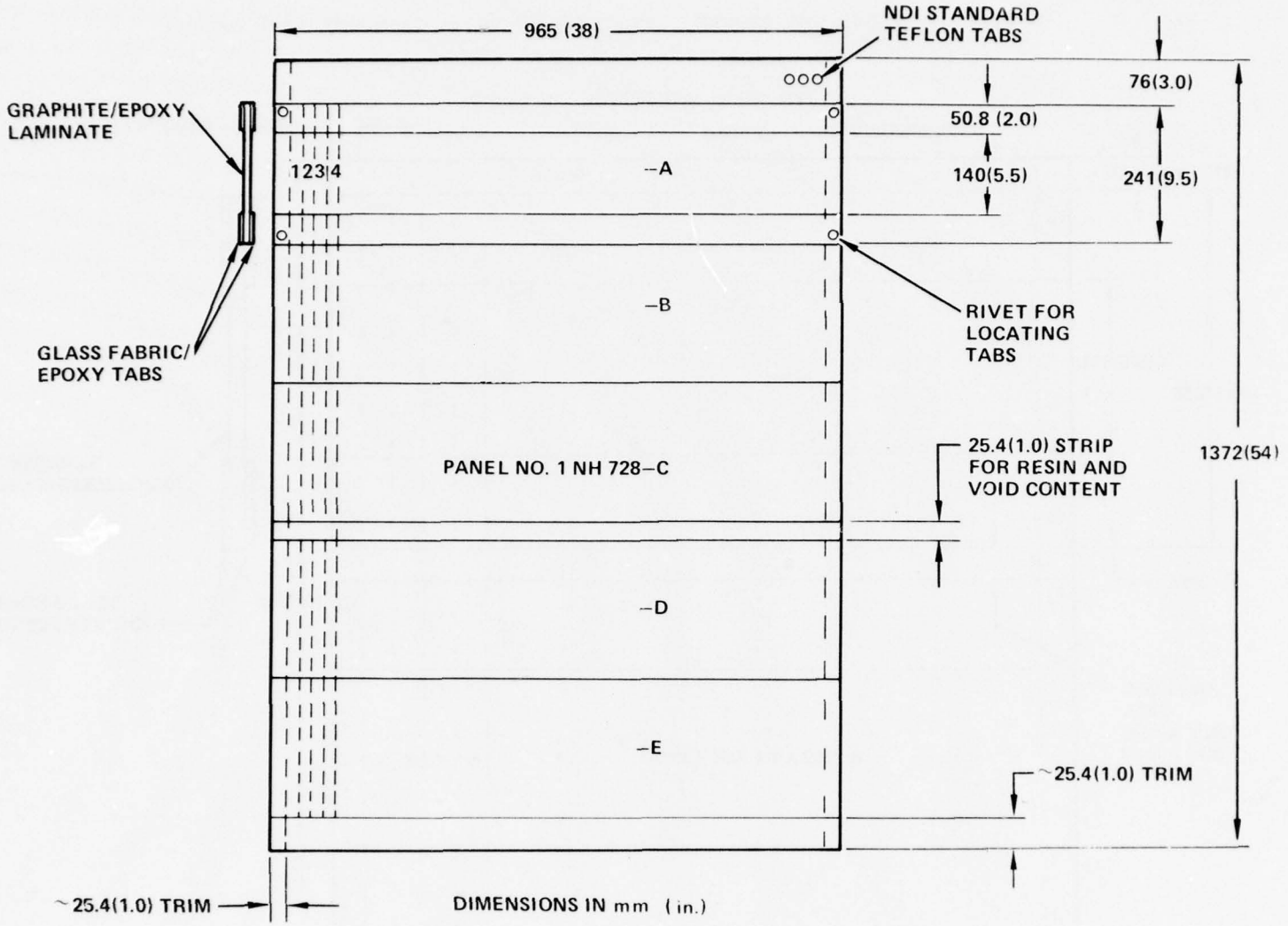


Figure 4A. Identification of Laminate 2 Panels and Coupon Locations

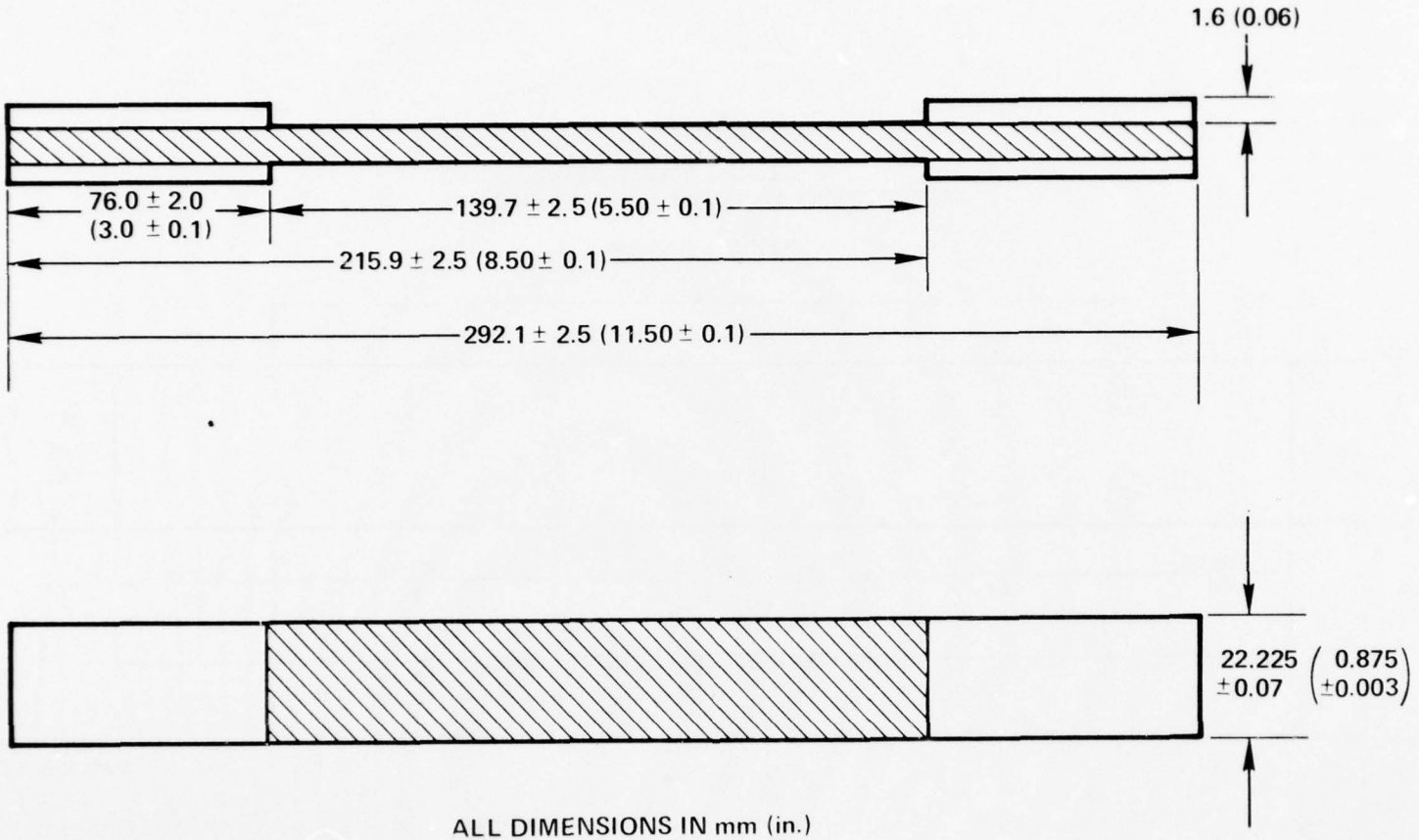


Figure 5A. Coupon Geometry

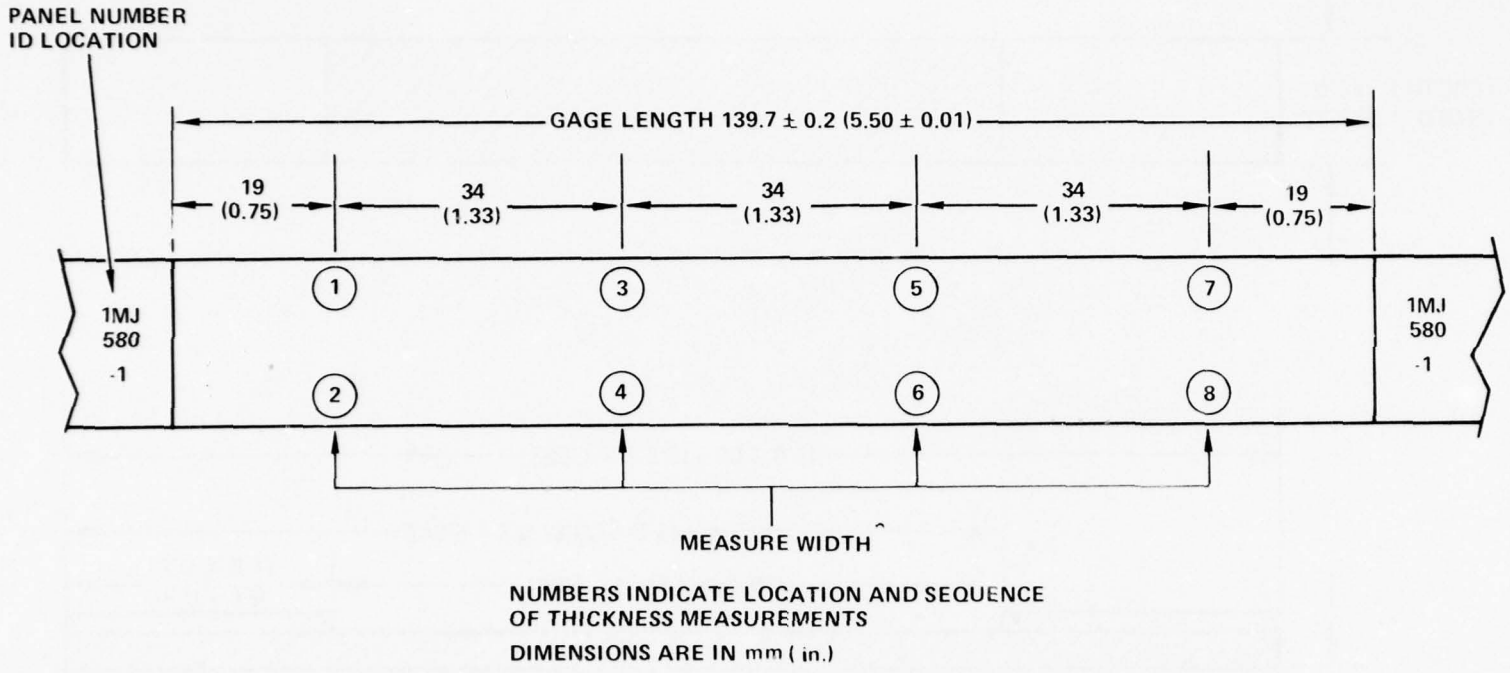


Figure 6A. Location of Thickness and Width Measurements

APPENDIX B

This appendix lists all of the fatigue data generated during this research investigation.

TABLE 1B

STRESS LIFE SCAN

TENSION-TENSION FATIGUE TEST RESULTS

OF LAMINATE 1

σ_{min} = 0 ksi, f = 10 Hz

Sample ID	Minimum Area, $in.^2$	Maximum Stress, σ_{max}, ksi	Cycles to Failure, N_F	Cycles to Delamination, N_{DL} (Approximate)
601- 7B	0.0822	62.0	2,079	-
603-18A	0.0825	62.0	229	-
606- 2B	0.0823	62.0	3	-
578-10A	0.0840	58.0	1,664	-
578-25B	0.0852	58.0	1,643	-
580- 2A	0.0846	58.0	5,705	-
580-21A	0.0812	54.0	30,520	-
603-26B	0.0815	54.0	7,798	-
604- 4A	0.0806	54.0	9,888	-
583-26A	0.0815	50.0	512,600	222,500
601-24B	0.0811	50.0	58,530	-
606-21A	0.0810	50.0	367,644	95,000
596-13A	0.0843	46.0	564,726	60,000
594-20B	0.0822	46.0	351,900	36,000
583-23A	0.0808	46.0	279,440	-
582-25A	0.0820	42.0	864,420	-
582- 9A	0.0821	42.0	1,698,100	1,400,000
594-21A	0.0819	42.0	2,876,860	1,100,000

TABLE 2B

STRESS LIFE SCAN

TENSION-COMPRESSION FATIGUE TEST RESULTS

OF LAMINATE 1

f = 10 Hz

Sample ID	Min Area, $in.^2$	Maximum Stress, σ_{max}, ksi	Minimum Stress, σ_{min}, ksi	Cycles to Failure, N_F	Cycles to Delamination, N_{DL} (Approximate)
578-20A	0.0835	62.0	-10.0	810	-
604-23A	0.0813	62.0	-10.0	1,127	-
606-15B	0.0841	62.0	-10.0	10	-
580-26A	0.0837	58.0	-10.0	4,840	3,000
594- 1A	0.0809	58.0	-10.0	4,980	-
603-10A	0.0815	58.0	-10.0	1,675	-
596-23B	0.0823	54.0	-10.0	10,500	9,500
582- 2B	0.0810	54.0	-10.0	11,055	7,200
601-18B	0.0821	54.0	-10.0	6,997	-
601-20B	0.0818	50.0	-10.0	10,651	-
580-16B	0.0837	50.0	-10.0	16,030	16,000
596-26A	0.0869	50.0	-10.0	10,000	9,000
582- 3A	0.0823	46.0	-10.0	25,520	25,180
603-18B	0.0834	46.0	-10.0	36,500	-
604- 5A	0.0824	46.0	-10.0	78,710	35,000
578-21A	0.0846	42.0	-10.0	130,720	125,500
583-13A	0.0849	42.0	-10.0	78,290	73,500
606-19B	0.0829	42.0	-10.0	188,887	38,000
594-22B	0.0818	38.0	-10.0	111,600	-
583- 7B	0.0833	38.0	-10.0	414,560	407,000
601-21A	0.0819	38.0	-10.0	485,190	436,020
582-25B	0.0808	34.0	-10.0	1,047,000	899,000
578-16B	0.0868	34.0	-10.0	1,322,440	677,000
596- 3A	0.0816	34.0	-10.0	2,104,510	1,241,000
580-26B	0.0859	58.0	-16.0	1,402	-
594-7A	0.0845	58.0	-16.0	3,251	-
601-17A	0.0856	58.0	-16.0	1,010	-
578-22A	0.0849	50.0	-16.0	10,906	-
582- 5B	0.0817	50.0	-16.0	11,445	2,500
604-24B	0.0808	50.0	-16.0	3,981	2,900
580-22A	0.0827	38.0	-16.0	213,539	187,000
603-16A	0.0823	38.0	-16.0	55,380	42,000
606-12A	0.0832	38.0	-16.0	43,485	38,000
604-16B	0.0873	34.0	-16.0	123,672	104,600
580-15A	0.0821	34.0	-16.0	749,444	-
606- 3A	0.0803	34.0	-16.0	638,880	-

TABLE 3B

STRESS LIFE SCAN

TENSION-TENSION FATIGUE TEST RESULTS

OF LAMINATE 2

σ_{min} = 0 ksi, f = 10 Hz

Sample ID	Average Area, $in.^2$	Maximum Stress, σ_{max}, ksi	Cycles to Failure, N_F
696-10B	0.1293	118.0	664,690
727-15A	0.1267	118.0	90
728-32C	0.1296	118.0	761,130
696- 5B	0.1275	112.0	2,350
696- 6B	0.1286	112.0	268,060
727-31C	0.1269	112.0	10^6 NF[a]
727- 5A	0.1273	112.0	1.1×10^6 NF
696- 2C	0.1270	106.0	210
728-29A	0.1292	106.0	933,780
728-30B	0.1310	106.0	10^6 NF
696-36C	0.1265	106.0	15,400
696-29A	0.1291	100.0	1.069×10^6 NF
699-30B	0.1235	100.0	10^6 NF
727-24A	0.1290	100.0	10^6 NF
699-34B	0.1276	94.0	1
727- 6B	0.1270	94.0	991,880 NF

a - NF indicates No Failure.

TABLE 4B

STRESS LIFE SCAN

TENSION-COMPRESSION FATIGUE RESULTS

OF LAMINATE 2

σ_{min} = -30 ksi, f = 10 H_z

Sample ID	Average Area, $in.^2$	Maximum Stress, σ_{max}, ksi	Cycles to Failure, N_F
699-26B	0.1270	100.0	Tab adhesive Failure
699- 6B	0.1281	100.0	Tab adhesive Failure
728- 9B	0.1322	100.0	Tab adhesive Failure
696-23B	0.1273	90.0	Tab adhesive Failure
727-27C	0.1248	90.0	Tab adhesive Failure
728-11A	0.1286	90.0	10^6 NF[a]
696-10C	0.1261	80.0	10^6 NF
699-19C	0.1299	80.0	10^6 NF
696-22A	0.1286	70.0	10^6 NF
727- 3A	0.1255	70.0	10^6 NF
728-24A	0.1301	70.0	380,800

a - NF indicates No Failure

TABLE 5B

TENSION-TENSION FATIGUE RESULTS OF LAMINATE 1

AT A MAXIMUM STRESS OF 25 ksi

σ_{min} = 0 ksi, f = 10 H_z

(Number of Tests = 20)

Sample ID	Minimum Area, $in.^2$	Number of Testing Cycles, N
578-13B	0.0873	10^6
578-19B	0.0847	10^6
580-6A	0.0825	10^6
580-16A	0.0828	10^6
582-8A	0.0824	10^6
582-3B	0.0814	10^6
583-23A	0.0809	10^6
583-26B	0.0820	10^6
594-4A	0.0811	10^6
594-25A	0.0818	10^6
596-9A	0.0831	10^6
596-26B	0.0816	10^6
601-8B	0.0827	10^6
603-4A	0.0810	10^6
603-13A	0.0841	10^7
604-11A	0.0836	10^7
604-12A	0.0836	10^6
606-9B	0.0836	10^7
606-10B	0.0844	10^7
606-23B	0.0803	10^6

NOTE: All tests ran out, no failures, no delamination.

TABLE 6B

TENSION-TENSION FATIGUE RESULTS
OF LAMINATE 1 AT A MAXIMUM STRESS OF 33.5 ksi

σ_{min} = 0 ksi, f = 10 Hz

(Number of Tests = 20)

Sample ID	Minimum Area, $in.^2$	Number of Testing Cycles, N
578-13A	0.0827	10^6
578-23A	0.0827	10^6
580-21A	0.0821	10^6
580-11B	0.0831	10^6
582-4A	0.0809	10^6
582-16A	0.0827	1.468×10^6
582-13B	0.0818	10^6
594-22A	0.0814	1.039×10^6
594-1B	0.0796	1.039×10^6
596-21A	0.0817	10^6
596-14B	0.0832	10^6
596-24B	0.0816	1.468×10^6
601-12A	0.0817	10^6
601-13A	0.0832	10^6
603-7A	0.0814	10^6
603-9B	0.0830	10^6
603-11B	0.0833	10^6
604-26A	0.0817	10^6
606-2A	0.0810	10^6
606-16B	0.0840	10^6

NOTE: All tests ran out, no failures, no delaminations.

TABLE 7B

TENSION-TENSION FATIGUE RESULTS

OF LAMINATE 1 AT A MAXIMUM STRESS OF 42 ksi

σ_{min} = 0 ksi, f = 10 Hz

(Number of Tests = 20)

Sample ID	Minimum Area, $in.^2$	Cycles to Failure, N_F	Cycles to Delamination, N_{DL} (Approximate)
578-25A	0.0835	1,872,851	142,000
578-17B	0.0869	1,437,800	500,000
580-15B	0.0835	215,984	185,000
580-18B	0.0829	2,359,300	142,000
582- 9A	0.0821	1,698,100	1,528,100
582-25A	0.0820	864,420	-
583- 1B	0.0823	1,291,505	197,000
583- 2B	0.0824	1,186,800	560,000
594-21A	0.0819	2,876,860	1,100,000
594- 6B	0.0817	3,347,500	1,983,800
596- 2A	0.0823	1,416,509	830,200
596-16A	0.0832	1,967,170	1,790,600
601- 1A	0.0799	632,406	326,000
601-11A	0.0827	245,455	-
603-14A	0.0845	350,363	-
603- 5B	0.0823	2,628,300	1,271,000
604-13B	0.0848	1,354,800	1,175,000
604-22B	0.0824	1,216,000	702,000
606-25A	0.0814	4,951,832	861,000
606-20B	0.0818	3,542,157	1,091,000

TABLE 8B

TENSION-TENSION FATIGUE RESULTS

OF LAMINATE 1 AT A MAXIMUM STRESS OF 50 ksi

σ_{min} = 0 ksi, f = 10 Hz

(Number of Tests = 20)

Sample ID	Minimum Area, $in.^2$	Cycles to Failure, N_F	Cycles to Delamination, N_{DL} (Approximate)
578- 4A	0.0850	87,373	70,000
578-18B	0.0859	11,491	-
580- 2B	0.0830	59,320	48,000
580- 5A	0.0825	60,912	-
582- 2A	0.0818	81,571	37,000
582-26B	0.0823	51,848	40,000
583-26A	0.0815	512,600	222,500
583-22B	0.0822	69,711	37,000
594- 7B	0.0823	54,187	50,000
594- 2A	0.0819	71,400	43,500
596- 5A	0.0820	116,667	-
596- 7A	0.0824	64,070	42,750
601-19A	0.0827	70,049	35,000
601-24B	0.0811	58,530	-
603-12B	0.0833	17,578	-
603-25B	0.0830	40,270	-
604- 9A	0.0837	44,830	-
604- 6B	0.0823	41,200	-
606- 8A	0.0839	70,497	-
606-21A	0.0810	367,644	95,000

TABLE 9B

TENSION-TENSION FATIGUE RESULTS

OF LAMINATE 1 AT A MAXIMUM STRESS OF 58 ksi

σ_{min} = 0 ksi, f = 10 Hz

(Number of tests = 20)

Sample ID	Minimum Area, $in.^2$	Cycles to Failure, N_F	Cycles to Delamination, N_{DL} (Approximate)
578-10A	0.0840	1664	-
578-25B	0.0852	1643	-
580- 2A	0.0846	5705	-
580- 3A	0.0836	5329	-
582-22A	0.0814	7954	4650
582- 4B	0.0812	6430	3500
583- 6A	0.0833	8430	-
583-15A	0.0848	7232	-
594- 2B	0.0810	690	-
594-16B	0.0823	100	-
596-12A	0.0838	1121	-
596-20B	0.0822	5347	-
601- 3A	0.0802	359	-
601-14B	0.0828	61	-
603- 1A	0.0817	1588	-
603-22A	0.0825	528	-
604-18A	0.0843	3558	-
604-21B	0.0817	9590	-
606- 7B	0.0831	4930	-
606-25B	0.0822	9060	-

TABLE 10B

TENSION-COMPRESSION FATIGUE RESULTS OF LAMINATE 1

AT A MAXIMUM STRESS OF 26 ksi

σ_{min} = -16 ksi, f = 10 Hz

(Number of Tests = 20)

Sample ID	Minimum Area, $in.^2$	Cycles to Failure, N_F
580-14A	0.0827	7,204,500 [a]
582-1B	0.0801	3,173,500
582-11B	0.0837	489,800
582-27B	0.0833	2,595,200
594-14A	0.0827	3,533,600
594-17A	0.0823	2,582,000
594-22A	0.0815	3,118,000
594-1B	0.0796	1,598,200
594-12B	0.0811	2,107,000
603-8A	0.0825	7,137,590
604-17A	0.0830	5,963,240
604-3B	0.0813	1,994,110
604-10B	0.0838	1,769,470
606-9A	0.0841	806,000
606-24A	0.0804	2,622,000
606-22B	0.0813	152,390
693-11A	0.0854	6,985,600
693-16B	0.0880	559,030
693-11C	0.0860	4,373,425
693-26C	0.0867	2,076,100

a - Failed due to equipment malfunction

TABLE 11B

TENSION-COMPRESSION FATIGUE RESULTS OF LAMINATE 1

AT A MAXIMUM STRESS OF 42 ksi

σ_{min} = -16 ksi, f = 10 Hz

(Number of Tests = 20)

Sample ID	Minimum Area, $in.^2$	Cycles to Failure, N_F	Cycles to Delamination, N_{DL} (Approximate)
578- 8A	0.0855	35,764	28,000
578-12B	0.0860	7,980	-
580- 3B	0.0846	20,400	-
580- 6B	0.0838	25,121	16,000
582- 9B	0.0824	39,580	-
582-16B	0.0835	23,400	-
583- 9B	0.0839	41,520	37,000
583-14B	0.0858	40,100	39,000
594-23A	0.0805	30,785	28,900
594- 4B	0.0808	20,340	-
596-14A	0.0831	38,600	33,500
596- 8B	0.0815	40,000	27,000
601- 2A	0.0804	21,610	-
601- 1B	0.0796	27,850	-
603-15A	0.0832	18,550	12,500
603- 8B	0.0832	72,935	-
604- 7A	0.0829	23,468	-
604-25A	0.0826	23,100	-
606-22A	0.0814	27,111	-
606-17B	0.0836	56,000	-

TABLE 12B

TENSION-COMPRESSION FATIGUE RESULTS OF LAMINATE 1

AT A MAXIMUM STRESS OF 50 ksi

σ_{min} = -16 ksi, f = 10 Hz

(Number of Tests = 20)

Sample ID	Minimum Area, $in.^2$	Cycles to Failure, N_F	Cycles to Delamination, N_{DL} (Approximate)
578-22A	0.0849	10,906	-
578- 1B	0.0856	142	-
580-12B	0.0828	3,671	-
580-24B	0.0824	5,586	-
582- 5B	0.0817	11,445	2,500
582-10B	0.0828	9,274	-
583- 2A	0.0827	11,960	9,670
583-11B	0.0841	1,650	-
594-11B	0.0817	8,490	4,500
594-19B	0.0825	21,774	7,800
596- 4B	0.0820	14,094	12,000
596-17A	0.0832	19,320	-
601- 9B	0.0829	13,655	12,000
601-10B	0.0830	7,833	-
603- 4B	0.0811	14,720	-
603-19B	0.0834	16,008	-
604- 5B	0.0826	7,002	-
604-24B	0.0808	3,981	4,400
606-15A	0.0847	8,580	-
606-21B	0.0806	700	-

TABLE 13B

TENSION-COMPRESSION FATIGUE RESULTS OF LAMINATE 1

AT A MAXIMUM STRESS OF 58 ksi

σ_{min} = -16 ksi, f = 10 H_z

(Number of Tests = 20)

Sample ID	Minimum Area, $in.^2$	Cycles to Failure, N_F	Cycles to Delamination, N_{DL} (Approximate)
578-21B	0.0843	1,473	-
578-24B	0.0832	3,453	-
580- 7A	0.0817	3,406	-
580-26B	0.0859	1,402	-
582- 1A	0.0790	1,930	-
582-13A	0.0822	330	-
583-21B	0.0824	57	-
583-10A	0.0819	2,685	580
594- 7A	0.0845	3,251	-
594-13A	0.0834	1,167	300
596- 5B	0.0818	1,385	-
596-10A	0.0838	2,356	1,100
601- 7A	0.0817	71	-
601-17A	0.0832	1,010	-
603-11A	0.0828	316	-
603-20A	0.0818	2,186	-
604-11B	0.0835	1,510	-
604-12B	0.0832	5	-
606-18A	0.0844	3,430	-
606-26B	0.0803	1,740	-

TABLE 14B

TENSION-TENSION FATIGUE RESULTS OF LAMINATE 2

AT A MAXIMUM STRESS OF 100 ksi

σ_{min} = 0 ksi, f = 10 Hz

(Number of Tests = 51)

Sample ID	Average Area, $in.^2$	Cycles to Failure, N_F	Sample ID	Average Area, $in.^2$	Cycles to Failure, N_F
696- 5A	0.1286	10^6 NF [a]	727-24A	0.1290	10^6 NF
696-16A	0.1286	10^6 NF	727-26A	0.1255	1.055×10^6 NF
696-23A	0.1279	930,000	727-30A	0.1270	10^6 NF
696-24A	0.1253	10^6 NF	727- 1B	0.1195	10^6 NF
696-29A	0.1291	10^6 NF	727- 7B	0.1195	10^6 NF
696- 2B	0.1239	10^6 NF	727-15B	0.1274	10^6 NF
696-20B	0.1262	10^6 NF	727-16B	0.1275	10^6 NF
696-31B	0.1282	495,040	727- 1C	0.1188	1
696-35B	0.1270	10^6 NF	727- 9C	0.1284	10^6 NF
696-11C	0.1256	10^6 NF	727-11C	0.1270	1.358×10^6 NF
696-28C	0.1276	10^6 NF	727-23C	0.1285	10^6 NF
696-29C	0.1264	10^6 NF	727-25C	0.1260	910
696-34C	0.1280	10^6 NF	727-33C	0.1276	10^6 NF
699- 1A	0.1201	10^6 NF	728- 6A	0.1287	826, 940
699-21A	0.1266	10^6 NF	728-37A	0.1300	10^6 NF
699-29A	0.1284	2,000	728- 2B	0.1236	10^6 NF
699-33A	0.1296	10^6 NF	728- 6B	0.1290	10^6 NF
699-34A	0.1302	10^6 NF	728- 7B	0.1304	1.47×10^6 NF
699- 1B	0.1176	1	728-26B	0.1288	1.212×10^6 NF
699-22B	0.1318	10^6 NF	728-27B	0.1271	10^6 NF
699-30B	0.1235	10^6 NF	728-34B	0.1300	10^6 NF
699-37B	0.1266	10^6 NF	728- 9C	0.1306	10^6 NF
699- 1C	0.1171	10^6 NF	728-27C	0.1265	1880
699-10C	0.1295	10^6 NF	728-31C	0.1282	10^6 NF
699-21C	0.1307	10^6 NF	728-33C	0.1302	10^6 NF
699-28C	0.1269	1			

a - NF indicates No Failure

TABLE 15B

TENSION - TENSION FATIGUE RESULTS OF LAMINATE 2

AT A MAXIMUM STRESS OF 112 ksi

σ_{min} = 0 ksi, f = 10 Hz

(NUMBER OF TESTS = 20)

Sample ID	Average Area, $in.^2$	Cycles to Failure, N_F
696-34A	0.1270	164,980
696-5B	0.1275	2,350
696-6B	0.1286	268,060
696-13C	0.1261	10^6 NF[a]
696-23C	0.1281	599,330
699-3A	0.1276	1.036×10^6 NF
699-15A	0.1135	10^6 NF
699-28A	0.1270	10^6 NF
699-11C	0.1285	25,000
699-20C	0.1255	10^6 NF
727-5A	0.1273	1.1×10^6 NF
727-19A	0.1283	910
727-17B	0.1287	10^6 NF
727-31C	0.1269	10^6 NF
727-36C	0.1255	390
728-31A	0.1285	17,191
728-19B	0.1294	1
728-10C	0.1299	574,260
728-17C	0.1320	1.065×10^6 NF
728-26C	0.1263	10^6 NF

a - NF indicates No Failure

TABLE 16B

TENSION-COMPRESSION FATIGUE RESULTS OF LAMINATE 2

AT A MAXIMUM STRESS OF 70 ksi

σ_{min} = -30 ksi, f = 10 Hz

(Number of Tests = 48)

Sample ID	Average Area, $in.^2$	Cycles to Failure, N_F	Sample ID	Average Area, $in.^2$	Cycles to Failure, N_F
696-19A	0.1279	10^6 NF[a]	727-6A	0.1270	10^6 NF
696-22A	0.1286	10^6 NF	727-21A	0.1295	10^6 NF
696-27A	0.1264	10^6 NF	727-4B	0.1258	1.198×10^6 NF
696-30A	0.1292	10^6 NF	727-22B	0.1291	10^6 NF
696-33A	0.1269	10^6 NF	727-35B	0.1268	696,420
696-1B	0.1146	10^6 NF	717-5C	0.1282	10^6 NF
696-7B	0.1285	10^6 NF	727-14C	0.1257	10^6 NF
696-8B	0.1279	10^6 NF	727-16C	0.1282	504,510
696-16B	0.1286	10^6 NF	727-17C	0.1270	10^6 NF
696-18C	0.1295	10^6 NF	727-26C	0.1243	10^6 NF
699-31A	0.1283	10^6 NF	727-28C	0.1264	10^6 NF
699-32A	0.1304	10^6 NF	727-34C	0.1289	10^6 NF
699-37A	0.1304	10^6 NF	728-1A	0.1150	10^6 NF
699-7B	0.1290	10^6 NF	728-10A	0.1300	10^6 NF
699-13B	0.1268	10^6 NF	728-20A	0.1312	53,090
699-14B	0.1258	10^6 NF	728-24A	0.1301	380,800
699-18B	0.1280	10^6 NF	728-28A	0.1268	10^6 NF
699-33B	0.1288	10^6 NF	728-34A	0.1292	10^6 NF
699-24C	0.1299	10^6 NF	728-1B	0.1177	10^6 NF
699-26C	0.1269	10^6 NF	728-22B	0.1320	10^6 NF
699-32C	0.1292	10^6 NF	728-25B	0.1284	10^6 NF
699-35C	0.1299	10^6 NF	728-29B	0.1300	10^6 NF
727-3A	0.1255	1.044×10^6 NF	728-37B	0.1258	1.120×10^6 NF
727-4A	0.1259	10^6 NF	728-23C	0.1317	10^6 NF

a - NF indicates No Failure

APPENDIX C

This appendix lists all of the results of the static residual strength tests conducted during this research investigation.

Preceding Page BLANK - FIL

TABLE 1C

RESIDUAL TENSION STRENGTH
TEST RESULTS OF LAMINATE 1 COUPONS
FATIGUE TESTED AT 0 to 42 ksi

Coupons fatigue tested to 364,000 cycles equal to a probability of survival, P_s, of 0.9. (Number of coupons static tested = 20)

Sample ID	Min. Area, $in.^2$	Ultimate Load, P_{ult}, lbs.	Ultimate Stress, σ_{ult}, ksi	Ultimate Strain, ε_{ult}, in 2.0 in.	Apparent Initial Modulus, E_a, psi X 10^6
578- 6A	0.0821	5970	72.4	0.0097	7.61
-26B	0.0849	5140	60.5	0.0090	6.93
580-20B	0.0826	5680	68.8	0.0100	7.12
-21B	0.0809	5630	69.6	0.0098	6.87
582-21A	0.0813	4830	59.4	-	7.03
- 6B	0.0821	5240	63.8	0.0096	6.41
583-21A	0.0821	5840	71.1	0.0091	6.41
-10B	0.0836	5770	69.0	0.0102	6.64
594-10A	0.0834	4850	58.2	0.0081	7.04
-16A	0.0826	Coupon failed at 51,792 cycles			
- 9B	0.0815	5050	62.0	0.0088	6.82
595-15A	0.0838	4900	58.5	0.0084	7.02
-22A	0.0813	5520	67.9	0.0092	7.45
601-23A	0.0810	4310	53.2	0.0079	6.86
- 3B	0.0824	Coupon failed at 245,030 cycles			
-16B	0.0821	5350	65.2	0.0091	7.16
603- 9A	0.0823	4900	59.5	0.0088	6.40
-22B	0.0822	4040	49.2	0.0074	6.76
604-20A	0.0838	4910	58.6	0.0090	6.63
-13A	0.0838	5200	62.0	-	6.63
606- 8B	0.0842	4900	58.2	0.0093	6.60
-14B	0.0835	5070	60.7	0.0091	6.47
Average			62.4	0.0090	6.84
			+10.0	+0.0012	+0.77
			-13.2	-0.0016	-0.43

TABLE 2C

RESIDUAL TENSION STRENGTH
TEST RESULTS OF LAMINATE 1 COUPONS
FATIGUE TESTED AT 0 TO 50 ksi

Coupons fatigue tested to 31,400 cycles equal to a probability of survival, P_s, of 0.9. (Number of coupons Static Tested = 20.)

Sample ID	Min. Area, $in.^2$	Ultimate Load, P_{ult}, lbs.	Ultimate Stress, σ_{ult}, ksi	Ultimate Strain, ε_{ult}, in./in. in 2.0 in.	Apparent Initial Modulus, E_a, psi X 10^6
578- 7A	0.0836	5640	67.5	0.0092	7.04
- 3B	0.0839	4580	54.6	0.0079	6.81
580 8A	0.0829	5700	68.8	-	6.70
-12A	0.0815	Coupon failed at 21,600 cycles			
- 9B	0.0833	5360	64.4	0.0102	7.06
582-23A	0.0820	5880	71.7	0.0099	7.17
-21B	0.0815	5380	66.0	0.0092	7.22
583- 3A	0.0821	5740	69.9	0.0105	6.77
-16A	0.0837	5800	69.3	0.0098	7.03
594- 9A	0.0817	5410	66.2	0.0091	7.16
-15B	0.0822	4740	57.7	0.0087	6.63
596-11A	0.0832	5360	64.4	0.0093	7.07
-16B	0.0840	5090	60.6	0.0079	7.68
601- 4A	0.0804	5780	71.4	0.0099	7.32
-13B	0.0830	6030	72.6	0.0102	7.09
603.23A	0.0817	4820	59.0	0.0092	6.80
- 3B	0.0808	4830	59.8	0.0094	6.51
604- 2B	0.0833	4820	57.9	0.0084	6.86
-17B	0.0833	5580	67.0	0.0096	7.06
606- 6B	0.0824	5910	71.7	0.0099	7.14
-18B	0.0835	5140	61.6	0.0088	7.04
Average			65.1	0.0093	7.01
			+ 7.5	+0.0012	+0.31
			-10.5	-0.0014	-0.38

TABLE 3C

RESIDUAL TENSION STRENGTH
TEST RESULTS OF LAMINATE 1 COUPONS
FATIGUE TESTED AT -16 TO 42 ksi

Coupons fatigue tested to 14,400 cycles equal to a probability of survival, P_s, of 0.9. (Number of coupons Static Tested = 20.)

Sample ID	Min. Area, $in.^2$	Ultimate Load, P_{ult}, lbs.	Ultimate Stress, σ_{ult}, ksi	Ultimate Strain, ε_{ult}, in./in. in 2.0 in.	Apparent Initial Modulus, E_a, psi X 10^6
578- 6B	0.0838	5830	69.6	0.0097	7.23
-11B	0.0850	5600	65.9	0.0100	6.92
-15B	0.0862	Coupon failed at 1,220 cycles			
580-20A	0.0826	5950	72.0	0.0102	7.12
-25B	0.0813	5320	65.4	0.0092	7.24
582- 5A	0.0819	6440	78.6	0.0107	7.51
-17B	0.0839	5780	68.9	0.0094	7.22
583- 5B	0.0848	5960	70.3	0.0097	6.21
-15B	0.0825	5980	72.5	0.0101	7.13
594-20A	0.0821	5860	71.4	0.0100	7.16
-13B	0.0830	5300	63.9	0.0093	7.13
596- 6B	0.0811	4900	60.4	0.0083	7.71
- 7B	0.0812	5440	67.0	0.0093	7.21
601- 5B	0.0819	5430	66.3	0.0088	7.63
- 9A	0.0832	5600	67.3	0.0094	7.07
603-17A	0.0831	5280	63.5	0.0093	7.08
-19A	0.0821	5780	70.4	-	7.16
604-15B	0.0843	5460	64.8	0.0095	6.78
- 3A	0.0809	Coupon failed at 12,289 cycles			
-16A	0.0823	5120	62.2	0.0092	7.15
606-17A	0.0848	5000	59.0	0.0077	7.37
-11B	0.0850	5540	65.2	0.0090	7.35
Average			67.2	0.0094	7.17
			+11.4	+0.0013	+0.54
			- 8.2	-0.0017	-0.96

TABLE 4C

RESIDUAL TENSION STRENGTH

TEST RESULTS OF LAMINATE 1 COUPONS
FATIGUE TESTED AT -16 TO 50 ksi

Coupons fatigue tested to 2,150 cycles equal to a probability of survival, P_s, of 0.90. (Number of coupons Static Tested = 20.)

Sample ID	Min. Area, $in.^2$	Ultimate Load, P_{ult}, lbs.	Ultimate Stress, σ_{ult}, ksi	Ultimate Strain, ε_{ult}, in./in. in 2.0 in.	Apparent Initial Modulus, E_a, psi X 10^6
578- 1A	0.0835	5880	70.4	0.0088	7.21
-19A	0.0821	5900	71.9	0.0101	7.16
580-17B	0.0834	5860	70.3	0.0097	7.05
-17A	0.0824	5840	70.9	0.0092	7.58
582- 7B	0.0824	5560	67.5	0.0097	7.14
-24B	0.0805	5490	68.2	0.0093	7.10
583-11A	0.0822	4960	60.3	-	7.16
-24A	0.0802	5120	63.8	0.0094	6.93
594-18A	0.0820	5300	64.6	0.0106	6.42
-17B	0.0825	5900	71.5	0.0107	6.73
596-25A	0.0807	5160	63.9	0.0095	6.70
-24A	0.0825	5520	66.9	0.0095	7.13
601- 2B	0.0819	6000	73.3	0.0099	7.40
- 4B	0.0817	5790	70.9	0.0093	7.65
-15B	0.0824	Coupon failed at 940 cycles			
603-12A	0.0830	5520	66.5	0.0097	7.09
-17B	0.0843	5880	69.8	0.0097	6.98
604- 2A	0.0819	5280	64.5	0.0088	7.63
-21A	0.0819	5560	67.9	0.0094	6.98
606- 7A	0.0816	5890	72.2	0.0103	7.21
-13B	0.0844	4920	58.3	0.0084	7.40
Average			67.7	0.0095	7.13
			+ 5.6	+0.0012	+0.50
			- 9.4	-0.0011	-0.71

TABLE 5C

RESIDUAL COMPRESSION STRENGTH TEST RESULTS OF
LAMINATE 1 COUPONS FATIGUE TESTED AT 0 TO 42 ksi

Coupons fatigue tested to 364,000 cycles equal to a probability of survival, P_s, of 0.90. (Number of coupons Static Tested = 20.)

Sample ID	Min. Area, $in.^2$	Ultimate Load, P_{ult}, lbs.	Ultimate Stress, σ_{ult}, ksi	Ultimate Strain, ε_{ult}, in./in. in 2.0 in.	Apparent Initial Modulus E_a, psi x 10^6	Amt. of Strain at Peak Load, ϵ, in./in. in 2.0 in.
578-26A	0.0852	5310	62.3	0.0108	6.34	0.0006
-22B	0.0831	5620	67.6	0.0129	6.68	0.003
580-11A	0.0821	3400	41.4	0.0069	6.25	-[a]
- 5B	0.0820	3870	47.2	0.0091	6.25	0.0027
582- 7A	0.0822	4280	52.1	0.0090	6.08	0.00045
-15B	0.0836	4440	53.1	0.0101	6.64	0.0021
583- 1A	0.0838	4680	55.8	0.0096	6.63	0.0006
-12A	0.0833	Coupon failed at 99,400 cycles				
-14A	0.0854	3620	43.4	0.0079	5.85	0.0009
594-24B	0.0794	4830	60.8	0.0105	5.60	-
-26B	0.0804	4240	52.7	0.0086	5.92	-
595-10B	0.0838	5020	59.9	0.0093	7.23	-
-22B	0.0823	5870	71.3	0.0120	5.93	0.00045
601-16A	0.0831	4290	51.6	0.0093	6.17	0.0019
- 8A	0.0825	Coupon failed at 238,061 cycles				
-20A	0.0828	5440	65.7	0.0113	6.36	0.0006
-12B	0.0816	Coupon failed at 118,000 cycles				
603- 2A	0.0825	4920	59.6	0.0102	6.22	0.0006
-24A	0.0804	5230	65.0	0.0109	6.91	0.0009
604-10A	0.0844	5630	66.7	0.0109	6.67	0.0006
-18B	0.0833	4410	52.9	0.0078	6.67	0.0005
606- 4A	0.0809	5530	68.4	0.0114	6.34	0.0012
-26A	0.0813	3800	46.7	0.0077	6.65	0.0006
Average			57.2	0.0098	6.37	
			+14.1	+0.0031	+0.86	
			-10.5	-0.0029	-0.77	

a - A dash (-) indicates no strain at peak load, sharp brittle fracture

TABLE 6C

RESIDUAL COMPRESSION STRENGTH TEST RESULTS OF
LAMINATE 1 COUPONS FATIGUE TESTED AT 0 TO 50 ksi

Coupons fatigue tested to 31,400 cycles equal to a probability of survival, P_s, of 0.90 (Number of coupons Static Tested = 20.)

Sample ID	Min. Area, $in.^2$	Ultimate Load, P_{ult}, lbs.	Ultimate Stress, σ_{ult}, ksi	Ultimate Strain, ϵ_{ult}, in./in. in 2.0 in.	Apparent Initial Modulus E_a, psi x 10^6	Amt. of Strain at Peak Load, ϵ, in./in. in 2.0 in.
578- 5A	0.0836	6010	71.9	0.0123	6.65	-[a]
- 2B	0.0838	Coupon failed at 14,200 cycles				
-14B	0.0817	5580	68.3	0.0119	6.44	0.0006
580- 4A	0.0830	5240	63.1	0.0097	7.09	-
- 8B	0.0835	5620	67.3	√[b]	6.30	√
582-14A	0.0835	5630	67.4	0.0112	6.65	0.00045
-19A	0.0835	5130	61.4	√	√	√
583- 8B	0.0835	5640	67.5	0.0108	6.14	-
-20B	0.0831	5310	63.9	0.0107	6.50	-
594- 5A	0.0812	5600	69.8	0.0116	6.32	0.0006
- 8A	0.0828	5330	64.4	0.0117	6.53	-
595-17B	0.0832	5280	63.5	0.0103	6.68	-
-21B	0.0817	5080	62.2	0.0097	6.80	-
601- 5A	0.0828	4270	51.6	0.0072	8.05	0.0006
-17B	0.0827	5810	70.2	0.0109	6.72	0.0006
603- 3A	0.0810	Coupon failed at 28,800 cycles				
-16B	0.0828	Coupon failed at 5,350 cycles				
-23B	0.0809	5510	68.1	0.0110	6.68	-
-24B	0.0810	4720	58.3	√	6.86	√
604- 7B	0.0833	5350	64.2	0.0108	6.49	-
-14B	0.0847	5000	59.0	0.0108	6.56	-
606-10A	0.0840	4650	55.4	0.0093	6.44	-
- 1B	0.0815	4540	55.7	0.0093	6.29	-
Average			63.7	0.0111	6.64	
			+ 8.2	+0.0012	+1.41	
			-12.1	-0.0039	-0.50	

a - A dash (-) indicates no strain at peak load, sharp brittle fracture.
b - A check (√) indicates not properly recorded by the measuring apparatus.

TABLE 7C

RESIDUAL COMPRESSION STRENGTH TEST RESULTS OF
LAMINATE 1 COUPONS FATIGUE TESTED AT -16 TO 42 ksi

Coupons fatigue tested to 14,400 cycles equal to a probability of survival, P_s, of 0.90. (Number of coupons Static Tested = 20.)

Sample ID	Min. Area, $in.^2$	Ultimate Load, P_{ult}, lbs.	Ultimate Stress, σ_{ult}, ksi	Ultimate Strain, ϵ_{ult}, in./in. in 2.0 in.	Apparent Initial Modulus F_a, psi x 10^6	Amt. of Strain at Peak Load, ϵ, in./in. in 2.0 in.
578-14A	0.0866	4960	57.3	0.0103	5.92	- [a]
- 7B	0.0833	5740	68.9	0.0117	6.67	0.0006
- 9B	0.0861	Coupon failed at 9,550 cycles				
580-14B	0.0842	5400	64.1	0.0102	6.99	0.0010
- 7B	0.0822	6260	76.2	√ [b]	6.58	-
582- 6A	0.0807	5520	68.4	0.0105	6.88	0.0006
-11A	0.0823	5770	70.1	0.0118	6.75	0.0004
583-17B	0.0841	5500	65.4	0.0109	6.61	0.0008
-19B	0.0836	6340	75.8	0.0130	6.64	0.0009
594-19A	0.0826	5860	70.9	0.0119	6.72	0.0006
- 8B	0.0816	5070	62.1	0.0103	6.62	0.0008
595- 2B	0.0818	5060	61.9	0.0111	6.79	0.0012
-13B	0.0835	5240	62.8	0.0099	6.65	0.0003
601-14A	0.0836	5970	71.4	0.0118	6.64	0.00045
-15A	0.0829	5300	63.9	0.0102	6.52	-
603-26A	0.0819	5510	67.3	0.0111	6.78	0.0006
-10B	0.0843	5400	64.1	0.0104	6.98	-
604-15A	0.0812	Coupon failed at 11,800 cycles				
- 4B	0.0808	5100	63.1	0.0096	6.88	0.0004
- 9B	0.0839	4980	59.4	√	√	√
606-16A	0.0847	4450	52.5	0.0084	6.56	0.0006
- 4B	0.0814	4940	59.5	0.0111	6.30	0.0009
Average			65.2	0.0108	6.66	
			+11.0	+0.0022	+0.32	
			-12.7	-0.0024	-0.74	

a - A dash (-) indicates no strain at peak load, sharp brittle fracture.

b - A check (√) indicates not properly recorded by the measuring apparatus.

TABLE 8C

RESIDUAL COMPRESSION STRENGTH TEST RESULTS OF
LAMINATE 1 COUPONS FATIGUE TESTED AT -16 TO 50 ksi

Coupons fatigue tested to 2,150 cycles equal to a probability of survival, P_s, of 0.9. (Number of coupons Static Tested = 20.)

Sample ID	Min. Area, $in.^2$	Ultimate Load, P_{ult}, lbs.	Ultimate Stress, σ_{ult}, ksi	Ultimate Strain, ϵ_{ult}, in./in. in 2.0 in.	Apparent Initial Modulus E_a, psi x 10^6	Amt. of Strain at Peak Load, ϵ, in./in. in 2.0 in.
578-12A	0.0849	4880	57.5	0.0102	6.19	0.0003
- 4B	0.0840	5560	66.2	0.0114	6.61	0.00075
580-13A	0.0842	6660	79.1	0.0125	6.60	0.0005
- 1B	0.0864	5200	60.2	0.0094	6.43	- [a]
582-26A	0.0826	5860	70.9	0.0116	6.73	0.00045
-22B	0.0813	5700	70.1	0.0113	6.65	-
583-22A	0.0823	5630	68.4	0.0114	6.75	0.00045
- 4B	0.0821	5990	73.0	0.0112	5.80	0.0006
594- 5B	0.0798	5610	70.3	0.0108	7.37	-
-18B	0.0821	5700	69.4	0.0108	6.41	-
596- 8A	0.0821	5830	71.0	0.0116	6.96	0.0005
-18B	0.0835	5330	63.8	0.0102	6.65	-
601-22A	0.0820	5730	69.9	0.0102	7.17	-
-25B	0.0804	5850	72.8	0.0116	6.91	0.0005
603- 1B	0.0823	5800	70.5	√ [b]	√	-
- 6B	0.0801	6020	75.2	0.0114	6.94	0.0003
604- 8A	0.0833	5500	66.0	0.0109	6.67	0.0006
- 1B	0.0823	4650	56.5	0.0087	6.75	0.0006
606-11A	0.0844	5800	68.7	0.0117	6.58	0.0006
- 5B	0.0819	5900	72.0	0.0117	6.43	0.0006
Average			68.6	0.0110	6.66	
			+10.5	+0.0015	+0.71	
			-12.1	-0.0023	-0.86	

a - A dash (-) indicates no strain at peak load, sharp brittle fracture

b - A check (√) indicates not properly recorded by the measuring apparatus.

TABLE 9C

RESIDUAL TENSION STRENGTH TEST RESULTS OF LAMINATE 2 COUPONS
FATIGUE TESTED AT 0 TO 100 ksi

(Number of coupons Static Tested = 20)

Sample ID	Average Area, $in.^2$	Ultimate Load, P_{ult}, lbs	Ultimate Stress, σ_{ult}, ksi	Ultimate Strain, ϵ_{ult}, in./in. in 2.0 in.	Apparent Modulus of Elasticity, E_a, psi $x10^6$	Amt. of Strain at Ultimate Load, ϵ, in./in. in 2.0 in.
696- 5A	.1236	18050	140.4	.0090	15.6	.0004
696-24A	.1253	15150	120.9	.0080	15.1	.0005
696-29A	.1291	18150	140.6	.0092	15.3	.0005
696- 2B	.1239	16650	134.4	.0084	16.0	.0004
696-29C	.1264	19000	150.3	.0088	17.1	.0005
699- 1A	.1201	18550	154.5	.0096	16.1	.0005
699-34A	.1302	19900	152.8	.0093	16.4	-[a]
699-22B	.1318	19650	149.1	.0096	15.5	-
699-30B	.1235	17200	139.3	.0084	16.6	-
699- 1C	.1171	16900	144.3	.0091	15.8	.0005
727-24A	.1290	18050	139.9	.0094	14.9	-
727-26A	.1255	16000	127.5	.0089	14.3	.0005
727- 7B	.1270	19000	149.6	.0097	15.4	.0005
727-16B	.1275	20300	159.2	.0102	15.6	0[b]
727-11C	.1270	17300	136.2	.0091	15.0	.0005
728-37A	.1300	18000	138.5	.0093	14.9	-
728- 2B	.1236	18250	147.7	.0096	15.4	-
728- 7B	.1304	18550	142.2	.0087	16.3	-
728-26B	.1288	19700	153.0	.0093	16.5	-
728- 9C	.1306	19600	150.1	.0097	15.5	-
Average			143.5 +15.7 -22.6	.0092 +.0010 -.0012	15.7 +1.4 -1.4	

a - A dash (-) indicates that the strain at ultimate load was not recorded.

b - A zero (0) indicates that no strain at ultimate load was observed.

TABLE 10C

RESIDUAL TENSION STRENGTH TEST RESULTS OF LAMINATE 2 COUPONS
FATIGUE TESTED AT -30 TO + 70 ksi
(Number of coupons Static Tested = 20)

Sample ID	Average Area, $in.^2$	Ultimate Load P_{ult}, lbs	Ultimate Stress, σ_{ult}, ksi	Ultimate Strain, ϵ_{ult}, in./in. in 2.0 in.	Apparent Modulus of Elasticity, E_a, psi x 10^6	Amt. of Strain at Ultimate Load, ϵ, in./in. in 2.0 in.
696-22A	.1286	16700	129.9	.0092	14.1	.0005
696-27A	.1264	17250	136.5	.0085	16.1	.0005
696-33A	.1269	18100	142.6	.0086	16.6	.0003
696- 8B	.1279	18700	146.2	.0103	14.3	0 [a]
696-20B	.1262	18750	148.6	.0096	15.5	.0005
699- 7B	.1290	19700	152.7	.0098	15.6	.0005
699-14B	.1258	18600	147.8	.0106	13.9	0
699-24C	.1299	18400	141.6	.0094	15.1	.0004
699-26C	.1269	18550	146.2	.0093	15.7	.0004
727- 3A	.1255	18000	143.4	.0094	15.3	.0005
727- 6A	.1270	18300	144.1	.0093	15.5	.0003
727-4B	.1258	17200	136.7	.0085	16.1	.0004
727- 5C	.1282	19600	152.9	.0099	15.4	.0004
727-28C	.1264	16600	131.3	.0087	15.1	.0005
728-10A	.1302	20100	154.6	.0104	14.9	0
728-34A	.1292	18450	142.8	.0090	15.9	.0004
728- 1B	.1177	18300	155.5	.0097	16.0	.0004
728-22B	.1320	18700	141.7	.0095	14.9	.0005
728-37B	.1258	17000	135.1	.0091	14.8	.0002
Average			143.7 +11.8 -13.8	.0094 +.0012 -.0009	15.3 +1.3 -1.4	

a - A zero (0) indicates that no strain at ultimate load was observed.

TABLE 11C

RESIDUAL COMPRESSION STRENGTH TEST RESULTS OF LAMINATE 2 COUPONS FATIGUE TESTED AT 0 TO 100 ksi

(Number of coupons Static Tested = 20)

Sample ID	Average Area, $in.^2$	Ultimate Load, P_{ult}, lbs.	Ultimate Stress, σ_{ult}, ksi	Ultimate Strain, ϵ_{ult}, in./in. in 2.0 in.	Apparent Modulus of Elasticity, E_a, psi x 10^6	Amt. of Strain at Ultimate Load, ϵ, in./in. in 2.0 in.	Secant Modulus at 70 ksi, E_{sec}, psi x 10^6
696-35B	.1270	12050	94.9	.0072	13.1	.0008	13.72
11C	.1256	10700	85.2	.0062	13.5	0[b]	13.86
28C	.1276	14800	116.0	.0093	11.9	.0008	13.21
34C	.1280	11000	85.9	.0066	12.6	.0014	13.46
699-21A	.1266	13200	104.3	.0080	12.9	.0006	13.73
33A	.1296	13550	104.6	.0087	12.2	0	12.96
37B	.1266	12500	98.7	.0078	12.4	.0003	13.21
10C	.1295	12700	98.1	.0077	12.5	.0011	13.46
21C	.1307	10150	77.7	.0057	13.3	0	13.08
727-30A	.1270	11250	88.6	-[a]	-	-	-
1B	.1195	11200	93.7	.0061	14.2	.0009	15.20
9C	.1284	13150	102.4	.0081	12.1	.0011	13.46
15B	.1274	13500	106.0	.0084	12.4	.0007	13.59
33C	.1276	11800	92.5	.0081	13.2	.0010	12.50
728- 6B	.1290	12850	99.6	.0078	12.5	.0009	13.46
27B	.1271	10800	85.0	.0067	11.8	.0003	12.50
34B	.1300	13550	104.2	.0083	12.6	0	13.86
31C	.1282	16125	125.8	.0101	11.9	.0007	13.21
33C	.1302	16250	124.8	.0099	12.4	0	13.73
		Average	99.3 +26.5 -21.6	.0078 +.0023 -.0021	12.7 + 1.5 - 0.9		13.46 + 0.40 - 0.96

a - A dash (-) indicates this value was not recorded.

b - A zero (0) indicates that no strain at ultimate load was observed.

TABLE 12C

RESIDUAL COMPRESSION STRENGTH TEST RESULTS OF LAMINATE 2 COUPONS FATIGUE TESTED AT -30 TO +70 ksi

(Number of coupons Static Tested = 20)

Sample ID	Average Area, $in.^2$	Ultimate Load, P_{ult}, lbs	Ultimate Stress, σ_{ult}, ksi	Ultimate Strain, ϵ_{ult}, in./in. in 2.0 in.	Apparent Modulus of Elasticity, E_a, psi x 10^6	Amt. of Strain at Ultimate Load, ϵ, in./in. in 2.0 in.	Secant Modulus at 70 ksi, E_{sec}, psi x 10^6
696-19A	.1279	15400	121.3	.0094	12.8	.0008	13.86
30A	.1292	12900	99.8	.0084	12.7	.0010	13.73
1B	.1146	10550	92.1	.0070	13.2	-	13.73
16B	.1286	13250	103.0	.0081	12.2	.0008	13.59
18C	.1295	13400	103.5	- [a]	13.8	-	12.96
699-31A	.1283	16600	129.4	.0109	11.6	.0008	13.33
37A	.1204	12250	101.7	.0078	12.9	.0009	13.86
18B	.1280	12050	94.1	.0071	12.9	0 [b]	13.73
33B	.1288	11950	92.8	.0072	13.0	.0009	13.86
35C	.1299	11250	86.6	.0066	12.7	.0011	13.59
727- 4A	.1259	13100	104.0	.0088	12.1	.0015	13.59
21A	.1295	11500	88.8	.0066	12.9	.0012	13.46
22B	.1291	10400	80.6	.0061	13.2	.0010	13.46
26C	.1243	10950	88.1	.0066	12.7	.0010	13.21
34C	.1289	10620	85.9	-	-	-	-
728-28A	.1268	11650	91.9	.0076	12.0	.0008	12.84
25B	.1284	10600	82.6	.0077	11.2	.0011	-
29B	.1300	16750	128.8	.0106	11.9	.0007	14.00
23C	.1317	13550	102.9	.0081	12.9	0	13.73
Average			98.8 +30.0 -18.2	.0079 +.0030 -.0018	12.6 + 1.2 - 1.4		13.56 +0.44 -0.72

a - A dash (-) indicates this value was not recorded.

b - A zero (0) indicates that no strain at ultimate load was observed.

TABLE 13C

COMPRESSION STRENGTH TEST RESULTS OF LAMINATE 2 COUPONS TESTED IN OCT, 1976

(No Prior Fatigue) (Number of coupons Static Tested = 20)

Sample ID	Average Area, $in.^2$	Ultimate Load, P_{ult}, lbs	Ultimate Stress, σ_{ult}, ksi	Ultimate Strain, ϵ_{ult}, in./in. in 2.0 in.	Apparent Modulus of Elasticity, E_a, psi x 10^6	Amt. of Strain at Ultimate Load, ϵ, in./in. in 2.0 in.	Secant Modulus at 70 ksi, E_{sec}, psi x 10^6
696- 4A	.1298	12900	99.4	.0077	12.4	.0005	13.21
17B	.1287	14000	108.8	.0087	12.4	.0006	13.21
21B	.1282	14000	109.2	.0087	12.4	0[b]	13.08
15C	.1296	15250	117.7	.0093	12.8	.0011	13.72
30C	.1289	15300	118.7	.0093	12.6	.0005	13.72
699- 6A	.1295	14100	108.9	.0092	11.8	.0009	12.73
11A	.1300	15750	121.2	.0099	11.9	.0008	13.70
20A	.1318	15150	114.9	.0099	11.4	-	12.96
28B	.1293	15500	119.9	.0101	12.2	.0008	13.46
6C	.1293	15150	117.2	.0099	11.7	.0011	12.84
727-16A	.1284	14200	110.6	.0087	12.4	0	13.21
14B	.1256	15000	119.4	.0102	11.3	.0008	12.61
31B	.1290	15500	120.2	.0099	11.7	.0007	13.26
2C	.1239	13600	109.8	.0085	12.8	.0007	14.00
29C	.1287	15000	116.6	.0099	12.2	.0010	13.72
728-22A	.1323	15200	114.9	.0099	11.5	.0006	12.96
25A	.1285	14950	116.3	-[a]	11.6	-	12.73
8B	.1312	15150	115.5	.0099	12.0	.0010	12.73
7C	.1317	12850	97.6	.0077	12.5	.0011	12.96
8C	.1303	14600	112.0	.0090	12.2	.0008	13.46
Average			113.4	.0093	12.1		13.21
			+ 15.2	+.0014	+ 0.7		+ 0.79
			- 10.0	-.0011	- 0.8		- 0.48

a - A dash indicates this value was not recorded

b - A zero indicates that no strain at ultimate load was observed

REFERENCES

1. Kaminski, B. E., "Narmco 5208/T300: A Graphite-Epoxy System Engineered for High-Performance Aircraft Structures," 5th National SAMPE Technical Conference, October, 1973.

2. Doner, Douglas R., and Novak, R. C., "Structural Behavior of Laminated Graphite Filament Composites," Proceedings of the Society of the Plastics Industry 24th Annual Technical Conference, February, 1969.

3. Sattar, S. A., and Kellog, D. H., "The Effect of Geometry on the Mode of Failure of Composites in the Short Beam Shear Test," Composite Materials: Testing and Deisgn, ASTM STP 460, American Society for Testing and Materials, 1969.

4. Pagano, N. J., and Pipes, R. Byron, "Some Observations on the Interlaminar Strength of Composite Laminates," Int. J. Mech. Sci., Vol. 15, 1973.

5. Lakman, L. M., et al, "Advanced Composites Data for Aircraft Structural Design, Vol. IV: Material and Basic Allowable Development-Graphite/ Epoxy," AFML TR 70-58, September, 1972.

6. Pagano, N. J., and Pipes, R. B., "Some Observations on the Interlaminar Strength of Composite Laminates," Int. J. Mech. Sci., Volume 15, 1973.

7. Spiegel, M. R., Theory and Problems of Statistics, Schaum's Outline Series, McGraw-Hill, 1961.

8. Gumbel, E. J., Statistics of Extremes, Columbia University Press, New York, 1958.

9. Bowie, G. E., Pettit, D. E., Ryder, J. T., and Krupp, W. E., "NDI Life Analysis Interface," Lockheed-California Company Report LR 27013, September,1974.

10. Advanced Composites Design Guide, Vol. IV, Test Methods Sec. 4.2, prepared by Rockwell International Corporation for the United States Air Force, January 1973, pp. 3-6.

11. " Test Methods - High Modulus, High Strength Graphite Materials and Assemblies," Specification IT-50, Revision B, Code Ident. No. 76823, Northrop Corporation, Aircraft Division, May 22, 1972.

12. "Material Specification, Cloth, Graphite Yarn, Epoxy Resin Impregnated, Fleet Ballistic Missile," Code Ident. 10001, prepared by Lockheed Missiles and Space Company, Inc. for Department of the Navy, Strategic Systems Project Office, Washington, D. C., April 5, 1974.

13. "Hercules Incorporated Graphite Composite Testing Procedures," HD-SG-2-6002B, Hercules Incorporated, Bacchus Works, Magna, Utah, January, 1975, pp. 14-16.

14. "Material Specification - Graphite Fiber Tape and Sheet, Epoxy Resin Impregnated," 207-8-410A, Vought Systems Division, LTV Aerospace Corporation, Dallas, Texas, June 3, 1974.

15. "Specification for Advanced Composite Material - Multiply Graphite/Epoxy Prepreg Broodgoods," LB0130-XXX, Code Ident. No. 43999, Rockwell International Corporation, B-1 Division, February 3, 1976.

16. "General Specification for Graphite Fiber Non-Woven Tape and Sheet, Resin Impregnated," C-22-1379, Lockheed-California Company, Burbank, California, November 12, 1975.

17. "Standard Method of Test for Compressive Properties of Oriented Fiber Composites," American Society for Testing and Materials, Designation: D3410-75.

18. "Standard Method of Test for Compressive Properties of Rigid Plastics," American Society for Testing and Materials, Designation: D695-69.

19. Halpin, J. C., Jerina, K. L., and Johnson, T. A., "Characterization of Composites for the Purpose of Reliability Evaluation," AFML, Technical Report No. AFML-TR-73-289, December, 1972.

20. Valluri, S. R., "Unified Engineering Theory of High Stress Level Fatigue," Aerospace Engineering, Vol. 20, No. 20, October, 1961.

21. Halpin, J. C., and Jerina, K. L., "Statistical Stress Concentration Effects in Composites," presented at UCLA Symposium, November, 1972.

22. Reed, D. L, and Eisenmann, J. R., "Reliability Aspects of a Composite Bolted Scarf Joint," Composite Reliability, ASTM STP 580, American Society for Testing and Materials, 1975, pp. 90-101.

23. Advanced Composites Design Guide, AFML, Advanced Development Division, Vol. IV, Third Edition, 1973.

24. Halpin, J. C., Jerina, K. L., and Johnson, T. A., "Characterization of Composites for the Purpose of Reliability Evaluation," Analysis of Test Methods for High Modulus Fibers and Composites, ASTM STP 521, American Society for Testing and Materials, 1973, pp. 5-64.

25. Berens, A. P., and West, B. S., "Evaluation of an Accelerated Characterization Technique for Reliability Assessment of Adhesive Joints," Composite Reliability, ASTM STP 580, American Society for Testing and Materials, 1975, pp. 90-101.

26. Berens, A. P., Johnson, P. E., and West, B. S., "Experimental Evaluation of a Reliability Assessment Model for Adhesively Bonded Joints," Air Force Materials Laboratory, Technical Report AFML-TR-74-120, June, 1974.

27. Halpin, J. C., "Structural Reliability Characterization of Advanced Composites," Proceedings of the Colloquium on Structural Reliability: The Impact of Advanced Materials on Engineering Design, Conducted with the cooperation of the U. S. Air Force Materials Laboratory, AFSC, held at Carnegie-Mellon University, 9-12 October, 1972, pp. 275-307.

28. Waddoups, M. E., and Halpin, J. C., "The Fracture and Fatigue of Composite Structures," Computers and Structures, Vol. V, 1974, pp. 659-673.

29. Air Force Military Standard,"Aircraft Structural Integrity Program, Airplane Requirements," MIL-STD-1530, U. S. Air Force Aeronautical Systems Command, Wright-Patterson AFB, Ohio, September, 1972.

30. Lavengood, R. E., and Ishai, O., "The Mechanical Performance of Cross-Plied Composites," Polymer Engineering and Science, Vol. 11, No. 3, May, 1971, pp. 226-232.

31. Reed-Hill, R. E., Physical Metallurgy Principles, D. Von Nostrand Company, Inc., Princeton, New Jersey, 1964.

32. Hoeppner, D. W., and Krupp, W. E., "Prediction of Component Life by Application of Fatigue Crack Growth Knowledge," Engineering Fracture Mechanics," Vol. 6, 1974, pp. 47-70.

33. Irwin, G. R., "Fracture Mechanics," Structural Mechanics, Pergamon Press, New York, 1960, p. 557.

34. Rice, J. R., and Rosengren, G. F., Journal of the Mechanics and Physics of Solids, Vol. 16, 1968, pp. 1-12.

35. Begley, J. A., and Landes, J. D., "The J Integral as a Fracture Criterion," Fracture Toughness, Proceedings of the 1971 National Symposium on Fracture Mechanics, Part II, ASTM STP 514, American Society for Testing and Materials, 1972, pp. 1-20.

36. Landes, J. D., and Begley, J. A., "The Effect of Specimen Geometry on J_{IC}," Fracture Toughness, Proceedings of the 1971 National Symposium on Fracture Mechanics, Part II, ASTM STP 514, American Society for Testing and Materials, 1972, pp. 24-39.

37. Ryder, J. T., "Fracture Control of H-O Engine Components," National Aeronautics and Space Administration Report, NASA CR-135137, February, 1977.

38. Adsit, N. R., and Waszczak, J. P., "Fracture Mechanics of Boron/Aluminum Coupons Containing Stress Risers," Fracture Mechanics of Composites, ASTM STP 593, American Society for Testing and Materials, 1975, pp. 163-176.

39. Slepetz, J. M., and Carlson, L., "Fracture of Composite Compact Tension Specimens," Fracture Mechanics of Composites, ASTM STP 593, American Society for Testing and Materials, 1975, pp. 143-162.

40. Konish, H. J., Jr., "Mode I Stress Intensity Factors for Symmetrically-Cracked Orthotropic Strips," Fracture Mechanics of Composites, ASTM STP 593, American Society for Testing and Materials, 1975, pp. 99-116.

41. Zimmer, J. E., "Fracture Mechanics of a Fiber Composite," J. Composite Materials, Vol. 6, April, 1972, p. 312.

42. Konish, H. J., Jr., and Swedlow, J. L , "On Fracture Phenomen in Advanced Fiber Composite Materials," Presented at the 13th Structures, Structural Dynamics, and Materials Conference, Sponsored by AIAA/ASME/SAE, San Antonio, Texas, April 10-12, 1972.

43. Beaumont, P. W. R., and Phillips, D. C., "Tensile Strengths of Notched Composites," J. Composite Materials, Vol. 6, January, 1972, p. 32.

44. Hancock, J. R., and Swanson, G. D., "Toughness of Filamentary Boron/Aluminum Composites," Composite Materials: Testing and Design (Second Conference) ASTM STP 497, American Society for Testing and Materials, 1971, p. 299.

45. Cooper, C. A., "The Fracture Toughness of Composites Reinforced with Weakened Fibers," J. Material Science, Fol. 5, 1970, pg. 645.

46. Beaumont, P. W. R., and Tetelman, A. S., "The Fracture Strength and Toughness of Fibrous Composites," Reports Group, School of Engineering and Applied Science, University of California, Los Angeles, August, 1972.

47. Pettit, D. E., Ryder, J. T., Krupp, W. E., and Hoeppner, D. W., "Investigation of the Effects of Stress and Chemical Environments on the Prediction of Fracture in Aircraft Structural Materials," Air Force Materials Laboratory Report, AFML-TR-74-183, December, 1974.

48. Nuismer, R. J., and Whitney, J. M., "Uniaxial Failure of Composite Laminates Containing Stress Concentrations," Fracture Mechanics of Composites, ASTM STP 593, American Society for Testing and Materials, 1975, pp. 117-142.

49. Roderick, G. L., and Whitcomb, J. D., "Fatigue Damage of Notched Boron/Epoxy Laminates Under Constant Amplitude Loading," presented at the Symposium on Filamentary Composites sponsored by ASTM in Denver, Colorado, November, 1976.

50. Chang, F. H., Gordon, D. E., and Gardner, A. H., "A Study of Fatigue Damage in Composites by Nondestructive Testing Techniques," presented at the Symposium on Filamentary Composites sponsored by ASTM in Denver, Colorado, November, 1976.

51. Freeman, R. B., and Durchlaub, E. C., "Designing for the Fracture Strength and Failure Modes of Notched Boron-Epoxy Composites," Proceedings of the Conference on Fibrous Composites in Flight Vehicle Design, AFFDL-TR-72-130, Dayton, Ohio, 26-28 September 1972, pp.739-755.

52. Kulkarni, S. V., McLaughlin, P. V., Jr., Pipes, R. B., and Rosen, B. W., "Fatigue of Notched Fiber Composite Laminates: Analytical and Experimental Evaluation," Composite Materials: Testing and Design (Fourth Conference), ASTM STP 617, American Society for Testing and Materials, 1977.

53. Reifsnider, K. L., "Fatigue in Composite Materials," North Atlantic Treaty Organization, Advisory Group for Aerospace Research and Development, AGARD, Report AGARD-R-638, February, 1976.

54. Reifsnider, K., Stinchcomb, W. E., and O'Brien, T. K., "Frequency Effects on a Stiffness Based Failure Criterion in Flawed Composite Specimens," Presented at the Symposium on Filamentary Composites Sponsored by ASTM in Denver, Colorado, November, 1976.

55. Halpin, J. C., "Structure- Property Relations and Reliability Concepts," J. Composite Materials, Vol. 6, April, 1972, pp. 208-231.

56. Halpin, J. C., Waddoups, M. E., and Johnson, T. A. "Kinetic Fracture Models and Structural Reliability," Int. J. Fracture Mechanics, Vol. 8, 1972, pp. 465-468.

57. Eisenman, J. R., Kaminski, B. E., Reed, K. L., Wilkens, D. J., "Toward Reliable Composites: An Examination of Design Methodology," J. Composite Materials, Vol. 7, 1973, pp. 298-308.

58. Paris, P. C., "The Growth of Cracks Due to Variations in Loads," Ph.D Thesis, Lehigh University, 1962.

59. Yang, J. N., "Analysis of Fatigue Data," presented at the Mechanics of Composites Review sponsored by the Air Force Materials Laboratory, Nonmetallic Materials Division and the Air Force Office of Scientific Research, Directorate of Aerospace Sciences in Dayton, Ohio, 26-28 October, 1976

60. Wu, E. M., "Strength and Fracture of Composites," Composite Materials, Vol. 5, Academic Press, 1974.

61. Rosen, B. W., and Zweben, C. H., "Tensile Failure Criteria for Fiber Composite Materials," NASA CR-2057, 1972.

62. Zweben, C. H., "Fracture Mechanics and Composite Materials: A Critical Analysis," Analysis of Test Methods for High Modulus Fibers and Composites, ASTM STP 521, American Society for Testing and Materials, 1972, pp. 65-97.

63. Kulkaini, S. V., and Rosen, B. W., "Design Data for Composite Structure Safe Life Prediction Analysis Evaluation, AFML-TR-73-225, 1973.

64. Zweben, C. H., "A Bounding Approach to the Strength of Composite Materials," J. Engineering Fracture Mechanics, Vol. 4, No. 1, March 1972, pp. 1-8.

65. Kanninen, M. F., Rybicki, E. F., and Brenson, H. F., " A Critical Look at Current Applications of Fracture Mechanics to the Failure of Fibre-Reinforced Composites," Composites, January, 1977, pp. 17-22.

66. Kanninen, M. F., Rybicki, E. F., and Griffith, W. L., "Preliminary Development of a Fundamental Analyses Model for Crack Growth in a Fibre-Reinforced Composite Material," Composite Materials: Testing and Design (Fourth Conference), ASTM STP 617, American Society for Testing and Materials, 1977.

67. Anthony, F. M., "Discussion of the Colloquium on Structural Reliability," Proceedings of the Colloquium on Structural Reliability: The Impact of Advanced Materials on Engineering Design, Conducted with the cooperation of the U. S. Air Force Materials Laboratory, AFSC, held at Carnegie-Mellon University, 9-12 October, 1972, pp. 527-534.

☆ U. S. GOVERNMENT PRINTING OFFICE: 1977 — 757-001/558